The University Of Sheffield.

Magnetohydrodynamic Waves in a Gravitationally Stratified Fluid

Alexander Brian Hague

School of Mathematics and Statistics

University of Sheffield

This dissertation is submitted for the degree of

Doctor of Philosophy

Supervisor:
Prof. Robert von
Fay-Siebenburgen

2016

For Josie

Acknowledgements

I would firstly like to thank my family and friends, in particular my Mum and Dad, for support. This thesis would not have been possible without them. The work in this thesis has doubtlessly been improved by the input of many people. I would like to thank my supervisor Robertus Erdélyi for guidance, Misha Ruderman for helpful discussions and feedback and the many friends and colleagues in the School of Mathematics and Statistics. Special thanks go to Stevie Chaffin for countless conversations which were invaluable to this thesis. I acknowledge the School of Mathematics and Statistics for funding this work. Finally, I would like to thank Josie.

Abstract

Waves and oscillations are ubiquitous in the Sun. Magnetohydrodynamic (MHD) waves in a gravitationally stratified medium are of fundamental importance in understanding the physical phenomena observed in the solar atmosphere. Waves may be generated by turbulent motion in the solar convection zone. Magnetic fields of varying scales permeate the atmosphere of the Sun; these may provide a channel for MHD waves to propagate into the solar atmosphere.

The theory of MHD waves in a stratified medium has been well developed, although it is far from complete. In this thesis we aim to contribute to the development of this theory. The work in this thesis can be broadly divided into two sections. The first of these concerns the role of buoyancy when MHD waves propagate within a gravitational field. Secondly, we study the global resonance of waves in a stratified atmosphere. We primarily employ analytical methods to make progress.

We study buoyancy-driven MHD waves with more depth and rigour than previous studies. We begin with a magnetic field that is parallel to gravity. We give a clearer picture of the situation, which has previously been misinterpreted. We generalise previous work to include a more complex and realistic background including temperature variation and partial ionisation. We also briefly consider a magnetic field perpendicular to gravity.

It has been shown that vertically propagating acoustic waves in a stratified atmosphere may be trapped by a varying acoustic cut-off frequency. This trapping leads to a global resonance in the entire solar atmosphere. We generalise previous work by including *e.g.* non-vertical wave propagation, buoyancy and a magnetic field. We conclude that the global resonance is a rather robust phenomenon and so may be an important mechanism in supplying energy into the higher solar atmosphere.

Table of contents

Chapter 1

Introduction

1.1 The Sun

The Sun is a main-sequence star located at the centre of the Solar System. From our perspective on Earth, the fundamental importance of the Sun cannot be overstated. The Sun contains the vast majority of the mass of the Solar System (approximately 99.9%) and so is responsible for the dynamics and conditions of the system. Whether pursued through the sky by a monstrous wolf or the source of Superman's power; the importance of the Sun to humanity is reflected by its place in the religions and mythologies of practically every culture. It is, therefore, unexpected that the Sun has been, and continues to be, a rich area of scientific study.

We study the Sun for many reasons. The primary reason is of "pure science"; it is human nature to study and understand the world we find ourselves in. We may study the Sun, not only to understand the Sun itself, but other stars in the universe. The Sun's proximity to Earth means that we may use the Sun as a laboratory to test stellar theories. Studying the Sun also has important practical applications. Space weather has its origin in solar phenomena. Space weather can have a drastic effect on electronics and satellites; for example, in 1989 a geomagnetic storm, due to a coronal mass ejection, caused extensive electricity blackouts in Quebec. A more powerful solar storm, known as the Carrington Event, occurred in 1859 resulting in a failure of telegraph systems throughout North America and Europe. Predicting and understanding space weather is, therefore, vital. We also do not know the extent of solar variability on Earth's climate. Making long term predictions of Earth's climate may then require a thorough understanding of solar processes.

Stars such as the Sun are composed of plasma. Plasmas are essentially gasses which are heated to such a degree that the molecules become ionised (either partially or fully). The medium therefore consists of a large number of ions and electrons. The medium overall is electrically neutral as, to a large extent, there is an equal number of ions and electrons. The solar plasma consists mainly of hydrogen and helium, with some heavier elements. The Sun, though, is not a uniform sphere of plasma. Rather, it is a highly structured, inhomogeneous medium which may be divided into several subsections where different physical processes are at play.

The very centre of the Sun is known as the solar core. The core represents the inner most 25% of the Sun, by radius ($0.25R_{Sun}$, where $R_{Sun} \approx 700$Mm). The solar core is the nuclear furnace that powers the Sun. The temperature and pressure are so high that nuclear fusion may take place. Energy is generated primarily via the proton-proton (PP) chain (although there are important contributions from the CNO cycle) in which hydrogen nuclei are fused to form helium. The energy generated in the core escapes this region in the form of photons. Beyond the core is the radiative zone. This is the region of the solar interior from $0.25R_{Sun}$ to $0.7R_{Sun}$. Energy is diffused very slowly through the radiative zone as photons are continuously absorbed and emitted.

The outermost 30% of the Sun's radius is represented by the region known as the convection zone. The conditions of the convection zone are such that it is unstable to convection, analogous to a pan of water heated from below. Convection represents the dominant form of energy transportation. There is a region of strong shear flow at base of the convection zone known as the tachocline. The tachocline is thought to be the site of the generation of the Sun's magnetic field through dynamo action. Many important and interesting phenomena on the Sun are caused by magnetism. Solar variability, including the well known 22-year sunspot cycle, is linked to the Sun's large scale dynamo. Above the tachocline, the Sun rotates differentially (*i.e.* the rotation rate varies with latitude); whereas below the tachocline, the solar interior rotates almost as a solid body.

The visible "surface" of the Sun is known as the photosphere. The photosphere is not a distinct surface, rather, it is a thin layer of plasma that represents the lowest part of the solar atmosphere. Like the interior, the solar atmosphere may also be divided into different regions having different physical properties. Each region is home to a variety of fascinating localised features. Localised magnetic structures are seen throughout the solar atmosphere, including sunspots, pores, prominences, coronal loops to name but a few. The photosphere is relatively opaque and emits the majority of the solar radiation. The motion in the convection zone may be seen in the photosphere in the form of photospheric granules (Rayleigh-Bénard convection cells). Above the photosphere is a more transparent layer known as the chromosphere. The depth of the chromosphere varies highly although averaged models, *e.g.* the VAL model (Vernazza, Avrett & Loeser, 1981), give its depth as 2Mm.

At the top of the chromosphere is the outer most part of the solar atmosphere, known as the corona. The temperature increases sharply by two orders of magnitude between the chromosphere and corona. The region in which the temperature increases is known as the transition region; the precise reason for this temperature increase is, at present, undecided. The solar corona is dominated by magnetic fields. Understanding the interaction and dynamics of the coronal magnetic fields is thought to be the key to understanding the long standing mystery of coronal heating. The chromosphere and corona are not normally visible to us due to emission from the photosphere. They can be seen, however, during an eclipse, when the Earth, Moon and Sun align in syzygy. When an eclipse occurs, emission from the photosphere is obscured so we may directly see the chromosphere and corona (this effect may be replicated with the use of equipment known as a coronagraph).

Material from the solar atmosphere flows continuously into interplanetary space in the form of the solar wind. We may define the extent of the solar atmosphere to be the point at which the solar wind speed is equal to the Alfvén speed, so that the lower layers of the Sun may not "communicate" with the solar wind plasma in the form of Alfvén waves. The Sun's magnetic field, carrying with it the solar wind plasma, extends to the far reaches of the solar system. This region, dominated by the solar magnetic field, is known as the heliosphere. The solar wind interacts with other bodies in the solar system. Special interest

is, of course, paid to the interaction of the Earth's magnetic field; this gives rise to so called space weather. Understanding space weather is of great practical importance given our reliance on satellites and electronic equipment. For details on the solar interior and atmosphere see *e.g.* Aschwanden (2005), Priest (2013).

We study the Sun by analysing the emitted radiation. Structures in the solar atmosphere may be seen directly (although not with our eyes). There are many telescopes on Earth and on-board satellites which we may use to view the solar atmosphere. These have been vital in advancing our understanding of solar structures. We have very briefly described the composition of the solar interior, although we cannot see into the Sun directly. How are we able to "see" the solar interior? It was long thought that the inside of the Sun would be forever invisible to us, but this is not so. The answer lies in analysing the waves and oscillations of the Sun.

1.2 Helioseismology and Waves on the Sun

The Sun is a huge sphere of plasma. On large length scales the plasma may be modelled as a fluid and may support hydrodynamic waves. Hydrodynamic waves in a gravitationally stratified, compressible medium have been well studied. There are two types of waves which may exist; the first is the gravitationally modified acoustic wave (Lamb, 1932), where pressure is the primary restoring force. There are also internal gravity, or buoyancy, waves (see *e.g.*, Lighthill, 1978). A fluid particle displaced vertically from equilibrium in a stratified medium is restored by buoyancy and will oscillate at a characteristic frequency known as the Brunt-Väisälä frequency. We will review these waves mathematically in Chapter 2.

In stars like the Sun, global internal oscillations (standing modes of the entire stellar interior) are known as p-modes and g-modes (Cowling, 1941) depending on the main driving force: pressure or buoyancy. There also exists a surface gravity mode, the incompressible f-mode. The linearised equations governing these modes in a spherical system are analysed by, *e.g.*, Cox (1980) and Unno *et al.* (1989). The perturbations are found to be described by spherical harmonics, Y_l^m, where l is the degree and m is the azimuthal order. A non-rotating, spherically symmetric star is independent of m, depending only on l and the radial order n. It can be shown that p-modes have higher frequencies than g-modes and display Sturmian behaviour (the frequency increases with n), while g-modes are anti-Sturmian (the frequency decreases with n increasing).

Acoustic p-modes were first observed by Leighton *et al.* (1962) and Evans & Michard (1962). The oscillations detected typically had periods of around 5 minutes. The theory of these solar 5-minute oscillations was developed by *e.g.* Ulrich (1970) and Leibacher & Stein (1971). These 5-minute oscillations were interpreted as acoustic modes generated by the convective motion in the convection zone and trapped in a resonant cavity below the photosphere. This interpretation became accepted when the predicted spectrum of

modes were observed by Deubner (1975) as a series of ridges in the power spectrum. The 5-minute oscillations were then indeed correctly interpreted as p-modes.

The period of p-modes is not limited to approximately 5 minutes; there may exist many p-modes with periods ranging from minutes to hours. In fact millions of modes of vibration have been observed with a combination of ground- and space-based instruments. Observations of p-modes are particularly interesting for what they reveal about the Solar interior. These modes are sensitive to background parameters, which can be determined from inversion of p-mode data, as suggested by Christensen-Dalsgaard & Gough (1976). This technique known as helioseismology, see *e.g.* Deubner & Gough (1984), Christensen-Dalsgaard (2002), Chaplin (2006) for details. The depth to which p-modes penetrate the solar interior depends upon spherical degree. High-frequency modes (large l) are trapped close to the solar surface and so studying these modes reveals only information about the high convection zone. Low-frequency modes (low l) may penetrate deeper into the Sun. The wide range of observed modes means we may see a clear picture of the solar interior.

Helioseismolgy has had many major successes. One of the earliest was to measure the depth of the convection zone, which was shown to be deeper than previously thought. Inverting p-mode data allows us to determine the properties of the medium through which the waves propagate, including elemental abundances. Helioseismology then allows a fairly accurate determination of the composition of the Sun (see *e.g.* Christensen-Dalsgaard *et al.* , 1996).

Rotation also has a significant effect on p-modes. Rotation breaks the spherical symmetry and so introduces another quantum number, the azimuthal order m. Instead of a single frequency for each l (plus the overtones from the number of radial modes, n) there may be several peaks in the frequency spectrum. For each l there are $2l+1$ possible values for m. A rotating star is said to split each mode of oscillation. Observing this splitting allows us to deduce the rotational profile of the star. Observing values of m other than $m = 0$, and so measurements of the solar internal rotation, was first achieved by Duvall & Harvey (1984) and Duvall *et al.* (1984). See *e.g.* Thompson *et al.* (2003) for more on the internal rotation of the Sun.

The achievements of helioseismology extend beyond the field of solar physics. One of the largest problems in 20th century physics was the so called solar neutrino problem. The nuclear fusion in the solar core produces particles knowns as neutrinos. The detected number of neutrinos emitted from the Sun was significantly fewer than solar models predicted. Helioseismology provided accurate information on the composition of the solar interior, so the predicted number of neutrinos should be as the solar models suggested. The resolution to this problem was the fact the neutrinos actually have mass and so undergo neutrino oscillation.

While a multitude of p-modes of varying degrees have been detected, g-modes have yet to be, unambiguously, observed on the Sun. The difficulty in detecting the g-modes of the solar interior arises for several reasons. Firstly, the waves are evanescent in the

convection zone. The amplitude of such perturbations is very small at the solar surface (around 0.1mm in contrast to *p*-mode amplitudes of hundreds of mm). Second, *g*-modes have very low frequencies and so require long observing times. The search for *g*-modes is summarised by Appourchaux *et al.* (2010).

The detection of *g*-modes would prove to be a beneficial tool to helioseismologists. The *g*-modes are trapped deep in the solar interior and so would be very sensitive to environmental factors near the core. An example is the rotation of the solar core. The rotation rate of the core and deep radiative is less well known, as very few *p*-modes penetrate this deep, giving us less reliable data. In addition, the sound speed is much greater in the core than the rest of the solar interior, hence the low-degree *p*-modes spend less time travelling through the core so are less sensitive to the environment there. It is hoped that measuring *g*-mode frequencies could better determine the conditions of the core.

The methods of helioseismology can be applied to other stars, this is the field of astroseismology. Although *g*-modes still prove to be elusive in the Sun, they have been detected in several other types of star including B-type stars and white dwarfs, see e.g. Waelkens (1991) and Winget & Kepler (2008), respectively. The field of astroseismology has greatly expanded in recent years with the COROT (Convection, Rotation & Planetary Transits) and Kepler space missions. For a review of asteroseismology applied to a number of solar-type and red giant stars see Chaplin & Miglio (2013) and references therein. It should be noted that in sufficiently evolved stars, *p*- and *g*-modes may couple together leading to modes of oscillations with a mixed character.

Sound waves and internal gravity waves (IGWs) are also supported by the solar atmosphere, where they are sometimes known as *atmospheric p*-modes and *g*-modes. In contrast to interior *g*-modes, atmospheric internal gravity waves have been observed by *e.g.* Komm, Mattig, & Nesis (1991), Stodilka (2008) and Straus *et al.* (2008). IGWs may be generated by convective motion in the solar convection region. Numerical simulations by Brun *et al.* (2013) have shown that internal *g*-modes may be excited in the solar radiative interior by turbulent convection. Atmospheric IGWs in the solar atmosphere may be excited in a similar fashion, as suggested by Komm *et al.* (1991).

Among the many, a major difference between the solar interior and atmosphere is magnetism. The solar atmosphere is permeated by magnetic fields, which play a vital role in structuring the atmosphere and in the dynamics of atmospheric plasma. We must use a magnetohydrodynamic (MHD) description of solar plasmas in the presence of a magnetic field. Magnetic structures are able to support magnetohydrodynamic waves: slow and fast magneto-acoustic and Alfvén waves. We review these waves in Section 2.3.1. MHD waves have been observed in various solar structures. It has long been known that oscillations are common in and around sunspots; in particular oscillations with periods of three and five minutes are well reported. These waves were interpreted as slow magnetoacoustic waves

guided by the magnetic field. See Bogdan & Judge (2006), and references therein for more on sunspot oscillations.

Many structures in the solar atmosphere are formed from structured magnetic fields. The magnetic field does not permeate the plasma of the solar atmosphere in a uniform manner, rather it forms localised structures such as magnetic flux tubes (*e.g.* Gent *et al.* , 2013). An important example of solar phenomena which may be modelled as magnetic flux tubes are coronal loops. Oscillations of coronal loops were first observed by Aschwanden *et al.* (1999). Coronal loop oscillations have been studied extensively because of what they may reveal about the coronal plasma. As in helioseismology, wave measurements may be inverted to deduce information about the background plasma such as the much sought-after magnetic field. This is a relatively new area of solar physics, and is labelled as solar magneto-seismology when applied to diagnostics, see Erdélyi (2006a,b). This is an important tool as other methods often used to directly measure the magnetic field strength, such as the Zeeman effect (which is sensitive to spatial resolution and so difficult to detect when noise levels are high) or methods based on gyroresonant emission (which require very strong magnetic fields), may be unsuitable for application in the solar corona.

The solar interior and atmosphere are not distinct, rather they are part of a coupled system. We therefore expect the magnetic atmosphere to influence and be influenced by the oscillating solar interior. It is well known that a magnetic field has significant implications for helioseismology, see *e.g.* the reviews by Thompson (2006b), Erdélyi (2006a,b). Chaplin *et al.* (2007) used data taken over three solar cycles to analyse changes to p-mode frequencies due to these cycles. These are global oscillations affected by variations to the overall magnetic field of the Sun. However, local magnetic fields are also important. We observe p-modes to be damped when propagating through a sunspot (Braun, Duvall and Labonte, 1987). The details of how the magnetic field changes the properties (*e.g.* frequency, amplitude, polarisation, reflection, refraction, etc.), of acoustic or internal gravity modes is a fundamental question. Once it is known how these changes scale with the presence of a magnetic field, magneto-seismology may be performed. The key to understanding the wave coupling of the interior and atmosphere is to study MHD waves in a gravitationally stratified medium, *i.e.* the MHD analogies to p- and g-modes. See *e.g.* Thomas (1983) for a review of MHD waves in a stratified atmosphere; where the waves are discussed in terms of their local dispersion relation.

Magnetohydrodynamic waves have different properties based on the configuration of the magnetic field in relation to the gravitational field. Two important configurations are when the magnetic field is perpendicular (termed a horizontal field, when a Cartesian coordinate system is used) or parallel (termed vertical) to gravity. In practice the magnetic field may be very complex and dynamic; loops, arcades, braided flux ropes *etc*. are all observed and may support MHD waves. In theoretical works these effects are difficult to analyse when combined with gravitational stratification, so horizontal and vertical magnetic fields are most often studied. A significant amount of theoretical work has been

carried out with a horizontal atmospheric magnetic field, the strength of which varies with height, modelling a chromospheric magnetic canopy as observed by, *e.g.*, Giovaneli (1980). The goal is to understand how global interior oscillations are effected by an atmospheric magnetic field and vice versa. Examples include Campbell & Roberts (1989), Evans & Roberts (1990), Jain & Roberts (1994a,b), Tirry *et al.* (1998), Pintér *et al.* (1998), Pintér & Goossens (1999), Goedbloed & Poedts (2004), Erdélyi (2006), Pintér, Erdélyi & Goossens (2007), and Pintér & Erdélyi (2011). It was shown in many of the works that the tendency of a magnetic field is to decrease the frequency of *p*-modes.

In the presence of a vertical magnetic field the distinction between fast and slow MHD modes is less clear. The slow and fast waves have mixed properties and mode conversion can occur when the sound and Alfvén speeds are equal. This phenomenon makes the mathematical treatment of MHD waves in this model very difficult. For an overview of mode conversion see *e.g.* Zhugzhda & Dzhalilov (1982), Cally (2001, 2006). A vertical magnetic field is directly applicable to phenomena such as sunspots, pores and coronal holes. It has also been shown by Reardon *et al.* (2011) that chromospheric fibrils, previously thought to be predominantly horizontal fields, have instead much "more" vertical magnetic flux than horizontal. The effect of a vertical magnetic field on *p*-modes has been investigated analytically by, *e.g.,* Zhugzhda & Dzhalilov (1981, 1982), Zhukov (1985), Zhukov & Efremov (1988), Spruit & Bogdan (1992), Cally & Bogdan (1993), Cally, Bogdan, & Zweibel (1994) and Hindman, Zweibel & Cally (1996). Most of the previous works were motivated by the conversion of *p*-modes in sunspots; where the *p*-modes were damped by mode conversion. As *p*-mode damping was the motivation, the effects of buoyancy were neglected in many of the previous studies. Bogdan *et al.* (1996), Hindman & Jain (2008), Jain *et al.* (2009) analysed absorption of *p*-modes by magnetic flux tubes as a damping mechanism.

The theory of MHD waves in stratified medium, in which the magnetic field is parallel to gravity, has also been investigated by, *e.g.*, Ferraro and Plumpton (1958), MacDonald (1961), Syrovatskii & Zhugzhda (1968), Zhugzhda (1979), Hollweg (1979), Moreno-Insertis & Spruit (1989), Hasan & Christensen-Dalsgaard (1992), Cally (2001), Zhukov (2002, 2005), and Roberts (2006). Some of these works focused on the effect of a magnetic field on convection, the unstable counterpart of buoyancy oscillations. One key result is that a sufficiently strong magnetic field can inhibit convection, *i.e.*, wave propagation may be possible when the square of the Brunt-Väisälä frequency is negative.

It should be noted that a significant difference between the case of a horizontal and vertical field is the presence of damping due to resonant absorption (see, *e.g.*, Goossens *et al.* , 2011 for a review). Resonance does not occur in a model with a vertical field, which is uniform in the horizontal directions. When the field is horizontal, the effect of gravity on damping due to resonant absorption has been analysed by, *e.g.*, Tirry *et al.* (1998), Pintér & Goossens (1999), Pintér, Erdélyi & Goossens (2007), and Pintér & Erdélyi (2011). Stratified plasmas may also introduce an important damping mechanism for

Alfvén waves known as phase mixing (Heyvaerts & Priest, 1983). Damping mechanisms are very important in wave theories. Waves are efficient mechanisms for transporting energy; damping allows this energy to be dissipated to the surrounding medium, resulting in heating. Wave heating of the solar corona is an attractive theory as we observe the Sun to be continuously oscillating (p-modes) and the magnetic field provides a channel for waves to propagate into the higher atmosphere. Dissipation of the energy in the waves could very well be a key contributor to coronal heating.

The wealth of observations of p-mode interaction with magnetic structures has steered theoretical works in this direction. Less attention has been paid to waves where buoyancy plays an important role in the motion, *i.e.* g-modes. A horizontal field, with a background flow, was analysed in the Boussinesq approximation by Barnes *et al.* (1998). It was shown that propagating IGWs have a buoyancy and a magnetic component in an MHD model. Studying buoyancy-driven MHD waves in a greater depth forms a significant part of this work.

1.3 Outline of Thesis

In this thesis we study problems concerning hydrodynamic and magnetohydrodynamic waves in a gravitationally stratified fluid. We are motivated by application of the results to the solar atmosphere, although the results are not limited to the Sun. This work can be split into two categories. Firstly, we study buoyancy-driven MHD waves. That is, the MHD analogue to g-modes. The second class involves the trapping of waves due to stratification, leading to a resonance which extends to the entire atmosphere. We are primarily interested in studying the problems analytically; that is, we seek to gain insight via the application of mathematics. The thesis is structured as follows.

Chapter 2 mostly consists of background material. We begin, in Section 2.1, by considering waves in a gravitationally stratified fluid. The two waves, acoustic and internal gravity waves, are discussed mathematically in terms of a local dispersion relation. We then (Section 2.2) review IGWs in more detail with the application of the Boussinesq approximation which is also discussed. This is applicable to the lower solar atmosphere in a region known as the Quiet Sun (QS), that is, an area with little to no magnetic activity. In addition to propagating waves, discussed in terms of a local dispersion relation, we consider waves in a polytropic atmosphere (both finite and semi-infinite). To do this we find the eigenfunctions describing the motion. To our knowledge, IGWs in a polytropic atmosphere have not previously been studied in detail. Chapter 2 ends, in Section 2.3, with a brief discussion of MHD theory and MHD waves in a homogeneous plasma.

After discussing hydrodynamic IGWs, we move onto the MHD case. This forms Chapter 3 of this thesis. We seek to address IGWs from the viewpoint of MHD waves and determine the modification of the frequency due to a magnetic field. This has not been studied in detail; in this chapter we generalise previous works and study the topic in a

greater depth than previously done. We therefore provide the theoretical basis for buoyancy-driven MHD waves in greater detail, and with more clarity, than previous authors. We begin by considering a vertical magnetic field. MHD waves in the Boussinesq approximation have previously been misinterpreted. Here, we look at the problem in such a way that the situation is clear. We see that buoyancy-driven MHD waves are slow MHD waves, not Alfvén waves as has been previously stated. We then move onto standing waves and waves in a two-layer atmosphere using an analysis similar to, but not exactly identical to, the Boussinesq approximation. Previous works have considered only simple models (that is standing waves in an isothermal slab). The effects of partial ionisation on buoyancy-driven MHD waves are discussed. We then study a model with a horizontal magnetic field.

The approximations used in this analysis lend themselves to the lower solar atmosphere, specifically the photosphere or low chromosphere. In this region we expect IGWs to be generated by convective motion and be influenced by the magnetic structures permeating the solar atmosphere. The conditions of the solar chromosphere may lead to some trapping of IGWs. A vertical or horizontal magnetic field may then be used to model the structures observed in chromosphere.

The remainder of this thesis is dedicated to studying the global resonance discovered by Taroyan & Erdelyi (2008). A variable background temperature, within a gravitationally stratified medium, may reflect vertically propagating acoustic waves so a resonant cavity is formed. Driving waves leads to a resonance which couples to the entire atmosphere. In Chapter 4 we further study this resonance by allowing non-vertical wave propagation. We show that IGWs are subject to the same type of resonance as acoustic waves. The effect of a non-zero horizontal wavenumber is studied. A key result is that the range of resonant frequencies is much larger than vertically propagating waves. This phenomenon is a potentially important mechanism for transferring energy into the upper solar atmosphere.

Chapter 5 generalises the hydrodynamic resonance to MHD waves. We find that the resonance is a rather robust phenomenon, occurring in a range of models for a variety of parameters. We firstly study vertically propagating waves in a model constructed from a polytropic, hydrodynamic interior and a magnetic atmosphere. Two cases are considered: a magnetic field that varies such that the Alfvén speed is constant and a uniform magnetic field. The magnetic field profile is seen to have a significant effect on the global resonance. Next, the effect of non-vertical wave propagation in a model with constant Alfvén speed is analysed. Finally, the case of a vertical magnetic field is analysed. Due to the difficulty in finding analytical solutions, the number of models is more restricted than the horizontal case. It is seen, however, that the resonance does exist in some models considered. We conclude in Chapter 6.

Chapter 2

Waves: Waves in a Stratified Fluid and Magnetohydrodynamic Waves

2.1 Waves in a Stratified Fluid: Basic Equations

The Sun consists of ionised gas known as plasma. To model the dynamics of the medium mathematically we may take two approaches the kinetic theory or the fluid theory. Both approaches lead to a system of equations governing the dynamics of the plasma. The kinetic theory studies the motion of a large number individual particles in terms of particle distribution functions. We find it more useful to treat the large number of particles as a macroscopic entity. This approach may be used when we work with length scales, such as in the Sun, *i.e.* on scales above the mean-free path of the ions. This is referred to as the continuum approximation. The fluid model is derived from the point of view of conserved quantities for a given volume. When the fluid is not affected by a magnetic field it may be described by the compressible Euler equations of fluid flow,

$$\frac{\partial \rho}{\partial t} = -\nabla \cdot (\rho \mathbf{v}), \tag{2.1}$$

$$\rho\left(\frac{\partial \mathbf{v}}{\partial t} + \mathbf{v} \cdot \nabla \mathbf{v}\right) = -\nabla p + \rho \mathbf{g}, \tag{2.2}$$

$$\frac{\partial p}{\partial t} + \mathbf{v} \cdot \nabla p = -\gamma p \nabla \cdot \mathbf{v}, \tag{2.3}$$

where $\mathbf{v}$ is the velocity field, $\mathbf{g}$ is acceleration due to gravity, ρ is the fluid density, p is the pressure and γ is the ratio of specific heats. The above equations represent the conservation of mass, momentum and entropy per unit volume for a fluid element, following the motion of the fluid element (using Eulerian variables). The equation representing the conservation of entropy is based on the assumption that the motion is adiabatic, *i.e.* when a fluid element is compressed no heat is exchanged to the surrounding fluid, and there are no sources or losses of heat. For a more general equation that allows non-adiabatic and more complex thermal effects see *e.g.* Priest (2013). Viscosity is neglected in our work and may be neglected in most solar applications (although it may become important in certain circumstances such as in shock waves; see Hollweg, 1986 for a discussion of the importance of viscosity in the solar corona). For more details, including the derivation of the Euler equations, and applications see one of the many classic texts *e.g.* Lamb (1932), Batchelor (1967), Landau & Lifshitz (1987).

The non-magnetic Euler equations may be used when the magnetic field is negligible. Solar applications include the regions of the lower atmosphere known as the Quiet Sun. The Euler equations are commonly employed in helioseismology, to study the standing oscillations of the entire Sun. The Sun's magnetic field is thought to be generated at the base of the solar convection zone. It's role in the dynamics of the plasma become more important in the solar atmosphere and so it is often neglected when not considering the atmosphere. We shall look at the effects of a magnetic field in later sections.

Waves play an important role in fluid dynamics. Waves carry energy without a bulk motion of the fluid and so provide an efficient mechanism for transferring energy with a fluid. Waves are also studied as a tool for diagnostic purposes. That is, information about a medium may be inferred from observations of waves propagating through it. Waves may be defined as perturbations to some background state; hence, to study them it is important to establish this background. We begin by writing the variable quantities as the background state plus some perturbation,

$$\rho(\mathbf{r},t) = \rho_0(\mathbf{r}) + \rho_1(\mathbf{r},t) \quad \text{where } |\rho_1| \ll \rho_0, \tag{2.4}$$

$$p(\mathbf{r},t) = p_0(\mathbf{r}) + p_1(\mathbf{r},t) \quad \text{where } |p_1| \ll p_0, \tag{2.5}$$

$$\mathbf{v}(\mathbf{r},t) = \mathbf{v}_0(\mathbf{r}) + \mathbf{v}_1(\mathbf{r},t) \quad \text{where } |\mathbf{v}_1| \text{ is small}, \tag{2.6}$$

The subscript 0 denotes the background state, while 1 denotes the perturbation and $\mathbf{r}$ is the position vector. We assume that the medium is initially in some time-independent equilibrium (though this can be relaxed to consider some variable background state), hence the background quantities do not depend on time. We also assume that there are no background flows $\mathbf{v}_0 = \mathbf{0}$, again for simplicity. Notice that we consider only small perturbations. This is linear theory. The case where the perturbed quantities are not small compared to the background may be studied (the non-linear theory) although this is beyond the scope of this work.

Considering the static, time-independent background gives us the equation of hydrostatic equilibrium

$$\nabla p_0 = \rho_0 \mathbf{g}. \tag{2.7}$$

The equation of hydrostatic equilibrium represents exact solutions to the full governing equations for the special case of $\mathbf{v} = \mathbf{0}$ and quantities which do not vary in time. This equation also results from substituting the expressions (2.4) to (2.6) into the momentum equation and retaining only the largest terms (formally, a perturbation series to leading order). We define the coordinate system such that gravity acts in the negative z-direction, $\mathbf{g} = (0, 0, -g)$. We assume that the gravitational field is constant. This is applicable to the solar atmosphere as approximately 90% of the Sun's mass is contained within 50% of it's radius. When studying the entire star we should allow the gravitational potential to vary as a function of density and radius. The background density and pressure then depend on height only, $p_0 = p_0(z)$, $\rho_0 = \rho_0(z)$. The equation of hydrostatic equilibrium takes the form

$$\frac{\mathrm{d}p_0}{\mathrm{d}z} = -g\rho_0. \tag{2.8}$$

The background also satisfies the equation of state,

$$p_0 = \frac{k_B}{\widehat{m}}\rho_0 T_0, \tag{2.9}$$

where k_B is Boltzmann's constant, T_0 is the background temperature and $\widehat{m}$ is the mean particle mass. This allows us to determine the background pressure and density profiles if the background temperature is known.

Around this static background we take small (*i.e.* linear), adiabatic, perturbations of the governing equations. Keeping now small terms to first order (neglecting terms quadratic and higher in the perturbed quantities) leads to the linearised governing equations of motion,

$$\frac{\partial \rho_1}{\partial t} + v_{1z}\frac{\mathrm{d}\rho_0}{\mathrm{d}z} + \rho_0 \nabla \cdot \mathbf{v}_1 = 0, \tag{2.10}$$

$$\rho_0 \frac{\partial \mathbf{v}_1}{\partial t} = -\nabla p_1 + \rho_1 \mathbf{g}, \tag{2.11}$$

$$\frac{\partial p_1}{\partial t} + v_{1z}\frac{\mathrm{d}p_0}{\mathrm{d}z} + \gamma p_0 \nabla \cdot \mathbf{v}_1 = 0, \tag{2.12}$$

These equations allow for the study of hydrodynamic waves in a gravitationally stratified fluid. When gravity is absent, $\mathbf{g} = \mathbf{0}$, the medium is homogeneous; the governing equations may be combined to form the familiar wave equation for sound waves.

In the above we neglected perturbations to the gravitational potential. This is known as the Cowling approximation after Cowling (1941) who first studied the justification. Effectively, the Cowling approximation states that perturbations to the gravitational potential are small compared to the perturbed density when the spherical degree l or radial order n is sufficiently large, *i.e.* the wave number is large. We may think of the Cowling approximation as being valid when the density variations cancel when integrating over them. For further details see *e.g.* Thompson (2006a).

2.1.1 Combined Theory of Sound and Internal Gravity Waves

Let us consider the waves described by the set of Equations (2.10) to (2.12). In terms of solar applications this is applicable to the non-magnetic regions of the solar atmosphere known as the Quiet Sun or standing modes of the solar interior. The latter is the foundation of helioseismology. In this case we should use spherical coordinates. The non-radial component of the oscillations can be shown to be described by spherical harmonics $Y_l^m(\theta, \phi)$. In this analysis the spherical nature of the Sun is neglected and we use a Cartesian coordinate system (x, y, z), applicable to large horizontal wavenumbers *i.e.* the l of perturbations in a spherical system is large (Pintér, 1999).

We form a single equation from Equations (2.10) to (2.12), using the divergence of velocity as a convenient variable. At this stage we assume normal modes, that is we Fourier analyse in x and t. This means we take all perturbed quantities to be of the form

$$f_1(x, z, t) = \widetilde{f_1}(z) e^{\mathrm{i}(k_x x - \omega t)}, \tag{2.13}$$

where f_1 represents any perturbed quantity, k_x is the horizontal wavenumber and ω is the frequency. Note that we assume no y-dependence, without loss of generality, by rotating the coordinate system such that the wave vector in the $x-y$ plane is in the direction of x only. We substitute above into the governing equations for the perturbed quantities; this has the effect of leaving ordinary differential equations for $\widetilde{f_1}(z)$ (we drop the tilde in the following for convenience) instead of partial differential equations. Mathematically, the above is valid when the coefficients in the governing equations do not depend upon the variable with which we Fourier transform (in linear theory Fourier components do not couple together and so may be treated separately). Physically, the normal modes (or plane waves) mean that the characteristics of the wave do not vary in a given direction; *i.e.* we may Fourier analyse the equations in the x-direction, for example, when quantities such as wavelength, phase speed etc. which depend upon the medium do not vary in the x-direction. Fourier transforming in time turns the system of equations into an eigenvalue problem where ω represents an eigenvalue of the differential operator acting on the system.

Letting

$$\Delta = \nabla \cdot \mathbf{v}_1, \tag{2.14}$$

we may form a single governing equation for χ from Equations (2.10) to (2.12),

$$\frac{\mathrm{d}^2\Delta}{\mathrm{d}z^2} + \frac{1}{c_s^2}\left(\frac{\mathrm{d}c_s^2}{\mathrm{d}z} - \gamma g\right)\frac{\mathrm{d}\Delta}{\mathrm{d}z} + \frac{1}{c_s^2}\left(\omega^2 - k_x^2 c_s^2 + \frac{g k_x^2}{\omega^2}\left(\frac{\mathrm{d}c_s^2}{\mathrm{d}z} + g(\gamma-1)\right)\right)\Delta = 0, \tag{2.15}$$

where c_s is the (adiabatic) sound speed defined by

$$c_s^2 = c_s^2(z) \equiv \frac{\gamma p_0}{\rho_0}. \tag{2.16}$$

Equation (2.15) has been investigated before by *e.g.* Lamb (1932), Campbell & Roberts (1989). Solutions to Equation (2.15) may be investigated by specifying a density and pressure profile. Equation (2.15) describes both sound waves, modified by buoyancy, and internal gravity (or buoyancy) waves, modified by compression.

Assuming that the equilibrium quantities ρ_0 and p_0 change slowly with height, we can apply the WKB method (see *e.g.*, Bender & Orszag, 1978) to obtain a local dispersion relation. The WKB method is a technique to find approximate solutions to singular perturbation problems. Physically, it is applicable to waves propagating in a medium that varies slowly. It was developed by Wentzel, Kramers and Brillouin in 1926 when investigating solutions to the Schrödinger equation and independently by Jeffreys in 1924; although its development can be traced earlier to *e.g.* Green and Liouville in 1837. First, we introduce a slowly varying spatial variable $\tilde{z} = \epsilon z$, where $\epsilon \ll 1$, and assume Δ takes the form

$$\Delta = w(\tilde{z}) e^{\mathrm{i}\theta(\tilde{z})/\epsilon}. \tag{2.17}$$

Substituting Equation (2.17) into (2.15) and keeping the leading order terms (*i.e.* terms order $O\left(\epsilon^0\right)$) we are left with

$$\frac{1}{c_s^2}\left(\omega^2 - k_x^2 c_s^2 + \frac{k_x^2}{\omega^2} c_s^2 N^2\right) - \frac{\gamma g \mathrm{i}}{c_s^2}\frac{\mathrm{d}\theta}{\mathrm{d}\tilde{z}} - \left(\frac{\mathrm{d}\theta}{\mathrm{d}\tilde{z}}\right)^2 = 0. \tag{2.18}$$

Using the WKB approximation to leading order is often referred to as the geometrical optics approach; to this order we are able to obtain an expression for the local frequencies but not the amplitude of the waves. To determine the amplitude we must keep terms proportional to ϵ, this is sometimes known as the physical optics approximation. Identifying the local vertical wavenumber, $k_z = \mathrm{d}\theta/\mathrm{d}\tilde{z}$, we find the local dispersion relation

$$\omega^4 - \left(k_x^2 c_s^2 + k_z^2 c_s^2 + \gamma g k_z \mathrm{i}\right)\omega^2 + k_x^2 c_s^2 N^2 = 0, \tag{2.19}$$

where N is the Brunt-Väisälä frequency defined by

$$N^2 = N^2(z) \equiv g\left(\frac{1}{\gamma p_0}\frac{\mathrm{d}p_0}{\mathrm{d}z} - \frac{1}{\rho_0}\frac{\mathrm{d}\rho_0}{\mathrm{d}z}\right) = -g\left(\frac{1}{\rho_0(z)}\frac{\mathrm{d}\rho_0(z)}{\mathrm{d}z} + \frac{g}{c_s^2}\right). \tag{2.20}$$

The Brunt-Väisälä frequency is the characteristic frequency at which a fluid element, displaced vertically in a gravitationally stratified medium, will oscillate. See *e.g.* Lighthill (1978), Priest (2013) for a simple demonstration of this. Introducing the transformed wave number k_z', as in Priest (2013),

$$k_z' = k_z + \frac{g\gamma}{2c_s^2}\mathrm{i}, \tag{2.21}$$

we may rewrite the local dispersion relation as

$$\omega^4 - \left(k^2 c_s^2 + \frac{\gamma^2 g^2}{4c_s^2}\right)\omega^2 + k_x^2 c_s^2 N^2 = 0, \tag{2.22}$$

where k is the total wavenumber $k^2 = k_x^2 + k_z'^2$. The imaginary second term of the transformed wavenumber, Equation (2.21), is due to the exponential variation in wave amplitude with height for propagating waves (when k_z' is real). This is seen, for example, in the case of an isothermal atmosphere where exact solutions may easily be found (Lamb, 1932).

The dispersion relation for sound waves, uncoupled to gravitational effects, can be extracted from Equation (2.22) by assuming that the frequency of these acoustic waves is greater than the Brunt-Väisälä frequency *i.e.*,

$$\omega^2 = c_s^2 k^2. \tag{2.23}$$

In the limit of vertical wave propagation, $k_x = 0$, only sound waves exist. The dispersion in such a limit is

$$\omega^2 = c_s^2 k_z'^2 + \frac{g^2\gamma^2}{4c_s^2}. \tag{2.24}$$

The term $g\gamma/2c_s$ is the acoustic cut-off frequency introduced into the system by gravitational stratification. When $\omega < g\gamma/2c_s$, k_z' is imaginary and the waves decay or grow exponentially as z varies, *i.e.* wave propagation does not occur. Note that this expression is the cut-off frequency when we assume the background to be slowly varying. For a more general background the acoustic cut-off was given by Deubner & Gough (1984),

$$\omega_c^2 = \frac{c_s^2}{4H^2}\left(1 - 2\frac{\mathrm{d}H}{\mathrm{d}z}\right), \tag{2.25}$$

where H is the density scale height defined by

$$H = H(z) \equiv \frac{p_0(z)}{g\rho_0(z)} = \frac{c_s^2}{g\gamma}. \tag{2.26}$$

When the background is isothermal, the expressions for the acoustic cut-off agree.

There is also a solution to the governing equation corresponding to $\Delta = 0$. This is the so called *f*-mode, a surface gravity mode which is independent of the thermal structure of the background state, satisfying the dispersion relation

$$\omega^2 = kg. \tag{2.27}$$

The dispersion relation, Equation (2.22), is a quadratic polynomial in ω^2. There are, therefore, two solutions for ω^2. Sound waves, where the primary restoring force is pressure, modified by buoyancy are given by the upper root of Equation (2.22). There is another wave that we have not yet discussed. These are internal gravity waves (note the terminology internal gravity to distinguish them from the surface gravity *f*-mode.). The primary restoring force of internal gravity waves (IGWs) is buoyancy. IGWs, with some modification due to compressibility are given by the lower root of Equation (2.22). It is helpful to study IGWs without the modification; this will be the subject of the next section.

2.2 Internal Gravity Waves

A fluid element within a stratified medium is subject to a force due to buoyancy, given by Archimedes' Principle. Displacing this fluid element vertically from equilibrium causes it to oscillate at a characteristic frequency, the Brunt-Väisälä frequency, if the medium is stable to convection. See *e.g.* Lighthill (1979), Priest (2013) for a simple mathematical demonstration of this phenomenon. This disturbance may propagate as an internal gravity wave. In this section we focus on the buoyancy-driven IGWs.

2.2.1 Governing Equations and the Boussinesq Approximation

To study internal gravity waves, uncoupled from sound waves, we apply the Boussinesq approximation. Essentially, the Boussinesq approximation is that perturbations to the

density are significant only when multiplied by the acceleration due to gravity, g, *i.e.* when a buoyancy force is provided. This approximation has been widely applied to flows driven by thermal gradients, *i.e.* convection. In the Sun, such flows are very applicable to the solar convection zone. In the Boussinesq approximation, the linearised governing equations are

$$\nabla \cdot (\rho_0 \mathbf{v}_1) = 0, \tag{2.28}$$

$$\rho_0 \frac{\partial \mathbf{v}_1}{\partial t} = -\nabla p_1 + \rho_1 \mathbf{g}, \tag{2.29}$$

$$\frac{\partial \rho_1}{\partial t} = \frac{N^2}{g} \rho_0 v_{1z}. \tag{2.30}$$

Equation (2.30) represents the excess density of a fluid particle over its background as it is displaced vertically from equilibrium (in a stratified fluid). This equation describes how the buoyancy force on a fluid element changes in time. Note that some works use the term Boussinesq approximation to mean a solenoidal velocity field ($\nabla \cdot \mathbf{v}_1$=0), applicable to a medium where the density may be considered as constant, however, we follow Lighthill (1978). This is sometimes referred to as the anelastic approximation. This approximation is more suited the solar atmosphere, where the density may vary significantly. For more on the anelastic approximation see *e.g.* Ogura & Phillips (1962), Gough (1969).

We shall now investigate the conditions of neglecting $\partial \rho_1 / \partial t$ in Equation (2.10) and the representation of $\partial \rho_1 / \partial t$ in Equation (2.30), following e.g. Lighthill (1978). In a fully compressible fluid, we may express the energy equation (2.12), via the continuity equation (2.10), as

$$\frac{\partial p_1}{\partial t} + v_{1z} \frac{\mathrm{d}p_0}{\mathrm{d}z} = c_s^2 \left(\frac{\partial \rho_1}{\partial t} + v_{1z} \frac{\mathrm{d}\rho_0}{\mathrm{d}z} \right), \tag{2.31}$$

or

$$\frac{\partial \rho_1}{\partial t} = \frac{N^2}{g} \rho_0 v_{1z} + \frac{1}{c_s^2} \frac{\partial p_1}{\partial t}, \tag{2.32}$$

using the definition of the Brunt-Väisälä frequency (2.20). Now, we may take the divergence of the momentum equation (2.29),

$$\frac{\partial}{\partial t} \nabla \cdot \rho_0 \mathbf{v} + \nabla^2 p_1 = -g \frac{\partial \rho_1}{\partial z}. \tag{2.33}$$

Taking the derivative with respect to t and substituting Equation (2.32)

$$\frac{\partial^2}{\partial t^2} \nabla \cdot \rho_0 \mathbf{v} + \frac{\partial}{\partial t} \left(\nabla^2 p_1 + g \frac{\partial}{\partial z} \frac{p_1}{c_s^2} \right) = -\frac{\partial}{\partial z} \left(N^2 \rho_0 v_{1z} \right). \tag{2.34}$$

We conclude, therefore, that the term

$$\frac{1}{c_s^2} \frac{\partial p_1}{\partial z} \tag{2.35}$$

has a negligible contribution to the perturbed density in Equation (2.30) when the wavenumber is large compared to g/c_s^2. This shows that by assuming Equation (2.28), Equation (2.30) may be used when the wavenumbers are large compared to g/c_s^2. We may also justify the use of $\nabla\cdot(\rho_0\mathbf{v}_1)=0$ in terms of wavenumber. The energy and continuity equation may be written together as

$$\frac{N^2}{g}\rho_0 v_{1z}+\frac{1}{c_s^2}\frac{\partial p_1}{\partial t}+\nabla\cdot(\rho_0\mathbf{v}_1)=0, \tag{2.36}$$

therefore if the wavenumber is large compared to N^2/g, and also g/c_s^2, the Boussinesq approximation (and so Equations (2.28) to (2.30)) may be used. The terms neglected from the Euler equations may be expected as they both relate to the compressibility of the fluid and so contribute to the generation of sound waves. Note that

$$\frac{N^2}{g}+\frac{g}{c_s^2}=-\frac{1}{\rho_0}\frac{\mathrm{d}\rho_0}{\mathrm{d}z}. \tag{2.37}$$

For more on the applicability of the Boussinesq approximation see *e.g.* Spiegel and Veronis (1960).

We may form a single equation from Equations (2.28) to (2.30), in terms of the vertical component of momentum $q=\rho_0 v_{1z}$, by taking the y-component of the curl of Equation (2.29) and eliminating v_{1x} and ρ_1,

$$\nabla^2\frac{\partial^2 q}{\partial t^2}=-\frac{\partial^2}{\partial x^2}N^2 q. \tag{2.38}$$

Note that we assume no y-dependence, without loss of generality, as there is no preferred horizontal direction. This is the governing equation for IGWs in the Boussinesq approximation. In deriving Equation (2.38), the y-component of the vorticity equation was employed, the x- and z-components do not correspond to interesting physics. The system of eigenvalues is complete by including the entropy wave ($\omega=0$). We may assume normal modes in Equation (2.38),

$$\frac{\mathrm{d}^2 q}{\mathrm{d}z^2}=k_x^2\left(1-\frac{N^2}{\omega^2}\right)q. \tag{2.39}$$

Under the assumption of normal modes, the assumption of no y -dependence is equivalent to rotating the coordinate system such that the wave vector in the $x-y$ plane is in the direction of x only. We shall investigate Equation (2.39) in the context of both propagating and standing waves.

2.2.2 Propagating Waves

Let us perform a local (WKB) analysis of Equation (2.39). First, we introduce a slowly varying spatial variable $\tilde{z}=\epsilon z$, where $\epsilon\ll 1$, and assume q takes the form

$$q=w(\tilde{z})\exp\left(\frac{\mathrm{i}}{\epsilon}\theta(\tilde{z})\right). \tag{2.40}$$

Substituting Equation (2.40) into (2.39) and keeping the leading order terms (*i.e.* terms order $O\left(\epsilon^0\right)$) we are left with

$$\left[\left(\frac{\mathrm{d}\theta}{\mathrm{d}\tilde{z}}\right)^2 + k_x^2\left(1 - \frac{N^2}{\omega^2}\right)\right] w(\tilde{z}) \exp\left(\frac{\mathrm{i}}{\epsilon}\theta(\tilde{z})\right) = 0. \tag{2.41}$$

Again, noting the local vertical wavenumber, we find the local dispersion relation

$$\omega^2 = \frac{k_x^2}{k_x^2 + k_z^2} N^2. \tag{2.42}$$

This is the well known dispersion relation for IGWs (Lighthill, 1978). The Brunt-Väisälä frequency is then the upper cut-off frequency of internal gravity waves. When k_x is large in comparison to k_z, $\omega^2 \approx N^2$. This agrees with the result that a plasma element displaced vertically from equilibrium will be restored by buoyancy and undergo simple harmonic motion at the Brunt-Väisälä frequency.

We may calculate the vertical component of the group velocity, the velocity at which energy is propagated, to be $\omega_g = -\omega k_z / k^2$. We see an interesting characteristic of IGWs, that the vertical components of the phase and group velocities are anti-parallel. An upwardly propagating wave, therefore, transfers energy downwards.

Equation (2.42) can also be found from Equation (2.22). Internal gravity waves correspond to the lower root in Equation (2.22), hence we can assume the frequencies to be small compared to that of acoustic waves. Assuming large wavenumbers (*i.e.* applying the Boussinesq approximation) we may neglect the term ω^4 in Equation (2.22), leaving the dispersion relation in the form given by Equation (2.42).

The discussion so far has been based on the assumption that acoustic waves and IGWs represent distinct solutions to the problem. If it is the case that the Brunt-Väisälä frequency is greater than the acoustic cut-off frequency there is overlap in the region for which the waves may propagate. This leads to modes that have a mixed character; that is, the mode may have a different character in different regions of the fluid. This manifests itself as "avoided crossings" in the dispersion diagram, as in *e.g.* Aizenman, Smeyers & Weigert (1977). This fact was not present in the above analysis as the WKB method in Section 2.1.1 implicitly assumes that the modes are distinct and so fails in the vicinity of avoided crossings. A different method of analysis must then be used to study coupled modes. The coupling of p-modes and g-modes is unlikely in the Sun, although it is important in red giants where the burning of helium may cause the Brunt-Väisälä frequency to become large.

2.2.3 Standing Waves

The Brunt-Väisälä frequency changes significantly throughout the solar chromosphere (see *e.g.* Newington & Cally, 2010). This may cause the trapping of IGWs in the solar

photosphere leading to a cavity in which standing modes may form. We should therefore, not restrict ourselves to propagating modes only and consider these standing modes. Further, standing modes are excellent tools to carry out solar magneto-seismology. Changes *e.g.* in the frequency or node/anti-node positions caused by inhomogeneity, structuring, or even time-dependence of the waveguide are popular applications in solar physics. Although there is an extensive literature to make such applications by means of MHD waves (*e.g.* slow sausage, fast kink, or even Alfvén), there is limited work on IGWs in this context.

We now consider standing waves and so must solve (2.39) with appropriate boundary conditions. The aim is to determine the global, rather than local, frequency of the oscillations. In calculating this we will also find the eigenfunctions, so that the amplitude of velocity and pressure can be specifically determined. This was not possible in the first order local analysis. Standing waves may occur in the solar atmosphere due to turning points or reflection by *e.g.* a sharp change in phase speeds caused *e.g.* by sharp changes in, for example, temperature. Let L be the length of the cavity, $z \in [-L, 0]$. Let us consider the case that the background temperature varies linearly with z,

$$T_0 = \widehat{T}_0\left(1 - \frac{z}{z_0}\right) \tag{2.43}$$

where $\widehat{T}_0$ is the temperature at $z = 0$ and $z_0\,(> 0)$ is the temperature scale height. The temperature, pressure and density are related by the equation of state, Equation (2.9). Using Equation (2.43) together with Equations (2.8) and (2.9) has the consequence that the density and pressure profiles are given by

$$\rho_0(z) = \widehat{\rho}_0\left(1 - \frac{z}{z_0}\right)^m, \quad p_0(z) = \widehat{p}_0\left(1 - \frac{z}{z_0}\right)^{m+1}, \tag{2.44}$$

where $\widehat{\rho}_0$ and $\widehat{p}_0$ are positive constants and represent density and pressure in the limit $z \to 0$, and m is a constant known as the polytropic index. Equation (2.8) implies that $m = z_0 g\gamma/c_s^2(0) - 1$. We see that pressure and density are related by $p_0 = K\rho_0^{1+1/m}$, where K is constant which may be determined using Equation (2.8). Applying the polytropic model, the Brunt-Väisälä frequency is given by

$$N^2 = N_0^2\left(1 - \frac{z}{z_0}\right)^{-1}, \quad N_0^2 = g\left(\frac{m}{z_0} - \frac{g}{c_{s0}^2}\right), \tag{2.45}$$

where N_0^2 is constant (note that N_0^2 can be negative). We also note that we consider a non-adiabatic polytrope, that is, $\gamma \neq 1 + 1/m$. We study a system where the effect of buoyancy is significant, and so the medium is not neutrally stable. The Schwarzschild criterion for convective stability (Lighthill, 1978) implies that $m > 3/2$ when $\gamma = 5/3$.

The governing equation (2.39) can be written

$$\frac{\mathrm{d}^2 q}{\mathrm{d}z^2} = k_x^2\left(1 - \frac{N_0^2}{\omega^2}\left(1 - \frac{z}{z_0}\right)^{-1}\right)q. \tag{2.46}$$

By making the variable change

$$\eta = -2k_x(z_0 - z), \tag{2.47}$$

we may rewrite Equation (2.46) as

$$\frac{\mathrm{d}^2 q}{\mathrm{d}\eta^2} + \left[-\frac{1}{4} - \frac{N_0^2 k_x z_0}{2\omega^2}\frac{1}{\eta}\right]q = 0. \tag{2.48}$$

This is Whittaker's equation (Abramowitz & Stegun, 1972)

$$\frac{\mathrm{d}^2 q}{\mathrm{d}\eta^2} + \left[-\frac{1}{4} + \frac{\kappa}{\eta} + \frac{\frac{1}{4} - \mu^2}{\eta^2}\right]q = 0, \tag{2.49}$$

where

$$\kappa = -\frac{N_0^2 k_x z_0}{2\omega^2}, \quad \mu = \frac{1}{2}. \tag{2.50}$$

Whittaker's equation has well known solutions denoted

$$q = C_1 M_{\kappa,\mu}(\eta) + C_2 W_{\kappa,\mu}(\eta), \tag{2.51}$$

where C_1, C_2 are constants. Although we have solved the governing equation exactly, it is instructive to also consider the case of slowly varying temperature (which has applications to the solar atmosphere and the magnetohydrodynamic case considered later), that is we assume $L \ll z_0$. Let $z = Lz^*$, $z^* \in [-1, 0]$, then the Brunt-Väisälä frequency can be written

$$N^2 = N_0^2\left(1 - \frac{Lz^*}{z_0}\right)^{-1} \approx N_0^2\left(1 + \frac{Lz^*}{z_0}\right) \quad \text{as} \quad \frac{L}{z_0} \ll 1. \tag{2.52}$$

Returning to the dimensional variable z, Equation (2.39) with the Brunt-Väisälä given by Equation (2.52) leads us to

$$\frac{\mathrm{d}^2 q}{\mathrm{d}z^2} = k_x^2\left(1 - \frac{N_0^2}{\omega^2}\left(1 + \frac{z}{z_0}\right)\right)q. \tag{2.53}$$

Making use of the variable substitution

$$\Theta = -\frac{1}{N_0^2}\left(\frac{k_x^2 N_0^2}{\omega^2 z_0}\right)^{\frac{1}{3}}\left(N_0^2(z + z_0) - \omega^2 z_0\right), \tag{2.54}$$

Equation (2.53) can be written

$$\frac{\mathrm{d}^2 q}{\mathrm{d}\Theta^2} - \Theta q = 0. \tag{2.55}$$

Equation (2.55) is Airy's equation, which has solutions

$$q = C_1 \mathrm{Ai}(\Theta) + C_2 \mathrm{Bi}(\Theta), \tag{2.56}$$

where Ai and Bi are the linearly independent Airy functions (see Abramowitz & Stegun, 1972). We note that while we are motivated here by standing waves in a cavity of length L, the solutions to the governing equation are not limited to this case. The solutions in terms of Whittaker functions represent general solutions, while the Airy functions are an approximation for a slowly varying medium.

We may also consider the case that the background temperature T_0 is constant. It is simple to show that when this is the case, the density and pressure profiles are

$$\rho_0(z) = \widehat{\rho_0} e^{-z/H}, \quad p_0(z) = \widehat{p_0} e^{-z/H}, \tag{2.57}$$

where H is the density scale height given by Equation (2.26). When the density and pressure are as above *i.e.*, Equations (2.57), the sound speed is constant. The Brunt-Väisälä frequency is also constant and given by

$$N^2 = \frac{g^2(\gamma - 1)}{c_s^2}. \tag{2.58}$$

The solution to Equation (2.39) is then

$$q = C_1 e^{\mathrm{i}\alpha z} + C_2 e^{-\mathrm{i}\alpha z}, \tag{2.59}$$

where

$$\alpha = k_x \left(\frac{N^2}{\omega^2} - 1 \right)^{\frac{1}{2}}. \tag{2.60}$$

We have solved the governing equation for q, that is, the amplitude of the waves. Let us now apply appropriate boundary conditions to determine the eigenfrequencies of the perturbations. Let us consider the case of slowly changing temperature, the solution of which is given by Equation (2.56). We are considering standing waves in a cavity of length L. The boundaries are fixed and perfectly reflecting. The boundary conditions for such a layer are

$$v_{1z}(0) = v_{1z}(-L) = 0, \tag{2.61}$$

or, in terms of q,

$$\left(\frac{q}{\rho_0} \right) \Big|_{-L} = \left(\frac{q}{\rho_0} \right) \Big|_{0} = 0. \tag{2.62}$$

Applying these boundary conditions to solution (2.56) gives two algebraic equations for the coefficients C_1, C_2

$$C_1 \mathrm{Ai}(\Theta_0) + C_2 \mathrm{Bi}(\Theta_0) = 0, \quad C_1 \mathrm{Ai}(\Theta_{-L}) + C_2 \mathrm{Bi}(\Theta_{-L}) = 0, \tag{2.63}$$

where Θ_0, Θ_{-L} denote Θ (Equation (2.54)) evaluated at $z = 0, -L$, respectively. For this system of equations to have a non-trivial solution (for the coefficients C_1 and C_2), the determinant must be zero. This condition gives the dispersion relation

$$\mathrm{Ai}(\Theta_0)\mathrm{Bi}(\Theta_{-L}) - \mathrm{Ai}(\Theta_{-L})\mathrm{Bi}(\Theta_0) = 0. \tag{2.64}$$

This equation cannot be inverted for the eigenfrequencies without some further simplification. The Boussinesq approximation is valid for large wavenumbers, hence we assume k to be large *i.e.* $k_x z_0 \gg 1$. This approximation is also very useful in the magnetic case. The wavenumber appears in Θ of order $(k_x z_0)^{\frac{2}{3}}$, *i.e.* Θ is large. An asymptotic expansion is therefore possible if $k_x z_0$ is sufficiently large. Let us make use of the asymptotic properties of the Airy functions (Abramowitz & Stegun, 1972),

$$\mathrm{Ai}(-z) \sim \pi^{-\frac{1}{2}} z^{-\frac{1}{4}} \sin\left(\zeta + \frac{\pi}{4}\right) + \ldots, \quad \mathrm{Bi}(-z) \sim \pi^{-\frac{1}{2}} z^{-\frac{1}{4}} \cos\left(\zeta + \frac{\pi}{4}\right) + \ldots, \quad z \to \infty, \tag{2.65}$$

where

$$\zeta = \frac{2}{3} z^{\frac{3}{2}}, \quad \text{and} \quad |\arg z| < \frac{2}{3}\pi. \tag{2.66}$$

Letting

$$\Theta = -\frac{1}{N_0^2}\left(\frac{k_x^2 N_0^2}{\omega^2 z_0}\right)^{\frac{1}{3}} \left(N_0^2 (z + z_0) - \omega^2 z_0\right) = -\widetilde{\Theta}, \tag{2.67}$$

we may write Equation (2.64) as

$$\pi^{-1}\Theta_0^{-\frac{1}{4}}\Theta_{-L}^{-\frac{1}{4}}\left[\sin\left(\zeta_0 + \frac{\pi}{4}\right)\cos\left(\zeta_{-L} + \frac{\pi}{4}\right) - \sin\left(\zeta_{-L} + \frac{\pi}{4}\right)\cos\left(\zeta_0 + \frac{\pi}{4}\right)\right] = \tag{2.68}$$

$$\pi^{-1}\Theta_0^{-\frac{1}{4}}\Theta_{-L}^{-\frac{1}{4}}\sin(\zeta_0 - \zeta_{-L}) = 0,$$

where

$$\zeta = \frac{2}{3}\widetilde{\Theta}^{\frac{3}{2}}. \tag{2.69}$$

Equation (2.68) implies

$$\zeta_0 - \zeta_{-L} = \frac{2}{3}\frac{1}{N_0^2}\left(\frac{k_x^2}{\omega^2 z_0}\right)^{\frac{1}{2}}\left[\left(z_0\left(N_0^2 - \omega^2\right)\right)^{\frac{3}{2}} - \left(N_0^2 z_0\left(1 + \frac{L}{z_0}\right) - \omega^2 z_0\right)^{\frac{3}{2}}\right] = n\pi. \tag{2.70}$$

Making use of the fact that $L/z_0 \ll 1$, we may Taylor expand (2.70) around $L/z_0 = 0$. Retaining the first term in L/z_0, the dispersion relation becomes

$$\omega^2 \approx \frac{k_x^2}{k_x^2 + \dfrac{n^2\pi^2}{L^2}} N_0^2. \tag{2.71}$$

A comparison to the local dispersion relation shows that the term $n\pi/L$ acts as a vertical "wavenumber". Equation (2.71) shows the familiar anti-Sturmian behaviour of internal gravity waves, that is, the eigenfrequencies decrease as n increases. Equation (2.71) is convenient for estimating the eigenfrequencies as it allows us to use the Brunt-Väisälä frequency evaluated at the top of the cavity. This is to be expected by the assumption of a slowly varying medium, this analysis, however, serves as justification.

We can also consider the case of constant sound speed (isothermal background temperature). We define the cavity to, again, be $z \in [-L, 0]$. The corresponding boundary conditions are again given by Equation (2.62). The solution (2.59) and boundary conditions (2.62) give the relations

$$C_1 e^{-\mathrm{i}\alpha L} + C_2 e^{\mathrm{i}\alpha L} = 0, \quad C_1 + C_2 = 0. \tag{2.72}$$

The determinant of this system of equations must be zero *i.e.*,

$$\sin(\alpha L) = 0 \tag{2.73}$$

or

$$\omega^2 = \frac{k_x^2}{k_x^2 + \dfrac{n^2\pi^2}{L^2}} N^2, \tag{2.74}$$

as expected. It can be shown that $N_0^2 = N^2 - g/z_0$, hence the eigenfrequencies are lower for the polytropic case than the isothermal case. That is, the effect of variable temperature is to slightly *decrease* the frequency of IGWs. This feature could be rather relevant for observational validation.

2.2.4 A Semi-infinite Polytrope

Consider a semi-infinite adiabatic polytrope, that is the case where the temperature varies linearly and the medium is such that $\gamma = 1 + 1/m$. When this is the case a fluid element is not subject to buoyancy and so g-modes are not present (the Brunt-Väisälä frequency is equal to zero). In such a model it can be shown that the frequency of p-modes satisfies the dispersion relation

$$\frac{\omega^2}{gk} = 1 + \frac{2n}{m}, \quad n = 1, 2, 3, \ldots. \tag{2.75}$$

For details on the derivation see Spiegel & Unno (1962), Christensen-Dalsgaard (1980), Campbell & Roberts (1989).

When the buoyancy effects are included ($\gamma \neq 1 + 1/m$), g-modes exist. Christensen-Dalsgaard (1980) considered the non-adiabatic case where both p-modes and g-modes exist. The starting point of this study was the full solution found by Lamb (1932). It is helpful to consider g-modes independent of p-modes, we employ the Boussinesq approximation to study these modes. The governing equation for the z-component of perturbed momentum, q, is

$$\omega^2 \frac{\mathrm{d}^2 q}{\mathrm{d}z^2} + k_x^2 \left(N^2 - \omega^2\right) q = 0, \tag{2.76}$$

having solution

$$q = C_1 e^{-\alpha/2} \alpha M(1-\kappa, 2, \alpha) + C_2 e^{-\alpha/2} \alpha U(1-\kappa, 2, \alpha), \tag{2.77}$$

where M and U are the Kummer functions and

$$\alpha = 2k_x(z - z_0), \quad \kappa = -\frac{k_x z_0 N_0^2}{2\omega^2}. \tag{2.78}$$

Note that we have defined the coordinate system such that the horizontal wave vector is in the x-direction, due to there being no preferred horizontal direction. We consider a closed atmosphere $z \in (-\infty, 0]$. The solutions are such that $q = 0$, at $z = 0$. Let us consider the asymptotic behaviour as $z \to -\infty$ (so $\alpha \to -\infty$). The Kummer functions have the properties

$$M(a, b, \sigma) \sim \frac{\Gamma(b)}{\Gamma(b-a)} e^{\mathrm{i}\pi a} \sigma^{-a} + \frac{\Gamma(b)}{\Gamma(a)} e^{\sigma} \sigma^{a-b}, \quad \text{for} \quad arg\,\sigma = \pi \tag{2.79}$$

$$U(a, b, \sigma) \sim \sigma^{-a}, \tag{2.80}$$

as $|\sigma| \to \infty$, where σ is a negative real variable (representing the argument of the Kummer functions). Using these properties we have

$$q \sim C_1 e^{-\alpha/2} \frac{\Gamma(b)}{\Gamma(b-a)} e^{\mathrm{i}\pi a} \alpha^{\kappa} + C_1 e^{-\alpha/2} \frac{\Gamma(b)}{\Gamma(a)} \alpha^{-2-\kappa} + C_2 e^{-\alpha/2} \alpha^{\kappa}. \tag{2.81}$$

As $\alpha \to -\infty$, the second term tends to 0, while the first and last terms tend to infinity. As a boundary condition we enforce the solution to stay regular as $z \to -\infty$. For this to be the case $C_2 = 0$ and $b - a$ is approximately 0 or a negative integer (so $e^{-\alpha/2}/\Gamma(b-a)$ does not increase without bound). That is

$$b - a = 1 + \kappa = 1 - \frac{k_x z_0 N_0^2}{2\omega^2} = -n, \quad n = 0, 1, 2, \ldots. \tag{2.82}$$

Rearranging gives

$$\omega^2 = \frac{k_x z_0 N_0^2}{2(1+n)}, \quad n = 0, 1, 2, \ldots. \tag{2.83}$$

These are the g-modes in an semi-infinite polytropic medium, analogous to the p-modes given by Equation (2.75). We see that the frequencies increase with k_x and decrease with n. The frequency also tends to 0 for $k \to 0$. Thus we see classic properties of g-modes. As in the case of the p-modes there are behaviours which are different to local (WKB) frequencies. The p-modes are not constrained to lie above the acoustic cut-off (when $k \to 0, \omega \to 0$) and do not act like sound waves in a homogeneous medium when $g \to 0$. The g-modes here have similar unexpected behaviours. Standing g-modes in a thin cavity are such that $\omega < N_0$, while here the solutions may or may not be less than N_0.

Note that flipping the coordinate system, for a comparison to other works, does not change the frequencies given above. To flip the system so that $z > 0$ and $z \to \infty$ is towards the solar centre, we apply the transformation $z_0 \to -z_0$. The Kummer U function tends to 0 as $z \to \infty$. To maintain regularity the condition is now $\Gamma(a) = -n$, which reproduces the frequencies (2.83) when κ is modified accordingly.

We have determined the frequencies of propagating and standing IGWs using the Boussinesq approximation. We found solutions (exact and approximate) to the governing equation of motion when the background is polytropic background. These solutions have, to our knowledge, not been derived previously. Expressions for the frequency of IGWs in a polytrope were found using these solutions. Magnetic fields are ubiquitous through the solar atmosphere and, as argued before, we must take into account their role in the dynamic processes at work as a next step. In the following chapter we consider the plasma to be embedded in a magnetic field. A comparison between the hydrodynamic and MHD problems will allow us to deduce the effect of a magnetic field on IGWs.

2.3 Magnetohydrodynamics

Magnetohydrodynamics is the study of electrically conducting fluids. The main application of MHD is to astrophysical and laboratory plasmas. MHD describes the fluid as a macroscopic continua *i.e.* there are a huge number of particles. The governing equations can be derived from a microscopic point of view, using kinetic theory, but they are equivalent to the MHD description. For a discussion of the theory of plasmas derived from a kinetic theory approach, see *e.g.* Choudhuri (1998), Goedbloed & Poedts (2004). When considering large length scales, such as in the Sun, the MHD description is much more useful than the kinetic description. Plasma is accurately described by MHD when the characteristic length scale is much greater than the mean free path. This condition implies that the motion of individual particles is negligible when considering the motion of the fluid as a whole. This is the continuum approximation. We assume that the velocities are much smaller than the speed of light, this means relativistic effects (including the displacement current in the Ampère-Maxwell law) are unimportant. We also assume quasi-neutrality; that is, the fluid may be considered to be electrically neutral. In the Sun these assumptions are valid to a high degree.

The governing equations for a fluid described by MHD consist of Maxwell's equations of electromagnetism, the momentum equation, the equation of conservation of mass (for a compressible fluid) and the conservation of entropy (for adiabatic motions). This is a system of eight coupled non-linear partial differential equations

$$\frac{\partial \mathbf{B}}{\partial t} = \nabla \times (\mathbf{v} \times \mathbf{B}) + \eta \nabla^2 \mathbf{B}, \quad \nabla \cdot \mathbf{B} = 0, \tag{2.84}$$

$$\frac{\partial \rho}{\partial t} = -\nabla \cdot (\rho \mathbf{v}), \tag{2.85}$$

$$\rho \left(\frac{\partial \mathbf{v}}{\partial t} + \mathbf{v} \cdot \nabla \mathbf{v} \right) = -\nabla p + \frac{1}{\mu} (\nabla \times \mathbf{B}) \times \mathbf{B} + \mathbf{F}, \tag{2.86}$$

$$\frac{\partial p}{\partial t} + \mathbf{v} \cdot \nabla p = -\gamma p \nabla \cdot \mathbf{v}, \tag{2.87}$$

where $\mathbf{B}$ is the magnetic field, $\mathbf{v}$ is the velocity field, ρ is the fluid density, p is the pressure and η, μ and γ are constants representing the magnetic diffusivity, magnetic permeability and the ratio of specific heats, respectively. $\mathbf{F}$ represents other forces that can be included such as gravity. The term $(\nabla \times \mathbf{B}) \times \mathbf{B}/\mu$ is the Lorentz force *i.e.* the force felt by a charged particle moving in a magnetic field. It is often convenient to decompose the Lorentz force into a magnetic tension and pressure force.

The above system of equations neglects viscosity, thermal conduction, radiation and rotation. There are many phenomena in the solar atmosphere where these effects play an important role. Other astrophysical and laboratory plasmas may be dominated by such effects. The MHD equations may be extended to include terms which represent these extra physical processes.

It should be noted that Maxwell's equations, in differential form, do not appear explicitly in the MHD equations (with the exception of $\nabla \cdot \mathbf{B} = 0$ which is treated as an initial condition for $\mathbf{B}$). The reason is that they have been combined with Ohm's law for a moving conductor, $\mathbf{E} + \mathbf{v} \times \mathbf{B} = \mu \eta \mathbf{j}$, to eliminate the electric field $\mathbf{E}$ and give one vector equation describing the evolution of the magnetic field - the induction equation, Equation (2.84). The set of equations (2.84) to (2.87) are collectively known as the MHD equations. The MHD equations show the key feature of MHD that gives the subject its complexity and beauty - the coupling between the momentum and induction equations. This means that the magnetic field determines the motion of the fluid which in turn feeds back to determine the magnetic field. For a further, more comprehensive, treatment of the MHD equations see *e.g.* Priest (2013) and Goedbloed & Poedts (2004).

It is useful to define a dimensionless quantity, the *magnetic Reynolds number*

$$Re_M = \frac{UL}{\eta}, \tag{2.88}$$

where U and L are the typical velocity and length scales of the flow respectively, and η is the magnetic diffusivity. Re_M is the ratio of the order of magnitude of the terms on the right hand side of the induction equation. Its value gives us an estimate of the effects of magnetic advection to magnetic diffusion. For very small values, $Re_M \ll 1$, diffusion dominates. This means that the magnetic field diffuses through the fluid as it moves. This is usually the case for laboratory plasmas due to the small length scales. For very large values, $Re_M \gg 1$, advection dominates. When this is the case the magnetic field lines are advected along by the fluid motion - we say that the magnetic field lines are "frozen" into the fluid (magnetic flux is conserved). This fact may be shown mathematically and is often referred to as Alfvén's theorem. This is the case, for example, in the Sun where we have very large length scales (although there are some very important exceptions). When $Re_M \gg 1$ we neglect the diffusive term in the induction equation. The MHD equations with diffusion (and viscosity, thermal conduction, radiation) neglected are known as the *ideal* MHD equations. The magnetic Reynolds number is named for its similarity to the Reynolds number in fluid dynamics which measures how important viscous effects are to the flow.

2.3.1 Magnetohydrodynamic Waves

Perturbations around some background state can give rise to *MHD waves*. This is the generalisation of hydrodynamic waves to MHD. We will see that perturbations in a homogeneous plasma, in the presence of a magnetic field, lead to not one, but three waves. Let us consider, for simplicity, that we have an infinite, homogeneous and time-independent background. This means that we do not include gravity and all background quantities are constant. We take small perturbations around this background. In addition to the hydrodynamic quantities, we also perturb the magnetic field

$$\mathbf{B}(\mathbf{r},t) = \mathbf{B}_0 + \mathbf{B}_1(\mathbf{r},t) \quad \text{where } |\mathbf{B}_1| \ll |\mathbf{B}_0|. \tag{2.89}$$

We also assume no background flows $\mathbf{v}_0 = 0$. We linearise the ideal MHD equations, as in Section 2.1, leading to

$$\rho_0 \frac{\partial \mathbf{v}_1}{\partial t} = -\nabla p_1 + \frac{1}{\mu}(\nabla \times \mathbf{B}_1) \times \mathbf{B}_0, \tag{2.90}$$

$$\frac{\partial \rho_1}{\partial t} = -\nabla \cdot (\rho_0 \mathbf{v}_1), \tag{2.91}$$

$$\frac{\partial \mathbf{B}_1}{\partial t} = \nabla \times (\mathbf{v}_1 \times \mathbf{B}_0), \quad \nabla \cdot \mathbf{B}_1 = 0, \tag{2.92}$$

$$\frac{\partial p_1}{\partial t} = -\gamma p_0 \nabla \cdot \mathbf{v}_1. \tag{2.93}$$

We have 8 equations with 8 unknowns and the solenoidal magnetic field condition (which is treated as an initial condition). We may write one component of the perturbed magnetic field in terms of the others through $\nabla \cdot \mathbf{B}_1 = 0$, hence we have 7 degrees of freedom and so

expect 7 eigenvalues. Some manipulation gives the wave equation for MHD waves in a homogeneous medium,

$$\frac{\partial^2 \mathbf{v}_1}{\partial t^2} - \left[\frac{1}{\mu\rho_0}(\mathbf{B}_0\cdot\nabla)^2\mathbf{I} + (v_A^2 + c_s^2)\nabla\nabla - \frac{1}{\mu\rho_0}\mathbf{B}_0\cdot\nabla(\nabla\mathbf{B}_0 + \mathbf{B}_0\nabla)\right]\cdot\mathbf{v}_1 = \mathbf{0}, \tag{2.94}$$

where

$$c_s^2 = \frac{\gamma p_0}{\rho_0} \quad \text{and} \quad v_A^2 = \frac{B_0^2}{\mu\rho_0}, \tag{2.95}$$

are the squares of the sound speed and Alfvén speed, respectively. Note that if we have no magnetic field, $\mathbf{B}_0 = 0$, the MHD wave equation reduces to the familiar equation for acoustic waves, as expected.

Next, we seek plane wave solutions. We assume the perturbations are proportional to $\exp(\mathrm{i}(\mathbf{k}\cdot\mathbf{r} - \omega t))$, where $\mathbf{k} = (k_x, k_y, k_x)$ is the wave vector, ω is the angular frequency and $\mathbf{r} = (x, y, z)$. This is possible as the background is homogeneous and so the properties of the wave do not change as it propagates. This turns the wave equation into an algebraic eigenvalue equation. We noted that there are 7 degrees of freedom, and so expect there to be 7 distinct eigenvalues *i.e.*, 7 different wave solutions. By assuming (without loss of generality) that $\mathbf{B}$ and $\mathbf{k}$ take the form $(0, 0, B_0)$ and $(k_\perp, 0, k_\parallel)$ for simplicity we find that we have non-trivial solutions to the eigenvalue equation when

$$(\omega^2 - k_\parallel^2 v_A^2)\left[\omega^4 - k^2(v_A^2 + c_s^2)\omega^2 + k_\parallel^2 k^2 v_A^2 c_s^2\right] = 0. \tag{2.96}$$

For a full derivation, refer to Goedbloed & Poedts (2004).

The solutions give our three MHD waves: the fast and slow magneto-acoustic waves (given by solving the quadratic in ω^2) and the Alfvén wave. The fast, slow and Alfvén modes represent orthogonal eignefunctions of the linear differential operator. The eigenfrequencies associated with the three MHD waves appear in the dispersion relation (2.96) as ω^2. This means there are two wave solutions for each of the MHD modes - waves propagating forward and backwards in space. There is another solution to the system of MHD equations corresponding to $\omega = 0$. This solution, known as the entropy wave, is lost when deriving the wave equation, Equation (2.94), but it can be shown to be a genuine solution to the system of linearised MHD equations (it is a perturbation to the entropy of the system which does not propagate). The entropy wave completes the spectrum of eigenvalues.

The Alfvén wave is a consequence of the magnetic field and the frozen flux condition solely; the restoring force is purely the magnetic tension component of the Lorentz force. The wave has frequency $\omega^2 = v_A^2 k_\parallel^2$ and propagates with group velocity equal to the Alfvén speed v_A along the magnetic field lines. Alfvén waves may not propagate perpendicular to the magnetic field. Energy is propagated parallel to the magnetic field only, that is the group velocity is in the direction of the magnetic field only. The perturbed velocity (and magnetic field, which is proportional to velocity) is perpendicular to the wave vector

($\mathbf{v}_1 \cdot \mathbf{k} = 0$); that is, Alfvén waves are incompressible, transverse waves. These waves were first predicted by Alfvén (1942). Alfvén waves have been observed in the solar atmosphere by Jess *et al.* (2009) (see also Mathioudakis, Jess & Erdélyi, 2013). There are numerous observations of Alfvén waves in laboratory experiments. Detections of Alfvén waves in laboratory plasmas include early reports by *e.g.* Lundquist (1949), Bostick & Levine (1952) and Lehnert (1954); and *e.g.* Alboussière *et al.* (2011), more recently. Berthold, Harris & Hope (1960) reported observations of Alfvén waves in the ionosphere following high-altitude nuclear detonations.

The fast and slow waves propagate with frequencies above and below the Alfvén frequency, respectively (the eigenfrequencies are well ordered). The frequencies are given by solving the quartic factor in Equation (2.96); the upper and lower roots corresponding to fast and slow waves, respectively. The key restoring forces are magnetic tension and pressure (kinetic and magnetic). The difference between the modes is the phase of the pressures: for fast modes the magnetic and kinetic pressures are in phase, whereas they are out of phase for slow modes. In homogeneous plasma, the group speeds are such that the fast wave propagates energy almost isotropically. The slow mode propagates most strongly along the field lines, but may transfer energy at some angle to the field. These properties often lead to the analogy that fast modes may be thought of as generalised sound waves with contributions from the magnetic field; while slow modes can be thought of as sound waves with strong guidance due to the magnetic field.

It is interesting to note some asymptotic properties of the magneto-acoustic modes. For $k_\perp$ fixed, the fast and slow waves are such that

$$\omega_f^2 = k_\perp^2\left(v_A^2 + c_s^2\right), \quad \omega_s^2 = 0 \quad \text{for} \quad k_\parallel = 0, \tag{2.97}$$

$$\omega_f^2 \to k_\parallel^2 \max(c_s^2, v_A^2) \quad \omega_s^2 \to k_\parallel^2 \min(c_s^2, v_A^2) \quad \text{for} \quad k_\parallel \to \infty. \tag{2.98}$$

When $k_\parallel$ is fixed,

$$\omega_f^2 = k_\parallel^2 \max(c_s^2, v_A^2), \quad \omega_s^2 = k_\parallel^2 \min(c_s^2, v_A^2) \quad \text{for} \quad k_\perp = 0, \tag{2.99}$$

$$\omega_f^2 \to \infty, \quad \omega_s^2 \to k_\parallel^2 \frac{v_A^2 c_s^2}{v_A^2 + c_s^2} \quad \text{for} \quad k_\perp \to \infty. \tag{2.100}$$

Note that there are no pure electromagnetic wave solutions (*i.e.*, light waves) to the linearised equations. This is a consequence of the displacement current being neglected in Maxwell's equations in the MHD approximation.

We can complicate matters by introducing specific geometry and inhomogeneity of the background quantities. In the solar atmosphere the magnetic field does not permeate the plasma in a uniform manner. Many solar phenomena, such as spicules, coronal loops, prominences, etc. are caused by localised, structured magnetic fields. MHD waves in a

structured magnetic field have been well studied, motivated in part by many observations of such waves in coronal loops. The theory of MHD waves in structured fields is given by *e.g.* Roberts (1981a,b), Edwin & Roberts (1983), Roberts, Edwin & Benz (1984), Roberts (2000), Ruderman & Erdélyi (2009) and Erdélyi, Hague & Nelson (2014), to name but a few articles. The properties of MHD waves are shown to depend very much on the geometry of the structure. In cylindrical geometry (a magnetic flux tube) for example, discussed in a review by Ruderman & Erdélyi (2009), the Alfvén wave manifests as a twisting of the tube while the magneto-acoustic waves are present as sausage, kink and flute modes. Kink waves displace the tube axis while sausage waves contract and expand the tube. There are many examples of observations of these MHD waves in the corona; for example, kink waves were observed by *e.g.* Aschwanden *et al.* (1999), Verwichte *et al.* (2004) (see Andries *et al.* , 2009, for a review). For a review of sausage modes, see *e.g* De Moortel (2009), Wang (2011).

Part of the appeal of studying MHD waves is their use as a diagnostic tool. Properties of the background medium such as density, temperature and the much sought after magnetic field may be inferred by measuring the waves and oscillations within solar structures. This practise is known as magneto-seismology. Magneto-seismology was suggested first by Uchida (1970) and Rosenberg (1970) and furthered by Roberts, Edwin & Benz (1984). Magneto-seismology has become a wide area of study in recent years; some examples include Nakariakov & Ofman (2001), Andries, Arregui & Goossens (2005), Erdélyi (2006b), Verth, Erdélyi & Jess (2008), and Erdélyi & Taroyan (2008).

In inhomogeneous plasma the properties of the modes are more subtle and complex. The plasma in the solar atmosphere should be considered to vary with space to give a realistic model. MHD waves in such plasmas has been well studied, motivated by observations of p-modes, although the theory is far from complete. Inhomogeneous plasmas have a rich theory due to the addition of additional physics such as resonant absorption (Goossens, Erdélyi & Ruderman, 2011), mode conversion (Zhugzhda & Dzhalilov, 1981, 1982) and phase mixing (Heyvaerts & Priest, 1983; Hood, Brooks & Wright, 2002). These are damping mechanisms in which the energy of the wave may be lost to the surrounding plasma. These mechanisms have been studied in an attempt to address the fundamental question of how the solar atmosphere is heated. So far, the specific mechanism (or combinations of mechanisms) responsible for heating the corona to its observed temperature has yet to be determined.

Inhomogeneity of the background plasma can be caused by, for example, gravity. We now consider the case of a gravitationally stratified plasma, embedded in a magnetic field. In the next section we discuss MHD waves where buoyancy plays a key role in the motion.

Chapter 3

Buoyancy-Driven Magnetohydrodynamic Waves

3.1 Introduction

Turbulent motions close to the visible solar surface may generate internal gravity waves (IGWs) that propagate through the lower solar atmosphere. IGWs have been observed by *e.g.* Komm, Mattig & Nesis (1991), Stodilka (2008) and Straus *et al.* (2008). Magnetic activity is ubiquitous throughout the solar atmosphere, so it is expected that the behaviour of IGWs is to be affected and modified.

Much of the previous work on MHD waves in a stratified fluid was motivated by observations of the interaction of p-modes with a magnetic field. This includes oscillations in sunspots. Oscillations with periods of 3 and 5 minutes have been reported in sunspots for some time. These signals were modelled as slow magneto-acoustic gravity modes in the low-β atmosphere above the sunspot. The generation mechanism of these slow waves was modelled by p-modes (or, more precisely, fast MHD modes in the high-β region), which undergo mode conversion into slow modes. For more on observations of sunspot oscillations see *e.g.* Bogdan & Judge (2006) and references therein.

The study of p-modes in a magnetic context has been well developed. Less attention has been paid to g-modes, observations of which are far less frequent in the solar atmosphere. This is partially due to the lower frequencies of the modes, which therefore require longer observing times. The fact that there are fewer observations of IGWs means that magnetic effects on these waves has not been well established empirically. One observational study by Straus *et al.* (2008) suggests that IGWs are not able to propagate within strong magnetic fields. Due to a lack of observational motivation, the theory of magnetic effects on g-modes has not been well developed analytically. In this chapter we study g-modes in a magnetic field in order to provide the theory which will be very useful when more observations are available.

In this chapter we investigate the role of a magnetic field on propagating and standing buoyancy oscillations in a gravitationally stratified medium. To do this, we make use of the Boussinesq approximation. A comparison between the hydrodynamic and magnetohydrodynamic cases allows us to deduce the effects due to a magnetic field. It is shown that the frequency of IGWs may depart significantly from the Brunt-Väisälä frequency, even for a weak magnetic field. The mathematical techniques employed in this chapter give a clearer picture of the situation which has previously been misinterpreted. New solutions are found for a polytropic density profile representing an upper interior or lower atmospheric density distribution. Expressions for the frequencies are derived. We then move onto a model which allows a more realistic depiction of the solar atmosphere. We primarily study a vertical magnetic field applicable to such phenomena as sunspots, pores etc. Some of this material is summarised in Hague & Erdélyi (2016). The case of a horizontal magnetic field, applicable to chromospheric canopy fields, is also studied. An observational test is urged to validate the theoretical findings.

Buoyancy has several other very important solar applications. The solar convection zone and so the granulation observed in the photosphere is a result of buoyancy. This

convective motion is the key to generating *p*-modes, the importance of which has been discussed, and in forming inter-granular magnetic structures.

An important area of study is that of flux emergence. The Sun's magnetic field is generated, through dynamo action, at the base of the convection zone. The magnetic field may form flux tubes which are subject to a buoyancy instability. These structures emerge from the solar photosphere, forming the many magnetic structures that dominate the solar atmosphere. The theory of this magneto-convection is outlined by *e.g.* Chandrasekhar (1961).

3.2 Wave Propagation in a Vertical Field

It is important to understand the wave processes in the solar atmosphere. There is plenty of evidence that the solar atmosphere contains structures which may be modelled as stratified plasma embedded in vertical magnetic fields. MHD waves in such structures (when stratification is along the magnetic field) are difficult to analyse. To gain some understanding of the situation we focus on MHD waves in the lower solar atmosphere where buoyancy plays a key role. With this knowledge we may measure and explain dynamic processes in the solar atmosphere.

It was shown by Straus *et al.* (2008) that IGWs are suppressed by a strong magnetic field. In this work we aim to determine the nature of IGWs in a magnetic environment. We aim to determine how the properties (*e.g.* frequency) of IGWs are modified by the presence of a magnetic field. In particular, we aim to determine how these changes (if any) scale with the magnetic field. Knowing such scaling may allow us to develop inversion techniques to determine the magnetic field present in such waveguides.

Let us now consider magntohydrodynamic (MHD) wave propagation, applicable to magnetically active regions such as pores and sunspots. It has already been observed that strong magnetic fields inhibit the propagation of IGWs (Straus *et al.* , 2008). We expect, however, that the weak magnetic fields found in the solar photosphere will also have some effect on IGWs. In particular, we aim to establish whether the frequencies of IGWs, present in a plasma embedded in a magnetic field, are effected. The magnetic field is vertical and uniform, $\mathbf{B}_0 = (0, 0, B_0)$. The linearised ideal MHD equations in the Cowling approximation, after some algebra, take the form

$$\left(\omega^2 + (c_s^2 + v_A^2)\frac{\partial^2}{\partial x^2} + v_A^2\frac{\partial^2}{\partial z^2}\right)\xi_x = \left(g - c_s^2\frac{\partial}{\partial z}\right)\frac{\partial \xi_z}{\partial x}, \tag{3.1}$$

$$\left(\omega^2 - g\gamma\frac{\partial}{\partial z} + c_s^2\frac{\partial^2}{\partial z^2}\right)\xi_z = \left(g(\gamma - 1) - c_s^2\frac{\partial}{\partial z}\right)\frac{\partial \xi_x}{\partial x}, \tag{3.2}$$

$$\left(\omega^2 + v_A^2\frac{\partial^2}{\partial z^2}\right)\xi_y = 0, \tag{3.3}$$

where we have Fourier analysed in time and introduced the Lagrangian displacement ξ such that

$$\mathbf{v}_1 = \frac{\partial \xi}{\partial t} = -\mathrm{i}\omega\xi. \tag{3.4}$$

These equations were first derived by Ferraro & Plumpton (1958) and have been widely applied. Equation (3.3) shows that the Alfvén wave, driven purely by magnetic tension, is decoupled from the system. Equations (3.1) and (3.2) govern the fast and slow magneto-acoustic gravity (MAG) waves which couple together in this model. Note that y-dependence has, again, been neglected. Exact solutions of this system, for the case of a constant background temperature, were found by Zhugzhda (1979) in terms of Meijer G-functions (or equivalently hypergeometric functions, as shown by Cally, 2001). Exact solutions for more complicated background states are not yet known.

Magnetohydrodynamic wave propagation, where the magnetic field is parallel to gravity has been studied by *e.g.* Ferraro & Plumpton (1958), MacDonald (1961), Syrovatskii & Zhugzhda (1968), Zhugzhda (1979), Hollweg (1979), Zhugzhda & Dzhalilov (1981, 1982), Zhukov (1985), Campos (1986), Zhukov & Efremov (1988), Moreno-Insertis & Spruit (1989), Hasan & Christensen-Dalsgaard (1992), Spruit & Bogdan (1992), Cally & Bogdan (1993), Cally, Bogdan & Zweibel (1994), Hindman, Zweibel & Cally (1996), Cally (2001), Zhukov (2002, 2005), Roberts (2006) and recently by Mather & Erdélyi (2016).

In this chapter we are primarily interested in buoyancy-driven motion and hence we neglect the effect of mode coupling as a first simplification. Our goal here is to derive analytical solutions to the governing equations, that may be used when buoyancy is the primary restoring force *i.e.* in the case of atmospheric g-modes. This motivates a different approach to the analysis than works focusing on mode conversion, *e.g.* Spruit & Bogdan (1992) and Cally & Bogdan (1993). Next, we derive the governing equation for buoyancy-driven motion.

Instead of using the full governing equations we may now derive a governing equation in the Boussinesq approximation. The linearised equations are

$$\nabla \cdot (\rho_0 \mathbf{v}_1) = 0, \tag{3.5}$$

$$\frac{\partial \rho_1}{\partial t} = \frac{N^2}{g}\rho_0 v_z, \tag{3.6}$$

$$\rho_0 \frac{\partial \mathbf{v}_1}{\partial t} = -\nabla p_1 - \nabla \frac{B_0 B_{1z}}{\mu} + \rho_1 \mathbf{g} + \frac{B_0}{\mu}\frac{\partial \mathbf{B_1}}{\partial z}, \tag{3.7}$$

$$\frac{\partial \mathbf{B_1}}{\partial t} = B_0 \frac{\partial \mathbf{v}_1}{\partial z} - \mathbf{B}_0 \nabla \cdot \mathbf{v}_1, \quad \nabla \cdot \mathbf{B}_1 = 0. \tag{3.8}$$

We may write a single equation for the z-component of perturbed momentum, $q = \rho_0 v_{1z}$, via the y-component of the curl of Equation (3.7). Eliminating the perturbed density and

magnetic field gives

$$\rho_0 v_A^2 \nabla^2 \frac{\partial}{\partial z}\left(\frac{1}{\rho_0}\frac{\partial q}{\partial z}\right) - \frac{\partial^2}{\partial x^2} N^2 q - \frac{\partial^2}{\partial t^2}\nabla^2 q = 0. \tag{3.9}$$

This is the governing equation for MHD perturbations in the Boussinesq approximation. The Boussinesq approximation has been applied to a vertical magnetic field by McKenzie & Axford (2000) who derived a simplified form of Equation (3.9).

We may now Fourier analyse Equation (3.9) in x and t,

$$\rho_0 v_A^2 \frac{\mathrm{d}^3}{\mathrm{d}z^3}\left(\frac{1}{\rho_0}\frac{\mathrm{d}q}{\mathrm{d}z}\right) + \omega^2 \frac{\mathrm{d}^2 q}{\mathrm{d}z^2} - \rho_0 v_A^2 k_x^2 \frac{\mathrm{d}}{\mathrm{d}z}\left(\frac{1}{\rho_0}\frac{\mathrm{d}q}{\mathrm{d}z}\right) + k_x^2\left(N^2 - \omega^2\right) q = 0. \tag{3.10}$$

Equation (3.10) describes buoyancy-driven MHD waves; there is also another wave solution of Equations (3.5) to (3.8) - the Alfvén wave. This corresponds to the x- and z-component of the curl of the momentum equation. The governing equation for Alfvén waves is

$$\left(\frac{\partial^2}{\partial t^2} - v_A^2 \frac{\partial^2}{\partial z^2}\right) v_y = 0. \tag{3.11}$$

This equation is decoupled from Equation (3.10), hence in a vertical field the Alfvén wave does not couple to internal gravity waves. This was not considered by McKenzie & Axford (2000) due to a cumbersome mathematical treatment of Equations (3.5) to (3.8). We find that Equation (3.10) is not easy to solve analytically. We will analyse Equation (3.10), via the WKB method, to study propagating waves.

3.2.1 Propagating Waves

For propagating waves we may perform a WKB analysis, as in the previous section, of Equation (3.10) to find the local dispersion relation

$$\omega^2 = v_A^2 k_z^2 + \frac{k_x^2}{k_x^2 + k_z^2} N^2. \tag{3.12}$$

The frequencies are plotted in Figure 3.1. We see that even for the case of a weak magnetic field, significant differences from the Brunt-Väisälä frequency are seen. The character of the solution may easily become magnetically dominated, the waves may therefore become high frequency as opposed to low frequency IGWs (although this is based on the specific values that the parameters take). In Figure 3.1 the frequencies are seen to increase as k_z increases, in contrast to the non-magnetic case. This is not a general property though as

$$\frac{\partial \omega^2}{\partial k_z^2} = v_A^2 - \frac{k_x^2}{\left(k_x^2 + k_z^2\right)^2} N^2, \tag{3.13}$$

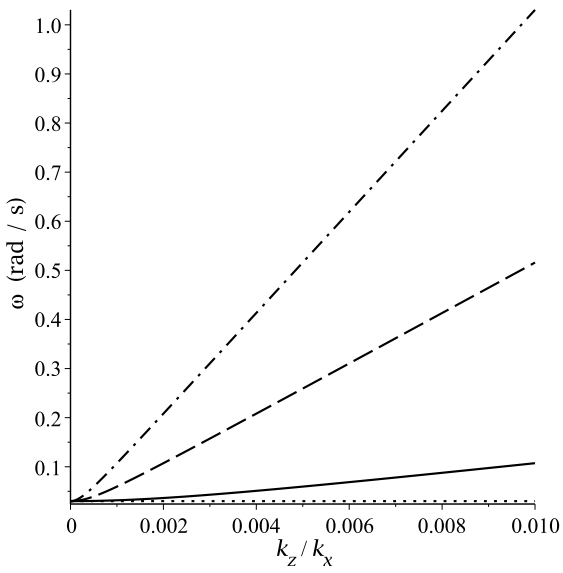

Fig. 3.1 A plot of frequencies (3.12) where $N_0 = 0.03\ \mathrm{s}^{-1}$, $\widehat{c_s} = 8\ \mathrm{km\ s}^{-1}$, $\beta = 50$. The solid line represents $k_x = 10\ \mathrm{km}^{-1}$, the dashed $k_x = 50\mathrm{km}^{-1}$ and the dot-dash $k_x = 100\ \mathrm{km}^{-1}$. The horizontal dotted line is the Brunt-Väisälä frequency N_0.

which may be positive or negative based on the parameters used. The local dispersion relation for Alfvén waves, found by a WKB analysis of Equation (3.3), is

$$\omega^2 = v_A^2 k_z^2. \tag{3.14}$$

The first term in Equation (3.12) resembles the frequency of an Alfvén wave and has lead to some authors labelling this wave as an Alfvén wave modified by gravity. This is not the case, as we have seen that the equation describing Alfvén waves is *decoupled* from the system of equations describing the wave given by the dispersion relation (3.12). This clarity owes to the elegance of using the components of the vorticity equation to derive the governing equations. To deduce what this wave is, in terms of the MHD spectrum, we note that the Boussinesq approximation is quasi-incompressible, *i.e.*, sound waves propagate at infinite phase speed. In a magnetic configuration, this corresponds to the plasma-β being large, where the plasma-β is defined by $\beta = \gamma c_s^2 / 2v_A^2$. The slow MHD mode, in the large horizontal wavenumber limit, propagates along the magnetic field lines with the phase speed c_T, where $c_T^2 = c_s^2 v_A^2 / (c_s^2 + v_A^2)$. In high-$\beta$ plasma, $c_T \approx v_A$, hence the first term in Equation (3.12) corresponds to a slow MHD mode propagating along the magnetic field lines. The absence of the fast MHD mode is due to the Boussinesq approximation, which corresponds to phase speed of the fast wave tending to infinity.

The implicit assumption of high-β plasma means that these results may be applied to regions of the Sun such as the upper interior or lower solar atmosphere, say the photosphere or low chromosphere. In the higher atmosphere, *i.e.* the solar corona, and in very strong magnetic structures in the lower atmosphere (low-β structures) the Boussinesq approximation, and so the previous result, is not applicable.

We have helped to clear up the picture of internal gravity waves in an MHD setting. We have shown that when a magnetic field is present, the internal gravity waves of hydrodynamics are slow MHD waves. Some previous authors have mistakenly identified internal gravity waves with Alfvén waves. This is important to recognize as Alfvén and slow waves are *orthogonal* eigenmodes of the MHD differential operator and hence are different and independent (in linear approximation). To gain a deeper understanding of system we should acknowledge the completeness of the spectrum of eigenmodes. Furthermore it is important to recognise the difference between the waves because they have different properties including: phase speed, group speed, polarisation, capability and capacity to carry energy, capability to dissipate, etc. A key difference in terms of energy transportation is that Alfvén waves carry energy along magnetic field lines while slow MHD waves may carry energy at an angle to the field lines. In the solar atmosphere, where the magnetic field is highly structured, these properties should be taken into account.

The buoyancy-driven slow MHD mode may have a phase speed greater than the Alfvén mode, hence the terminology "slow" may be misleading. If the Boussinesq approximation is not applied, there are two magneto-acoustic gravity (MAG) wave solutions. By taking limits of these solutions, equivalent to applying the Boussinesq approximation, the slow magneto-acoustic gravity solution tends to the buoyancy-driven solution we discuss here. Hence, the terminology "slow wave" makes sense in terms of limiting forms of MAG waves.

The dispersion relation, Equation (3.12), demonstrates the well known fact that a sufficiently strong magnetic field may inhibit convection. When the medium is unstable to convection, the square of the Brunt-Väisälä frequency is negative $N^2 < 0$. In a hydrodynamic system this implies that the eigenfrequency is complex; this is the convection instability. An example of such a model is that of a constant density and so a linear pressure profile. A magnetic field may stabilise the medium. This is the reason that sunspots are observed to be cooler than the surrounding medium.

Note also the well known property of IGWs that the vertical components of the phase and group velocities have opposing signs. This result may or may not persist in the case of buoyancy-driven slow MAG waves. We may calculate the vertical component of the group velocity, the velocity at which energy is transferred, to be

$$\omega_g \equiv \frac{\partial \omega}{\partial k_z} = \frac{k_z}{\omega}\left(-\frac{k_x^2}{\left(k_x^2+k_z^2\right)^2}N^2 + v_A^2\right). \tag{3.15}$$

We see that depending on the parameters, energy may be transferred parallel or antiparallel to the phase speed. In the limit of vanishing magnetic field, the group speed is negative. The magnetic field acts to oppose this. Depending on the character of the solution, we may expect either magnetism or buoyancy to be more dominant. In the lower solar atmosphere, the Brunt-Väisälä frequency is low hence the waves may transfer energy predominantly upwards. The character of the waves may be then said to be more of MHD waves modified

	$B_0(G)$			
k_z (km^{-1})	0	1	10	100
0.1	4.19	4.19	4.28	9.56
1	4.19	4.28	9.56	68.1
10	4.19	9.56	86.1	860

Table 3.1 The frequency, determined by Equation (3.12), at the base of the photosphere. The horizontal wavenumber is taken to be $k_x = 1\text{Mm}^{-1}$.

	$B_0(G)$			
k_z (km^{-1})	0	1	10	100
0.1	5.31	5.31	8.33	64.3
1	5.31	8.33	64.3	641
10	5.31	64.3	641	6410

Table 3.2 The frequency, determined by Equation (3.12), at the top of the photosphere. The horizontal wavenumber is taken to be $k_x = 1\text{Mm}^{-1}$.

by gravity than magnetic IGWs (although we stress that these are not independent solutions, rather the dominant character of the waves).

The connection between slow MHD waves and IGWs has been briefly commented upon by *e.g.* Hasan & Christensen-Dalsgaard (1992), Goedbloed & Poedts (2004) and Priest (2013); although here we present for the first time a detailed, rigorous demonstration of this fact. Using the starting point of the Boussinesq approximation, we are able to derive the correct governing equation and see explicitly the link between slow and internal gravity waves.

It is possible to derive the expressions (3.12) and (3.14) without rotating the coordinate system. When this is the case Equation (3.10) is unchanged (except k_x^2 is replaced by $k_x^2 + k_y^2$), while Equation (3.3) has a forcing term on the right hand side. This does not change the essential physics (a WKB analysis returns Equations (3.12) and (3.14)), but represents the displacement in the y-direction forcing Alfvén waves.

We expect to observe the waves in the lower solar atmosphere, *e.g.* the photosphere. In this region even plasma embedded in a strong magnetic field may be considered to be in the high-β regime. In Tables 3.1 and 3.2 we give the frequency (in mHz), determined by Equation (3.12), for a realistic solar atmosphere (the VAL-C model, Vernazza *et al.* , 1981). For simplicity, we use the expression for the Brunt-Väisälä frequency in an isothermal atmosphere $N^2 = g^2(\gamma - 1)/c_s^2$. Table 3.1 corresponds to the base of the photosphere ($z \approx 0$ km in the VAL-C model), where the plasma is such that the sound speed is $c_s \approx 8.5$ km s^{-1}. Table 3.2 expresses the frequencies at the top of the photosphere ($z \approx 500$ km) where $c_s \approx 6.7$ km s^{-1}. Many of these frequencies are well within current instrumental capabilities. The frequency is highly dependent on the vertical wavenumber; simulations or observational data is needed to determine the typical vertical wavelengths of magnetic IGWs in a realistic solar atmosphere. Note that the horizontal wavenumber is taken to be 1 Mm^{-1}, satisfying the large wavenumber criteria of the Boussinesq approximation.

Equation (3.12) predicts the frequencies that we expect to observe. The waves we discuss are quasi-incompressible so intensity variations are unlikely to be of use as an identifying tool. Doppler velocities and Stokes parameters are probably the key to observing these waves. Straus *et al.* (2008) were able to identify IGWs in the lower solar atmosphere using line of sight Doppler velocities. These were seen using lower solar atmospheric lines (Fe I 7090, Na I D1, Mg I b_2, Ni I 6764 lines) using the Interferometric Bidimensional Spectropolarimeter (IBIS, Cavallini, 2006) and Echelle spectrograph instruments at the Dunn Solar Telescope (DST) and the Michelson Doppler Imager (MDI, Scherrer *et al.* , 1995) onboard the Solar and Heliospheric Observatory (SOHO) spacecraft. In the hydrodynamic regime we expect a similar analysis to observe the waves. In the magnetic regime, this may not be applicable as periods may be too low, although this is based on the vertical wavelength. We suggest that a super-sensitive MDI-type of instrument could pick up such signals, or using magneto-optical filters (MOFs) at various heights (*e.g.* Na D2, the K lines, through the Ca I line could also be used).

There remains the question of how to distinguish magnetic IGWs from other wave modes. There should be no confusion with acoustic or fast MHD waves, as the frequency of such waves should be significantly different. The frequency of the magnetic IGWs (slow MHD waves) that we discuss is determined by the Alfvén frequency and the Brunt-Väisälä frequency, which are significantly less than the frequency of fast or p-modes in high-β plasma (where our results are applied, this region is the lower part of the solar atmosphere, *i.e.* the photosphere embedded in a magnetic field). The distinction between the Alfvén mode may be more difficult, based on instrumental capabilities, but in principle is possible. The frequency, as we have determined, is greater than the Alfvén frequency. When the magnetic field has a very small effect, the waves may be observed as almost pure IGWs (as in Straus *et al.* , 2008), the magnetic effect is seen by the deviation from the frequency of IGWs. Such deviations could be observed in Dopplergrams, known in helioseismology. Unfortunately, even a very weak magnetic field may cause the frequencies to become very close to the frequency of Alfvén waves. The frequency is not exactly the same, although the difference may be challenging to observe. A more significant difference may be observed in the phase and group velocities, expressions for which may be determined from Equation (3.12) with ease. When the waves take on a magnetic character, the distinction between Alfvén waves is in the velocity perturbations relative to the magnetic field. If one can determine the magnetic surfaces, the slow MHD waves may have velocity both parallel (the dominant component) and perpendicular to the magnetic field, while Alfvén waves have velocity only perpendicular, within constant magnetic surfaces. In Alfvén waves the perturbations are to the magnetic and velocity field components, and they would be out of phase. Observationally it is not easy to establish what the magnetic iso-surfaces are, but using for example Local Correlation Tracking (LCT) it is possible.

In this section we have confirmed that IGWs in a slowly varying medium embedded in a weak, vertical magnetic field are slow MHD waves. The frequencies of the oscillations

are modified by a term corresponding to a slow MHD wave. In the next section we will show that this is also the case for standing waves.

3.2.2 Standing Waves

It has been shown by Newington & Cally (2010) that a weak, vertical magnetic field has a tendency to refract and reflect upward propagating IGWs. This typically occurs below the region where the sound and Alfvén speeds are comparable. This fact, in addition to temperature variations in the low solar atmosphere may create some cavity in the photosphere/chromosphere where IGWs are trapped, leading to standing modes in the high-β medium.

It has been shown that when the magnetic field is weak and vertical, and the background temperature is constant, the frequencies of standing IGWs are modified. In this section we generalise this result to the case of a varying temperature.

To analyse buoyancy-driven MHD standing waves, we find it preferable to further simplify Equations (3.1) and (3.2) via the method of coordinate stretching (see *e.g.*, Roberts, 2006), which we outline here for reference. We take this approach as the governing equation in the Boussinesq approximation is still difficult to analyse analytically, even for simple background states. This method is equivalent to assuming large horizontal wavelength and so some analogy with the Boussinesq approximation may be drawn.

We are interested in vertical, buoyancy-driven motion *i.e.*, we wish to consider motion that is predominantly along the magnetic field lines. Let us introduce the scaling

$$x = \epsilon\bar{x}, \quad \xi_x = \epsilon\bar{\xi}_x, \quad z = \bar{z}, \quad \xi_z = \bar{\xi}_z, \quad \frac{\partial}{\partial x} = \frac{1}{\epsilon}\frac{\partial}{\partial \bar{x}}, \quad \frac{\partial}{\partial z} = \frac{\partial}{\partial \bar{z}}, \tag{3.16}$$

where ϵ is dimensionless and small, *i.e.*, $\epsilon \ll 1$. Substituting the scaled variables into Equations (3.1) and (3.2) leaves Equation (3.2) unchanged but (3.1) becomes

$$(c_s^2 + v_A^2)\frac{\partial^2 \bar{\xi}_x}{\partial \bar{x}^2} + \epsilon^2\left(\omega^2 + v_A^2\frac{\partial^2}{\partial \bar{z}^2}\right)\bar{\xi}_x = \left(g - c_s^2\frac{\partial}{\partial \bar{z}}\right)\frac{\partial \bar{\xi}_z}{\partial \bar{x}}. \tag{3.17}$$

Since $\epsilon \ll 1$, the term $O(\epsilon^2)$ can be neglected. Equation (3.17) can be integrated with respect to $\bar{x}$. Let us now return to the original, unscaled variables. Elimination of $\partial\xi_x/\partial x$ between Equations (3.2) and (3.17) leads us to

$$c_T^2\frac{\partial^2 \xi_z}{\partial z^2} - g\gamma\frac{c_T^4}{c_s^4}\frac{\partial \xi_z}{\partial z} + \left(\omega^2 - \frac{c_T^2}{v_A^2}\left(N^2 + \frac{g}{H}\frac{c_T^2}{c_s^2}\right)\right)\xi_z = 0. \tag{3.18}$$

Equation (3.18) is the governing equation for MHD buoyancy oscillations. The scaling (3.16) is equivalent to assuming that the horizontal *wavelength* of the perturbations is small (so the horizontal *wavenumber* is large), *i.e.*, taking the limit $k_x H \to \infty$. We can relate the horizontal wavenumber k_x to the azimuthal order l of spherical harmonics (for standing waves of the entire Sun) as $k_x^2 = l(l+1)/R_{\text{Sun}}^2$, where R_{Sun} is the radius of the Sun. The

assumption of large wavenumber implies that l is large, that is, the analysis performed here is applicable to waves trapped close to the solar surface. Large values of l also agree with the use of Cartesian coordinates. The spherical nature of the Sun can be neglected when the horizontal wavelength is small compared to the solar radius. It can be shown that Cartesian coordinates may be used when $l \gg 6$ (Pintér, 1999).

Note, if the magnetic field is absent from the model, $v_A = 0$, we have the dispersion relation $\omega^2 = N^2$. This is the well known dispersion relation for a fluid particle (displaced vertically from equilibrium) undergoing either simple harmonic motion due to buoyancy, or convection in the case of complex ω. This is the dispersion relation for internal gravity waves in the limit of large horizontal wavenumber.

Equation (3.18) is Equation (3.9) of Roberts (2006). This equation has also been derived previously by *e.g.* Moreno-Insertis & Spruit (1989) in the context of modelling convective motion in sunspots; and, it was also applied by *e.g.*, Hasan & Christensen-Dalsgaard (1992) to study MHD waves in a high-β approximation in an isothermal atmosphere. McDougal & Hood (2007) found approximate solutions to a simplified version of Equation (3.18) (where the cut-off and effects of buoyancy are neglected), using the WKB method for the case of large frequencies, in the analysis of mode conversion in an isothermal plasma.

We may Fourier analyse Equation (3.18) in the x direction,

$$c_T^2 \frac{\mathrm{d}^2\xi_z}{\mathrm{d}z^2} - g\gamma\frac{c_T^4}{c_s^4}\frac{\mathrm{d}\xi_z}{\mathrm{d}z} + \left(\omega^2 - \frac{c_T^2}{v_A^2}\left(N^2 + \frac{g}{H}\frac{c_T^2}{c_s^2}\right)\right)\xi_z = 0. \tag{3.19}$$

The assumption of normal modes is not absolutely necessary as we may solve the governing partial differential equation, Equation (3.18), for ξ_z in terms of z, with the dependence upon x acting as a parameter. In later work however, solving an ordinary differential equation is preferable for simplicity. Equation (3.19) is the governing equation we shall use to investigate the slow MAG wave. To gain a greater insight into the implications of the coordinate stretching it is useful to consider the total pressure perturbation P_T defined by

$$P_T = p_1 + \frac{\mathbf{B}_0 \cdot \mathbf{B}_1}{\mu}. \tag{3.20}$$

The linear MHD equations (with gravity included) allow us to write an expression for P_T,

$$P_T = g\rho_0\xi_z + \rho_0 v_A^2 \frac{\mathrm{d}\xi_z}{\mathrm{d}z} - \rho_0\left(c_s^2 + v_A^2\right)\nabla\cdot\xi. \tag{3.21}$$

After using the coordinate stretching (3.16), Equation (3.17) gives us a relationship between ξ_x and ξ_z (after neglecting the terms $O(\epsilon^2)$),

$$\mathrm{i}k(c_s^2 + v_A^2)\xi_x = \left(g - c_s^2\frac{\mathrm{d}}{\mathrm{d}z}\right)\xi_z. \tag{3.22}$$

This latter relation combined with Equation (3.21) shows that $P_T = 0$ (*i.e.*, P_T is $O(\epsilon^2)$). We therefore conclude that the primary restoring forces driving the motion are gravitational

forces (buoyancy and weight) and magnetic tension. This removal of the pressure term is analogous to removal of compressive terms in the Boussinesq approximation.

Let us consider a temperature profile that increases linearly with depth, given by Equation (2.43). The density and pressure are given by Equation (2.44). The square of the sound and Alfvén speeds take the form

$$c_s^2 = \widehat{c}_s^2\left(1 - \frac{z}{z_0}\right), \quad v_A^2 = \widehat{v}_A^2\left(1 - \frac{z}{z_0}\right)^{-m}, \tag{3.23}$$

where $\widehat{c}_s^2$ and $\widehat{v}_A^2$, the value of sound and Alfvén speed squared at $z = 0$, are constants. The Brunt-Väisälä frequency is as in the hydrodynamic case, given by Equation (2.45).

A polytropic model has been considered before by *e.g.* Scheuer & Thomas (1981), Spruit & Bogdan (1992), Cally & Bogdan (1993), Cally, Bogdan & Zweibel (1994), Hindman, Zweibel & Cally (1996) and Zhukov (2002, 2005) although it has not been studied as extensively as an isothermal model. Scheuer & Thomas (1981) investigated numerically a sunspot model, in cylindrical coordinates, constructed from a polytropic layer and two isothermal layers. They found the resonant frequencies and energy density for forced oscillations modelling forcing by overstable convection. Free oscillations were considered when the motion parallel to the background magnetic field is neglected. Many of the previous works have been motivated by oscillations in sunspots and the mode conversion of magnetically modified p-modes (fast MHD modes) into slow MHD modes.

Let us make a note when $\beta = \gamma/2$, Equations (3.1) and (3.2) are difficult to analyse due to mode coupling in this case. Spruit & Bogdan (1992) considered mode conversion of magnetically modified p-modes (fast MHD modes) into slow MHD modes in a polytropic density profile. Cally & Bogdan (1993) extended the work of Spruit & Bogdan (1992), finding Frobenius series solutions around $z = 0$ and $z \to -\infty$. These results were then compared to numerical solutions. They found that the eigenfrequencies were complex, indicating wave damping in the context considered. These works are motivated by the observed damping of p-modes in sunspots; mode conversion as a mechanism for the damping was suggested. The mathematical models of the MAG perturbations had the slow and fast modes coupled except in the asymptotic behaviour $z \to \infty$. Hindman, Zweibel & Cally (1996) added an isothermal atmosphere (where mode conversion occurred) to the model studied by Cally & Bogdan (1993) to investigate the effect of a vertical magnetic field on p-modes. It was shown that the damping of p-modes due to coupling of fast and slow MHD modes is smaller than the observed damping, suggesting other damping mechanisms are at play. Mode conversion in a two-layer model was also investigated by Cally, Bogdan & Zweibel (1994). These studies neglected the effects of buoyancy by considering a neutrally stable medium ($m = 3/2$).

The previous works were extended by Zhukov (2002, 2005). Conversion of fast to slow modes in a sunspot umbra (modelled by a vertical field) was studied numerically in a model consisting of a polytopic layer and a layer that represents the chromosphere

and corona. This work improved on the previous by not using $m = 3/2$ and by finding an asymptotic solution for the high-β polytrope to use with the numerical simulations. It was found that in the high-β polytrope, the system may be described by gravitationally modified acoustic modes and slow MHD modes. The asymptotic solutions, however, may not be used to analyse g-modes as the slow mode had no contribution due to buoyancy. This was due to no assumption being made on the wavenumber, hence buoyancy effects were not included. To study the g-modes in detail then, we must find solutions that include the relevant effects.

On the other hand, a low-β polytropic profile was studied by Syrovatskii & Zhugzhda (1968), when analysing the effect of a strong vertical magnetic field on convection. The vertical wave motion was found to be described by Bessel functions.

Let us now make the assumption of high-β plasma, in accordance with the Boussinesq approximation. A high value of β (*i.e.* a "hot" and dense plasma, such that the kinetic pressure is dominant) implies $v_A^2 \ll c_s^2$ and so $c_T^2 \approx v_A^2$. Under this assumption Equation (3.19) becomes

$$v_A^2 \frac{\mathrm{d}^2 \xi_z}{\mathrm{d}z^2} + \left(\omega^2 - N^2\right)\xi_z = 0. \tag{3.24}$$

This is a Sturm-Liouville type problem in contrast to the anti-Sturmian hydrodynamic case. The Brunt-Väisälä frequency now plays the role of the lower cut-off frequency, that is, there is only wave propagation if $\omega^2 > N^2$. If $N^2 > \omega^2$ the waves are evanescent.

Now, substituting the expressions (3.23) and (2.45) for v_A^2 and N^2 into (3.24), we obtain the governing equation for longitudinal MHD wave propagation in a polytropic high-β plasma

$$\widehat{v}_A^2 \frac{\mathrm{d}^2 \xi_z}{\mathrm{d}z^2} + \left[\omega^2 \left(1 - \frac{z}{z_0}\right)^m - N_0^2 \left(1 - \frac{z}{z_0}\right)^{m-1}\right]\xi_z = 0. \tag{3.25}$$

To solve Equation (3.25) analytically one needs to make further simplification. We reduce the complexity of Equation (3.25) when the temperature varies slowly throughout the medium. In this approximation we find that the resulting governing equation can be solved analytically, in terms of special functions.

Here, we consider standing waves in a cavity of thickness L, *i.e.*, $z \in [-L, 0]$. Now, we assume that the thickness of the cavity is much smaller than the temperature scale-height, $L \ll z_0$ (*i.e.*, the temperature changes slowly throughout the cavity). This assumption is relevant for a thin layer close to the solar surface, and so complements the scaling (3.16) in deriving the governing equation. If we introduce a new variable, z^*, such that $z = Lz^*$ where $z^* \in [-1, 0]$, we can rewrite equation (3.25) as

$$\frac{\widehat{v}_A^2}{L^2} \frac{\mathrm{d}^2 \xi_z}{\mathrm{d}z^{*2}} + \left[\omega^2 \left(1 - \frac{z^* L}{z_0}\right)^m - N_0^2 \left(1 - \frac{z^* L}{z_0}\right)^{m-1}\right]\xi_z = 0. \tag{3.26}$$

Next, we Taylor expand the above equation for small L/z_0, as $L/z_0 \ll 1$ by assumption. To first order in L/z_0 this is

$$\frac{\widehat{v}_A^2}{L^2}\frac{\mathrm{d}^2\xi_z}{\mathrm{d}z^{*2}} + \left[\left(\omega^2 - N_0^2\right) - \left(\omega^2 m - N_0^2(m-1)\right)\frac{z^* L}{z_0}\right]\xi_z = 0, \tag{3.27}$$

or, returning to the dimensional variable z in favour of z^*

$$\widehat{v}_A^2\frac{\mathrm{d}^2\xi_z}{\mathrm{d}z^2} + \left[\left(\omega^2 - N_0^2\right) - \left(\omega^2 m - N_0^2(m-1)\right)\frac{z}{z_0}\right]\xi_z = 0. \tag{3.28}$$

The transformation

$$Q = \left(\frac{1}{\widehat{v}_A^2 z_0}\right)^{1/3}\left(N_0^2(m-1) - m\omega^2\right)^{-2/3}\left[\omega^2(mz - z_0) + N_0^2(z_0 + z(1-m))\right] \tag{3.29}$$

turns equation (3.28) into

$$\frac{\mathrm{d}^2\xi_z}{\mathrm{d}Q^2} - Q\xi_z = 0. \tag{3.30}$$

This is, again, Airy's equation having well known solutions of the form

$$\xi_z = C_1\mathrm{Ai}(Q) + C_2\mathrm{Bi}(Q). \tag{3.31}$$

If we choose to not make the assumption of plane waves in the horizontal direction, the solution to the partial differential equation is given by solution (3.31) where C_1 and C_2 are not constant, but arbitrary functions of x. The Airy functions have the property that they are spatially oscillatory for $Q < 0$. When $Q > 0$, Ai decays while Bi tends to infinity. The transition from wave propagation to evanescent or unstable behaviour occurs when $Q = 0$. Equations (3.28) and (3.29) show that the condition $Q = 0$ is equivalent to

$$\omega^2(mz - z_0) + N_0^2(z_0 + z(1-m)) = 0, \tag{3.32}$$

this implies a critical value of z, *i.e.*,

$$z_{\text{critical}} = \frac{\left(\omega^2 - N_0^2\right)z_0}{\left(m\omega^2 - N_0^2(m-1)\right)}, \tag{3.33}$$

where $z_{\text{critical}} \notin [-L, 0]$ unless $N_0^2(1-1/m) < \omega^2 < N_0^2$ or $N_0^2 < \omega^2 < N_0^2(1-1/m)$. If we assume $\omega^2 > N_0^2$ and $m > 1$ then $Q < 0$ and, so, the solution (3.31) is spatially oscillatory.

It should be stressed that the above is not limited to standing waves. The eigenfunctions are not only valid for a fixed cavity, but may describe the motion so long as the medium may be considered to be slowly varying. The parameter L then represents the vertical length scale of the motion. When $L/z_0 \ll 1$, the above eigenfunctions may be used. A fixed cavity satisfies this, although it is not the sole application.

Note that Equation (3.19) also describes the well known behaviour of the slow MAG wave in a strong magnetic field. For low plasma-β (a strong magnetic field in a "cold" and rarefied plasma) $c_s^2 \ll v_A^2$ and so $c_T^2 \approx c_s^2$. Equation (3.19) can be written

$$c_s^2 \frac{\mathrm{d}^2 \xi_z}{\mathrm{d}z^2} - g\gamma \frac{\mathrm{d}\xi_z}{\mathrm{d}z} + \omega^2 \xi_z = 0. \tag{3.34}$$

We recognise the governing equation as a description of vertically acoustic waves in a gravitationally stratified medium (*e.g.*, Lamb, 1932; Whitham, 1973). Roberts (2006), for example, notes that in a strong field slow MAG waves take the form of sound waves propagating along the, rigid, magnetic field lines. This accounts for the absence of magnetic terms in Equation (3.34), *i.e.,* terms containing v_A. It should be noted that Equation (3.19) can actually be solved exactly for the case of an isothermal background without making an a priori assumption on the plasma-β although the solution is complicated (see next section).

We consider now standing waves in a cavity of length L. We assume the boundaries of the cavity to be perfectly reflecting. As in the hydrodynamic case, reflection can occur due to an abrupt change in the background, see *e.g.* Scheuer & Thomas (1981). Slow waves may also be reflected in a region where the Alfvén and sound speeds are equal, due to mode conversion (Zhugzhda & Dzhalilov, 1984). As mentioned in the previous section, this work is restricted to the case of a weak magnetic field hence there is no region in which mode conversion can occur.

We are considering a standing wave problem in a finite cavity

$$\xi_z(-L) = \xi_z(0) = 0. \tag{3.35}$$

The desired dispersion relation is

$$\mathrm{Ai}(Q_{-L})\mathrm{Bi}(Q_0) - \mathrm{Ai}(Q_0)\mathrm{Bi}(Q_{-L}) = 0, \tag{3.36}$$

where Q_0 and Q_{-L} are $Q|_{z=0}$ and $Q|_{z=-L}$.

This equation is highly transcendental and cannot be solved easily for ω, which appears implicitly in Q_0, Q_{-L}. We can probe some information by noting that the parameter z_0 is large in comparison to L *i.e.*, the lower medium has slow temperature variation. Using the variable z^*, defined earlier, we note that Q is of order $(z_0/L)^{2/3}$ in the large parameter z_0/L. An asymptotic expansion around large Q is therefore possible. Letting

$$Q_0 = -\widetilde{Q}_0, \quad Q_{-L} = -\widetilde{Q}_{-L}, \tag{3.37}$$

where, for spatially oscillating solutions, $\widetilde{Q}_0$, $\widetilde{Q}_{-L} > 0$. The asymptotic expansions (2.65) allow Equation (3.36) to be rewritten

$$\pi^{-1}\widetilde{Q}_0^{-1/4}\widetilde{Q}_{-L}^{-1/4}\left(\sin\left(\zeta_0+\frac{\pi}{4}\right)\cos\left(\zeta_{-L}+\frac{\pi}{4}\right)-\sin\left(\zeta_{-L}+\frac{\pi}{4}\right)\cos\left(\zeta_0+\frac{\pi}{4}\right)\right)$$

$$= \pi^{-1} \widetilde{Q}_0^{-1/4} \widetilde{Q}_{-L}^{-1/4} \sin(\zeta_0 - \zeta_{-L}) = 0, \tag{3.38}$$

where

$$\zeta_0 = \frac{2}{3} \widetilde{Q}_0^{3/2}, \quad \zeta_{-L} = \frac{2}{3} \widetilde{Q}_{-L}^{3/2}. \tag{3.39}$$

Equation (3.38) implies

$$\zeta_0 - \zeta_{-L} = \frac{2}{3} \left(\frac{1}{\widetilde{v}_A^2 z_0} \right)^{1/2} z_0^{3/2} \left(N_0^2 (m-1) - m\omega^2 \right)^{-1} \times$$

$$\left[\left(\omega^2 - N_0^2 \right)^{3/2} - \left(\omega^2 \left(1 + m \frac{L}{z_0} \right) - N_0^2 \left(1 - (1-m) \frac{L}{z_0} \right) \right)^{3/2} \right] = n\pi. \tag{3.40}$$

This is an algebraic equation in ω although it still cannot be solved exactly analytically. We can, however, solve Equation (3.40) if we Taylor expand around the small parameter L/z_0. We retain only the first term in L/z_0. The frequencies can then be expressed as

$$\omega^2 = \frac{n^2 \pi^2 \widetilde{v}_A^2}{L^2} + N_0^2. \tag{3.41}$$

These are asymptotic approximations of the eigenfrequencies of the interior. Equation (3.41) is useful for estimating the frequencies as it used only the values of v_A and N evaluated at $z = 0$. The frequency consists of a magnetic contribution modifying the Brunt-Väisälä frequency. Based on photospheric measurements of the Brunt-Väisälä frequency (Komm *et al.*, 1991), the frequencies are low for small n. Figure 3.2 plots values of ω against n for typical photospheric parameters. The sound speed, at $z = 0$, is taken to be 8 km s^{-1}, and $L = 500$ km corresponding to a relatively thin layer in the upper interior/photosphere. Figure 3.2 shows that higher values of β (a smaller Alfvén speed for fixed sound speed) return lower frequencies, as is expected due to the lower phase speed of the wave. For small n the character is that of an internal gravity wave, as the magnetic field is weak by assumption. When n increases sufficiently the Brunt-Väisälä term is negligible; the curve of ω against n behaves linearly. This represents the magnetic restoring forces dominating the gravitational one. Note the Sturmian behaviour of slow MAG in contrast to the anti-Sturmian behaviour of non-magnetic internal gravity waves.

Note also that for the case of an isothermal, high-β plasma, Hasan & Christensen-Dalsgaard (1992) solved Equation (3.24) in terms of Bessel functions. A dispersion relation for standing waves may be inverted by assuming the frequency, appropriately non-dimensionalised, is large. When the medium is assumed to vary slowly, the square of the eigenvalues of the isothermal medium may be expressed in the same form as Equation (3.41). A comparison of this analysis to the isothermal case shows that a slowly varying temperature does not change the form of the equation for frequency. This is not a surprising result, but it can now be applied with confidence. The polytropic Brunt-Väisälä frequency N_0 is smaller than the isothermal Brunt-Väisälä frequency, the frequency of

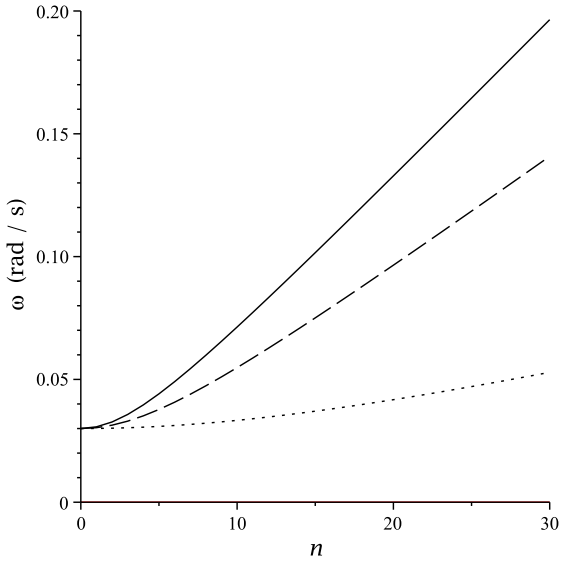

Fig. 3.2 A plot of frequencies (3.41) where $L = 500$ km, $N_0 = 0.03$ s^{-1}, $\widehat{c_s} = 8$ km s^{-1}. The solid line represents $\widehat{\beta} = 50$, the dashed $\widehat{\beta} = 100$ and the dotted $\widehat{\beta} = 1000$.

the magnetically modified IGW is then decreased by the changing temperature as in the non-magnetic case.

We have determined the eigenfunctions for the case of slowly varying temperature. The layer here is representative of a thin layer in the lower solar atmosphere. The eigenfunctions determined may be used, via appropriate boundary conditions, to establish the eigenfrequencies of buoyancy-driven oscillations. In this way we provide a theoretical underpinning for small-scale waves in the solar atmosphere.

We can also investigate the effect of different boundary conditions. For the case of a constant temperature, the effect of zero-gradient boundary conditions was analysed by Banerjee, Hasan & Christensen-Dalsgaard (1995). The analysis was carried out using a perturbation series approach based on the exact solutions derived by Zhugzhda (1979). It was shown that there exists a mode termed the gravitationally modified Lamb mode. The zero velocity gradient boundary conditions imply anti-nodes at the ends of the cavity. The modes are standing waves as in the rigid wall boundary conditions. Let us apply zero velocity gradient boundary conditions to our polytropic model. We apply zero velocity gradient to each boundary

$$\frac{\mathrm{d}v_z}{\mathrm{d}z} = 0 \quad \text{at} \quad z = -L, 0. \tag{3.42}$$

Applying this to the solution we have non-trivial solutions when

$$\mathrm{Ai}'(Q_0)\mathrm{Bi}'(Q_{-L}) - \mathrm{Ai}'(Q_{-L})\mathrm{Bi}'(Q_0) = 0. \tag{3.43}$$

We may use the asymptotic expansions for large negative argument (assuming $\omega > N_0$) to simplify the dispersion relation to

$$\pi^{-1}\widetilde{Q}_0^{\frac{1}{4}}\widetilde{Q}_{-L}^{1}4\sin(\zeta_0-\zeta_{-L})=0, \tag{3.44}$$

where $\widetilde{Q}=-Q$, $\zeta=(2/3)\widetilde{Q}^{3/2}$. The eigenmodes are then given by solving $\zeta_0-\zeta_{-L}=n\pi$. Taylor expanding this expression we may approximate the eigenfrequncies as

$$\omega^2 \approx \frac{n^2\pi^2\widetilde{v}_A^2}{L^2}+N_0^2. \tag{3.45}$$

This approximate solution is exactly the same as the rigid boundaries, and so the change in boundary conditions has no effect on the frequencies. The Lamb mode as described by Hasan & Christensen-Dalsgaard (1992) and Banerjee, Hasan, & Christensen-Dalsgaard (1995) is a limiting form of a sound wave and is not present in our analysis to the "removal" of compressive effects.

Let us consider the case of an open boundary and a closed boundary. We choose the closed boundary to be the lower boundary and the open to be the upper boundary,

$$v_z=0 \quad \text{at} \quad z=-L, \qquad \frac{\mathrm{d}v}{\mathrm{d}z}=0 \quad \text{at} \quad z=0. \tag{3.46}$$

Applying these boundary conditions gives us the dispersion relation

$$\mathrm{Ai}(Q_{-L})\mathrm{Bi}'(Q_0)-\mathrm{Bi}(Q_{-L})\mathrm{Ai}'(Q_0)=0. \tag{3.47}$$

An asymptotic expansion of the dispersion relation, using the well known asymptotic expressions for Airy functions, leads to

$$\pi^{-1}\widetilde{Q}_{-L}^{-\frac{1}{4}}\widetilde{Q}_0^{\frac{1}{4}}\cos(\zeta_0-\zeta_{-L})=0. \tag{3.48}$$

Hence, the eigenfrequencies are solutions to

$$\zeta_0-\zeta_{-L}=\frac{2n-1}{2}\pi, \quad n=1,2,3,\ldots, \tag{3.49}$$

that is,

$$\frac{2}{3}\left(\frac{1}{\widetilde{v}_A^2 z_0}\right)^{\frac{1}{2}} z_0^{\frac{3}{2}}\left(N_0^2(m-1)-m\omega^2\right)^{-1}\times \tag{3.50}$$

$$\left\{\left(\omega^2-N_0^2\right)^{\frac{3}{2}}-\left[\omega^2\left(1+\frac{mL}{z_0}\right)-N_0^2\left(1-\frac{L}{z_0}(1-m)\right)\right]^{\frac{3}{2}}\right\}=\frac{2n-1}{2}\pi.$$

Taylor expanding this expression, as in the case of rigid and zero-gradient boundary conditions, around $L/z_0 = 0$ to first order, the frequencies may be approximated as

$$\omega^2 \approx N_0^2 + \frac{\widehat{v}_A^2 \pi^2 (2n-1)^2}{4L^2}, \quad n = 1, 2, 3, \ldots. \tag{3.51}$$

These are the analytical expressions for the frequencies for the case of mixed boundary conditions. A comparison to the case of rigid boundary conditions shows that the effect of letting one boundary be open is the same as the case of an oscillating taut string. There is a node at the lower boundary and an anti-node at the upper boundary, hence the cavity allows odd multiples of half a wavelength.

It can be shown that inverting the cavity so that the bottom boundary is open and the upper is closed does not change the frequencies despite the temperature asymmetry. The dispersion relation for this case is

$$\mathrm{Ai}(Q_0)\mathrm{Bi}'(Q_{-L}) - \mathrm{Bi}(Q_0)\mathrm{Ai}'(Q_{-L}) = 0. \tag{3.52}$$

The approximate frequencies are the same as those given by Equation (3.47).

The approximations made when deriving Equation (3.19) lend themselves naturally to consider waves trapped close the solar surface, as investigated in the previous section. The coordinate stretching may also be used to model a larger cavity, provided that $k_x H$ is still large. When this is the case the assumption of slowly varying temperature, $z_0 \gg L$, is unlikely to be valid. In this subsection, we choose a cavity such that the assumption $L \gg z_0$ is applicable. A layer with rapidly varying temperature is representative of a deeper layer in the lower solar atmosphere than was considered in the previous subsection. The governing equation (3.25), in terms of the dimensionless variable z^* is, again,

$$\frac{\widehat{v}_A^2}{L^2}\frac{\mathrm{d}^2\xi_z}{\mathrm{d}z^{*2}} + \left[\omega^2\left(1 - \frac{z^*L}{z_0}\right) - N_0^2\right]\left(1 - \frac{z^*L}{z_0}\right)^{m-1}\xi_z = 0. \tag{3.53}$$

Making use of the binomial theorem, the coefficient of ξ_z can now be expressed as an asymptotic series

$$\left[\omega^2\left(1 - \frac{z^*L}{z_0}\right) - N_0^2\right]\left(1 - \frac{z^*L}{z_0}\right)^{m-1} \sim \omega^2\left(\frac{-Lz^*}{z_0}\right)^m$$

$$+\left(m\omega^2 - N_0^2\right)\left(\frac{-Lz^*}{z_0}\right)^{m-1} + O\left(\left(\frac{L}{z_0}\right)^{m-2}\right) \quad \text{as} \quad \frac{L}{z_0} \to \infty. \tag{3.54}$$

We retain only the first (*i.e.* the dominant) term in the asymptotic series. After returning to dimensional coordinates, the governing equation becomes

$$\widehat{v}_A^2\frac{\mathrm{d}^2\xi_z}{\mathrm{d}z^2} + \omega^2\left(\frac{-z}{z_0}\right)^m\xi_z = 0. \tag{3.55}$$

The transformation

$$\alpha = -\left(\frac{\omega z_0}{\widehat{v}_A\,(2+m)}\right)^2\left(-\frac{z}{z_0}\right)^{2+m} \tag{3.56}$$

allows us to rewrite Equation (3.55) as

$$\alpha\frac{\mathrm{d}^2\xi_z}{\mathrm{d}\alpha^2} + \frac{1+m}{2+m}\frac{\mathrm{d}\xi_z}{\mathrm{d}\alpha} - \xi_z = 0, \tag{3.57}$$

which has general solutions

$$\xi_z = C_1\,{}_0F_1\left(\frac{1+m}{2+m};\alpha\right) + C_2\,{}_0F_1\left(2-\frac{1+m}{2+m};\alpha\right)\alpha^{1-\frac{1+m}{2+m}}, \tag{3.58}$$

where ${}_0F_1$ is defined by

$${}_0F_1(b,x) = \lim_{a\to\infty} M\left(a,b;\frac{x}{a}\right), \tag{3.59}$$

where M is the confluent hypergeometric function (or Kummer function) of the first kind. We have now solved the governing equation for the lower layer for the cases of $L \ll z_0$ and $L \gg z_0$, representing different aspects of a lower solar atmosphere. A slowly varying background is applicable to a thin layer while a rapidly varying profile is representative of a layer much deeper than the temperature scale-height. A similar analysis as in the case of a slowly varying solution may be used here to analyse standing waves. The dispersion relation may be shown to be

$${}_0F_1\left(2-\frac{1+m}{2+m};\alpha_{-L}\right) = 0. \tag{3.60}$$

Analytic estimates of these frequencies can be made by exploiting the fact that $L/z_0 \gg 1$. This suggests an asymptotic expansion for large α_{-L} (if $m > -2$ is and non-zero). The first term in the asymptotic expansion of the ${}_0F_1$ function is

$${}_0F_1(b;z) \sim \frac{\Gamma(b)}{\sqrt{\pi}}(-z)^{\frac{1-2b}{4}}\cos\left(2\sqrt{-z} - \frac{2b-1}{4}\pi\right) + \ldots \quad |z| \to \infty, \tag{3.61}$$

where $\Gamma(b)$ denotes the Gamma function of b (b arbitrary). The asymptotic series of ${}_0F_1$ can be found by its relation to the Bessel J_ν function, the asymptotic expansion of which is well known (Abramowitz & Stegun, 1972). This expansion allows us to rewrite the dispersion relation (3.60), for non-trivial ω, as

$$\cos\left(2\sqrt{-\alpha_{-L}} - \frac{1}{4}\left(3-\frac{2+2m}{4+2m}\right)\pi\right) = 0, \tag{3.62}$$

and so

$$2\sqrt{-\alpha_{-L}} - \frac{1}{4}\left(3-\frac{2+2m}{4+2m}\right)\pi = \frac{(2n-1)\pi}{2}, \qquad n = 1,2,3,\ldots. \tag{3.63}$$

Substituting α, as defined in Equation (3.56), into the above gives the eigenfrequencies

$$\omega = \frac{\widehat{v}_A \pi (2+m)}{2z_0} \left(\frac{L}{z_0}\right)^{\frac{-2-m}{2}} \left[\frac{2n-1}{2} + \frac{1}{4}\left(3 - \frac{2+2m}{4+2m}\right)\right], \quad n = 1,2,3\ldots. \tag{3.64}$$

The expression for the frequencies is linear in n rather than parabolic, as in Equation (3.41). This is due to the asymptotic expansion (3.54), which has removed N_0 (which played the role of the lower cut-off frequency when the temperature varied slowly) and hence the acceleration due to gravity, g. The Brunt-Väisälä frequency is not removed entirely as the factor $(1 - z/z_0)^{-1}$ has contributed to the asymptotic expansion. Acknowledging this limitation, we may use Equation (3.64) to estimate the frequencies when L/z_0 is sufficiently large. It can be shown that for typical solar parameters the frequencies are much lower in the case of rapidly varying temperature than slowly varying.

3.2.3 Waves in a Two-layer Model

In the previous section we considered only a medium consisting of high-β plasma. We have established that in the high-β regions of the solar atmosphere, IGWs are slow magneto-acoustic gravity waves. The character of slow MHD waves depends upon the plasma-β; when the medium is dominated by the magnetic field (low-β), the slow wave has the character of a sound wave. For a more realistic picture of slow waves in vertical magnetic structures we will now include these effects.

The plasma-β typically falls below unity in the solar chromosphere (see *e.g.* Gent *et al.*, 2013). The temperature profile of the solar chromosphere is such that we may use an isothermal background plasma as a model. To connect the photospheric conditions studied previously to the solar chromosphere we construct a two-layer model consisting of a polytropic lower layer and an isothermal upper layer. The depth of the chromosphere is much greater than the photosphere; hence, we may consider the chromospheric layer to be infinite.

The slowly varying polytropic solution, Equation (3.31), may be used in the lower layer; although, as we shall see, this is not the most convenient representation of the solution. We begin by studying the upper isothermal layer.

3.2.3.1 Upper Isothermal Layer

We now consider an isothermal (constant temperature) atmosphere. Isothermal plasmas in the presence of a vertical magnetic field have been studied extensively by *e.g.* Ferraro & Plumpton (1958), Zhugzhda (1979), Hollweg (1979), Leroy (1980, 1981), Bel & Leroy (1981), Zhugzhda & Dzhalilov (1981, 1982), Leory & Schwartz (1982), Schwartz & Leory (1982), Zhugzhda & Dzhalilov (1984a, b), Hasan & Christensen-Dalsgaard (1992), Cally (2001), McDougal & Hood (2007) and Mather & Erdélyi (2016). Much of the previous work has been motivated by oscillations in sunspots, and most of the above

consider both fast and slow MAG waves. An isothermal medium implies a constant sound speed; when this is the case the operators acting on $\partial\xi_z/\partial x$ and ξ_z in Equations (3.1) and (3.2), respectively, commute. It is straightforward to eliminate ξ_z to obtain a fourth-order differential equation for ξ_x. Zhugzhda (1979) showed, in a seminal paper, that this equation can be solved exactly in terms of Meijer G-functions. Cally (2001) demonstrated that this solution is equivalent to a combination of hypergeometric ${}_2F_3$ functions. In what follows we, again, use the coordinate stretching technique to analyse the longitudinal slow mode.

We consider an upper layer, $z > 0$, in which the sound speed is constant. The pressure and density are given by

$$p_0 = \widehat{p}_0 e^{-z/H}, \quad \rho_0 = \widehat{\rho}_0 e^{-z/H}. \tag{3.65}$$

The Alfvén speed increases exponentially with height

$$v_A^2 = \frac{B_0^2}{\mu\rho_0} = \frac{B_0^2}{\mu\widehat{\rho}_0} e^{z/H} \equiv \widehat{v}_A^2 e^{z/H}. \tag{3.66}$$

The governing equations (3.1) and (3.2) possess exact solutions in terms of Meijer G-functions, Zhugzhda (1979). These solutions describe slow and fast MAG waves which may couple together. We are interested in slow modes, uncoupled from fast modes, hence we use Equation (3.19) as the basis for our investigation. This is also needed to accurately connect the solution with that of the lower layer.

Taking the low-β limit returns the equation

$$c_s^2 \frac{\mathrm{d}^2\xi_z}{\mathrm{d}z^2} - g\gamma\frac{\mathrm{d}\xi_z}{\mathrm{d}z} + \omega^2\xi_z = 0. \tag{3.67}$$

which is the equation of vertically propagating acoustic waves. This is the well known behaviour of slow MAG waves in low-β plasma. The solutions are simply given by

$$\xi_z = D_1 \exp\left(\frac{z}{2H} + \frac{\mathrm{i}}{2c_s^2}\left[4\omega^2c_s^2 - g^2\gamma^2\right]^{1/2} z\right) + D_2 \exp\left(\frac{z}{2H} - \frac{\mathrm{i}}{2c_s^2}\left[4\omega^2c_s^2 - g^2\gamma^2\right]^{1/2} z\right). \tag{3.68}$$

We are interested in case where we allow the layer to transition from high to low-β. Substituting the isothermal pressure and density profiles into Equation (3.19), we have

$$\left(c_s^2 + \widehat{v}_A^2 e^{z/H}\right) c_s^2 \widehat{v}_A^2 e^{z/H} \frac{\mathrm{d}^2\xi_z}{\mathrm{d}z^2} - g\gamma\widehat{v}_A^4 e^{2z/H}\frac{\mathrm{d}\xi_z}{\mathrm{d}z}$$

$$+\left(\omega^2\left(c_s^2 + \widehat{v}_A^2 e^{z/H}\right)^2 - c_s^2N^2\left(c_s^2 + \widehat{v}_A^2 e^{z/H}\right) - \frac{gc_s^2\widehat{v}_A^2}{H}e^{z/H}\right)\xi_z = 0. \tag{3.69}$$

We note that in a low-β plasma, the wave propagating along the field line takes the form of a sound wave in a gravitationally stratified medium. For this reason we expect that the solution for a sound wave is a limiting cases of the solution of Equation (3.69). This

motivates us to make the ansatz

$$\xi_z = f(z)\exp\left(\frac{z}{2H} + \frac{\mathrm{i}}{2c_s^2}\left[4\omega^2 c_s^2 - g^2\gamma^2\right]^{1/2} z\right), \tag{3.70}$$

where $f(z)$ is some function to be determined. The variable transformation

$$\eta = -\frac{c_s^2}{\widetilde{v}_A^2} e^{-z/H} \tag{3.71}$$

allows Equation (3.69) to be cast into the form

$$\eta(\eta-1)\frac{\mathrm{d}^2 f(\eta)}{\mathrm{d}\eta^2} + \left[\left(1 + \frac{\mathrm{i}}{g\gamma}\sqrt{4\omega^2 c_s^2 - g^2\gamma^2}\right)(\eta-1) - \eta\right]\frac{\mathrm{d}f(\eta)}{\mathrm{d}\eta} +$$

$$\left[\frac{1}{2} + \frac{c_s^2}{g^2\gamma^2}\left(\omega^2 - N^2\right) - \frac{1}{\gamma} - \frac{\mathrm{i}}{2g\gamma}\sqrt{4\omega^2 c_s^2 - g^2\gamma^2} + \frac{c_s^2}{g^2\gamma^2}\left(N^2 - \omega^2\right)\eta\right] f(\eta) = 0. \tag{3.72}$$

This equation is the *confluent Heun equation* (CHE)

$$\frac{d^2 f(\eta)}{d\eta^2} + \left[a_1 + \frac{a_2}{\eta} + \frac{a_3}{\eta-1}\right]\frac{\mathrm{d}f(\eta)}{\mathrm{d}\eta} + \left[\frac{a_4\eta - a_5}{\eta(\eta-1)}\right] f(\eta) = 0, \tag{3.73}$$

where

$$a_1 = 0, \quad a_2 = 1 + \frac{\mathrm{i}}{g\gamma}\sqrt{4\omega^2 c_s^2 - g^2\gamma^2}, \quad a_3 = 1, \quad a_4 = \frac{c_s^2}{g^2\gamma^2}\left(N^2 - \omega^2\right),$$

$$a_5 = \frac{1}{\gamma} - \frac{c_s^2}{g^2\gamma^2}\left(\omega^2 - N^2\right) - \frac{1}{2} + \frac{\mathrm{i}}{2g\gamma}\sqrt{4\omega^2 c_s^2 - g^2\gamma^2}. \tag{3.74}$$

For further details on the CHE see *e.g.* Ronveaux (1995). The CHE has two regular singularities at $\eta = 0, 1$ and one irregular singularity at infinity. The solutions to the CHE are not well studied, however, we can investigate local (Frobenius) expansions around the singularities (*c.f.* the ${}_2F_1$ hypergeometric function). Let us denote the local solution around $\eta = 0$ by $\mathrm{Hc}(a_1, a_2, a_3, a_4, a_5; \eta)$. The power series solution is normalised such that

$$\mathrm{Hc}(a_1, a_2, a_3, a_4, a_5; 0) = 1. \tag{3.75}$$

The radius of convergence of this solution is 1, *i.e.*, it is valid up to the singularity at $\eta = 1$. The condition $z \in (0, \infty)$ corresponds to $\eta \in \left(-c_s^2/\widetilde{v}_A^2, 0\right)$. For the case of low-$\beta$, the local solution around $\eta = 0$ is valid for all z. When $c_s^2 \geq \widetilde{v}_A^2$ the series does not converge. It is sometimes possible that the solution can be continued to other regions by analytic continuation, or that the local solution around $\eta = 1$ matches the solution around 0. A

second linearly independent solution is found by taking the negative root in (3.70), *i.e.*

$$\xi_z = D_1 \mathrm{Hc}(0, a_{2+}, a_3, a_4, a_{5+}; \eta) \exp\left(\frac{z}{2H} + \frac{\mathrm{i}}{2c_s^2}\left[4\omega^2 c_s^2 - g^2\gamma^2\right]^{1/2} z\right) + D_2 \mathrm{Hc}(0, a_{2-}, a_3, a_4, a_{5-}; \eta) \exp\left(\frac{z}{2H} - \frac{\mathrm{i}}{2c_s^2}\left[4\omega^2 c_s^2 - g^2\gamma^2\right]^{1/2} z\right). \quad (3.76)$$

This solution may be used when $\beta < 2/\gamma$. The low-β solution, satisfying Equation (3.67), can be obtained from (3.76) by taking the asymptotic limit $v_A \to \infty$.

Asymptotic solution

The complex nature of the exact solution is such that it is difficult to apply it to high-β plasma. This motivates a different approach to finding a solution in the upper layer. We let the initial plasma-β be high, that is

$$\epsilon = \frac{\widetilde{v_A^2}}{c_s^2} \ll 1. \quad (3.77)$$

The parameter ϵ is defined such that it is proportional to $1/\beta$. Writing Equation (3.18) in terms of the parameter ϵ,

$$c_s^2 \epsilon e^{z/H}\left(\epsilon e^{z/H} + 1\right)\frac{\mathrm{d}^2\xi_z}{\mathrm{d}z^2} - e^{2z/H} g\gamma\epsilon^2 \frac{\mathrm{d}\xi_z}{\mathrm{d}z} + \left[\omega^2\left(\epsilon e^{z/H} + 1\right)^2 - \left(\epsilon e^{z/H} + 1\right)N^2 - \frac{\epsilon g}{H} e^{z/H}\right]\xi_z = 0. \quad (3.78)$$

We shall attempt to find an asymptotic solution to Equation (3.78) as $\epsilon \to 0$. Examining the coefficient of the 1st term we may expect to encounter some problems with the asymptotic series when

$$\epsilon e^{z/H} \sim 1 \quad \text{or} \quad z \sim -H \log \epsilon. \quad (3.79)$$

This is a potential problem as we may neglect terms that are initially small but become important in some other region. This is reflected in the physics of the problem where we have mainly hydrodynamic effects when z is small, but due to the decreasing density magnetic effects dominate higher in the solar atmosphere. In anticipating this problem let us make the variable transformation

$$\alpha = e^{z/H}. \quad (3.80)$$

In terms of α, the set $z \in [0, \infty)$ is equivalent to $\alpha \in [1, \infty)$. The exact reason for this change will become apparent later. Recasting Equation (3.78) in terms of the new variable α,

$$\epsilon\alpha^3(1 + \epsilon\alpha)\frac{\mathrm{d}^2\xi_z}{\mathrm{d}\alpha^2} + \epsilon\alpha^2\frac{\mathrm{d}\xi_z}{\mathrm{d}\alpha} + \frac{H^2}{c_s^2}\left[\omega^2(1 + \epsilon\alpha)^2 - N^2(1 + \epsilon\alpha) - \frac{g\epsilon\alpha}{H}\right]\xi_z = 0. \quad (3.81)$$

Attempting to solve via a regular perturbation series does not allow us to determine the solution. The first term returns $\omega^2 = N^2$ and does not allow us to determine the amplitude of ξ_z. This is analogous to assuming plane wave solutions and ignoring the magnetic effects.

This is due to the singular nature of the problem. Rescaling does not help as it leads to spurious problems further down the line.

We may, however, solve the equation using the WKB method,

$$\xi_z \sim A(\alpha) e^{\epsilon^{-1/2} S(\alpha)}. \tag{3.82}$$

The standard form of the WKB solution is recovered using the small term $\epsilon^{1/2}$. The square root is needed as the equation is a second order ODE where the global singularity is of order ϵ. This approach is more suited due to singular nature of the problem. It should be noted that the terminology WKB has become synonymous with the physical assumption that the wavelength of the waves is much smaller than the scale over which the background quantities vary; such application of the WKB method has used in previous local analysis. Here, we refer to the WKB method in its mathematical form - a technique to analyse singular perturbation problems. Let us expand the amplitude of the WKB form into a perturbation series,

$$\xi_z \sim \left(A_0(\alpha) + \epsilon^{1/2} A_1(\alpha) + \epsilon A_2(\alpha) + O\left(\epsilon^{3/2}\right)\right) e^{\epsilon^{-1/2} S(\alpha)}. \tag{3.83}$$

Substituting ξ_z given by Equation (3.83) into the governing equation (3.81). Retaining terms of order $O(\epsilon^0)$, we have

$$\alpha^3 \left(\frac{\mathrm{d}S}{\mathrm{d}\alpha}\right)^2 + \frac{H^2}{c_s^2}\left(\omega^2 - N^2\right) = 0, \tag{3.84}$$

which may be integrated to give

$$S = \mp 2\alpha^{-1/2} \frac{H}{c_s} \left(N^2 - \omega^2\right)^{1/2}, \tag{3.85}$$

where the two roots represent ingoing/outgoing wave solutions. To $O(\epsilon^{1/2})$ we have

$$\frac{\mathrm{d}A_0}{\mathrm{d}\alpha} - \frac{1}{4\alpha} A_0 = 0, \tag{3.86}$$

hence

$$A_0 = \mathcal{D}\alpha^{1/4}. \tag{3.87}$$

The form of A_0 does not depend on the sign of S, we let the constant of integration $\mathcal{D} = C_1$ correspond to the negative root, while $\mathcal{D} = D_1$ represents the positive root. Finally, to $O(\epsilon)$,

$$\alpha^2 \frac{\mathrm{d}S}{\mathrm{d}\alpha}\left(2\alpha \frac{\mathrm{d}A_1}{\mathrm{d}\alpha} - \frac{1}{2} A_1\right) + \mathcal{D}\alpha^{5/4}\left(\frac{1}{16} + \frac{H^2\omega^2}{c_s^2} - \frac{gH}{c_s^2}\right) = 0. \tag{3.88}$$

Taking the negative root,

$$\frac{\mathrm{d}A_1}{\mathrm{d}\alpha} - \frac{1}{4\alpha} A_1 = -\frac{C_1 c_s}{2H} \alpha^{-1/4} \left(N^2 - \omega^2\right)^{-1/2} \left(\frac{1}{16} + \frac{H^2\omega^2}{c_s^2} - \frac{gH}{c_s^2}\right). \tag{3.89}$$

It is simple to obtain the solution for A_1 using the integrating factor $\alpha^{-1/4}$,

$$A_1 = -\frac{C_1 c_s}{H}\alpha^{3/4}\left(N^2-\omega^2\right)^{-1/2}\left(\frac{1}{16}+\frac{H^2\omega^2}{c_s^2}-\frac{gH}{c_s^2}\right)+C_2\alpha^{1/4}. \tag{3.90}$$

Repeating the above, taking the positive root gives

$$A_1 = \frac{D_1 c_s}{H}\alpha^{3/4}\left(N^2-\omega^2\right)^{-1/2}\left(\frac{1}{16}+\frac{H^2\omega^2}{c_s^2}-\frac{gH}{c_s^2}\right)+D_2\alpha^{1/4}. \tag{3.91}$$

The full solution is then given by

$$\begin{aligned}\xi_z \sim &\left[C_1\alpha^{1/4}+\epsilon^{1/2}\left(-\frac{C_1 c_s}{H}\alpha^{3/4}\left(N^2-\omega^2\right)^{-1/2}\left(\frac{1}{16}+\frac{H^2\omega^2}{c_s^2}-\frac{gH}{c_s^2}\right)+C_2\alpha^{1/4}\right)+O(\epsilon)\right]e^{\epsilon^{-1/2}S}\\ &+\left[D_1\alpha^{1/4}+\epsilon^{1/2}\left(\frac{D_1 c_s}{H}\alpha^{3/4}\left(N^2-\omega^2\right)^{-1/2}\left(\frac{1}{16}+\frac{H^2\omega^2}{c_s^2}-\frac{gH}{c_s^2}\right)+D_2\alpha^{1/4}\right)+O(\epsilon)\right]e^{-\epsilon^{-1/2}S},\end{aligned} \tag{3.92}$$

where

$$S = -\frac{2H}{c_s}\alpha^{-1/2}\left(N^2-\omega^2\right)^{1/2}. \tag{3.93}$$

Comparing the functions A_0 and $\epsilon^{1/2}A_1$, we see that these terms are of the same order in ϵ when $\alpha^{1/4} \sim \epsilon^{1/2}\alpha^{3/4}$, that is when $\alpha \sim \epsilon^{-1}$. There is, therefore, a loss of regularity when $\alpha \sim \epsilon^{-1}$. This is the same breaking point we expected from inspecting the governing equation.

This is, therefore, a singular perturbation problem requiring the use of a matched asymptotic expansion (Van Dyke, 1975) well known to fluid dynamics where, for example, a viscous boundary layer is included. Matched asymptotic expansions have been applied to many areas of applied mathematics, including important developments in topics such as aerodynamics. We have a solution valid when the exponential term is greater than ϵ and a solution with the exponential term is smaller than ϵ. The point where the solution changes is where the character of the wave changes from hydrodynamic effects to magnetically dominated effects, *i.e.* high-β effects to low-β effects. We apply the method of matched asymptotic expansions to form an asymptotic solution that takes into account this change in behaviour. The fact that we are required to use both the WKB method and the method of matched asymptotic expansions is interesting and unusual. This is due to effectively having two singularities in the first term in Equation (3.81).

The WKB solution is valid in the regime $\alpha \in [1, \epsilon^{-1})$ or $z/H \in [0, -\log\epsilon)$. In the theory of matched asymptotic expansions, this solution is referred to as the outer solution. We now seek a solution that is valid beyond $\alpha \sim \epsilon^{-1}$, termed the inner solution. The terminology is somewhat confusing as the inner solution is so called as it refers to the solution valid inside some boundary layer. In our problem, the boundary layer is, in effect, located at $z = \infty$. This is analogous to the resolution of the Stokes-Whitehead paradox of incompressible,

viscous flow over a sphere. We seek a new variable $\widetilde{\alpha} \sim 1$, when $\alpha \sim \epsilon^{-1}$, that is we introduce

$$\widetilde{\alpha} = \epsilon\alpha. \tag{3.94}$$

In terms of the variable $\widetilde{\alpha}$, Equation (3.81) may be written

$$\widetilde{\alpha}^3(1+\widetilde{\alpha})\frac{\mathrm{d}^2\xi_z}{\mathrm{d}\widetilde{\alpha}^2} + \widetilde{\alpha}^2\frac{\mathrm{d}\xi_z}{\mathrm{d}\widetilde{\alpha}} + \frac{H^2}{c_s^2}\left[\omega^2(1+\widetilde{\alpha})^2 - N^2(1+\widetilde{\alpha}) - \frac{g\widetilde{\alpha}}{H}\right]\xi_z = 0. \tag{3.95}$$

Following the low-β isothermal case mentioned above, we assume ξ_z takes the form

$$\xi_z = f(\widetilde{\alpha})\widetilde{\alpha}^{\frac{1}{2}-\kappa}, \tag{3.96}$$

where

$$\kappa = \frac{1}{2c_s}\sqrt{c_s^2 - 4H^2\omega^2} \tag{3.97}$$

and $f(\widetilde{\alpha})$ is some function to be determined. Substituting ξ_z, given by Equation (3.96), into the governing equation, we have

$$\widetilde{\alpha}^3(1+\widetilde{\alpha})\frac{\mathrm{d}^2 f}{\mathrm{d}\widetilde{\alpha}^2} + \widetilde{\alpha}^2[2-2\kappa(1+\widetilde{\alpha})+\widetilde{\alpha}]\frac{\mathrm{d}f}{\mathrm{d}\widetilde{\alpha}} + \left[\widetilde{\alpha}\left(\frac{1}{2}-\kappa-\frac{gH}{c_s^2}\right) + \frac{H^2}{c_s^2}\left(\omega^2-N^2\right)(1+\widetilde{\alpha})\right]f = 0. \tag{3.98}$$

Making one further variable change, let

$$q = -\widetilde{\alpha}^{-1}, \tag{3.99}$$

which transforms Equation (3.98) into

$$q(q-1)\frac{\mathrm{d}^2 f}{\mathrm{d}q^2} + [(1+2\kappa)(q-1)-q]\frac{\mathrm{d}f}{\mathrm{d}q} + \left[\frac{H^2}{c_s^2}\left(N^2-\omega^2\right)q + \frac{1}{2} - \kappa - \frac{gH}{c_s^2} + \frac{H^2}{c_s^2}\left(\omega^2-N^2\right)\right]f = 0. \tag{3.100}$$

This equation is in the form of the confluent Heun equation (3.73) with

$$a_1 = 0, \quad a_2 = 1+2\kappa, \quad a_3 = -1, \quad a_4 = \frac{H^2}{c_s^2}\left(N^2-\omega^2\right), \quad a_5 = \kappa - \frac{1}{2} + \frac{gH}{c_s^2} - \frac{H^2}{c_s^2}\left(\omega^2-N^2\right). \tag{3.101}$$

This is, in fact, the isothermal governing equation rewritten. It is customary to write the solution to the CHE in terms of the parameters

$$\alpha = a_1, \quad \beta = a_2 - 1, \quad \gamma = a_3 - 1, \quad \delta = a_4 - \frac{a_1}{2}(a_2+a_3), \quad \eta = \frac{1}{2}(a_1a_2 - a_2a_4 + 1) - a_5, \tag{3.102}$$

where the labels should not be confused with physical parameters or variables used previously. The two linearly independent solutions to the CHE are given by

$$f = \widehat{C}_1 \mathrm{Hc}(0,\beta,\gamma,\delta,\eta;q) + \widehat{C}_2 q^{-\beta}\mathrm{Hc}(0,-\beta,\gamma,\delta,\eta;q). \tag{3.103}$$

The solution for ξ_z is then,

$$\xi_z = \widehat{C}_1 \mathrm{Hc}\left(0,\beta,\gamma,\delta,\eta;-\widetilde{\alpha}^{-1}\right)\widetilde{\alpha}^{\frac{1}{2}-\kappa} + \widehat{C}_2 \mathrm{Hc}\left(0,-\beta,\gamma,\delta,\eta;-\widetilde{\alpha}^{-1}\right)\widetilde{\alpha}^{\frac{1}{2}+\kappa}. \tag{3.104}$$

The WKB solution derived previously is valid for the regime $\alpha < \epsilon^{-1}$, the confluent Heun solution derived here is used for the regime $\alpha > \epsilon^{-1}$ or $\widetilde{\alpha} \in (1,\infty)$. The radius of convergence of the solution (3.104) is $|-\widetilde{\alpha}| < 1$, hence we are inside the radius of convergence in the region $\alpha > \epsilon^{-1}$.

Let us now apply a boundary condition as $z \to \infty$. We require the kinetic energy density to tend to 0 as $z \to \infty$, *i.e.* $\rho_0 \xi_z^2 \to 0$. The Heun function is such that $\mathrm{Hc}(\alpha,\beta,\gamma,\delta,\eta;0) = 1$, hence $\mathrm{Hc}(\alpha,\beta,\gamma,\delta,\eta;-\widetilde{\alpha}) \to 1$ as $z \to \infty$. $\rho_0 \propto \widetilde{\alpha}^{-1}$ so to satisfy $\rho_0 \xi_z^2 \to 0$, $\widehat{C}_2 = 0$ and $\Omega > \omega$ (for which κ is real and positive; if $\Omega < \omega$ then our boundary condition is the statement of only outgoing waves). The solution is then

$$\xi_z \sim \widehat{C}_1 \mathrm{Hc}\left(0,\beta,\gamma,\delta,\eta;-\widetilde{\alpha}^{-1}\right)\widetilde{\alpha}^{\frac{1}{2}-\kappa}. \tag{3.105}$$

We have two solutions valid in two regions; we must now match the inner solution to the outer solution. To do this, we apply Van Dyke's matching rule (Van Dyke, 1975; Hinch, 1991). This method is simpler to perform than other methods, such as using an intermediate matching variable. The advantage of using Van Dyke's rule is its simplicity although it does not show that there is some region where the inner and outer solutions are the same. There are also examples where Van Dyke's rule fails where a matching variable succeeds, for more see *e.g.* Hinch (1991). A rigorous justification of Van Dyke's matching rule is given by Fraenkel (1969a,b,c).

To apply Van Dyke's matching rule we substitute the inner variable into the outer solution and take the asymptotic limit as $\epsilon \to 0$ (while holding $\widetilde{\alpha}$ constant). We also substitute the outer variable into the inner solution and let $\epsilon \to 0$. These solutions match by the matching rule, up to a rescaling of the solution by a constant.

Firstly, we let $\alpha = \epsilon^{-1}\widetilde{\alpha}$ in the lower (outer) solution,

$$\begin{aligned}\xi_z \sim &\left[C_1\widetilde{\alpha}^{1/4}\epsilon^{-1/4} + C_2\widetilde{\alpha}^{1/4}\epsilon^{1/4} - \epsilon^{-1/4}\frac{C_1 c_s}{H}\widetilde{\alpha}^{3/4}\left(N^2-\omega^2\right)^{-1/2}\left(\frac{1}{16}+\frac{H^2\omega^2}{c_s^2}-\frac{gH}{c_s^2}\right)+\ldots\right]e^{S}\\ &+\left[D_1\widetilde{\alpha}^{1/4}\epsilon^{-1/4} + D_2\widetilde{\alpha}^{1/4}\epsilon^{1/4} + \epsilon^{-1/4}\frac{D_1 c_s}{H}\widetilde{\alpha}^{3/4}\left(N^2-\omega^2\right)^{-1/2}\left(\frac{1}{16}+\frac{H^2\omega^2}{c_s^2}-\frac{gH}{c_s^2}\right)+\ldots\right]e^{-S},\end{aligned} \tag{3.106}$$

$$S = -\frac{2H}{c_s}\widetilde{\alpha}^{-1/2}\left(N^2-\omega^2\right)^{1/2}, \tag{3.107}$$

Note that there are now no terms in ϵ in the exponential functions. We take the asymptotic limit $\epsilon \to 0$, holding $\widetilde{\alpha}$ constant, and keep the dominant terms,

$$\xi_z \sim C_1\epsilon^{-1/4}\left[\widetilde{\alpha}^{1/4} - \frac{c_s}{H}\widetilde{\alpha}^{3/4}\left(N^2-\omega^2\right)^{-1/2}\left(\frac{1}{16}+\frac{H^2\omega^2}{c_s^2}-\frac{gH}{c_s^2}\right)+\ldots\right]e^S + D_1\epsilon^{-1/4}\left[\widetilde{\alpha}^{1/4} + \frac{c_s}{H}\widetilde{\alpha}^{3/4}\left(N^2-\omega^2\right)^{-1/2}\left(\frac{1}{16}+\frac{H^2\omega^2}{c_s^2}-\frac{gH}{c_s^2}\right)+\ldots\right]e^{-S}, \quad (3.108)$$

or, in terms of α,

$$\xi_z \sim C_1\left[\alpha^{1/4} - \epsilon^{1/2}\frac{c_s}{H}\alpha^{3/4}\left(N^2-\omega^2\right)^{-1/2}\left(\frac{1}{16}+\frac{H^2\omega^2}{c_s^2}-\frac{gH}{c_s^2}\right)+\ldots\right]e^{\epsilon^{-1/2}S} + D_1\left[\alpha^{1/4} + \epsilon^{1/2}\frac{c_s}{H}\alpha^{3/4}\left(N^2-\omega^2\right)^{-1/2}\left(\frac{1}{16}+\frac{H^2\omega^2}{c_s^2}-\frac{gH}{c_s^2}\right)+\ldots\right]e^{-\epsilon^{-1/2}S}, \quad (3.109)$$

$$S = -\frac{2H}{c_s}\alpha^{-1/2}\left(N^2-\omega^2\right)^{1/2}. \quad (3.110)$$

Let us now apply the procedure to the upper (inner) solution. Letting $\widetilde{\alpha} = \epsilon\alpha$,

$$\xi_z \sim \widehat{C}_1\epsilon^{\frac{1}{2}-\kappa}\alpha^{\frac{1}{2}-\kappa}\mathrm{Hc}\left(0,\beta,\gamma,\delta,\eta;-\epsilon^{-1}\alpha^{-1}\right). \quad (3.111)$$

We need to take the limit $\epsilon \to 0$, so we need to know the behaviour of the Heun function for a large argument. For the case $a_1 = 0$ (or $\alpha = 0$, where here α is the first parameter of the Heun function) it can be shown that the first term in the asymptotic series is, see *e.g.* Figueiredo (2005), El-Jaick & Figueiredo (2009),

$$\mathrm{Hc}\left(\alpha,\beta,\gamma,\delta,\eta;x\right) \sim e^{\pm 2\mathrm{i}\sqrt{\delta x}}x^{\frac{1}{4}-\frac{\pm\beta+\gamma+2}{2}}, \quad x\to\infty, \quad (3.112)$$

where the positive and negative roots correspond to the two solutions to the CHE. For asymptotic solutions for the case $a_1 \neq 0$, see *e.g.* Decarreau, Maroni & Robert (1978), Staicova (2012). Using this expression for the positive root in the Heun functions, we have

$$\xi_z \sim (-1)^{\frac{1}{4}-\kappa}\widehat{C}_1\alpha^{1/4}\epsilon^{1/4}e^{\left[2H\left(N^2-\omega^2\right)^{1/2}\alpha^{-1/2}\epsilon^{-1/2}/c_s\right]} = (-1)^{\frac{1}{4}-\kappa}\widehat{C}_1\alpha^{1/4}\epsilon^{1/4}e^{-\epsilon^{1/2}S}, \quad (3.113)$$

where S is as above. This must match the limit of the lower solution, hence $C_1 = 0$; this is a consequence of the upper boundary condition. It is also clear that we must rescale the upper solution by $\epsilon^{-1/4}$ to make the orders in epsilon match. The matching also implies that

$$D_1 = (-1)^{\frac{1}{4}-\kappa}\widehat{C}_1. \quad (3.114)$$

To see that this is indeed correct, we should calculate the next term in the asymptotic expansion expansion of the confluent Heun function. The asymptotic relation used above is

derived by investigating the behaviour of the confluent Huen function around the irregular singular point at infinity, using the method of dominant balance (Bender & Orszag, 1978). We apply this to Equation (3.100) to extend the asymptotic expansion. This method of analysing behaviour around irregular singular points is often attributed to Green. We begin by making the substitution

$$f = e^{s(q)}, \tag{3.115}$$

so Equation (3.100), takes the form

$$q(q-1)\left(s'' + (s')^2\right) + (2\kappa q - 1 - 2\kappa)\, s' + \left[\frac{H^2}{c_s^2}\left(N^2 - \omega^2\right)q + \frac{1}{2} - \kappa - \frac{gH}{c_s^2} + \frac{H^2}{c_s^2}\left(\omega^2 - N^2\right)\right] = 0. \tag{3.116}$$

We are interested in the behaviour as $q \to \infty$. We assume that $s'' \ll (s')^2$, which we will see to be valid (and is in fact valid for the case of an irregular singular point, the inequality fails only around regular points). When q tends to infinity, the dominate terms in Equation (3.116) must balance, leading to

$$q(s')^2 \sim \frac{H^2}{c_s^2}\left(\omega^2 - N^2\right), \quad q \to \infty, \tag{3.117}$$

or

$$s \sim \frac{2H}{c_s}\left(\omega^2 - N^2\right)^{1/2} q^{1/2}. \tag{3.118}$$

We shall use only the positive root as we need only the expansion of the Heun function corresponding to the positive root. We see the asymptotic behaviour of s, hence we know s takes the form $s(q) = 2H\sqrt{\omega^2 - N^2}q^{1/2}/c_s + c(q) = s_0 + c$, where $c \ll q^{1/2}$. This last inequality implies that $c' \ll q^{-1/2}, (c')^2 \ll q^{-1}, c'' \ll q^{-3/2}$ which will become important at the next stage. Substituting $f = \exp(s_0 + c)$ into Equation (3.116) gives

$$q(q-1)\left(s_0'' + c'' + \left(s_0'\right)^2 + (c')^2 + 2s_0'c'\right) + (2\kappa q - 1 - 2\kappa)\left(s_0' + c'\right) + \left[\frac{H^2}{c_s^2}\left(N^2 - \omega^2\right)q + \frac{1}{2} - \kappa - \frac{gH}{c_s^2} + \frac{H^2}{c_s^2}\left(\omega^2 - N^2\right)\right] = 0. \tag{3.119}$$

We now consider the dominant terms as $q \to \infty$. We remove the highest order terms, which balance each other from the previous step. To correctly retain the dominant terms we use the inequalities on c, stated previously. We also use the fact that $q^{3/2}c' \ll q$. The dominant terms then give the relation

$$q^2 s_0'' + 2q^2 s_0' c' \sim -2\kappa q s_0', \quad q \to \infty, \tag{3.120}$$

so

$$c' \sim \left(\frac{1}{4} - \kappa\right)q^{-1}, \quad c \sim \log\left(q^{\frac{1}{4}-\kappa}\right). \tag{3.121}$$

Using the asymptotic relations for s and c give the first term in the expansion for the Heun function used previous, to find the next term in the series we use $s(q) = 2H\sqrt{\omega^2 - N^2}q^{1/2}/c_s + \log\left(q^{1/4-\kappa}\right) + v = s_0 + c_0 + v$, where $v \ll \log\left(q^{1/4-\kappa}\right)$, or $v' \ll q^{-1}$. Repeating the process, we have

$$q(q-1)\left(s_0'' + c_0'' + v'' + \left(s_0' + c_0' + v'\right)^2\right) + (2\kappa q - 1 - 2\kappa)\left(s_0' + c_0' + v'\right) + \left[\frac{H^2}{c_s^2}\left(N^2 - \omega^2\right)q + \frac{1}{2} - \kappa - \frac{gH}{c_s^2} + \frac{H^2}{c_s^2}\left(\omega^2 - N^2\right)\right] = 0. \quad (3.122)$$

For large q, we remove the terms which balance at the previous steps and use the expressions for s_0 and c_0, and the fact that $v' \ll c_0'$ etc., to deduce the largest terms. It may be shown that

$$2q^2 s_0' v' \sim -q^2 c_0'' - q^2 (c_0')^2 + q(s_0')^2 - 2\kappa q c_0' - \left[\frac{1}{2} - \kappa - \frac{gH}{c_s^2} + \frac{H^2}{c_s^2}\left(\omega^2 - N^2\right)\right]. \quad (3.123)$$

Using the above, and the expression for κ, this may be rewritten

$$\frac{2H}{c_s}\left(\omega^2 - N^2\right)^{1/2} q^{3/2} v' \sim -\left(\frac{1}{16} + \frac{H^2\omega^2}{c_s^2} - \frac{gH}{c_s^2}\right), \quad (3.124)$$

$$v \sim \frac{c_s}{H}\left(\omega^2 - N^2\right)^{-1/2}\left(\frac{1}{16} + \frac{H^2\omega^2}{c_s^2} - \frac{gH}{c_s^2}\right)q^{-1/2}. \quad (3.125)$$

The function f, which satisfies the confluent Heun equation then has the asymptotic behaviour

$$f = e^{s_0 + c_0 + v} \sim \exp\left[\frac{2H}{c_s}\left(\omega^2 - N^2\right)^{1/2} q^{1/2}\right]\left(q^{\frac{1}{4}-\kappa}\right)\times \exp\left[\frac{c_s}{H}\left(\omega^2 - N^2\right)^{-1/2}\left(\frac{1}{16} + \frac{H^2\omega^2}{c_s^2} - \frac{gH}{c_s^2}\right)q^{-1/2}\right], \quad q \to \infty. \quad (3.126)$$

The second exponential term has a small argument when $q \to \infty$, and hence may be Taylor expanded so

$$\mathrm{Hc}(q) \sim e^{2H(\omega^2 - N^2)^{1/2} q^{1/2}} q^{1/4-\kappa}\left[1 + \frac{c_s}{H}\left(\omega^2 - N^2\right)^{-1/2}\left(\frac{1}{16} + \frac{H^2\omega^2}{c_s^2} - \frac{gH}{c_s^2}\right)q^{-1/2} + \ldots\right], \quad (3.127)$$

as $q \to \infty$, where the parameters of the confluent Heun function are as above. Writing the above in terms of α, we see that the next term in the expansion of the inner solution for ξ_z matches perfectly with the outer solution. Hence, the matching process applied above is indeed correct.

The complete solution is then

$$\xi_z \sim \left[D_1\alpha^{1/4} + \epsilon^{1/2}\left(\frac{D_1 c_s}{H}\alpha^{3/4}\left(N^2-\omega^2\right)^{-1/2}\left(\frac{1}{16}+\frac{H^2\omega^2}{c_s^2}-\frac{gH}{c_s^2}\right)+D_2\alpha^{1/4}\right)+O(\epsilon)\right]e^{-S/\epsilon^{1/2}} + \left[\epsilon^{1/2}C_2\alpha^{1/4}+O(\epsilon)\right]e^{S/\epsilon^{1/2}}, \quad (3.128)$$

where

$$S = -\frac{2H}{c_s}\left(N^2-\omega^2\right)^{1/2}\alpha^{-1/2}, \quad (3.129)$$

for the region $\alpha < \epsilon^{-1}$ and

$$\xi_z \sim \epsilon^{1/4-\kappa}(-1)^{-1/4+\kappa}D_1\alpha^{1/2-\kappa}\mathrm{Hc}\left(0,\beta,\gamma,\delta,\eta;-\epsilon^{-1}\alpha^{-1}\right), \quad (3.130)$$

for the region $\alpha > \epsilon^{-1}$ where

$$\kappa = \frac{H}{c_s}\sqrt{\Omega^2-\omega^2}, \quad (3.131)$$

and $\Omega > \omega$, for evanescent waves.

Equivalence of WKB Solution to High-β Bessel Function Solution

Under the assumption of high-β plasma, the governing Equation (3.18) reduces to Equation (3.24). For the case of an isothermal background we have the solution,

$$\xi_z = D_1 J_0\left(\frac{2H}{c_s\epsilon^{1/2}}\left(\omega^2-N^2\right)^{1/2}\alpha^{-1/2}\right)+D_2 Y_0\left(\frac{2H}{c_s\epsilon^{1/2}}\left(\omega^2-N^2\right)^{1/2}\alpha^{-1/2}\right). \quad (3.132)$$

We now show that in the region $\alpha < \epsilon^{-1}$, the WKB approach to the problem is equivalent to the solution in terms of Bessel functions. In the limit $\epsilon \to 0$, the argument of the Bessel functions may be considered to be large. By specifying that the region of interest is $\alpha < \epsilon^{-1}$, α may not become large itself with the effect of making the argument small or order 1 *i.e.* a small ϵ and a large α do not "cancel each other out". The asymptotic expansion of the Bessel functions, for the case of the order being equal to 0, is

$$J_0\left(\frac{2H}{c_s\epsilon^{1/2}}\left(\omega^2-N^2\right)^{1/2}\alpha^{-1/2}\right) \sim \frac{1}{\sqrt{\pi}}\left[\frac{2H}{c_s\epsilon^{1/2}}\left(\omega^2-N^2\right)^{1/2}\right]^{-1/2}\alpha^{1/4}\left[\sin\left(-\mathrm{i}\epsilon^{1/2}S\right)+\cos\left(-\mathrm{i}\epsilon^{1/2}S\right)\right], \quad (3.133)$$

$$Y_0\left(\frac{2H}{c_s\epsilon^{1/2}}\left(\omega^2-N^2\right)^{1/2}\alpha^{-1/2}\right) \sim \frac{1}{\sqrt{\pi}}\left[\frac{2H}{c_s\epsilon^{1/2}}\left(\omega^2-N^2\right)^{1/2}\right]^{-1/2}\alpha^{1/4}\left[\sin\left(-\mathrm{i}\epsilon^{1/2}S\right)-\cos\left(-\mathrm{i}\epsilon^{1/2}S\right)\right], \quad (3.134)$$

where S is as in the WKB solution,

$$S = -\frac{2H}{c_s}\left(N^2-\omega^2\right)^{1/2}\alpha^{-1/2}. \tag{3.135}$$

Making use of the exponential definition of the circular functions, the solution may be written

$$\xi_z \sim \alpha^{1/4}e^{S/\epsilon^{1/2}}\{D_1-D_2-\mathrm{i}(D_1+D_2)\}\frac{\lambda}{2} + \alpha^{1/4}e^{-S/\epsilon^{1/2}}\{D_1-D_2+\mathrm{i}(D_1+D_2)\}\frac{\lambda}{2}, \tag{3.136}$$

where λ is equal to the constant factor in the expansions of the Bessel functions. We see that this is equivalent to the leading order term in the WKB solution in the previous section, where the constants of integration are suitably chosen. Hence, we see that there is an equivalence between the asymptotic approach to the governing equation and the solution to the high-β equation given in terms of special functions.

3.2.3.2 Asymptotic Solution for the Lower Layer

We now wish to construct a two-layer model by connecting the lower polytropic layer to the upper isothermal layer. As the solution in the upper layer is in the form of a perturbation series, to formally connect the layers we must apply boundary conditions to the right orders, *i.e.* apply the boundary conditions at order ϵ^0, order $\sqrt{\epsilon}$, etc. We may do this with the existing polytropic solution via a Taylor expansion. We take another approach, however, by using a WKB, solution as in the isothermal layer. This will allow us to apply boundary conditions at each order. Another advantage to deriving a solution via the WKB method is that it may allow us to generalise the existing solution to a larger or infinite layer, whereas the previously derived solution is valid for a thin layer.

When the background temperature varies linearly, the sound speed, Alfvén speed, Brunt-Väisälä frequency and scale-height take the form

$$c_s^2 = \widehat{c}_s^2\left(1-\frac{z}{z_0}\right),\ v_A^2 = \widehat{v}_A^2\left(1-\frac{z}{z_0}\right)^{-m},\ N^2 = N_0^2\left(1-\frac{z}{z_0}\right)^{-1},\ H = \frac{\widehat{c}_s^2}{g\gamma}\left(1-\frac{z}{z_0}\right). \tag{3.137}$$

Substituting these into the Equation (3.18), the governing equation to be solved is

$$\frac{\widehat{c}_s^2\widehat{v}_A^2\left(1-\frac{z}{z_0}\right)^{1-m}}{\widehat{c}_s^2\left(1-\frac{z}{z_0}\right)+\widehat{v}_A^2\left(1-\frac{z}{z_0}\right)^{-m}}\frac{\mathrm{d}^2\xi_z}{\mathrm{d}z^2} - g\gamma\frac{\widehat{v}_A^4\left(1-\frac{z}{z_0}\right)^{-2m}}{\left(\widehat{c}_s^2\left(1-\frac{z}{z_0}\right)+\widehat{v}_A^2\left(1-\frac{z}{z_0}\right)^{-m}\right)^2}\frac{\mathrm{d}\xi_z}{\mathrm{d}z} + \Bigg[\omega^2 - \frac{\widehat{c}_s^2\left(1-\frac{z}{z_0}\right)}{\widehat{c}_s^2\left(1-\frac{z}{z_0}\right)+\widehat{v}_A^2\left(1-\frac{z}{z_0}\right)^{-m}}\left(N_0^2\left(1-\frac{z}{z_0}\right)^{-1} + \frac{g^2\gamma}{\widehat{c}_s^2\left(1-\frac{z}{z_0}\right)}\frac{\widehat{v}_A^2\left(1-\frac{z}{z_0}\right)^{-m}}{\widehat{c}_s^2\left(1-\frac{z}{z_0}\right)+\widehat{v}_A^2\left(1-\frac{z}{z_0}\right)^{-m}}\right)\Bigg]\xi_z = 0. \tag{3.138}$$

We consider the lower layer to be high-β plasma, that is,

$$\epsilon = \frac{\widehat{v_A^2}}{\widehat{c_s^2}} \ll 1, \tag{3.139}$$

when the density and temperature are continuous at the interface of the two layers, $\widehat{c_s}$ and $\widehat{v_A}$ are equal to c_s and $\widehat{v_A}$, respectively, in the upper layer. This means that ϵ has the same value in the entire domain. Introducing ϵ, and a little manipulation, allows Equation (3.138) to be rewritten as

$$\begin{aligned}\epsilon\widehat{c_s^2}\left(1-\frac{z}{z_0}\right)^{1-m}\left[\epsilon\left(1-\frac{z}{z_0}\right)^{-m}+\left(1-\frac{z}{z_0}\right)\right]\frac{\mathrm{d}^2\xi_z}{\mathrm{d}z^2}-g\gamma\epsilon^2\left(1-\frac{z}{z_0}\right)^{-2m}\frac{\mathrm{d}\xi_z}{\mathrm{d}z}+\\ \left[\omega^2\left[\epsilon\left(1-\frac{z}{z_0}\right)^{-m}+\left(1-\frac{z}{z_0}\right)\right]^2-N_0^2\left[\epsilon\left(1-\frac{z}{z_0}\right)^{-m}+\left(1-\frac{z}{z_0}\right)\right]-\frac{\epsilon g}{\widehat{H}}\left(1-\frac{z}{z_0}\right)^{-m}\right]\xi_z=0.\end{aligned} \tag{3.140}$$

For convenience we let $\alpha = 1 - z/z_0$, where $\alpha \in [1, \infty]$,

$$\frac{\epsilon\widehat{c_s^2}}{z_0^2}\alpha^{1-m}\left[\epsilon\alpha^{-m}+\alpha\right]\frac{\mathrm{d}^2\xi_z}{\mathrm{d}\alpha^2}+\frac{g\gamma\epsilon^2}{z_0}\alpha^{-2m}\frac{\mathrm{d}\xi_z}{\mathrm{d}\alpha}+\left[\omega^2\left[\epsilon\alpha^{-m}+\alpha\right]^2-N_0^2\left[\epsilon\alpha^{-m}+\alpha\right]-\frac{\epsilon g}{\widehat{H}}\alpha^{-m}\right]\xi_z=0. \tag{3.141}$$

We may apply the WKB method, by seeking a solution of the form

$$\xi_z \sim \left(A_0+\epsilon^{1/2}A_1+\epsilon A_2+\ldots\right)\exp\left(S\left(\alpha\right)\epsilon^{-1/2}\right). \tag{3.142}$$

The parameter m is the polytropic index, which for a convectively stable medium satisfies $m > 3/2$. In the lower layer $z < 0$, hence the term $(1 - z/z_0)^{-m}$ (the varying contribution to the Alfvén speed) decreases as with increasing $|z|$. We do not, therefore, expect a breakdown in the solution as the first term in the square brackets is always smaller in magnitude than the second term. Physically, this is to be expected as the loss of regularity in the isothermal solution was caused by the change in the dominant parameter between c_s and v_A as z increases. In the lower layer the density and pressure vary in such a way that as $|z|$ increases, c_s increases while v_A decreases. Based on the assumption of high-β plasma at $z = 0$ ($\epsilon \ll 1$), the assumption of high-β plasma is valid for the whole lower layer.

Applying the WKB form of the solution, we may determine the phase function S by retaining terms of order ϵ^0 and simplifying gives

$$\frac{\widehat{c_s^2}}{z_0^2}\alpha^{1-m}\left(\frac{\mathrm{d}S}{\mathrm{d}\alpha}\right)^2+\alpha\omega^2-N_0^2=0, \tag{3.143}$$

or

$$\frac{\mathrm{d}S}{\mathrm{d}\alpha}=\pm\frac{z_0}{\widehat{c_s}}\alpha^{\frac{m-1}{2}}\left(N_0^2-\alpha\omega^2\right)^{1/2}=\pm\frac{z_0\mathrm{i}}{\widehat{c_s}}\alpha^{\frac{m-1}{2}}\left(\alpha\omega^2-N_0^2\right)^{1/2}. \tag{3.144}$$

We see the solution oscillates in space if $\omega > N_0$. The function S is given by

$$S = \pm\frac{\mathrm{i}z_0\omega}{\widehat{c_s}}\int \alpha^{(m-1)/2}\left(\alpha - \frac{N_0^2}{\omega^2}\right)^{1/2}\mathrm{d}\alpha. \tag{3.145}$$

We may write S in a more convenient form. To do this we firstly make the variable transformation $t = 1/\alpha$ and Taylor expand the square root term in the integral (which we write in terms of the Pochammer symbol, $(x)_n$, for convenience), so

$$\begin{aligned}
\int \alpha^{(m-1)/2}\left(\alpha - \frac{N_0^2}{\omega^2}\right)^{1/2}\mathrm{d}\alpha &= -\int t^{-m/2-2}\left(1 - \frac{N_0^2 t}{\omega^2}\right)^{1/2}\mathrm{d}t = \\
-\int t^{-m/2-2}\sum_{n=0}^{\infty}\left(-\frac{1}{2}\right)_n\left(\frac{N_0^2}{\omega^2}\right)^n\frac{t^n}{n!}\mathrm{d}t &= t^{-m/2-1}\sum_{n=0}^{\infty}\left(\frac{m}{2}+1-n\right)^{-1}\left(-\frac{1}{2}\right)_n\left(\frac{N_0^2}{\omega^2}\right)^n\frac{t^n}{n!} \\
&= t^{-m/2-1}\frac{2}{m+2}\sum_{n=0}^{\infty}\frac{\left(-\frac{1}{2}\right)_n\left(-1-\frac{m}{2}\right)_n}{\left(-\frac{m}{2}\right)_n}\left(\frac{N_0^2}{\omega^2}\right)^n\frac{t^n}{n!} \\
&= \frac{2}{m+2}t^{-m/2-1}\,{}_2F_1\left(-\frac{1}{2},-1-\frac{m}{2};-\frac{m}{2};\frac{N_0^2 t}{\omega^2}\right).
\end{aligned} \tag{3.146}$$

The phase function S is then given by

$$S = \pm\mathrm{i}\frac{2\omega z_0}{\widehat{c_s}(m+2)}\alpha^{\frac{m+2}{2}}\,{}_2F_1\left(-\frac{1}{2},-1-\frac{m}{2};-\frac{m}{2};\frac{N_0^2}{\alpha\omega^2}\right). \tag{3.147}$$

If $\omega > N_0$, the solution is always inside of the radius of convergence of the hypergeometric function around zero. If we choose to study, for example, a driven problem such that $\omega < N_0$, we may use Euler's hypergeometric transformations to obtain the correct solution. This is the reason for introducing t above; to obtain the form of the solution valid when $\omega > N_0$. We note that the condition for convergence of the hypergeometric series is that of the Taylor expansion used to determine the integral, as expected. We also see that the function converges absolutely on the unit circle as $c-a-b = 3/2$.

To determine the leading order term in the amplitude we keep terms of order $\epsilon^{1/2}$ leading to

$$2\frac{\mathrm{d}A_0}{\mathrm{d}\alpha}\frac{\mathrm{d}S}{\mathrm{d}\alpha} + A_0\frac{\mathrm{d}^2 S}{\mathrm{d}\alpha^2} = 0. \tag{3.148}$$

Using the positive root of S' given by the zero-th order approximation, gives

$$\frac{\mathrm{d}A_0}{\mathrm{d}\alpha} + \frac{A_0}{4}\left[(m-1)\alpha^{-1} + \omega^2\left(\alpha\omega^2 - N_0^2\right)^{-1}\right] = 0, \tag{3.149}$$

this separable equation may be integrated to give

$$\log A_0 = \frac{1-m}{4}\log\alpha - \frac{1}{4}\log\left(\alpha\omega^2 - N_0^2\right) + C_1^*, \tag{3.150}$$

or

$$A_0 = C_1\left[\frac{\alpha^{1-m}}{\alpha\omega^2 - N_0^2}\right]^{1/4}. \tag{3.151}$$

It can be shown that choosing the negative root in S' returns the same solution for A_0. It is interesting to note the behaviour as $z \to -\infty$. When α is large, the denominator acts like α, hence A_0 is asymptotic to $\alpha^{-m/4}$. In the limit $\alpha \to \infty$, $A_0 \to 0$ as m is some real number greater than $3/2$. Let us now work out the term A_1 by applying the WKB method to order ϵ. The equation to be solved is

$$\frac{\widehat{c_s^2}}{z_0^2}\alpha^2\left(2\frac{\mathrm{d}A_1}{\mathrm{d}\alpha}\frac{\mathrm{d}S}{\mathrm{d}\alpha} + A_1\frac{\mathrm{d}^2S}{\mathrm{d}\alpha^2}\right) + \frac{\widehat{c_s^2}}{z_0^2}\alpha^2\frac{\mathrm{d}^2A_0}{\mathrm{d}\alpha^2} + \left[\frac{\widehat{c_s^2}}{z_0^2}\alpha^{1-m}\left(\frac{\mathrm{d}S}{\mathrm{d}\alpha}\right)^2 + 2\omega^2 - N_0^2 - \frac{g}{\widehat{H}}\right]A_0 = 0, \tag{3.152}$$

or

$$\frac{\mathrm{d}A_1}{\mathrm{d}\alpha} + \frac{1}{4}\left(\frac{m-1}{\alpha} + \frac{\omega^2}{\alpha\omega^2 - N_0^2}\right)A_1 + \frac{\alpha^{\frac{1-m}{2}}}{2}\left(N_0^2 - \alpha\omega^2\right)^{-1/2}\left(\frac{\widehat{c_s}}{z_0}\frac{\mathrm{d}^2A_0}{\mathrm{d}\alpha^2} + \frac{z_0}{\widehat{c_s}}\alpha^{-2}\left(\alpha\omega^2 - \frac{g}{\widehat{H}}\right)A_0\right) = 0. \tag{3.153}$$

Multiplying by the integrating factor $\left(\alpha^{m-1}\left(\alpha\omega^2 - N_0^2\right)\right)^{1/4}$ and substituting the expression for A_0,

$$\begin{aligned}&\frac{\mathrm{d}}{\mathrm{d}\alpha}\left(\alpha^{\frac{m-1}{4}}\left(\alpha\omega^2 - N_0^2\right)^{1/4}A_1\right) = \\ &-\frac{C_1\widehat{c_s}\mathrm{i}}{32z_0}\alpha^{\frac{-3-m}{2}}\left(\alpha\omega^2 - N_0^2\right)^{-5/2}\left[a\alpha^2 + b\alpha + c\right] - \frac{C_1z_0\mathrm{i}}{2\widehat{c_s}}\alpha^{\frac{-3-m}{2}}\left(\alpha\omega^2 - N_0^2\right)^{-1/2}\left(\alpha\omega^2 - \frac{g}{\widehat{H}}\right),\end{aligned} \tag{3.154}$$

where

$$a = \omega^4 m(m+4), \quad b = 2\omega^2N_0^2(1-m)(m+4), \quad c = (m-1)(m+3)N_0^4. \tag{3.155}$$

Integrating the equation for A_1 gives

$$\begin{aligned}\alpha^{\frac{m-1}{4}}\left(\alpha\omega^2 - N_0^2\right)^{1/4}A_1 = &-\frac{C_1\widehat{c_s}\alpha^{-m/2}\mathrm{i}}{16z_0\omega^5}\left[\frac{a\alpha^{-1}}{m+2}\,{}_2F_1\left(\frac{5}{2},\frac{m}{2}+1;\frac{m}{2}+2;\frac{N_0^2}{\omega^2\alpha}\right) + \right.\\ &\left.\frac{b\alpha^{-2}}{m+4}\,{}_2F_1\left(\frac{5}{2},\frac{m}{2}+2;\frac{m}{2}+3;\frac{N_0^2}{\omega^2\alpha}\right) + \frac{c\alpha^{-3}}{m+6}\,{}_2F_1\left(\frac{5}{2},\frac{m}{2}+3;\frac{m}{2}+4;\frac{N_0^2}{\omega^2\alpha}\right)\right] + \\ &\frac{C_1z_0\alpha^{-m/2}\mathrm{i}}{\widehat{c_s}}\left[\frac{\omega}{m}\,{}_2F_1\left(\frac{1}{2},\frac{m}{2};\frac{m}{2}+1;\frac{N_0^2}{\omega^2\alpha}\right) - \frac{g\alpha^{-1}}{\widehat{H}\omega(m+2)}\,{}_2F_1\left(\frac{1}{2},\frac{m}{2}+1;\frac{m}{2}+2;\frac{N_0^2}{\omega^2}\alpha\right)\right] + D_1.\end{aligned} \tag{3.156}$$

It should be noted that the derivation of the above involved the transformation $t = \alpha^{-1}$. This has the advantage of writing the hypergeomtric function in terms of an argument that converges for values of α we use, rather than some over representation of the hyperge-

ometric function. The function A_1 was calculated in the same manner as S previously (details omitted). Some of the hypergeometric functions above also have the issue that $c-a-b<-1$ (where a,b,c are the parameters of the function, not the quantities given by Equation (3.155)) so the series representations of the hypergeometric functions diverge on the unit circle. We may construct a convergent series via Euler's transformations, although we need not concern ourselves with this matter when $\omega > N_0$. The above analysis may be repeated using the negative root of S to determine the wave travelling in the opposite direction.

Let us note the asymptotic behaviour of A_1. Using the fact that

$$ {}_2F_1(a,b;c,z) \approx 1 + \frac{ab}{c}z \quad \text{for} \quad |z| \ll 1, \tag{3.157}$$

we see that in the limit $\alpha \to \infty$,

$$ A_1 \propto \alpha^{-m/4} + \alpha^{-3m/4}\left(1+\alpha^{-1}+\alpha^{-2}+\alpha^{-3}\right), \tag{3.158}$$

note that we have ignored all the coefficients, to focus on how A_1 varies with α. The polytropic index is such that $m > 3/2$, hence the dominant term is $\alpha^{-m/4}$. The asymptotic amplitude of ξ_z can be shown to be (again neglecting the coefficients)

$$ A_0 + \epsilon^{1/2}A_1 \sim \alpha^{-m/4} + \epsilon^{1/2}\alpha^{-m/4}. \tag{3.159}$$

The above expression, coupled with the fact that $\epsilon^{1/2}A_1$ is order $\epsilon^{1/2}$ when $\alpha = 1$, shows that the there is no loss of regularity in the perturbation series for the amplitude of ξ_z.

The WKB solution in the lower layer is then given by

$$ \xi_z \sim \left(C_1\left[\frac{\alpha^{1-m}}{\alpha\omega^2 - N_0^2}\right]^{1/4} + \epsilon^{1/2}A_{1+} + \ldots\right)e^{S/\epsilon^{1/2}} + \left(C_2\left[\frac{\alpha^{1-m}}{\alpha\omega^2 - N_0^2}\right]^{1/4} + \epsilon^{1/2}A_{1-} + \ldots\right)e^{-S/\epsilon^{1/2}}, \tag{3.160}$$

where S is given by taking the positive sign in Equation (3.147).

Let us use the above solution to determine the frequency of standing waves in a one-layer polytropic model. With the WKB solution we may generalise somewhat the dispersion relation of a thin layer found in terms of Airy functions previously. The solution found via the WKB method can then be applied to high-β plasma with an arbitrary temperature scale-height. We now briefly show the equivalence of the WKB solution to the slowly varying solution found previously.

We apply reflecting boundary conditions $\xi_z = 0$, when $z = 0, -L$ or $\alpha = 1, 1 + L/z_0$. For simplicity we apply the boundary conditions to order ϵ^0 (in the perturbation series for the

amplitude), resulting in the equations,

$$C_1\left(\omega^2-N_0^2\right)^{-1/4}\exp(S(1)\epsilon^{-1/2})+C_2\left(\omega^2-N_0^2\right)^{-1/4}\exp(-S(1)\epsilon^{-1/2})=0, \tag{3.161}$$

$$C_1\left[\frac{\left(1+\frac{L}{z_0}\right)^{1-m}}{\left(1+\frac{L}{z_0}\right)\omega^2+N_0}\right]^{1/4}\exp(S\left(1+\frac{L}{z_0}\right)\epsilon^{-1/2}) + C_2\left[\frac{\left(1+\frac{L}{z_0}\right)^{1-m}}{\left(1+\frac{L}{z_0}\right)\omega^2+N_0}\right]^{1/4}\exp(-S\left(1+\frac{L}{z_0}\right)\epsilon^{-1/2})=0. \tag{3.162}$$

The condition for non-trivial solutions for C_1 and C_2 gives the dispersion relation

$$\sin\left(\frac{\epsilon^{-1/2}}{\mathrm{i}}\left[S\left(1+\frac{L}{z_0}\right)-S(1)\right]\right)=0, \tag{3.163}$$

or, using the expression for S,

$$\frac{2\omega z_0}{m+2}\left[\left(1+\frac{L}{z_0}\right)^{\frac{m}{2}+1}{}_2F_1\left(-\frac{1}{2},-1-\frac{m}{2};-\frac{m}{2};\frac{N_0^2}{\omega^2}\left(1+\frac{L}{z_0}\right)^{-1}\right)- {}_2F_1\left(-\frac{1}{2},-1-\frac{m}{2};-\frac{m}{2};\frac{N_0^2}{\omega^2}\right)\right]=\widehat{c}_s\epsilon^{1/2}n\pi. \tag{3.164}$$

Equation (3.164) is the generalisation of the Airy function dispersion relation valid for larger lengths of the cavity. Equation (3.164) cannot be inverted exactly and so a numerical approach may be taken. We may find an analytical expression for the frequency by noting that $N_0/\omega<1$. The hypergeometric functions are a convergent power series in N_0^2/ω^2; if we approximate the series by truncating the series after the second term, *i.e.*,

$$\begin{aligned}{}_2F_1\left(-\frac{1}{2},-1-\frac{m}{2};-\frac{m}{2};\frac{N_0^2}{\omega^2}\right)&\approx 1-\frac{1}{2m}(m+2)\frac{N_0^2}{\omega^2},\\ {}_2F_1\left(-\frac{1}{2},-1-\frac{m}{2};-\frac{m}{2};\frac{N_0^2}{\omega^2}\left(1+\frac{L}{z_0}\right)^{-1}\right)&\approx 1-\frac{1}{2m}(m+2)\left(1+\frac{L}{z_0}\right)^{-1}\frac{N_0^2}{\omega^2},\end{aligned} \tag{3.165}$$

the dispersion relation may be approximated by

$$\frac{2z_0}{m+2}\left[\left(1+\frac{L}{z_0}\right)^{\frac{m}{2}+1}-1\right]\omega^2-\widehat{c}_s\epsilon^{1/2}n\pi\omega+\frac{z_0N_0^2}{m}\left[1-\left(1+\frac{L}{z_0}\right)^{\frac{m}{2}}\right]=0. \tag{3.166}$$

The frequency is given by

$$\omega = \frac{\widehat{v}_A n\pi(m+2)}{4z_0}\left[\left(1+\frac{L}{z_0}\right)^{\frac{m}{2}+1}-1\right]^{-1}+$$
$$\frac{m+2}{4}\left[\left(1+\frac{L}{z_0}\right)^{\frac{m}{2}+1}-1\right]^{-1}\left[\frac{\widehat{v}_A^2 n^2\pi^2}{z_0^2}-\frac{8N_0^2}{m(m+2)}\left(\left(1+\frac{L}{z_0}\right)^{\frac{m}{2}+1}-1\right)\left(1-\left(1+\frac{L}{z_0}\right)^{\frac{m}{2}}\right)\right]^{1/2}. \tag{3.167}$$

It is helpful to consider the case of a thin lower layer $L/z_0 \ll 1$, under this approximation

$$\omega \approx \frac{\widehat{v}_A n\pi}{2L}+\frac{z_0}{2L}\left[\frac{\widehat{v}_A^2 n^2\pi^2}{z_0^2}+2N_0^2\frac{L^2}{z_0^2}\right]^{1/2}. \tag{3.168}$$

We may further simplify the expression by expanding the square root around the small parameter L/z_0,

$$\omega \approx \frac{\widehat{v}_A n\pi}{L}+\frac{N_0^2 L}{2\widehat{v}_A n\pi}. \tag{3.169}$$

Let us consider the frequency derived from the starting point of a thin layer,

$$\omega = \left(\frac{\widehat{v}_A^2 n^2\pi^2}{L^2}+N_0^2\right)^{1/2}. \tag{3.170}$$

This may be written

$$1 = \left(\frac{n^2\pi^2\widehat{v}_A^2}{\omega^2 L^2}+\frac{N_0^2}{\omega^2}\right)^{1/2}. \tag{3.171}$$

If we assume that $\omega^2/N_0^2 < 1$ we may approximate the square root as

$$1 \approx \frac{n\pi\widehat{v}_A}{\omega L}+\frac{\omega L}{2n\pi\widehat{v}_A}\frac{N_0^2}{\omega^2} \implies \omega \approx \frac{n\pi\widehat{v}_A}{L}+\frac{LN_0^2}{2n\pi\widehat{v}_A}. \tag{3.172}$$

This shows that taking equivalent limits return the same expression for the frequency, as they should. That is, assuming N_0/ω is small in the dispersion relation found from the starting point of a thin layer ($L/z_0 \ll 1$) and assuming L/z_0 and N_0/ω are small in the hypergeometric (WKB) solution are the same. It should be noted that ω grows significantly larger than N_0 as n increases. This justifies the truncation of the hypergeometric series used a priori.

The dispersion relation, Equation (3.164), may also be used to investigate a larger cavity. Let us take the asymptotic limit $L/z_0 \to \infty$. In this limit the dispersion relation reduces to

$$\frac{2\omega z_0}{m+2}\left[\left(\frac{L}{z_0}\right)^{\frac{m+2}{2}}-{}_2F_1\left(-\frac{1}{2},-1-\frac{m}{2};-\frac{m}{2};\frac{N_0^2}{\omega^2}\right)\right]=\widehat{v}_A n\pi. \tag{3.173}$$

When n is sufficiently large, we may neglect the hypergeometric function to give

$$\omega \sim \frac{(m+2)\widehat{v}_A n\pi}{2z_0}\left(\frac{L}{z_0}\right)^{\frac{-2-m}{2}}. \tag{3.174}$$

We recognise this as the eigenfrequency (3.64) in the limit or large n. Note that it can be shown that when the frequency takes this form, the hypergeometric function can indeed be neglected, that is, there are no inconsistencies in the above analysis. We see, therefore, that the dispersion relation (3.164) represents a generalisation of the one-layer models considered previously.

Now that we have investigated the lower layer and have the solution in a suitable form, let us connect the solutions to these two layers together.

3.2.3.3 Connection of the Layers

We form a two-layer model by applying two appropriate boundary conditions at the interface $z = 0$. We also need to apply an extra boundary condition in the lower layer to close the system of equations. We use the subscripts i and e to denote the lower interior and upper exterior layers, respectively. For simplicity let us apply a rigid boundary at $z = -L$ as in the one-layer model

$$\xi_{zi} = 0 \quad \text{at} \quad z = -L. \tag{3.175}$$

The second boundary condition is the continuity of displacement at $z = 0$,

$$\xi_{zi} = \xi_{ze} \quad \text{at} \quad z = 0. \tag{3.176}$$

We make the assumption that the density (and temperature) are continuous at $z = 0$, when this is the case the continuity of (Lagrangian) pressure perturbation is a restatement of the continuity of displacement. A discontinuous density acts as a reflecting barrier; if this is the case the frequencies are those given by the single layer above. Note that this is only the case for a significant density discontinuity. If the discontinuity is small or infinitesimal we Taylor expand the boundary conditions. To first order, the boundary condition is independent of the jump in density. We use the condition of continuity of magnetic field $\mathbf{B}_1 \cdot \mathbf{n}$ where $\mathbf{n}$ is the unit normal vector to the boundary; or $B_{1zi} = B_{1ze}$. In terms of ξ_z this condition can be written

$$\frac{\mathrm{d}\xi_{zi}}{\mathrm{d}z} = \frac{\mathrm{d}\xi_{ze}}{\mathrm{d}z} \quad \text{at} \quad z = 0. \tag{3.177}$$

When applying these boundary condition to the asymptotic solutions we apply them in turn at each order. Due to the complicated nature of the second order terms we will, for simplicity, only apply the boundary conditions to leading order. To leading order the

boundary conditions give us the equations

$$C_1 \exp\left[S_i(-L)\epsilon^{-1/2}\right] + C_2 \exp\left[-S_i(-L)\epsilon^{-1/2}\right] = 0, \tag{3.178}$$

$$C_1\left(\omega^2 - N_0^2\right)^{-1/4} \exp\left[S_i(0)\epsilon^{-1/2}\right] + C_2\left(\omega^2 - N_0^2\right)^{-1/4} \exp\left[-S_i(0)\epsilon^{-1/2}\right] - D_1 \exp\left[-S_e(0)\epsilon^{-1/2}\right] = 0, \tag{3.179}$$

$$\frac{C_1}{z_0}\left(\omega^2 - N_0^2\right)^{-1/4} S_i'|_0 \exp\left[S_i(0)\epsilon^{-1/2}\right] - \frac{C_2}{z_0}\left(\omega^2 - N_0^2\right)^{-1/4} S_i'|_0 \exp\left[-S_i(0)\epsilon^{-1/2}\right] - \frac{D_1}{H} S_e'|_0 \exp\left[-S_e(0)\epsilon^{-1/2}\right] = 0. \tag{3.180}$$

Note that the derivative of $S_{i,e}$ in the third boundary condition is with respect to the argument of the function, not z itself. The upper boundary condition of finite kinetic energy density has been applied during the method of matched asymptotic expansions to the isothermal solution. For non-trivial solutions the determinant of the system of equation must be zero. After some algebra the dispersion relation takes the form

$$\tan Q = \mathrm{i}\frac{\left(\omega^2 - N_0^2\right)^{1/2}}{\left(\omega^2 - N^2\right)^{1/2}}, \tag{3.181}$$

where

$$Q = \frac{2\omega z_0}{\widehat{v}_A(m+2)}\left[\left(1 + \frac{L}{z_0}\right)^{\frac{m+2}{2}} {}_2F_1\left(-\frac{1}{2}, -1 - \frac{m}{2}; -\frac{m}{2}; \frac{N_0^2}{\omega^2}\left(1 + \frac{L}{z_0}\right)^{-1}\right) - {}_2F_1\left(-\frac{1}{2}, -1 - \frac{m}{2}; -\frac{m}{2}; \frac{N_0^2}{\omega^2}\right)\right]. \tag{3.182}$$

The dispersion relation reveals a surprising consequence for waves in the two-layer model. Let us begin by noting that for real parameters, Q, and so $\tan Q$, are real. The dispersion relation only has solutions when the right-hand side is real. To see more clearly we may square both sides of the dispersion relation to give

$$\tan^2 Q = -\frac{\omega^2 - N_0^2}{\omega^2 - N^2}. \tag{3.183}$$

Real solutions of the dispersion relation exist only if the right-hand side is positive. Noting that $N_0 < N$, this is only possible if $N_0 < \omega < N$. The waves exist above the lower cut-off N_0 as in the one-layer model, but there is now an upper cut-off. The effect of adding an upper layer is then to introduce a cut-off effect. This may be a manifestation of the boundary condition at infinity, although this is surprising as the requirement for this condition to be met is ω is less than the *acoustic* cut-off Ω. This boundary condition is met whether the

solution is oscillatory or not in the high-β regime; that is, the upper boundary condition is satisfied for both $\omega < N$ and $N < \omega < \Omega$.

This cut-off effect would have significant implications for solar oscillations. It is well known that g-modes decay throughout the solar convection zone and so they are not easily observable in the atmosphere. A magnetic field can inhibit convection and so provide a channel for these slow MHD modes to propagate into the solar atmosphere. The above analysis suggests that the atmosphere itself may act to stop the wave propagation. It is usually the case that N_0 is close to N, hence there is only a narrow band of frequencies which may exist. This may add to the reasons that g-modes are difficult to observe in the solar atmosphere.

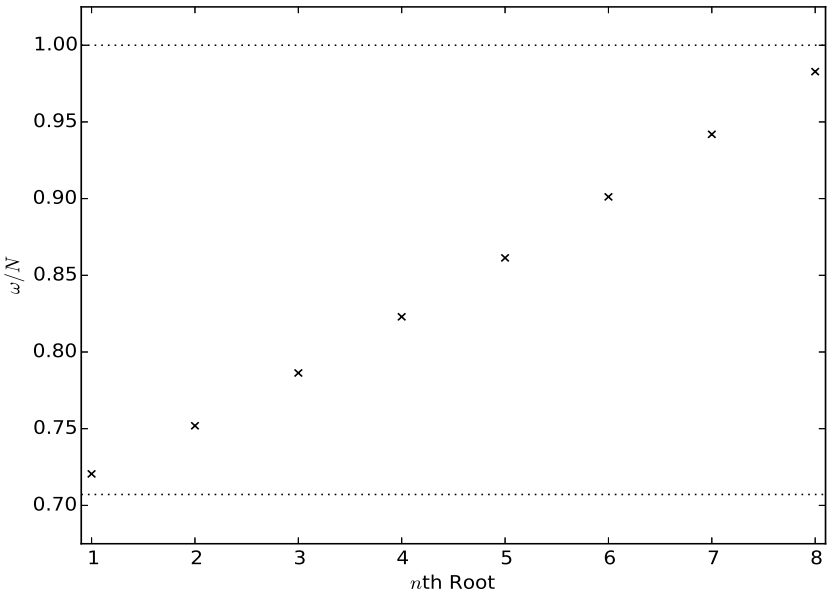

Fig. 3.3 Numerical solutions to Equation (3.181).

Numerical solutions to the dispersion relation, normalised to the Brunt-Väisälä frequency in the upper layer, are plotted in Figure 3.3. Typical values representing the lower solar atmosphere are used for the parameters, $g = 0.274$ km s^{-2}, $\gamma = 5/3$, $c_s = 8$ km s^{-1}. The Alfvén speed is 0.8 km s^{-1}, so that $\epsilon^{1/2} = 0.1$. We take $L = z_0 = 5H$. This choice of temperature scale height matches with estimates of the Brunt-Väisälä frequency in the lower solar atmosphere. The depth of the lower layer, L, is chosen to represent the photosphere and low chromosphere. Using these parameters, the polytropic index m is approximately 4, and the Brunt-Väisälä frequencies are $N_0 \approx 0.02$ s^{-1} and $N \approx 0.03$ s^{-1}. As $N_0 < N$, there are real solutions to the dispersion relation, as shown in Figure 3.3. The upper dotted line marks N, while the lower is N_0; we clearly see the frequencies are located between the two dotted lines. It can be shown that there are no other real solutions to the dispersion relation. For the parameters used, there are precisely 8 solutions to the dispersion relation, the first of which is close to N_0. In the solar atmosphere, we therefore

expect that the number of overtones of buoyancy-driven MHD waves is relatively low. The difference, in frequency, between the modes is small; observing distinct overtones may be challenging.

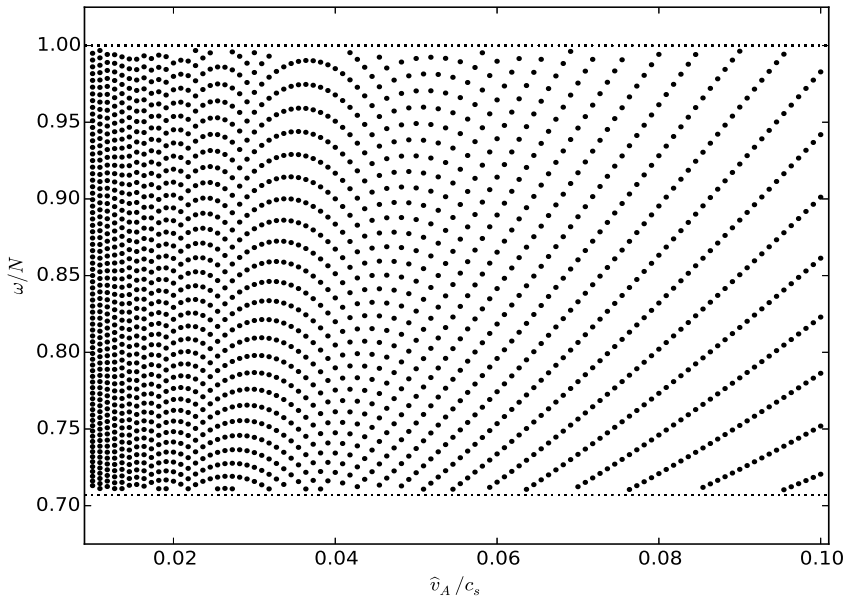

Fig. 3.4 Numerical solutions to Equation (3.181).

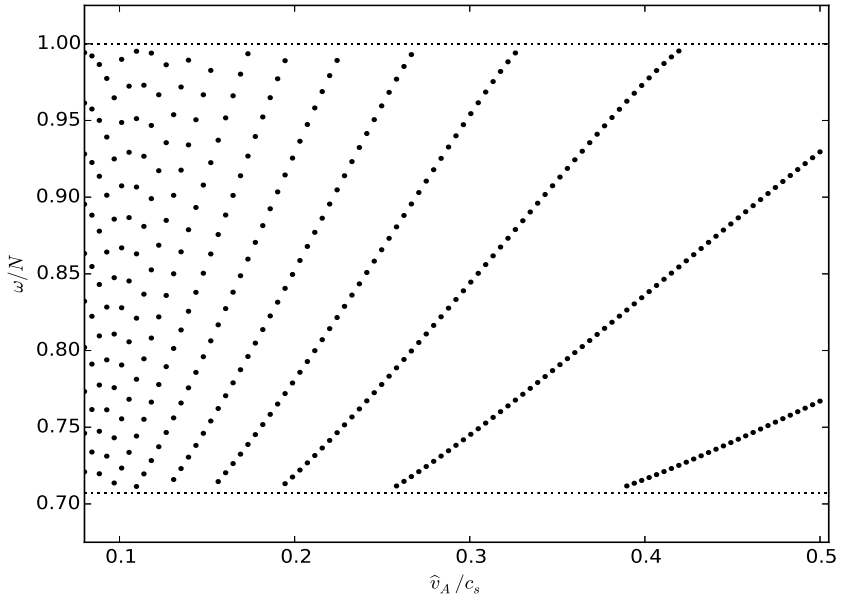

Fig. 3.5 Numerical solutions to Equation (3.181).

Figures 3.4 and 3.5 show the effect of varying the Alfvén speed. The other parameters are as in Figure 3.3. Each marker shows a solution to Equation (3.181), normalised to the

Brunt-Väisälä frequency in the upper layer, N. The horizontal dotted lines mark the Brunt-Väisälä frequencies. Figure 3.4 shows solutions where $\epsilon^{1/2}$ takes values between 0.01 and 0.1. The first notable point is that while the Brunt-Väisälä frequencies are relatively close together there can be many oscillating solutions that exist. The number of solutions that exist decreases as ϵ increases. This is due to the proportionality of the eigenfrequency to the phase speed; increasing ϵ increases the phase speed of the waves. Increasing n increases the vertical wavenumber, and so there are fewer modes which may exist within the range of frequencies. We may see this fact by noting that distance between branches of frequency, for a given ϵ, is $\Delta\omega = c_{ph}\Delta k_z$. When $\epsilon^{1/2} = 0.1$, the 8 solutions are those plotted in Figure 3.3. This trend is continued in Figure 3.5 for higher values of ϵ.

Following a given root, we see that the eigenfrequency of the wave increases with ϵ as in the one-layer case. The key difference is that due to the cut-off effect of the upper layer the waves do not take on a magnetic character as in the one-layer case. The rate at which the frequency of the wave increase decreases with ϵ, suggesting that ω depends on ϵ^n where $0 < n < 1$.

We may investigate these frequencies analytically. We begin by taking the inverse tangent function of the dispersion relation (3.181),

$$\frac{2\omega z_0}{\widehat{v}_A(m+2)}\left[\left(1+\frac{L}{z_0}\right)^{\frac{m+2}{2}} {}_2F_1\left(-\frac{1}{2},-1-\frac{m}{2};-\frac{m}{2};\frac{N_0^2}{\omega^2}\left(1+\frac{L}{z_0}\right)^{-1}\right)\right.$$
$$\left. - {}_2F_1\left(-\frac{1}{2},-1-\frac{m}{2};-\frac{m}{2};\frac{N_0^2}{\omega^2}\right)\right] = n\pi + \arctan\left[-\frac{\left(\omega^2-N_0^2\right)^{1/2}}{\left(N^2-\omega^2\right)^{1/2}}\right], \quad n = 0,1,2,\ldots. \tag{3.184}$$

The factor $n\pi$ is due to the periodicity of the tangent function. The dispersion relation may be simplified if we assume that ω is close to N_0, this assumption is likely to be valid due to the fact that ω is between N_0 and N. We will Taylor expand the inverse tangent function. To see the conditions for this series to converge let us write the frequency as $\omega^2 = N_0^2 + \delta^2$, where $\delta \ll N_0$. The argument of the inverse tangent function is then

$$\frac{\delta/N_0}{\left(\frac{g}{z_0N_0}-\frac{\delta^2}{N_0^2}\right)^{1/2}} \approx \delta\left(\frac{g}{z_0}\right)^{-1/2} \tag{3.185}$$

The series form of the inverse tangent has a radius of convergence 1 (due to singularities at ±i). The series then converges for $\delta(g/z_0)^{-1/2} < 1$ or $\delta^2 < g/z_0$. That is, the Taylor series converges for frequencies within the interval of propagation. For simplicity, let us assume the parameters are such that we may approximate the function by the first term in its Taylor series. Strictly speaking, this requires that $\delta^2 \ll g/z_0$, although we proceed in a non-rigorous way specifying only that $\delta^2 < g/z_0$. In the interest of simplicity we shall adopt a non-rigorous approach until a more rigorous solution presents itself. Letting

$\omega \approx N_0$, the dispersion relation may be written

$$\frac{2\omega z_0}{\widehat{v}_A(m+2)}\left[\left(1+\frac{L}{z_0}\right)^{\frac{m+2}{2}} {}_2F_1\left(-\frac{1}{2},-1-\frac{m}{2};-\frac{m}{2};\left(1+\frac{L}{z_0}\right)^{-1}\right) - \frac{1}{2}B\left(\frac{1}{2},-\frac{m}{2}\right)\right] - n\pi = -\frac{\left(\omega^2-N_0^2\right)^{1/2}}{\left(N^2-\omega^2\right)^{1/2}}, \quad (3.186)$$

where we have used the fact that

$${}_2F_1\left(-\frac{1}{2},-1-\frac{m}{2};-\frac{m}{2};\frac{N_0^2}{\omega^2}\right) \approx {}_2F_1\left(-\frac{1}{2},-1-\frac{m}{2};-\frac{m}{2};1\right) = \frac{1}{2}B\left(\frac{1}{2},-\frac{m}{2}\right), \quad (3.187)$$

where $B(x,y)$ denotes the Beta function (Abramowitz & Stegun, 1972). Squaring each side of Equation (3.186), the dispersion relation can be approximated by

$$\left[\frac{4z_0^2\omega^2A^2}{\widehat{v}_A^2(m+2)^2} - \frac{4z_0 n\pi\omega A}{\widehat{v}_A(m+2)} + n^2\pi^2\right]\left(N^2-\omega^2\right) = \omega^2 - N_0^2, \quad (3.188)$$

where

$$A = \left(1+\frac{L}{z_0}\right)^{\frac{m+2}{2}} {}_2F_1\left(-\frac{1}{2},-1-\frac{m}{2};-\frac{m}{2};\left(1+\frac{L}{z_0}\right)^{-1}\right) - \frac{1}{2}B\left(\frac{1}{2},-\frac{m}{2}\right). \quad (3.189)$$

The exact dispersion relation was a transcendental equation that could not be inverted; the simplified equation is a quartic polynomial. Quartic polynomials may be solved analytically but the solution is very complex. It is perhaps more instructive to simplify the dispersion relation further rather than finding the solution to the quartic equation. Let us consider the case of slow temperature variation, $L/z_0 \ll 1$, as in Section 3.2.2. Under this approximation,

$$\begin{aligned} {}_2F_1\left(-\frac{1}{2},-1-\frac{m}{2};-\frac{m}{2};\left(1+\frac{L}{z_0}\right)^{-1}\right) &\approx {}_2F_1\left(-\frac{1}{2},-1-\frac{m}{2};-\frac{m}{2};1-\frac{L}{z_0}\right) \\ &\approx {}_2F_1\left(-\frac{1}{2},-1-\frac{m}{2};-\frac{m}{2};1\right) + \frac{m+2}{2m}\,{}_2F_1\left(\frac{1}{2},-\frac{m}{2};1-\frac{m}{2};1\right)\frac{L}{z_0} + O\left(\frac{L^2}{z_0}\right) \\ &= \frac{1}{2}B\left(\frac{1}{2},-\frac{m}{2}\right)\left[1-\frac{2+m}{2}\frac{L}{z_0}+O\left(\frac{L^2}{z_0^2}\right)\right], \end{aligned} \quad (3.190)$$

and so

$$\begin{aligned} A &\approx \left[1+\frac{m+2}{2}\frac{L}{z_0}+O\left(\frac{L^2}{z_0^2}\right)\right]\frac{1}{2}B\left(\frac{1}{2},-\frac{m}{2}\right)\left[1-\frac{2+m}{2}\frac{L}{z_0}+O\left(\frac{L^2}{z_0^2}\right)\right] - \frac{1}{2}B\left(\frac{1}{2},-\frac{m}{2}\right) \\ &= \frac{1}{2}B\left(\frac{1}{2},-\frac{m}{2}\right)O\left(\frac{L^2}{z_0^2}\right). \end{aligned} \quad (3.191)$$

To first order in the parameter L/z_0, we may approximate A by zero, and so the eigenfrequencies of the two-layer model may be approximated by

$$\omega^2 = \frac{n^2\pi^2 N^2 + N_0^2}{1 + n^2\pi^2}. \tag{3.192}$$

For $n = 0$, the frequency is approximately N_0; while as $n \to \infty$, $\omega \to N^2$. We, therefore, see that the frequencies are located between the Brunt-Väisälä frequencies and how they transition from one to another. It is worth noting that the Alfvén speed does not appear in the expression for the frequency when approximated to leading order in L/z_0. The explicit dependence on the magnetic parameter can be seen via the numerical solutions to the exact dispersion relation, plotted in Figures 3.4 and 3.5. The effect of the magnetic field may be seen implicitly via the fact that the frequencies increase with n, as opposed to well known decrease seen in a hydrodynamic system.

Analytical progress may also be achieved based on other approximations, for example when the lower layer is close to adiabatic $N_0 \approx 0$. For details see Appendix A.

3.2.4 A Note on Mode Conversion

The coupled equations (3.1) and (3.2) allow for mode conversion between slow and fast MAG waves. Mode conversion occurs at points where the phase speeds, and so frequencies for a given wavenumber (*i.e.* avoided crossings), are equal and allows energy to be transmitted between wave modes. This typically occurs when the sound and Alfvén speeds are equal (or close when gravitational effects are included). In the above analysis we have concentrated only on the slow mode without considering the possibility of mode conversion. Let us now see if this was a feasible approach.

Let us perform a local (WKB) analysis of the frequencies of MAG modes. Mode conversion is possible if the local frequencies of the modes are close. The WKB method is restricted to the case when the medium varies slowly. Although this is not entirely applicable to the solar atmosphere, where the background may vary exponentially, it allows for some insight into the problem.

We begin by Fourier analysing in the x-direction, and introducing a slowly varying vertical variable $\widetilde{z} = \epsilon z$. Applying the WKB ansatz, we substitute

$$\xi_x = \widehat{\xi}_x(\widetilde{z})\, e^{\mathrm{i}\theta(\widetilde{z})/\epsilon}, \quad \xi_z = \widehat{\xi}_z(\widetilde{z})\, e^{\mathrm{i}\theta(\widetilde{z})/\epsilon}, \tag{3.193}$$

into Equations (3.1) and (3.2). Retaining the dominant terms (neglecting terms of order ϵ and higher) leaves the equations

$$\left[\omega^2 - k_x^2\left(c_s^2 + v_A^2\right) - v_A^2(\theta')^2\right]\widehat{\xi}_x = \mathrm{i}k_x\left(g - \mathrm{i}c_s^2\theta'\right)\widehat{\xi}_z, \tag{3.194}$$

$$\left[\omega^2 - \mathrm{i}g\gamma\theta' - c_s^2(\theta')^2\right]\widehat{\xi_z} = \mathrm{i}k_x\left[g(\gamma-1) - \mathrm{i}c_s^2\theta'\right]\widehat{\xi_x}. \tag{3.195}$$

Elimination of either of the displacement amplitudes leads to the local dispersion relation

$$\omega^4 - \left(k^2\left(c_s^2+v_A^2\right) + \mathrm{i}g\gamma k_z\right)\omega^2 + c_s^2v_A^2k_z^2k^2 + k_x^2g^2(\gamma-1) + \mathrm{i}g\gamma v_A^2k_zk^2 = 0, \tag{3.196}$$

where $k_z \equiv \theta'$ and $k^2 = k_x^2 + k_z^2$. This local dispersion relation has been studied previously by *e.g.* MacDonald (1961), Thomas (1982). The two modes are given by the roots, *i.e.*

$$\omega^2 = \frac{1}{2}\left(k^2\left(c_s^2+v_A^2\right) + \mathrm{i}g\gamma k_z\right) \pm \frac{1}{2}\Big[\left(k^2\left(c_s^2+v_A^2\right) + \mathrm{i}g\gamma k_z\right)^2 - 4\left(c_s^2v_A^2k_z^2k^2 + k_x^2g^2(\gamma-1) + \mathrm{i}g\gamma v_A^2k_zk^2\right)\Big]^{1/2}. \tag{3.197}$$

Mode conversion typically occurs when c_s is close to v_A; hence let us equate the two speeds $c_s = v_A = v$, the corresponding frequencies are

$$\omega^2 = \frac{1}{2}\left(2k^2v^2 + \mathrm{i}g\gamma k_z\right) \pm \frac{1}{2}\sqrt{\left(2k^2v^2 + \mathrm{i}g\gamma k_z\right)^2 - 4\left(v^4k_z^2k^2 + k_x^2g^2(\gamma-1) + \mathrm{i}g\gamma v^2k_zk^2\right)}. \tag{3.198}$$

In our previous analysis we removed fast modes from consideration by taking the small horizontal wavelength limit, $k_xH \to \infty$. In the same limit, the local frequencies may be approximated by

$$\omega^2 \approx k_x^2v^2 + \frac{g\gamma}{2}\mathrm{i}k_z \pm k_x^2\sqrt{v^4 - \frac{v^4k_z^2 + g^2(\gamma-1)}{k_x^2}} \approx k_x^2v^2 + \frac{g\gamma}{2}\mathrm{i}k_z \pm \left(k_x^2v^2 - \frac{g^2(\gamma-1)}{2v^2} - \frac{1}{2}v^2k_z^2\right), \tag{3.199}$$

hence $\omega^2 \approx \left(v^2k_z^2 + N^2 + g\gamma k_z\mathrm{i}\right)/2,\ 2k_x^2v^2$. We see there is a large separation between the modes and so mode conversion may be neglected in our previous analysis.

It should be noted that the WKB method fails in regions where mode conversion takes place as the WKB method assumes distinct modes. The problem has been addressed by Cally (2005), for a vertical field, using a perturbation method and Cally (2006), for an inclined field, using a variational method founded by Tracy, Kaufman & Brizard (2003). When the magnetic field is vertical the two approaches yield the same results. Schunker & Cally (2006) extended the previous work stressing the field inclination and the role of the so-called attack angle in mode conversion.

It was shown by Cally (2006) that the transmission coefficient (here transmission means transmission from the slow branch to fast or vice versa), where gravitational effects are neglected, is given by

$$T = \exp\left[-\frac{\pi k_\perp^2}{k_z\left|\frac{\mathrm{d}}{\mathrm{d}z}\frac{c_s^2}{v_A^2}\right|}\right]\Bigg|_{c_s=v_A}. \tag{3.200}$$

The derivative term is a measure of the thickness of the layer over which mode conversion takes place. We see that $T \to 0$ when the horizontal wavelength is large, hence, as we noted in the WKB analysis, the effects of mode conversion may be ignored.

3.2.5 The Effect of Partial Ionisation

Magnetohydrodynamic effects are observed in the lower solar atmosphere. Sunspots, pores, bright points etc. show that magnetic fields do indeed interact with the solar plasma in the photosphere. In our analysis we have so far assumed that the particles are ionised and so we may use an MHD description of the fluid. In reality, the solar plasma is not composed of fully ionised hydrogen particles, rather the fluid also consists of neutral hydrogen particles (and some heaver elements which may display varying levels of ionisation). To include the effects of the magnetic field we employ the most simple MHD model, a single-fluid description. To include the more realistic effects of partial ionisation, we may have to use a modified description of MHD. A three-fluid description of a plasma, where distinctions are made between electrons, ions and neutral hydrogen is discussed by *e.g.* Braginskii (1965). MHD waves in a two-fluid MHD model (where the electrons and ions may be considered as a single fluid, valid for time scales longer than the ion-electron collision time) were studied by *e.g.* Zaqarashvili, Khodachenko & Rucker (2011b), Soler, Carbonell & Ballester (2013), Soler *et al.* (2013b,c). Note that these alternate MHD models do not include the effects of elemental abundances, although these effects are included in many widely used numerical codes. Alfvén waves in plasma containing hydrogen and helium were studied by Zaqarashvili, Khodachenko & Rucker (2011a).

The effect of partial ionisation on Alfvén waves have been studied by *e.g* Haerendel (1992), De Pontieu & Haerendel (1998), James & Erdélyi (2002), James, Erdélyi & De Pontieu (2003), Erdélyi & James (2004), Leake, Arber & Khodachenko (2005), Vranjes *et al.* (2008) to name but a few. Some of these works suggested the damping of Alfvén waves as a mechanism for the formation of spicules. The damping of MHD waves in partially ionised plasmas was studied by *e.g.* Khodachenko *et al.* (2004), Forteza *et al.* (2007), Forteza, Oliver & Ballester (2008), Soler, Oliver & Ballester (2009a,b, 2010), Carbonell *et al.* (2010). These works did not consider a two-fluid model; rather used a single fluid description where the fluid consists of ions and neutrals. This is valid on time scales much greater than the ion-neutral collision time. For a discussion on the differences between a two-fluid model and a single-fluid model see Zaqarashvili *et al.* (2011b). Instabilities in partially ionised plasmas have been studied by *e.g.* Soler *et al.* (2012), Díaz, Soler & Ballester (2012), Ballai, Oliver & Alexandrou (2015).

To study the effects of partial ionisation we use a two-fluid model. This approach treats the plasma as a mixture of an ion-electron gas and a neutral hydrogen gas. The ion-electron gas is taken to be quasi-neutral ($n_i \approx n_e$). We are interested in the effect of partial ionisation on buoyancy-driven MHD waves, hence we apply the Boussinesq approximation to the ion-electron and neutral gasses. For simplicity, we neglect the Hall

term, magnetic diffusion, and collisions between electrons and neutrals. The linearised equations are

$$\nabla\cdot\rho_{n0}\mathbf{v_{n1}}=0,\quad \nabla\cdot\rho_{i0}\mathbf{v_{i1}}=0, \tag{3.201}$$

$$\rho_{n0}\frac{\partial\mathbf{v_{n1}}}{\partial t}=-\nabla p_{n1}+\alpha_{in}\left(\mathbf{v_{i1}}-\mathbf{v_{n1}}\right)+\rho_{n1}\mathbf{g}, \tag{3.202}$$

$$\rho_{i0}\frac{\partial\mathbf{v_{i1}}}{\partial t}=-\nabla p_{i1}-\nabla\left(\frac{B_0B_{1z}}{\mu}\right)+\frac{1}{\mu}\frac{\partial\mathbf{B_1}}{\partial z}-\alpha_{in}\left(\mathbf{v_{i1}}-\mathbf{v_{n1}}\right)+\rho_{n1}\mathbf{g}, \tag{3.203}$$

$$\frac{\partial\mathbf{B_1}}{\partial t}=B_0\frac{\partial\mathbf{v_{i1}}}{\partial z}-\mathbf{B_0}\nabla\cdot\mathbf{v_{i1}},\quad \nabla\cdot\mathbf{B_1}=0, \tag{3.204}$$

$$\frac{\partial\rho_{n1}}{\partial t}=\frac{N_n^2\rho_{n0}}{g}v_{n1z},\quad \frac{\partial\rho_{i1}}{\partial t}=\frac{N_i^2\rho_{i0}}{g}v_{i1z}, \tag{3.205}$$

where the subscripts n and i refer to the neutral and ionised fluids, respectively, and α_{in} is the equilibrium coefficient of friction between neutrals and ions. We assume no y-dependence, so that we may separate Alfvén and slow waves. The Alfvén waves are given by the y-component of the velocity field, which we do not consider. First, we Fourier analyse in x and t; some algebra leads to the coupled governing equations for the vertical velocity components,

$$\begin{aligned}\mathrm{i}\omega\left[\frac{\mathrm{d}}{\mathrm{d}z}\frac{\alpha_{in}}{\rho_{i0}}\frac{\mathrm{d}}{\mathrm{d}z}\rho_{i0}v_{iz}-\alpha_{in}k_x^2v_{iz}\right]=&\\ \omega^2\frac{\mathrm{d}^2}{\mathrm{d}z^2}\rho_{n0}v_{nz}+\mathrm{i}\omega\frac{\mathrm{d}}{\mathrm{d}}\frac{\alpha_{in}}{\rho_{n0}}\frac{\mathrm{d}}{\mathrm{d}z}\rho_{n0}v_{nz}+k_x^2\left(\rho_{n0}N_n^2-\rho_{n0}\omega^2-\mathrm{i}\omega\alpha_{in}\right)v_{nz},&\end{aligned} \tag{3.206}$$

$$\begin{aligned}\mathrm{i}\omega\left[\frac{\mathrm{d}}{\mathrm{d}z}\frac{\alpha_{in}}{\rho_{n0}}\frac{\mathrm{d}}{\mathrm{d}z}\rho_{n0}v_{nz}-\alpha_{in}k_x^2v_{nz}\right]=\rho_0v_A^2\frac{\mathrm{d}^3}{\mathrm{d}z^3}\frac{1}{\rho_{i0}}\frac{\mathrm{d}}{\mathrm{d}z}\rho_{i0}v_{iz}-k_x^2\rho_0v_A^2\frac{\mathrm{d}}{\mathrm{d}z}\frac{1}{\rho_{i0}}\frac{\mathrm{d}}{\mathrm{d}z}\rho_{i0}v_{iz}+&\\ \omega^2\frac{\mathrm{d}^2}{\mathrm{d}z^2}\rho_{i0}v_{iz}+\mathrm{i}\omega\frac{\mathrm{d}}{\mathrm{d}z}\frac{\alpha_{in}}{\rho_{i0}}\frac{\mathrm{d}}{\mathrm{d}z}\rho_{i0}v_{iz}+k_x^2\left(\rho_{i0}N_i^2-\rho_{i0}\omega^2-\mathrm{i}\omega\alpha_{in}\right)v_{iz},&\end{aligned} \tag{3.207}$$

where $\rho_0=\rho_{i0}+\rho_{n0}$ and $v_A^2=B_0^2/(\mu\rho_0)$. These are the governing equations which we may use to study buoyancy-driven MHD waves in a simplified two-fluid model. We study the wave solutions via the local dispersion relation which may be found using the WKB method as in previous sections. The local dispersion relation is

$$\begin{aligned}\xi_n\xi_ik^4\omega^4+\mathrm{i}\nu_{in}k^4\omega^3-\xi_nk^2\left(v_A^2k_z^2k^2+\xi_ik_x^2N^2\right)\omega^2-&\\ \mathrm{i}\nu_{in}k^2\left(k_x^2\xi_iN_i^2+k_x^2\xi_nN_n^2+k^2k_z^2v_A^2\right)\omega+k_x^2N_n^2\xi_n\left(\xi_ik_x^2N_i^2+v_A^2k_z^2k^2\right)=0,&\end{aligned} \tag{3.208}$$

where $\nu_{in}=\alpha_{in}/\rho_0$ is the ion-neutral collision frequency, $\xi_i=\rho_{i0}/\rho_0$, $\xi_n=\rho_{n0}/\rho_0$, $k^2=k_x^2+k_z^2$ and $N^2=N_i^2+N_n^2$. The fourth order system can be solved exactly although the

expressions themselves do not reveal the nature of the solutions. We note that there are four solutions, hence there are two branches of solutions. Zaqarashvili *et al.* (2011b) also found four slow solutions. In the high-frequency domain (compared to the collision frequency), the two gases do not couple strongly so each may support oscillatory wave modes. In the low frequency regime these modes have zero real part. In this case, the solutions were termed vortex modes; these are solutions to the fluid equations that damp due to collisions. The solutions do not represent oscillatory waves as the ions and neutrals are coupled strongly through collisions. Therefore, the medium behaves as a single fluid, hence there are only two slow solutions. We will investigate these solutions in more detail. First, we note on some limiting forms of the dispersion relation. In the non-magnetic, collisionless ($\nu_{in} = 0$) limit the dispersion relation becomes

$$\left(k^2\omega^2 - k_x^2 N_i^2\right)\left(k^2\omega^2 - k_x^2 N_n^2\right) = 0, \tag{3.209}$$

which represent IGWs in each of the non-interacting fluids. In the collisionless, homogeneous ($N_{i,n} = 0$) limit the dispersion relation becomes $\omega^2\left(\omega^2 - v_A^2 k_z^2\right) = 0$, which represents the familiar slow MHD wave. Let us now consider the more interesting cases where the two-fluids may interact. Firstly, we consider the plasma to be strongly ionised, $\xi_n \ll 1$. In this limit, the dispersion relation reduces to

$$\omega^2 = v_A^2 k_z^2 + \xi_i \frac{k_x^2}{k^2} N_i^2. \tag{3.210}$$

This represents the buoyancy-driven slow mode with a correction due to the presence of a small amount of neutral fluid. The form of the dispersion equation is similar to the case of the fully ionised plasma, Equation (3.12), studied previously in Section 3.2.1. In this limit, the fourth order equation has reduced to a second order, hence some solutions have been removed. These are the modes associated with the neutral gas.

Perhaps of more interest, when considering the lower solar atmosphere, is the limit of a weakly ionised plasma. As discussed previously, we expect the Boussinesq approximation to be more applicable in the lower solar atmosphere where a significant proportion of the fluid may be neutral. At the base of the photosphere the level of ionisation is placed at around 1% (Carlsson & Stein, 2002). Let us consider the case of $\xi_i \ll 1$, where the dispersion relation takes the form

$$\mathrm{i}\nu_{in}\omega^3 - \xi_n v_A^2 k_z^2 \omega^2 - \mathrm{i}\nu_{in}\left(\frac{k_x^2}{k^2}\xi_n N_n^2 + k_z^2 v_A^2\right)\omega^2 + \frac{k_x^2}{k^2} N_n^2 \xi_n v_A^2 k_z^2 = 0. \tag{3.211}$$

This is the dispersion relation with which we may study photospheric plasma. Again, we have lost a solution associated with the ionised gas. While this equation is less complex than the full dispersion relation, the solutions are not in a simple form. In the interest of simplicity, we will investigate the solutions by making a further approximation, that of small/large collision frequency. These limits represent the extent to which fluid species

interact. For processes that act on time-scales shorter than the collision time, the waves do not strongly feel the interaction between the two fluids. On long time-scales, the waves are highly influenced by the interaction of the fluids. We begin by assuming that ν_{in} is small (when non-dimensionalised appropriately by *e.g.* the Alfvén or Brunt-Väisälä frequency). The dispersion relation is singular with regards to ν_{in}, hence the second solution associated with the ionised gas is removed. We use a perturbation series $\omega = \omega_0 + \nu_{in}\omega_1/(v_A k_z) + \ldots$. The leading order solution may be found to be

$$\omega_0^2 = \frac{k_x^2}{k^2} N_n^2, \tag{3.212}$$

which represents IGWs. The leading order effect of small collision frequency is that magnetic effects are unimportant. The next term may be found to be

$$\omega_1 = \frac{\mathrm{i}}{2\xi_n v_A k_z}\left(\frac{k_x^2}{k^2} N_n^2 (1-\xi_n) + v_A^2 k_z^2\right). \tag{3.213}$$

In the above analysis we made the assumption that $\xi_i \ll 1$, which implies that $\xi_n \approx 1$. The first term in ω_1 may then be considered to be small, and so contributes to the third term in the perturbation series. The frequency then takes the form

$$\omega \sim \pm\frac{k_x}{k} N_n + \frac{\mathrm{i}\nu_{in}}{2\xi_n}. \tag{3.214}$$

We see that for the case of a small collision frequency, the waves may be considered damped IGWs in the mostly neutral plasma. The damping is due to ion-neutral collision and the damping rate is given by the imaginary part of the frequency. The above analysis is valid when the g-mode frequency is larger than the collision frequency.

In the solar atmosphere the Brunt-Väisälä frequency is relatively small hence we should also consider the case of a large collision frequency. Zaqarashvili *et al.* (2011b) estimate the ion-neutral collision frequency in the chromosphere, based on the FAL-3 model (Fontenla, Avrett & Loeser, 1990), to be 4 s^{-1}. Hence, the case of high collision frequency may be more applicable to the lower solar atmosphere. Let the frequency take the form $\omega = \omega_0 + v_A k_z \omega_1/\nu_{in} + \ldots$. The leading order term is

$$\omega_0^2 = v_A^2 k_z^2 + \frac{k_x^2}{k^2}\xi_n N_n^2. \tag{3.215}$$

We see, when the collision frequency is large, the frequency is of the form of a fully ionised plasma and magnetic effects may be important even when the fluid is weakly ionised. There is also a solution $\omega_0 = 0$, representing a damped vortex mode (see below). The next term in the series is given by

$$2\omega_1 = \mathrm{i}\xi_n v_A k_z\left(\frac{k_x^2 N_n^2}{k^2\omega_0^2} - 1\right), \tag{3.216}$$

which is imaginary and so the damping rate is given by $\nu_A k_z \omega_1/\nu_{in}$. In the above analysis we have shown that the frequency, derived for the case of fully ionised fluid, may be used in partially ionised plasmas when either the plasma is strongly ionised or weakly ionised and the ion-neutral collision frequency is high. We have calculated generalisations to these results for either case.

The nature of the solutions may also be investigated by applying the limit of small collision frequency to the full fourth order dispersion relation, Equation (3.208). In this limit the dispersion relation is not singular hence we have all four solutions. These results are valid for arbitrary proportion of ionised and neutral material. As above, let us use a perturbation series of the form $\omega = \omega_0 + \nu_{in}\omega_1/(\nu_A k_z) + \ldots$, where $\nu_{in} \ll \nu_A k_z$. To lowest order, we find the leading order solutions to be

$$\omega_0^2 = v_A^2 k_z^2 \xi_i^{-1} + \frac{k_x^2}{k^2} N_i^2,\ \frac{k_x^2}{k^2} N_n^2. \tag{3.217}$$

These solutions represent buoyancy-driven waves in each of the fluids. As the collision frequency is small the coupling of the fluids is weak. We also observe the transformation of oscillatory wave modes to vortex modes. In the limit $k_z \to \infty$, the first branch represents slow MHD waves unaffected by gravity $\omega_0^2 \sim v_A^2 k_z^2 \xi_i^{-1}$. The frequency of the second branch tends to zero; hence we can think of these as becoming vortex modes in the low frequency limit. For large vertical wavenumbers the frequency decreases, a property of IGWs; this is in contrast to the case of slow modes in a homogeneous medium where the vortex modes become oscillatory in the large wavenumber limit. As in the above, the damping rate is given by the next term in the series, which may be shown to be

$$\frac{\nu_{in}}{\nu_A k_z}\omega_1 = \mathrm{i}\nu_{in}\frac{\left(k_x^2/k^2\right)\left(\xi_i N_i^2 + \xi_n N_n^2\right) + v_A^2 k_z^2 - \omega_0^2}{4\omega_0^2\xi_n\xi_i - 2\xi_n v_A^2 k_z^2 - 2\xi_n\xi_i N^2 k_x^2/k^2}. \tag{3.218}$$

In the large wavenumber limit, the solutions take the form

$$\omega \sim \pm\frac{v_A k_z}{\sqrt{\xi_i}} + \mathrm{i}\nu_{in}\frac{\xi_i - 1}{2\xi_i\xi_n},\ \pm\frac{k_x}{k_z}N_n - \frac{\mathrm{i}\nu_{in}}{2\xi_n}. \tag{3.219}$$

Note that we should be careful taking the large vertical wavenumber limit as we may lose regularity in the perturbation series, and so this type of analysis is unable to study the vortex modes. They may be studied, however, by taking the large wavelength limit in the dispersion relation. Neglecting small terms leads to

$$\xi_i\xi_n\omega^4 + \mathrm{i}\nu_{in}\omega^3 - \xi_n v_A^2 k_z^2\omega^2 - \mathrm{i}\nu_{in}k_z^2 v_A^2\omega + k_x^2 N_n^2\xi_n v_A^2 = 0. \tag{3.220}$$

If we consider only the dominant terms we have the vortex solution,

$$\omega = -\frac{\mathrm{i}\nu_{in}}{\xi_n}. \tag{3.221}$$

As the previous analysis suggests, in the large wavenumber limit, there is a vortex mode with zero real frequency. We see that the damping rate is actually twice as fast as previously suggested. This discrepancy is attributed to the fact the perturbation approach is, as discussed previously, not valid in the large vertical wavenumber limit. When the wavenumber is not large, the damping rate is lower. Note also that the solutions lost correspond to the slow waves, the frequency of which is proportional to $v_A k_z$; hence, these represent the singular solutions. A perturbation series, for small collision frequency, is possible to investigate the solutions of Equation (3.220), resulting in the first two slow solutions in Equation (3.219).

Finally, analytical expressions are available for the frequency in the limit of high collision frequency. The oscillatory solutions are given, to leading order, by

$$\omega^2 \sim \frac{k_x^2}{k^2}\left(\xi_i N_i^2 + \xi_n N_n^2\right) + v_A^2 k_z^2. \tag{3.222}$$

In this limit, the vortex modes are purely imaginary. The propagating solutions are purely real in this limit, hence we see that the damping tends to 0 in the limit of high collision frequency. When the collision frequency is high the plasma acts as a single fluid; the solution here then represents a buoyancy-driven MHD wave in the single fluid composed of ions and neutrals.

Let us now consider the full dispersion relation (3.208) by plotting the solutions numerically. We assume that the temperature of all three species are equal, that is $T_i = T_e = T_n$; hence, $c_{si}^2 = 2c_{sn}^2$. For simplicity, we consider the gasses to be isothermal so the square of the Brunt-Väisälä frequency is given by $N_{(i,n)}^2 = g^2(\gamma - 1)/c_{s(i,n)}^2$. These two assumptions lead to $N_i^2/N^2 = 1/3, N_n^2/N^2 = 2/3$. We use these values in the following numerical solutions.

Let us begin by investigating the effect of varying the collision frequency. Figures 3.6 and 3.7 show the real and imaginary parts of the frequency when ν_{in}/N varies from 0 to 1.5. We plot the case of 70% neutral gas and 30% ionised gas, representative of conditions which may be found in the chromosphere (Carlsson & Stein, 2002). The other parameters take the values $k_z/k_x = 1, v_A k_z/N = 1$. It can be shown that the curves plotted follow the same paths for a large range of ν_{in}/N. The behaviour plotted here is, therefore, representative of arbitrarily large ν_{in}. The solid blue curves, in Figure 3.6, represent forwards and backwards propagating slow MAG waves that remain oscillatory for all values of ν_{in}. In the limit of small collision frequency, the frequency of these waves may be given by the first solution in Equation (3.217). This expression is close to the numerical solution for $\nu_{in}/N < 0.2$. Figure 3.6 clearly shows two regimes for the solution. For increasing collision frequency the wave frequency decreases. When $\nu_{in}/N \approx 0.55$ the real part of the solutions cease to depend on the collision frequency. The frequency is given by Equation (3.222), valid for 'large' collision frequencies. Beyond this value the plasma acts as a single fluid, a higher collision frequency does not change this fact so the real part of the propagating wave is unaffected by the collision frequency.

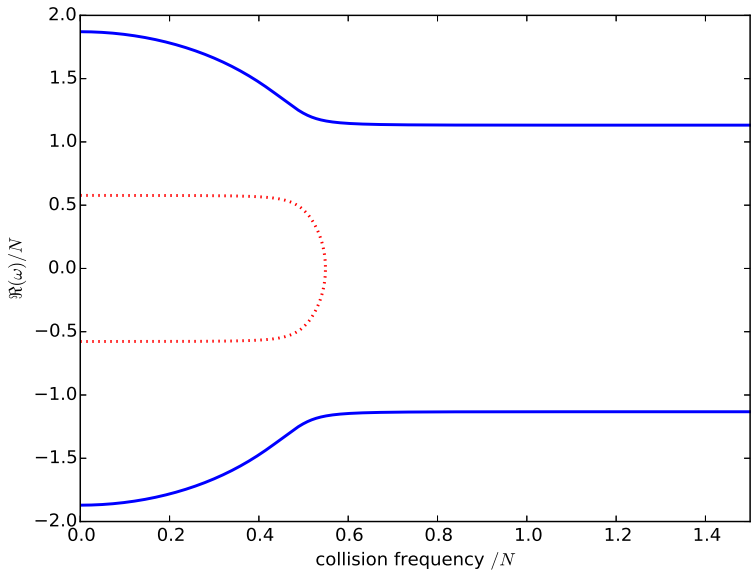

Fig. 3.6 Real part of the frequency for varying collision frequency, normalised to N. The other parameters take the values $\xi_n = 0.7, \xi_i = 0.3, k_z/k_x = 1, v_A k_z/N = 1$.

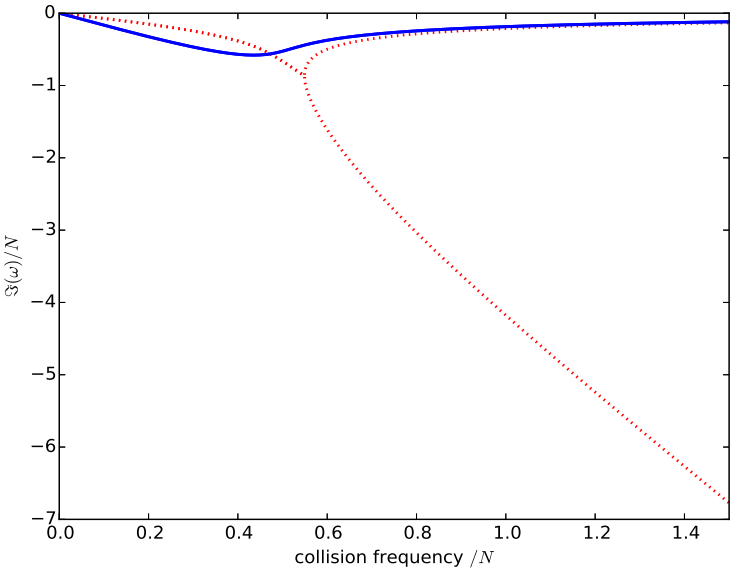

Fig. 3.7 Imaginary part of the frequency (damping rate) for varying collision frequency, normalised to N. The other parameters take the values $\xi_n = 0.7, \xi_i = 0.3, k_z/k_x = 1, v_A k_z/N = 1$.

There is another solution present represented by the red dotted line. This solution is a propagating mode in the low collision frequency regime and a purely damped vortex mode when the partially ionised plasma acts as a single fluid. The value of the real part of the frequency when the wave is propagating is given by the second term of Equation (3.217) for $\nu_{in}/N < 0.4$. Beyond this value the real part of the frequency tends to 0. When the partially ionised particles interact weakly the red dotted curves correspond to IGWs in the neutral fluid while the blue solid curves are buoyancy-driven MHD waves in the

ionised fluid. When the plasma species interact strongly as a single fluid, the blue curves represent buoyancy-driven MHD waves in the whole fluid.

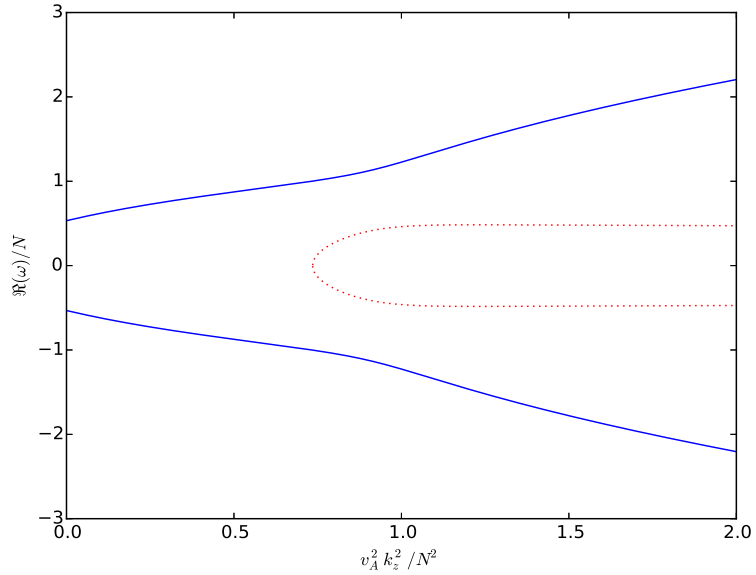

Fig. 3.8 Real part of the frequency for Alfvén frequency (or magnetic field strength), normalised to N. The other parameters take the values $\xi_n = 0.7, \xi_i = 0.3, k_z/k_x = 1, \nu_{in}/N = 0.5$.

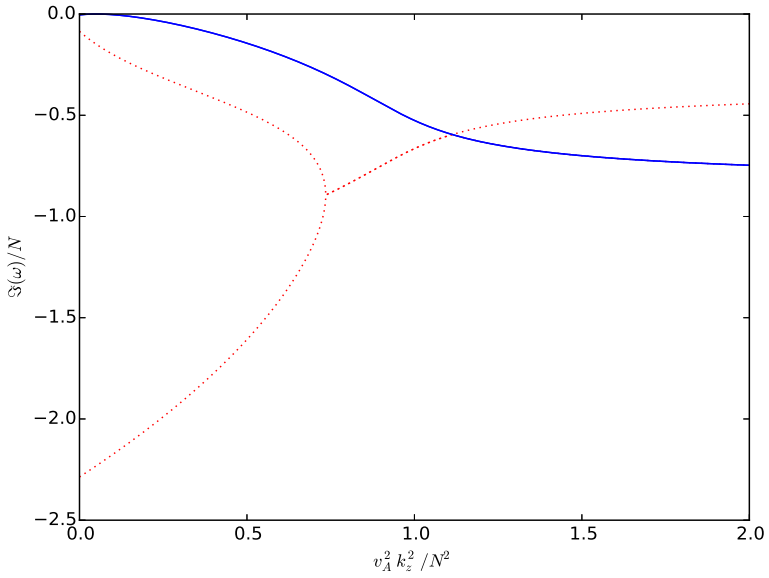

Fig. 3.9 Imaginary part of the frequency (damping rate) for varying Alfvén frequency (or magnetic field strength), normalised to N. The other parameters take the values $\xi_n = 0.7, \xi_i = 0.3, k_z/k_x = 1, \nu_{in}/N = 0.5$.

Figure 3.7 shows the imaginary part of the frequency. We see that all curves take negative values, indicating that the solutions are damped. We, again, see the two regimes where the fluid may be treated as separate fluids or a single fluid. In the low ν_{in} region

the blue MHD wave is damped more strongly than the red IGW. The damping rates for small ν_{in} are given by Equation (3.218). As expected, the damping rates for the forwards and backwards wave are equal by symmetry. In the high ν_{in} region, the damping rate of the propagating modes decrease with ν_{in}, tending asymptotically to 0. This is expressed in the solution (3.222) which contains no imaginary part. The physical reason for this is that the wave acts on a greater time-scale than the ion-neutral collision time-scale and so does not feel the particle interactions in this limit. When the propagating IGWs become imaginary vortex modes the damping rate bifurcates; there are two vortex solutions which are strongly and weakly damped, respectively.

Figures 3.8 and 3.9 show the effect of varying the magnetic field strength. Again, the blue solid curve shows the propagating solutions and red dotted show the vortex/propagating modes. As above, we set the parameters to the values $\xi_n = 0.7, \xi_i = 0.3, k_z/k_x = 1$. The collision frequency is set so that $\nu_{in}/N = 0.5$, close to the region where propagating modes become vortex modes. It can be shown that the trends seen in Figures 3.8 and 3.9 persist for larger Alfvén frequencies. A key point depicted here is that the behaviour of the solutions can be split into magnetically or gravitationally dominated regions. The propagating MHD waves undergo a change in the gradient of the real part of the frequency around $v_A k_z/N = 1$. The gradient of the imaginary part also undergoes a similar change.

It is interesting to note that the parameters of magnetic field strength and collision frequency produce contrasting effects. That is, for a weak magnetic field the vortex modes are purely imaginary; increasing the magnetic field causes them to become propagating modes. There is, again, a weakly and strongly damped vortex mode.

Note that for large Alfvén frequency the solutions here do not match up with the analytical results for large vertical wavenumber. This is due to the fixing of the ratio $k_z/k_x = 1$. It can be shown that plotting the solutions for large Alfvén frequency and large values of k_z/k_x does indeed agree with the asymptotic results.

3.3 Wave Propagation in a Horizontal Field

The solar atmosphere contains structures that may not be described by a vertical magnetic field only. In reality, the magnetic field topology may be very complex, and time-dependent, leading to the formation of arcades, braided loops, etc. The solar chromosphere contains regions that may be considered as a magnetic canopy over the photosphere, as observed by *e.g.* Giovaneli (1980). We may model these structures simply by a horizontal (perpendicular to gravity) magnetic field.

The governing equations of motion are simpler to work with when the background field is horizontal, and permit exact solutions to several useful magnetic field profiles. The theory of MHD waves in a horizontal model and the coupling of p-modes to a magnetic atmosphere (or interior in some cases) has been analysed by *e.g.*Yu (1965), Goedbloed (1971), Chen & Lykoudis (1972), Nye & Thomas (1976), Thomas (1982), Campbell &

Roberts (1989), Musielak *et al.* (1989), Evans & Roberts (1990), Miles & Roberts (1992), Miles, Allen & Roberts (1992), Jain & Roberts (1994a,b), Tirry *et al.* (1998), Pintér *et al.* (1998), Pintér & Goossens (1999), Pintér, Čadež & Roberts (1999), Erdélyi & Taroyan (1999), Pintér, Erdélyi & New (2001), Foullon & Roberts (2005), Erdélyi (2006), Pintér, Erdélyi & Goossens (2007), Pintér (2008), Pintér & Erdélyi (2011) and Jovanović (2014).

As in the case of a vertical magnetic field, atmospheric g-modes have received less attention. Propagating waves were analysed by Barnes *et al.* (1998). In this section we extend this work by finding the eigenfunctions and dispersion relations for g-modes, coupling to a magnetic atmosphere. We see that while exact solutions are available to the governing equations, the dispersion relations are difficult to analyse.

3.3.1 Boussinesq Approximation in a Horizontal Field

Let the magnetic field be in the x-direction and vary with height, $\mathbf{B}_0 = (B_0(z), 0, 0)$. Gravity is constant and points in the negative z-direction $\mathbf{g} = (0, 0, -g)$. The background satisfies the equation of magnetohydrostatic equilibrium

$$\frac{\mathrm{d}}{\mathrm{d}z}\left(p_0 + \frac{B_0^2}{2\mu}\right) = -g\rho_0. \tag{3.223}$$

Note that the Brunt-Väisälä frequency N includes a magnetic contribution, that is the buoyancy force on a fluid element is modified by the gradient of the magnetic field,

$$N^2 = -g\left(\frac{1}{\rho_0}\frac{\mathrm{d}\rho_0}{\mathrm{d}z} + \frac{g}{c_s^2 + v_A^2}\right). \tag{3.224}$$

See Chen & Lykoudis (1972) for the derivation of the modified Brunt-Väisälä frequency. The linearised equations of motion, in the Boussinesq approximation, may be manipulated into the two coupled, first order equations

$$\rho_0\left(\omega^2 - v_A^2 k_x^2\right)\frac{\mathrm{d}\xi_z}{\mathrm{d}z} + \omega^2\frac{\mathrm{d}\rho_0}{\mathrm{d}z}\xi_z = k^2 P_T, \tag{3.225}$$

$$\rho_0\left(\omega^2 - v_A^2 k_x^2 - N^2\right)\xi_z = \frac{\mathrm{d}P_T}{\mathrm{d}z}, \tag{3.226}$$

where $k^2 = k_x^2 + k_y^2$. These two equations govern MHD internal gravity waves. Equations (3.225) and (3.226) reduce to the familiar equation for internal gravity waves, Equation (2.38),

$$\omega^2\frac{\mathrm{d}^2 q}{\mathrm{d}z^2} = k^2\left(\omega^2 - N^2\right)q, \tag{3.227}$$

where $q = \rho_0 v_z$ is the vertical component of perturbed momentum, in the hydrodynamic limit.

There is also another solution to the MHD equations - the Alfvén wave. For the special case of parallel wave propagation, $k_y = 0$, the y-component of velocity is decoupled from the other components. The resulting equation describing Alfvén waves is

$$\left(\omega^2 - v_A^2 k_x^2\right) v_y = 0. \tag{3.228}$$

When the wave propagation is oblique ($k_y \neq 0$), we can recover the Alfvén wave by noting that Alfvén waves are incompressible $\nabla \cdot \mathbf{v}_1 = 0$. Assuming $\nabla \cdot \mathbf{v}_1 = 0$, Equation (2.28) implies that $v_z = 0$. Setting $v_z = 0$ in the equations of motion returns the Alfvén wave.

Let us now investigate the frequency of internal gravity waves modified by a horizontal magnetic field. First we combine Equations (3.225) and (3.226) by eliminating the total pressure,

$$\rho_0\left(\omega^2 - v_A^2 k_x^2\right)\frac{\mathrm{d}^2\xi_z}{\mathrm{d}z^2} + \left[\left(\omega^2 - v_A^2 k_x^2\right)\frac{\mathrm{d}\rho_0}{\mathrm{d}z} - \rho_0 k_x^2 \frac{\mathrm{d}v_A^2}{\mathrm{d}z} + \omega^2 \frac{\mathrm{d}\rho_0}{\mathrm{d}z}\right]\frac{\mathrm{d}\xi_z}{\mathrm{d}z} + \left[\omega^2 \frac{\mathrm{d}^2\rho_0}{\mathrm{d}z^2} - k^2\rho_0\left(\omega^2 - v_A^2 k_x^2 - N^2\right)\right]\xi_z = 0. \tag{3.229}$$

We make the assumption that the background medium varies slowly and apply the WKB approximation (see *e.g.* Bender & Orszag, 1978). Applying the WKB approximation to Equation (3.229) and keeping terms of order $O\left(\epsilon^0\right)$, we have

$$\left(\omega^2 - v_A^2 k_x^2\right)\left(\frac{\mathrm{d}\theta}{\mathrm{d}\tilde{z}}\right)^2 + \left(k_x^2 + k_y^2\right)\left(\omega^2 - v_A^2 k_x^2 - N^2\right) = 0, \tag{3.230}$$

or

$$\omega^2 = k_x^2 v_A^2 + \frac{k_x^2 + k_y^2}{k_x^2 + k_y^2 + k_z^2} N^2, \tag{3.231}$$

where we have identified the local wavenumber $k_z \equiv \mathrm{d}\theta/\mathrm{d}\tilde{z}$. This result has been derived previously be e.g Barnes *et al.* (1998). In the framework of MHD this is a slow MHD wave. Note that resonant absorption does not occur as $\omega^2 - v_A^2 k_x^2 \neq 0$ due to the contribution of the Brunt-Väisälä frequency.

There exists exact solutions to the governing equation (3.229). If the background temperature T_0 is constant, the sound speed and Brunt-Väisälä frequency do not vary with height. We have some freedom in choosing B_0, provided the medium is in magnetohydrostatic equilibrium, so we let

$$B_0(z) = \widehat{B}_0 e^{-z/2H_B}, \tag{3.232}$$

where $\widehat{B}_0$ and H_B are constants, representing the magnetic field strength at $z = 0$ and the magnetically modified scale-height of the medium, respectively. When the temperature is constant, the density is given by

$$\rho_0(z) = \widehat{\rho}_0 e^{-z/H_B}. \tag{3.233}$$

The Alfvén speed is therefore constant for this choice of magnetic field. The magnetically modified scale height is determined from the equation of magentohydrostatic equilibrium to be

$$H_B \equiv \frac{\rho_0}{\rho_0'} = \frac{c_s^2 + \frac{1}{2}\gamma v_A^2}{\gamma g}. \tag{3.234}$$

In the hydrodynamic limit H_B tends to the familiar scale-height H. Substituting this density and magnetic field into Equation (3.229),

$$\widehat{\rho}_0 e^{-\frac{z}{H_B}}\left(\left(\omega^2 - v_A^2 k_x^2\right)\frac{\mathrm{d}^2\xi_z}{\mathrm{d}z^2} - \frac{1}{H_B}\left(2\omega^2 - v_A^2 k_x^2\right)\frac{\mathrm{d}\xi_z}{\mathrm{d}z} + \left[\frac{\omega^2}{H_B^2} - k^2\left(\omega^2 - v_A^2 k_x^2 - N^2\right)\right]\xi_z\right) = 0, \tag{3.235}$$

which has solutions

$$\xi_z = C_1 e^{m_+ z} + C_2 e^{m_- z}, \tag{3.236}$$

where

$$m_\pm = \frac{1}{2H_B}\left(\frac{\omega^2}{\omega^2 - v_A^2 k_x^2} + 1\right) \pm \mathrm{i}\left[\frac{k^2\left(v_A^2 k_x^2 + N^2 - \omega^2\right)}{\omega^2 - v_A^2 k_x^2} - \frac{v_A^4 k_x^4}{4H_B^2\left(\omega^2 - v_A^2 k_x^2\right)^2}\right]^{\frac{1}{2}}. \tag{3.237}$$

Exact solutions also exist for the case of a uniform magnetic field, *i.e.*, the Alfvén speed varies exponentially, in terms of generalised Heun functions. The properties of these functions are little known so we shall work with the solutions (3.236). We may also find solutions when B_0 and c_s are constant by assuming c_s is large. When this is the case the Brunt-Väisälä frequency may be approximated by its first term, and Equation (3.229) has solutions in terms of ${}_2F_1$ hypergeometric functions. Changing the density and magnetic field profiles would be an interesting avenue for further study.

The modes are propagating if the term in the square brackets is positive. This condition leads to the inequality

$$-\omega^4 + (2v_A^2 k_x^2 + N^2)\omega^2 - v_A^2 k_x^2\left(v_A^2 k_x^2 + N^2\right) - \frac{v_A^4 k_x^4}{4H_B^2 k^2} > 0, \tag{3.238}$$

hence the condition for propagating wave solutions is

$$v_A^2 k_x^2 + \frac{N^2}{2} - \frac{1}{2}\left(N^4 - \frac{v_A^4 k_x^4}{H_B^2 k^2}\right)^{1/2} < \omega^2 < v_A^2 k_x^2 + \frac{N^2}{2} + \frac{1}{2}\left(N^4 - \frac{v_A^4 k_x^4}{H_B^2 k^2}\right)^{1/2}. \tag{3.239}$$

For real quantities $N^2 > v_A^2 k_x^2 / H_B k$. When this is the case, the square root of the term in brackets is less than N^2. The lower root is then above the square of the Alfvén frequency, while the upper root is below the square of the Alfvén frequency plus the square of the Brunt-Väisälä frequency. Noting this, the frequency of propagating waves also satisfies the inequality

$$v_A^2 k_x^2 < \omega^2 < v_A^2 k_x^2 + N^2. \tag{3.240}$$

In the hydrodynamic limit, this reduces to $0 < \omega^2 < N^2$. The Alfvén frequency acts as a lower cut-off for the modes. This means that propagating low frequency IGWs will become evanescent as they propagate through a sufficiently strong magnetic field.

Let us consider standing waves in a slab of plasma of thickness L. A plasma slab is representative of structures with abrupt changes in background quantities such as, for example, density, temperature or magnetic field. We assume that the slab is infinite in the $x-$ and $y-$directions and that the boundaries are located at $z = 0$ and $z = L$. We further assume that the boundaries are perfectly reflecting, due to *e.g.* a turning point formed by the cut-off frequency or a sharp change in the temperature of the medium. The boundary conditions are then

$$\xi_z = 0 \quad \text{at} \quad z = 0,\, L. \tag{3.241}$$

Applying these conditions leads to

$$C_1 + C_2 = 0, \tag{3.242}$$

$$C_1 e^{m_- L} + C_2 e^{m_+ L} = 0. \tag{3.243}$$

The condition for a non-trivial solution to these equations, after a little algebra, leads us to our dispersion relation

$$\left(\omega^2 - v_A^2 k_x^2\right)\left(\omega^2 - v_A^2 k_x^2 - N^2 \frac{k_\perp^2}{k_\perp^2 + \frac{n^2\pi^2}{L^2}}\right) + \frac{v_A^4 k_x^4}{4H_B^2\left(k_\perp^2 + \frac{n^2\pi^2}{L^2}\right)} = 0, \tag{3.244}$$

where $k_\perp^2 = k_x^2 + k_y^2$ is the square of the wavenumber perpendicular to gravity. This equation describes slow MHD waves. Here, we see one of the key differences between the cases of a horizontal and vertical field - that there are two branches of slow MHD waves. One branch is the buoyancy-driven slow mode, the magnetic analogue of internal gravity waves. The other is a magnetic slow mode. We note too that $n\pi/L$ acts as a vertical wavenumber.

When the wavenumber is large, in accordance with the Boussinesq approximation, or when the medium varies slowly (the assumption behind the local WKB approximation) we may assume $kH \gg 1$, where k represents the total effective wavenumber $k^2 = k_\perp^2 + n^2\pi^2/L^2$, and so we may approximate the dispersion relation as

$$\left(\omega^2 - v_A^2 k_x^2\right)\left(\omega^2 - v_A^2 k_x^2 - N^2 \frac{k_\perp^2}{k_\perp^2 + \frac{n^2\pi^2}{L^2}}\right) = 0. \tag{3.245}$$

The solutions here are the magnetic slow wave wave with gravitational effects neglected and the buoyancy-driven slow magnetoacoustic-gravity wave. It may seem that the magnetic slow mode is an Alfvén mode by the appearance of the Alfvén frequency as a solution to Equation (3.245), although this is not the case. Equation (3.244) shows that the Alfvén type slow mode does not decouple from the g-mode type slow mode when $k_y = 0$, as would be the case for the Alfvén mode.

3.3.1.1 Two-layer Model

Let us consider a two-layer model consisting of a non-magnetic polytropic layer and a magnetic isothermal layer. We consider the whole model to be infinite. The polytropic layer is representative of the solar interior, while the upper layer represents the solar atmosphere. IGWs in a polytrope were studied in Chapter 2. The model used is simplistic in that it does not take into account the effects of solar curvature or the complex structuring of the solar atmosphere. We model the effect of an atmosphere on g-modes. It is well known that g-modes are sensitive to the convection zone. The polytropic layer in our model may be representative of the convectively stable solar interior ($N_0^2 > 0$) or the unstable convection zone ($N_0^2 < 0$). When the layer is stable to convection our model may be applicable to stars with thin or no convection zones.

It is helpful to work in a 'flipped' coordinate system in which gravity takes the form $\mathbf{g} = (0, 0, g)$, $z > 0$ is the solar interior while $z < 0$ is the solar atmosphere. We use the subscripts "i" and "e" for the interior and exterior, respectively. The solution to the governing equation for $q_i = \rho_{0i} v_{1zi}$, derived in Section 2.2.4, that remains regular as $z \to \infty$ is given in terms of the Kummer U function,

$$q_i = A_1 e^{-\alpha/2} \alpha U(1-\kappa, 2, \alpha), \tag{3.246}$$

where

$$\kappa = \frac{k z_0 N_0^2}{2\omega^2}, \quad \alpha = 2k(z+z_0), \tag{3.247}$$

where A_1 is some constant. In the atmosphere we seek an evanescent solution. This is the case when $\omega^2 < v_A^2 k_x^2$, or $\omega^2 > v_A^2 k_x^2 + N^2$ and $C_1 = 0$ (in Equation 3.236). The solution is then given by

$$\xi_e = C_2 e^{m_- z}, \tag{3.248}$$

where

$$m_- = -\frac{1}{2H_B}\left(\frac{\omega^2}{\omega^2 - v_A^2 k_x^2} + 1\right) + \left[\frac{v_A^4 k_x^4}{4H_B^2\left(\omega^2 - v_A^2 k_x^2\right)^2} + \frac{k^2\left(v_A^2 k_x^2 + N^2 - \omega^2\right)}{v_A^2 k_x^2 - \omega^2}\right]^{\frac{1}{2}}. \tag{3.249}$$

The boundary conditions at the interface $z = 0$ are the continuity of Lagrangian displacement and pressure (the Lagrangian perturbation is $\delta P_T = P_T + \xi \cdot \nabla P_{T0}$). These may be expressed

$$\xi_{zi} = \xi_{ze}, \quad p_{1i} + g\rho_{0i}\xi_{zi} = P_T + g\rho_{0e}\xi_{ze} \quad \text{at } z = 0. \tag{3.250}$$

A relation for the pressure p_1 can be deduced from the x and y components of the momentum equation to be

$$\frac{\mathrm{d}}{\mathrm{d}z}\rho_{0i}\xi_{zi} = \frac{k_\perp^2}{\omega^2} p_{1i}. \tag{3.251}$$

The total pressure perturbation, P_{Te}, in the atmosphere is

$$\rho_{0e}\left(\omega^2 - v_A^2 k_x^2\right)\frac{\mathrm{d}\xi_{ze}}{\mathrm{d}z} + \omega^2\frac{\mathrm{d}\rho_{0e}}{\mathrm{d}z}\xi_{ze} = k_\perp^2 P_{Te}. \tag{3.252}$$

The boundary conditions at $z = 0$ can then be expressed as

$$\frac{\mathrm{i}}{\omega\rho_{0i}}q_i = \xi_{ze}, \tag{3.253}$$

$$\frac{\mathrm{i}\omega}{k^2}\frac{\mathrm{d}q_i}{\mathrm{d}z} + \frac{\mathrm{i}g}{\omega}q_i = \frac{\rho_{0e}}{k^2}\left(\omega^2 - v_A^2 k_x^2\right)\frac{\mathrm{d}\xi_{ze}}{\mathrm{d}z} + \frac{\omega^2}{k^2}\frac{\mathrm{d}\rho_{0e}}{\mathrm{d}z}\xi_{ze} + g\rho_{0e}\xi_{ze}. \tag{3.254}$$

For simplicity, we restrict the following to the case where the wave vector is located in the $x-z$ plane only ($k_y = 0$), although the results may be generalised with ease. Applying these boundary conditions gives

$$\frac{2k_x z_0 \mathrm{i}}{\omega\widehat{\rho}_{0i}}A_1 e^{-k_x z_0}U(1-\kappa, 2, 2k_x z_0) = C_2, \tag{3.255}$$

$$\begin{aligned}2\mathrm{i}e^{-k_x z_0}A_1\left[U(1-\kappa,2,2k_x z_0)\left(-\omega z_0 + \frac{\omega}{k_x} + \frac{gk_x z_0}{\omega}\right) + 2z_0\omega U'(1-\kappa,2,2k_x z_0)\right]\\ = \frac{\widehat{\rho}_{0e}}{k_x^2}\left[\left(\omega^2 - v_A^2 k_x^2\right)m_- + \frac{\omega^2}{H_B} + gk_x^2\right]C_2.\end{aligned} \tag{3.256}$$

The dispersion relation is found, from the determinant of the above system, to be

$$\begin{aligned}\left[\omega^2 H_B(1-k_x z_0) + gk_x^2 z_0 H_B\left(1 - \frac{\widehat{\rho}_{0e}}{\widehat{\rho}_{0i}}\right) - z_0\frac{\widehat{\rho}_{0e}}{\widehat{\rho}_{0i}}\left(\left(\omega^2 - v_A^2 k_x^2\right)m_- H_B + \omega^2\right)\right]U(1-\kappa,2,2k_x z_0)\\ + 2k_x z_0 H_B\omega^2 U'(1-\kappa,2,2k_x z_0) = 0.\end{aligned} \tag{3.257}$$

This is the dispersion relation for g-modes in an infinite polytrope, modified by a magnetic chromosphere. A numerical approach is needed to pick out the solutions clearly. We return to this further on. Some information may be extracted from the dispersion relation analytically. In accordance with the Boussinesq approximation we look for solutions in the limit of large $k_x z_0$. For simplicity, we make the a priori assumption that while $k_x z_0$ is large the quantity $k_x z_0 N_0^2/\omega^2$ does not become large. The motivation for this simplifying assumption is that the argument of the Kummer U functions may be assumed to be large, but the a parameter $(1-\kappa)$ is fixed. The frequency of the semi-infinite polytrope considered previously would satisfy this assumption. We shall see that there is indeed a solution in this limit that satisfies the a priori assumption.

In the limit $k_x z_0 \to \infty$, the Kummer functions may be approximated by their asymptotic formula,

$$U(a,b,x) \sim x^{-a}. \tag{3.258}$$

Using the formula for the derivative of the U function, the asymptotic dispersion relation is

$$\left[\omega^2 H_B(1-k_x z_0)+gk_x^2 z_0 H_B\left(1-\frac{\widehat{\rho}_{0e}}{\widehat{\rho}_{0i}}\right)-z_0\frac{\widehat{\rho}_{0e}}{\widehat{\rho}_{0i}}\left(\left(\omega^2-v_A^2k_x^2\right)m_- H_B+\omega^2\right)\right]+H_B\left(\frac{k_x z_0 N_0^2}{2}-\omega^2\right)=0. \tag{3.259}$$

We have made the assumption $k_x z_0 \gg 1$; we shall simplify the dispersion relation further under this assumption. This may be achieved by introducing a dimensionless wavenumber $\widetilde{k}=k_x z_0$, and assuming $\widetilde{k}\gg 1$. Keeping large terms in the dispersion relation, that is terms including $\widetilde{k}$ we have

$$\begin{aligned}\left(1-\rho^2\right)\omega^4+\left[\rho^2\left(\frac{2v_A^2\widetilde{k}^2}{z_0^2}+N^2\right)-\frac{2g\widetilde{k}}{z_0}(1-\rho)-N_0^2+\frac{\rho v_A^2\widetilde{k}}{2z_0H_B}\right]\omega^2\\ +\left(\frac{g\widetilde{k}}{z_0}(1-\rho)+\frac{N_0^2}{2}-\frac{\rho v_A^2\widetilde{k}}{2z_0H_B}\right)^2-\frac{\rho^2v_A^4\widetilde{k}^2}{4z_0^2H_B^2}-\frac{\rho^2v_A^2\widetilde{k}^2}{z_0^2}\left(\frac{v_A^2\widetilde{k}^2}{z_0^2}+N^2\right)=0,\end{aligned} \tag{3.260}$$

where $\rho=\widehat{\rho}_{0e}/\widehat{\rho}_{0i}$. This equation may be solved easily to give the full solutions

$$\begin{aligned}\omega^2=&\frac{2g(\widetilde{k}/z_0)(1-\rho)+N_0^2-\rho^2\left(2v_A^2(\widetilde{k}/z_0)^2+N^2\right)}{2(1-\rho^2)}-\frac{\rho v_A^2(\widetilde{k}/z_0)}{4H_B(1-\rho^2)}\pm\\ &\frac{1}{2(1-\rho^2)}\Bigg[\left(\rho^2\left(2v_A^2(\widetilde{k}/z_0)^2+N^2\right)-2g(\widetilde{k}/z_0)(1-\rho)-N_0^2+\frac{\rho v_A^2(\widetilde{k}/z_0)}{2H_B}\right)^2-4\left(1-\rho^2\right)\times\\ &\left(\left(g(\widetilde{k}/z_0)(1-\rho)+\frac{N_0^2}{2}-\frac{\rho v_A^2(\widetilde{k}/z_0)}{2H_B}\right)^2-\rho^2v_A^2(\widetilde{k}/z_0)^2\left(v_A^2(\widetilde{k}/z_0)^2+N^2\right)-\frac{\rho^2v_A^2(\widetilde{k}/z_0)^2}{4H_B^2}\right)\Bigg]^{1/2}.\end{aligned} \tag{3.261}$$

It can be shown that real solutions may exist for a weak magnetic field. When the magnetic field is strong, real solutions cease to exist. This is likely due to the fact that for a strong field the perturbations may become propagating in the atmosphere, hence the solutions no longer satisfy the upper boundary condition. For a sufficiently strong field, the solutions may exist below the Alfvén frequency hence real solutions may, once again, exist.

Due to the complex form of Equation (3.261), it is instructive to simplify the solutions further. Let us consider the dominant contribution to the frequency in the limit of $\widetilde{k}\to\infty$. Taylor expanding the solution, it can be shown that the solution corresponding to taking the positive root is approximately

$$\omega^2\sim gk_x\frac{1-\rho}{1+\rho}+\frac{v_A^2k_x^2\rho}{1+\rho}-\frac{v_A^2k_x\rho}{4H_B}. \tag{3.262}$$

Note that we return to a dimensional wavenumber. This analysis shows that when the magnetic field is weak, the dominant contribution to the frequency has the form of the frequency of an f-mode. The a priori assumption that κ does not grow large as the

wavenumber grows large is seen to be justified. In the hydrodynamic limit (with continuous temperature) this reduces to $\omega^2 \approx 0$, so we should keep more terms in the Taylor expansion; see below for a discussion about the non-magnetic solutions. The first term resembles the f-mode, a surface gravity mode, which has the dispersion relation $\omega^2 = gk_x$. This leads us to conjecture that this solution is a g-mode. The f-mode is located between the p-mode and g-mode branches, hence frequencies below the f-mode may be considered as g-modes. As in the case of an isolated polytrope, the frequency may be above the Brunt-Väisälä frequency. If gravitational effects are negligible, the frequency is approximated by $\omega^2 = v_A^2 k_x^2/2$. This is below the frequency range for propagating waves in the lower layer, hence waves below the Alfvén frequency may exist. In the limit of large wavenumber the second term may be the dominant term, so the wave may take on a magnetic character. It should also be noted that the third term may be considered to be smaller than the other terms due to the high-β assumption, implicit in the Boussinesq approximation.

It is interesting to note that the existence of a density discontinuity causes the character of the waves to change. Waves in an isolated polytrope are determined in relation to the Brunt-Väisälä frequency, while buoyancy-driven waves in a two-layer model have the characteristic of the f-mode. Note that while the waves may have an f-mode character, the solution may be oscillatory in the interior, while the f-mode is a surface mode that decays away from the surface.

The solution corresponding to the negative root can be shown to be

$$\omega^2 \sim gk_x - \frac{v_A^2 k_x^2 \rho}{1-\rho} - \frac{v_A^2 k_x \rho}{4H_B(1-\rho)}. \tag{3.263}$$

Equation (3.260) is singular in the limit $\rho \to 1$ (no magnetic field and continuous density at $z = 0$); furthermore as $\rho < 1$, (when the sound speed is continuous) the frequency is complex, hence the solution ceases to exist in the hydrodynamic limit. The atmosphere may, therefore, be subject to some instability. When the magnetic field does not vanish there may be a real frequency. The singular solution may correspond to a surface mode modified by buoyancy in the solar interior. The classical f-mode is a surface gravity mode that decays away from the surface, having a frequency given by $\sqrt{gk_x}$. Previous studies, making use of an adiabatic polytrope ($N_0 = 0$) concluded that the thermal profile of the interior had no effect on the f-mode. The solution presented here may be considered to be the helioseismic f-mode, or, depending on the character of the solution it is closer to a surface mode related to the tangential discontinuity in the magnetic field. The dispersion relation is singular in the limit $\rho \to 1$, this is due to the surface discontinuity vanishing in this limit so this solution ceases to exist.

Let us investigate the dispersion relation numerically. Figures 3.10 and 3.11 show numerical solutions of Equation (3.257), where we write the frequency in dimensionless form $\Omega = z_0\omega/c_s$. The sound speed is continuous at $z = 0$. Figure 3.10 shows the effect of varying the horizontal wavenumber. We choose the other parameters such that the

polytropic layer is stable to convection ($z_0 = 5H$) and the magnetic layer consists of plasma in the high-β regime. Note that in terms of the dimensionless frequency here the Brunt-Väisälä frequencies are $z_0 N/c_s \approx 2.5$ and $z_0 N_0/c_s \approx 1.7$.

We see that there are two distinct branches of solutions. When the dimensionless wavenumber kz_0 is order 1 we have parabolic ridges corresponding to g-modes. When kz_0 reaches ≈ 5 a new solution appears. This is a magnetically dominated mode. This mode appears to follow a linear trajectory increasing without bound. This mode can be shown to be described accurately by the second term (*i.e.* the dominant term) in Equation (3.262), which may be approximated by $\omega^2 \approx v_A^2 k^2/2$. In the Boussinesq approximation, fast modes are excluded while slow modes remain. The lower branch of solutions have a g-mode character, and so may be termed g-type slow modes, while the upper solution is a slow mode with a magnetic character.

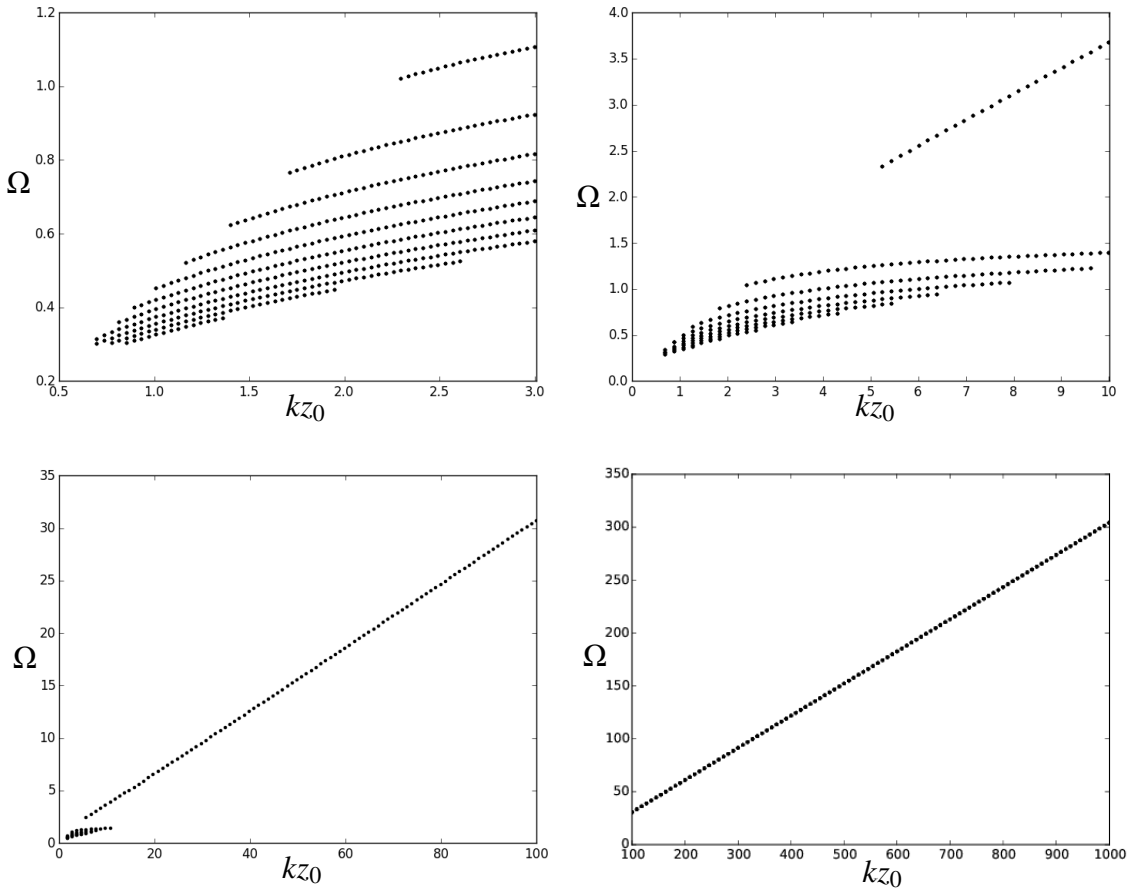

Fig. 3.10 Numerical solutions to Equation (3.257) for varying horizontal wavenumber. The other parameters are set at $v_A^2/c_s^2 = 0.2, z_0 = 5H, c_s = 8$ km s^{-1}.

The solutions are located between two cut-off frequencies. The upper cut-off is responsible for the appearance of the magnetic mode and higher frequency g-modes. For evanescent solutions in the magnetic layer the frequency must satisfy the conditions

$\omega^2 < \omega_{C1}^2 \approx v_A^2 k^2$, or $\omega^2 > \omega_{C2}^2 \approx v_A^2 k^2 + N^2$. The upper cut-off shown in Figure 3.10 is the first of these inequalities, that is the lower cut-off for the magnetic atmosphere. This means that it is possible that another branch of frequencies could exist in principle, although we do not see any for this choice of parameters.

For this choice of parameters we would not see any oscillatory solutions in the non-magnetic limit $v_A/c_s \to 0$ as the upper cut-off tends to zero. A horizontal magnetic field may then allow g-modes from the lower solar atmosphere to propagate into the higher atmosphere. Contrast this to a vertical magnetic field where the propagation of g-modes is inhibited.

The g-modes are constrained to exist above a lower cut-off frequency. The g-modes were not seen in the asymptotic analysis as they are below the lower cut-off in the limit taken. This cut-off is likely due to the polytropic as the curve resembles a g-mode frequency. This cut-off is not immediately evident from the dispersion relation. Further investigation is needed to identify this cut-off frequency.

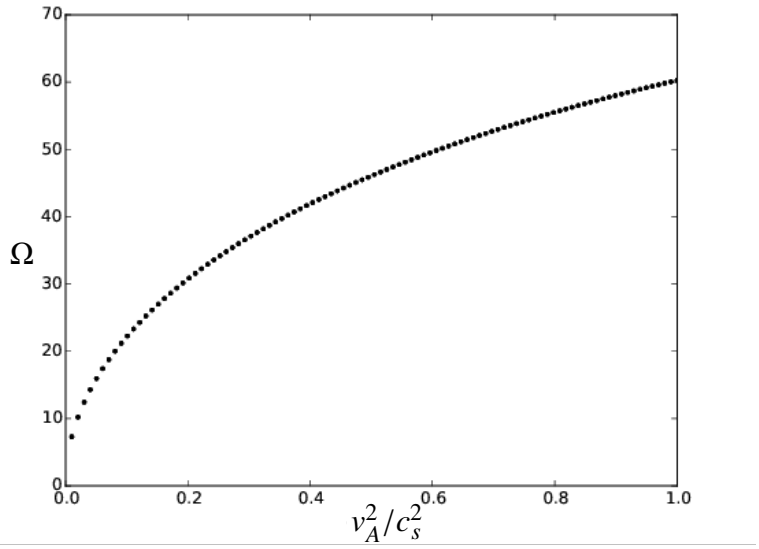

Fig. 3.11 Numerical solutions to Equation (3.257) for varying Alfvén speed. The other parameters are set at $kz_0 = 100, z_0 = 5H, c_s = 8$ km s^{-1}.

Figure 3.11 shows the effect of varying the Alfvén speed on the magnetic mode. The frequency tends to 0 as $v_A/c_s \to 0$. The mode does not exist when $v_A/c_s = 0$ as the cut-off tends to zero. We see that the dimensionless frequency changes significantly for small increases in the Alfvén frequency.

The f-mode is not present in this numerical analysis. There are two reasons for this fact. Firstly, in the low wavenumber regime the frequency of the f-mode is above the upper cut-off. When the wavenumber grows the wave may become magnetically dominated. As shown in Equation (3.269), the f-mode frequency may become imaginary if the mode is magnetically dominated. Hence, for the parameters used here there is no f-mode.

Let us make a note of the hydrodynamic solutions to the dispersion relation. We assume there is no discontinuity in temperature, that is the sound speed is continuous. The

approximate dispersion relation, Equation (3.260) is singular, hence one of the solutions is lost when taking the limit $\rho \to 1$. The non-singular solution may be found from the dispersion relation to be

$$\omega^2 \sim -\frac{N_0^4}{4\left(N^2 - N_0^2\right)}. \tag{3.264}$$

The non-singular solution may also be obtained from the positive root of the exact solution by Taylor expansion. The singular solution to the dispersion relation may be found from the negative root of the exact solution to be

$$\omega^2 \sim -\frac{N^2 - N_0^2}{2(1-\rho)}. \tag{3.265}$$

Each of these two solutions are negative, so we may expect that there are no stable solutions to the dispersion relation. Physically, this may be a consequence of the isothermal layer. The boundary condition of finite kinetic energy implies that the frequency must be greater than the Brunt-Väisälä frequency of the isothermal layer $\omega > N$, *i.e.* the solution is evanescent in the isothermal layer. It may be that polytropic layer does not allow oscillatory solutions that also decay in the isothermal. That is, there are no solutions that satisfy both boundary conditions in this limit. We should be careful not to over-interpret this result. These frequencies do not depend on k_x, hence the a priori assumption that κ stays finite is not valid. We should analyse the non-magnetic dispersion relation in a different manner, analytically or numerically.

We may also consider the case of no magnetic field in the isothermal layer, but we allow a discontinuity in the density. Such a system may model the solar photosphere where the physical quantities decrease quickly from their sub-surface values to atmospheric. When this is the case $\rho = \widehat{\rho}_{0e}/\widehat{\rho}_{0i} = \widehat{c}_{si}^2/c_{se}^2 \neq 1$. The simplified dispersion (3.260) relation takes the form

$$\left(1-\rho^2\right)\omega^4 + \left[\rho^2 N^2 - N_0^2 - 2gk_x(1-\rho)\right]\omega^2 + \left(gk_x(1-\rho) + \frac{N_0}{2}\right)^2 = 0, \tag{3.266}$$

which has solutions

$$\omega^2 = \frac{2gk_x(1-\rho) - \rho^2 N^2 + N_0^2}{2(1-\rho^2)} \pm \frac{gk_x\rho}{2(1-\rho^2)}\left[4(1-\rho)^2 - \frac{4(1-\rho)\left(N^2 - N_0^2\right)}{gk_x} + \frac{\rho^2 N^4 - 2N^2 N_0^2 + N_0^4}{g^2 k_x^2}\right]^{1/2}. \tag{3.267}$$

It is helpful to further simplify these solutions. These solutions are derived in the large wavenumber approximation. When the wavenumber is large we may assume that

$gk_x \gg N^2, N_0^2$. Taylor expanding the solutions gives

$$\omega^2 \sim gk_x - \frac{\rho N^2 - N_0^2}{2(1-\rho)}, \tag{3.268}$$

$$\omega^2 \sim gk_x \frac{1-\rho}{1+\rho} + \frac{\rho N^2 + N_0^2}{2(1+\rho)}. \tag{3.269}$$

We see that ω^2 depends on k_x, hence these solutions are such that κ does not grow with k_x and so we may be use these solutions with confidence. First, we consider the case that $\widehat{\rho}_{0i} > \widehat{\rho}_{0e}$, or $\rho < 1$. When this is the case the first solution is larger than the second; the first is approximately $\omega^2 \approx gk_x$, whereas the dominant contribution to the second is below the f-mode. The first solution has the character of the f-mode. Previous studies not in the Boussinesq approximation, making use of an adiabatic polytrope ($N_0 = 0$), concluded that the thermal profile of the interior had no effect on the f-mode. This may not be the case, as we see some modification due to the second term. The second solution, below the f-mode is a g-mode.

Let us now consider the case of a less dense isothermal exterior $\widehat{\rho}_{0i} < \widehat{\rho}_{0e}$, or $\rho > 1$. The dominant contribution to the first solution is unchanged $\omega^2 \approx gk_x$. The leading contribution to the second solution is negative and we have some instability. A heavier fluid over a lighter fluid causes the famous Rayleigh-Taylor instability to form. This unstable solution is a manifestation of this instability.

The non-magnetic dispersion relation, when there is no discontinuity in density, is

$$\left[\omega H(1-k_x z_0) - z_0 H k_x \left(\omega^2 - N^2\right)^{1/2}\right] U(1-\kappa, 2, 2k_x z_0) + 2k_x z_0 H \omega U'(1-\kappa, 2, 2k_x z_0) = 0. \tag{3.270}$$

It may be shown that in the small wavelength approximation, the resulting frequency is imaginary frequency given by Equation (3.264). As mentioned previously, this solution may be unreliable as the quantity κ does not remain finite when the frequency takes this form and so the assumptions are seen to be flawed.

The model used here may be extended to include to include a third layer. Such a model may include the simultaneous effects of a stable and unstable polytrope, which may model the effects of convection and a magnetic atmosphere on g-modes in the Sun. Some preliminary results with such a model are given in Appendix B.

3.4 Conclusions

In this chapter we have analysed buoyancy oscillations, which may be considered to be slow MHD waves propagating along the magnetic field lines. We are motivated by contributing to the theory of determining global oscillations present in the solar atmosphere.

There is growing evidence that oscillations from the solar interior penetrate deeply in the solar atmosphere. Good examples of such penetration is the reporting of 5-minute oscillations in the lower solar atmosphere by *e.g.* Didkovsky *et al.* (2011, 2013), Ireland *et al.* (2015). Here, we focus on perturbations taking into account the role of gravity. We focus on IGWs. When the field is parallel to gravity, the full coupled governing equations for MHD perturbations can be shown to have exact solutions when the temperature is constant (Zhugzhda, 1979). For more complicated (and realistic) density profiles the governing equations cannot be solved exactly to the best of our knowledge. We find that, by considering longitudinal motion, we are able to solve the resulting governing equation under certain simplifying assumptions that are applicable to solar atmospheric conditions.

Here, we have used the Boussinesq approximation to study hydrodynamic IGWs and derived the analogous governing equation for the case of a vertical magnetic field. Our aim was to determine the modification by the magnetic field, applicable to magnetic structures in the lower solar atmosphere. We, firstly, analysed propagating waves using the WKB approximation, similar to the case of a horizontal field studied by Barnes *et al.* (1998). A comparison between the hydrodynamic and MHD cases shows that the magnetic contribution to the frequency is a term corresponding to a slow MHD wave. This term is similar to the frequency of an Alfvén wave, which has led some to believe that in this model, Alfvén waves modified by gravity correspond to IGWs in a non-magnetic model. We have now shown that this is not the case. The Boussinesq approximation is applicable to high-β plasma, and so the lower solar atmosphere, in which the slow wave propagating along the magnetic field lines has a frequency comparable to an Alfvén wave, but the wave solution is not an Alfvén wave.

In this chapter we studied the effect of a variable temperature profile. Hasan & Christensen-Dalsgaard (1992) analysed the frequencies of standing wave modes in an isothermal plasma in a vertical magnetic field based on the exact solution of Zhugzhda (1979). The frequency shifts of solutions to a simplified dispersion relation due to coupling with the other modes are calculated. This analysis requires an in-depth mathematical treatment. In this work, the case of a large horizontal wavenumber was considered. Roberts (2006) found that for predominantly vertical motion, *i.e.* large horizontal wavenumbers, the slow wave is governed by a Klein-Gordon equation. This is a much simpler equation to analyse than the coupled second order equations obtained by Ferraro & Plumpton (1958).

We considered the case of standing waves using the method of Roberts (2006). This method is similar to the Boussinesq approximation in that it assumes large wavenumbers. Applying the high-β approximation we may study standing IGWs. Hasan & Christensen-Dalsgaard (1992) studied the case of a constant temperature; we have generalised this result to the case of propagating waves and standing waves in a polytropic model, where the background varies slowly, which is more applicable to the case of the lower solar photosphere. In the cases of standing and propagating waves we see that a weak magnetic field has a significant effect, leading to frequencies greater than the Brunt-Väisälä frequency.

The Boussinesq approximation was not applied in the analysis of Hasan & Christensen-Dalsgaard (1992), hence this study gives a clearer picture of IGWs in the lower solar atmosphere.

The, perhaps over simplistic, case of standing waves in a finite cavity is relaxed to add a semi-infinite upper layer in which the plasma-β may vary and become large. Such an atmosphere may model the chromosphere, where the plasma-β typically reaches unity. The character of the waves changes drastically through this region, meaning a mathematical analysis is difficult. We find asymptotic expressions for the eigenfunctions. The key result is that an upper cut-off is introduced via the Brunt-Väisälä frequency in the upper layer. This may contribute to the reason IGWs are elusive - the atmosphere itself may inhibit the propagation of magnetic IGWs.

The case of a partially ionised plasma was studied using a two-fluid model. We calculated the corrections to the frequencies and the damping rates in several physical limits. A key result was that the frequency, derived from the starting point of a fully ionised fluid, is close to that of a weakly ionised fluid when the ion-neutral collision frequency is large. The major difference is that damping due to ion-neutral collisions is present. That is, magnetic effects may still be very important even to a weakly ionised plasma. When the collision frequency is low the two fluids interact weakly so oscillatory solutions are present in each of the gasses: buoyancy-driven MHD waves in the ionised fluid and IGWs in the neutral fluid. For large collision frequency the two gasses act as a single fluid. The oscillatory IGWs become purely damped vortex modes and we have MHD waves in the ion/neutral single fluid.

We also consider the case of a horizontal field. While the governing equations may be solved easier than the case of a vertical field, information about the eigenfrequencies is difficult to obtain from the dispersion relation. Limiting expressions, including surface modes, may be found.

The application of this work is to atmospheric magnetic buoyancy oscillations, that is oscillations where buoyancy is the primary restoring force but magnetic tension also has a contribution. These internal gravity waves (internal here does not refer to the solar interior, it refers to the interior of the fluid to distinguish the waves from *surface* gravity waves) have been observed in the solar photosphere and low atmosphere by *e.g.*, Stodilka (2008) and Straus *et al.* (2008). A detailed study to observe the effect of a magnetic field on IGWs has, to the author's knowledge, not yet been undertaken. It is anticipated that the techniques applied in this survey will be extended to study MAG waves in the lower solar atmosphere. The theoretical results in this chapter may prove important when such studies are carried out.

Note that the atmospheric buoyancy oscillations are not to be confused with the internal g-modes of helioseismology. The internal g-modes that are trapped in the solar interior, below the convection zone, have well known properties although they have not been

convincingly observed on the Sun yet. The search for interior g-modes is summarised by Appourchaux *et al.* (2010).

Our model is representative of the photosphere or upper interior. It is natural then that we include in our model forcing due to convective motion just below the photosphere. The governing equation in the lower layer has a z-dependent cut-off frequency. The Brunt-Väisälä frequency plays the role of the cut-off frequency here. It is possible that the system will be subject to a global resonance of the type discovered by Taroyan & Erdélyi (2008). This will be discussed in a following chapter.

Chapter 4

Global Resonance in a Hydrodynamic Model

4.1 Global Resonance of Vertically Propagating Acoustic Waves

4.1.1 Introduction and Summary of Previous Work

Many of the myriad of observed wave phenomena in the solar atmosphere owe their origin to the turbulent motion in the convection zone. The convection zone is an efficient generator of p-modes in particular; millions of p-modes of varying spherical degree have been observed. The decreasing density in the lower solar atmosphere may cause some reflection or refraction of p-modes, effectively trapping them in the solar interior. This is, however, an idealised picture. The photosphere is not a free surface, the solar interior and atmosphere is a coupled system. Waves generated in the convection zone may propagate into the atmosphere. It has been shown that vertically propagating waves may be trapped by the varying temperature, leading to a resonance that extends to the whole atmosphere. In this chapter we outline the resonance as discovered by Taroyan & Erdélyi (2008) and extend the work to non-vertical wave propagation in a hydrodynamic atmosphere.

We begin with a discussion of the work of Taroyan & Erdélyi (2008). Let the background equilibrium consist of a lower layer in which the temperature varies slowly and an isothermal upper layer

$$T_0(z) = \begin{cases} T_0(1 - z/z_0), & 0 < z < L, \\ T_2, & z > L, \end{cases} \tag{4.1}$$

where T_0, T_2 and z_0 are positive constants and $L/z_0 < 1$ to ensure the temperature remains positive. Gravity acts in the negative z direction, $\mathbf{g} = (0, 0, -g)$. In this section we consider the lower layer to be $z \in [0, L]$, as in Taroyan & Erdélyi (2008). The medium is in hydrostatic equilibrium, we consider only the hydrostatic case; that is, there is no magnetic field, and there are no background flows. The background pressure, p_0, and density, ρ_0, are functions of z only. The background in the lower layer is polytropic while in the upper layer the pressure and density decay exponentially

$$p_0(z) = \begin{cases} p_0(0)(1 - z/z_0)^{m+1}, & 0 < z < L, \\ p_0(L)\exp(-z/H), & z > L, \end{cases} \tag{4.2}$$

$$\rho_0(z) = \begin{cases} \rho_0(0)(1 - z/z_0)^{m}, & 0 < z < L, \\ \rho_0(L)\exp(-z/H), & z > L, \end{cases} \tag{4.3}$$

where H is the pressure scale height, c_s is the sound speed, γ is the ratio of specific heats and m is the polytropic index. Around this background we analyse the propagation of small amplitude, *i.e.* linear, waves. We restrict ourselves to the case of vertical wave propagation,

equivalent to $k_\perp = 0$. The linearised equations of continuity, momentum and energy are

$$\frac{\partial \rho_1}{\partial t} + \frac{\partial}{\partial z}(\rho_0 u) = 0, \tag{4.4}$$

$$\rho_0 \frac{\partial u_1}{\partial t} = -\frac{\partial p_1}{\partial z} - \rho_1 g, \tag{4.5}$$

$$\frac{\partial p_1}{\partial t} + \frac{\partial p_0}{\partial z} u_1 = c_s^2 \left(\frac{\partial \rho_1}{\partial t} + \frac{\partial \rho_0}{\partial z} u_1 \right), \tag{4.6}$$

where p_1, ρ_1, u_1 are the perturbed pressure, density and velocity. Equations (4.4) to (4.6) may be combined to give

$$\rho_0 \frac{\partial^2 u_1}{\partial t^2} = \frac{\partial}{\partial z} \left(\rho_0 c_s^2 \frac{\partial u_1}{\partial z} \right), \tag{4.7}$$

which may be written in Klein-Gordon form

$$\frac{\partial^2 Q}{\partial t^2} - c_s^2 \frac{\partial^2 Q}{\partial z^2} + \Omega^2 Q = 0, \tag{4.8}$$

where

$$Q(z,t) = \sqrt{\frac{\rho_0(z) c_s^2(z)}{\rho_0(0) c_s^2(0)}} u(z,t) \tag{4.9}$$

is a scaled velocity and

$$\Omega^2(z) = \frac{c_s^2}{4H^2} \left(1 + 2 \frac{\mathrm{d}H}{\mathrm{d}z} \right) \tag{4.10}$$

is the square of the acoustic cut-off frequency. We let Q be proportional to $\exp(-\mathrm{i}\omega t)$. Equation (4.9) has solutions in the lower layer in terms of Bessel functions

$$Q = e^{-\mathrm{i}\omega t} \sqrt{1 - z/z_0} \left[A_1 J_m \left(\frac{2\omega z_0}{c_s(0)} \sqrt{1 - z/z_0} \right) + B_1 Y_m \left(\frac{2\omega z_0}{c_s(0)} \sqrt{1 - z/z_0} \right) \right], \quad 0 < z < L, \tag{4.11}$$

where m may also be expressed as

$$m = \frac{g \gamma z_0}{c_s^2(0)} - 1. \tag{4.12}$$

In the upper layer the solutions are given by

$$Q = A_2 \exp\left(\mathrm{i}\left(kz - \omega t\right)\right), \quad z > L, \tag{4.13}$$

where

$$k = \begin{cases} \mathrm{i} \dfrac{\sqrt{\Omega_2^2 - \omega^2}}{c_2}, & \omega < \Omega_2, \\ \dfrac{\sqrt{\omega^2 - \Omega_2^2}}{c_2}, & \omega > \Omega_2, \end{cases} \tag{4.14}$$

where the subscript "2" denotes the sound speed or cut-off in the upper layer. Solution (4.13) represents an outgoing wave when $\omega > \Omega_2$. When $\omega < \Omega_2$, the solution is a manifestation of the boundary condition of finite wave energy density as $z \to \infty$.

Let us now connect these two layers together by applying boundary conditions. Firstly, the cavity is driven periodically at $z = 0$ with frequency ω and amplitude $I = I(\omega)$,

$$\lim_{z\to 0} Q(z,t) = I(\omega)\exp(-\mathrm{i}\omega t). \tag{4.15}$$

At $z = L$ we apply the continuity of Lagrangian displacement which, with the continuity of background pressure, leads to

$$Q(z,t)|_{z=L-} = Q(z,t)|_{z=L+} \tag{4.16}$$

The final boundary condition is a consequence of the continuity of Lagrangian pressure perturbation, $\delta p = p_1 + \xi\, \mathrm{d}p_0/\mathrm{d}z$, where ξ is the Lagrangian displacement $u = \partial\xi/\partial t$. The governing equations (4.4) to (4.6) may be combined to show

$$\frac{\partial}{\partial t}\delta p = -\gamma p_0 \frac{\partial u}{\partial z}, \tag{4.17}$$

δp is continuous in space (and smooth in time) and p_0 is continuous to maintain equilibrium, hence the second boundary condition may be expressed as the continuity of $\partial u/\partial z$. In terms of the scaled variable Q, this is

$$\left(\frac{\partial Q}{\partial z} + \frac{1}{2H_1}Q\right)\bigg|_{z=L-} = \left(\frac{\partial Q}{\partial z} + \frac{1}{2H_2}Q\right)\bigg|_{z=L+}. \tag{4.18}$$

Applying these boundary conditions gives the relations

$$A_1 J_m(\theta_0) + B_1 Y_m(\theta_0) = I(\omega), \tag{4.19}$$

$$\sqrt{1 - L/z_0}\,(A_1 J_m(\theta_L) + B_1 Y_m(\theta_L)) - A_2 e^{\mathrm{i}kL} = 0, \tag{4.20}$$

$$\frac{\omega}{c_s(0)} J_{m+1}(\theta_L) + \frac{\omega}{c_s(0)} Y_{m+1}(\theta_L) - \left(\mathrm{i}k + \frac{1}{2H_2}\right) e^{\mathrm{i}kL} = 0, \tag{4.21}$$

where

$$\theta_0 = \frac{2\omega z_0}{c_s(0)}, \quad \theta_L = \frac{2\omega z_0}{c_s(0)}\sqrt{1 - L/z_0}. \tag{4.22}$$

The inhomogeneous system of equations (4.19) to (4.21) may be inverted to obtain expressions for the coefficients A_1, B_1 and A_2, *i.e.* the amplitudes of the waves,

$$A_2 = \frac{-\frac{\omega}{c_s(0)} I(\omega) e^{-\mathrm{i}kL} W\left(J_m(\theta_L), Y_m(\theta_L)\right)}{\frac{\omega}{c_s(L)}\left(Y_{m+1}(\theta_L) J_m(\theta_0) - Y_m(\theta_0) J_{m+1}(\theta_L)\right) + \left(\mathrm{i}k + \frac{1}{2H_2}\right)\left(J_m(\theta_L) Y_m(\theta_0) - J_m(\theta_0) Y_m(\theta_L)\right)}, \tag{4.23}$$

$$A_1 = \frac{\left[Y_m(\theta_L)\left(\mathrm{i}k + \frac{1}{2H_2}\right) - \frac{\omega}{c_s(L)} Y_{m+1}(\theta_L)\right] e^{\mathrm{i}kL} A_2}{\frac{\omega}{c_s(0)} W\left(J_m(\theta_L), Y_m(\theta_L)\right)}, \tag{4.24}$$

$$B_1 = \frac{\left[-J_m(\theta_L)\left(\mathrm{i}k + \frac{1}{2H_2}\right) + \frac{\omega}{c_s(L)} J_{m+1}(\theta_L)\right] e^{\mathrm{i}kL} A_2}{\frac{\omega}{c_s(0)} W\left(J_m(\theta_L), Y_m(\theta_L)\right)}, \tag{4.25}$$

where $W(f,g) = fg' - gf'$ is the Wronskian, and the Wronskian of the Bessel functions is given by (Abramowitz & Stegun, 1979)

$$W\left(J_\nu(x), Y_\nu(x)\right) = \frac{2}{\pi x}. \tag{4.26}$$

Note that the coefficients A_1 and B_1 are corrections of those in Taroyan & Erdélyi (2008), but this does not change the key results of that work.

We see that A_2 may be singular, for some imaginary k. There may, therefore, be resonant frequencies below the acoustic cut-off frequency in the upper layer. The coefficients A_1 and B_1 are proportional to A_2 so this resonance is global. Finding these frequencies requires numerical analysis as the expression for A_2 is transcendental in ω. We may, however, make analytical progress by assuming the lower layer is thin and the temperature varies slowly throughout the layer,

$$\frac{L}{H} \ll 1, \quad 1 - T(z)/T_0 \ll 1, \quad 0 < z < L. \tag{4.27}$$

We may simplify A_2 by Taylor expanding around the small parameters (4.27) to give

$$A_2 = \frac{I(\omega) e^{\mathrm{i}kL}}{1 - \frac{L}{2H_2} + L\frac{\sqrt{\Omega_2^2 - \omega^2}}{c_{s2}}}. \tag{4.28}$$

The waves are then amplified when driven at the frequency

$$\omega = \frac{c_{s2}}{L}\sqrt{\frac{L}{H_2} - 1}. \tag{4.29}$$

The resonant frequencies lie between the acoustic cut-off frequencies in the lower and upper layers, $\Omega_1 < \omega < \Omega_2$. We see that for a resonance to occur, $L/H_2 > 1$. This fact used with the simplifications applied in the previous analysis imply that $\widehat{c}_{si}^2 \gg c_{se}^2$ and so $\Omega_1 \ll \omega < \Omega_2$. Equation (4.29) may then be applied when there is a significant drop in temperature between the two-layers. This is applicable to the solar atmosphere where the

temperature decrease rapidly from its sub-surface value to the value in the lower solar atmosphere. The assumptions simplify the analysis although they are not fundamental to the existence of the global resonance, as a numerical analysis may show.

Taroyan & Erdélyi (2008) give the varying temperature in the lower layer as the cause of the resonance. The decreasing temperature causes an increasing acoustic cut-off frequency which acts as a potential barrier, reflecting low-frequency waves. This effect is analogous to the well known phenomena in quantum mechanics where some potential reflects a portion of the incoming wave solution. The acoustic cut-off in the above wave equation is analogous to the potential function in the time-dependent Schrödinger equation. When the driver matches the driving frequency, standing waves are created in the resonant cavity and amplified. The analytical result, when the lower layer is thin, represents only the fundamental mode of oscillation. See Taroyan & Erdélyi (2008) for numerical results.

4.1.2 Effect of the Polytropic Temperature Profile

In the interest of consistency with previous chapters, let us apply the driven boundary condition at $z = -L$ and connect the layers at $z = 0$. We also use the same notation used elsewhere. The coefficient of the outgoing wave can be written

$$D_1 = \frac{\frac{\omega}{\widehat{c}_{si}} I(\omega)(-z_0)^{-\frac{m}{2}}(-L-z_0)^{\frac{m}{2}} W(J_m(\theta_0), Y_m(\theta_0))}{\frac{\omega}{\widehat{c}_{si}}[J_m(\theta_{-L})Y_{m+1}(\theta_0) - J_{m+1}(\theta_0)Y_m(\theta_{-L})] - [J_m(\theta_{-L})Y_m(\theta_0) - J_m(\theta_0)Y_m(\theta_{-L})]\left(\frac{1}{2H_e} + \mathrm{i}\kappa\right)}, \tag{4.30}$$

where D_1 represents the amplitude of the outgoing wave in the upper layer (replacing A_2 used in the previous subsection), we also use i and e rather than 1 and 2 to denote the lower and upper layers. Let us assume the lower layer is thin $L/z_0 \ll 1$. Applying this assumption we may Taylor expand the Bessel functions $\mathscr{C}_m(\theta_{-L})$, where $\mathscr{C}$ denoted either of the Bessel functions J and Y,

$$\mathscr{C}_m\left(\theta_0\sqrt{1+\frac{L}{z_0}}\right) = \mathscr{C}_m(\theta_0) + (m\mathscr{C}_m(\theta_0) - \mathscr{C}_{m+1}(\theta_0)\theta_0)\frac{L}{2z_0} + O\left(\frac{L^2}{z_0^2}\right). \tag{4.31}$$

The series expansions for the Bessel functions may be used to show that

$$J_m(\theta_{-L})Y_m(\theta_0) - J_m(\theta_0)Y_m(\theta_{-L}) \approx -\frac{L}{2z_0}\theta_0 W(J_m(\theta_0), Y_m(\theta_0)), \tag{4.32}$$

$$J_m(\theta_{-L})Y_{m+1}(\theta_0) - J_{m+1}(\theta_0)Y_m(\theta_{-L}) \approx -W(J_m(\theta_0), Y_m(\theta_0))\left(1 + \frac{Lm}{2z_0} - \frac{\theta_0^2 L^2}{8z_0^2}\right). \tag{4.33}$$

The polytropic index m is determined by $m = (z_0/H_i) - 1$ and $\theta_0 = 2\omega z_0/\widehat{c}_{si}$; hence for the Taylor expansions (4.32) and (4.33) to be truncated as above, we make the assumption $L/H_i \ll 1$. Note that H_i is H in the lower layer evaluated at $z = 0$. Small terms appearing

higher than first order have been neglected. It can be shown that all first-order small quantities are contained within in the series above. Physically, the assumption of $L/H_i \ll 1$ complements the assumption $L/z_0 \ll 1$ in describing the lower layer as thin. Used together, these assumptions are equivalent to $|f_0' L/f_0| \ll 1$, where f_0 represents the equilibrium quantities of pressure, density and temperature. The coefficient D_1 may be simplified to

$$D_1 \approx \frac{-I(\omega)\left(1+\dfrac{L}{2H_i}-\dfrac{L}{2z_0}\right)}{1+\dfrac{L}{2H_i}-\dfrac{L}{2z_0}-\dfrac{L^2\omega^2}{2g\gamma H_i}-\dfrac{L}{2H_e}+\dfrac{L}{c_{se}}\sqrt{\Omega_e^2-\omega^2}}, \tag{4.34}$$

where we drive below the cut-off frequency $\omega < \Omega_e$. Finding the resonant frequency is then given by the solution to

$$1+\frac{L}{2H_i}-\frac{L}{2z_0}-\frac{L^2\omega^2}{2g\gamma H_i}-\frac{L}{2H_e}+\frac{L}{c_{se}}\sqrt{\Omega_e^2-\omega^2}=0. \tag{4.35}$$

In analysing the resonance, Taroyan & Erdélyi (2008) neglected the small terms L/z_0 and L/H_i. Neglecting these terms in the above returns their result. Let us keep these terms in order to see the correction due to the slow parameter variation in the lower layer. Rearranging for the frequency ω, and neglecting second order small quantities, gives us

$$\omega = \frac{c_{se}}{L}\left[\frac{L}{H_e}-1+\left(1-\frac{L}{2H_e}\right)\frac{L}{z_0}+\frac{1}{2}\left(1-\frac{2H_e}{L}\right)\frac{L}{H_i}\right]^{\frac{1}{2}}. \tag{4.36}$$

Equation (4.36) is the expression for the fundamental resonant frequency with a correction due to the slow variation of equilibrium quantities throughout the lower layer. When $L/2H_e > 1$, the tendency of the L/z_0 term is to decrease the resonant frequency, whereas the L/H_i term increases the frequency. The combination of these competing effects is to overall increase the resonant frequency, relative to the case of neglecting first-order small terms, if

$$\left(1-\frac{2H_e}{L}\right)\frac{L}{2H_i} > \left(\frac{L}{2H_e}-1\right)\frac{L}{z_0}. \tag{4.37}$$

The resonant frequency is smaller than the zero-th order frequency if

$$\left(1-\frac{2H_e}{L}\right)\frac{L}{2H_i} < \left(\frac{L}{2H_e}-1\right)\frac{L}{z_0}. \tag{4.38}$$

When there is equality of these terms, there is no overall effect and the resonant frequency is the same as that investigated by Taroyan & Erdélyi (2008).

4.2 Internal Gravity Waves

The above analysis assumed the case of vertical wave propagation, $k_x = 0$, hence only sound waves were considered. In this section we perform a similar analysis to investigate whether the resonance exists for the case of internal gravity waves. We use the Boussinesq approximation, solutions to the governing equations of which were found previously. There is no magnetic field so let us assume no y-dependence. In the lower layer we assume, for simplicity, that the temperature varies slowly (although the governing equation may be solved without this assumption). The solution for the vertical component of momentum is

$$q_i = C_1 \mathrm{Ai}(\Theta) + C_2 \mathrm{Bi}(\Theta), \tag{4.39}$$

where

$$\Theta = -\frac{1}{N_0^2}\left(\frac{k_x^2 N_0^2}{\omega^2 z_0}\right)^{\frac{1}{3}}\left(N_0^2(z+z_0) - \omega^2 z_0\right). \tag{4.40}$$

Note that this solution is the function representing the z-dependent amplitude, *i.e.* the governing equations have already been Fourier analysed. The solution in the upper layer is

$$q_e = D_1 e^{\mathrm{i}\kappa z}, \tag{4.41}$$

where

$$\kappa = \begin{cases} k_x\left(\dfrac{N^2}{\omega^2} - 1\right)^{\frac{1}{2}}, & \omega < N, \\ \mathrm{i}k_x\left(1 - \dfrac{N^2}{\omega^2}\right)^{\frac{1}{2}}, & \omega > N, \end{cases} . \tag{4.42}$$

This full solution, $q_e = D_1 \exp(\mathrm{i}\kappa z - \mathrm{i}\omega t)$, represents an outgoing wave when $\omega < N$. When $\omega > N$ the solution expresses the condition of finite kinetic energy as $z \to \infty$.

Let us now apply boundary conditions. Firstly we drive the waves at $z = -L_1$,

$$\lim_{z \to -L} v_{zi} = \frac{q_i}{\rho_{0i}} = I(\omega). \tag{4.43}$$

The boundary conditions are continuity of velocity and Lagrangian pressure perturbations at $z = 0$,

$$\frac{q_i}{\rho_{0i}} = \frac{q_e}{\rho_{0e}}, \quad \text{at} \quad z = 0, \tag{4.44}$$

and

$$\frac{\omega}{k_x^2}\frac{\mathrm{d}q_i}{\mathrm{d}z} - \frac{g}{\omega}q_i = \frac{\omega}{k_x^2}\frac{\mathrm{d}q_e}{\mathrm{d}z} - \frac{g}{\omega}q_e, \quad \text{at} \quad z = 0. \tag{4.45}$$

Applying these conditions we have the relations

$$\frac{1}{\widehat{\rho_{0i}}}\left(1 + \frac{L}{z_0}\right)^{-m}\left[C_1 \mathrm{Ai}(\Theta_{-L}) + C_2 \mathrm{Bi}(\Theta_{-L})\right] = I(\omega), \tag{4.46}$$

$$\frac{1}{\widehat{\rho}_{0i}}\left[C_1\mathrm{Ai}\left(\Theta_0\right)+C_2\mathrm{Bi}\left(\Theta_0\right)\right]-\frac{1}{\widehat{\rho}_{0e}}D_1=0, \tag{4.47}$$

$$\left[\frac{\omega}{k_x^2}\Theta'\mathrm{Ai}'\left(\Theta_0\right)-\frac{g}{\omega}\mathrm{Ai}\left(\Theta_0\right)\right]C_1+\left[\frac{\omega}{k_x^2}\Theta'\mathrm{Bi}'\left(\Theta_0\right)-\frac{g}{\omega}\mathrm{Bi}\left(\Theta_0\right)\right]C_2-\left[\frac{\mathrm{i}\omega\kappa}{k_x^2}-\frac{g}{\omega}\right]D_1=0. \tag{4.48}$$

These equations may be used to determine the coefficients,

$$D_1=\frac{-\omega^2\Theta'\widehat{\rho}_{0i}\widehat{\rho}_{0e}I(\omega)\left(1+\frac{L}{z_0}\right)^m W\left(\mathrm{Ai}\left(\Theta_0\right),\mathrm{Bi}\left(\Theta_0\right)\right)}{\left[\mathrm{Ai}'\left(\Theta_0\right)\mathrm{Bi}\left(\Theta_{-L}\right)-\mathrm{Bi}'\left(\Theta_0\right)\mathrm{Ai}\left(\Theta_{-L}\right)\right]\widehat{\rho}_{0i}\omega^2\Theta'+\left[\mathrm{Ai}\left(\Theta_0\right)\mathrm{Bi}\left(\Theta_{-L}\right)-\mathrm{Bi}\left(\Theta_0\right)\mathrm{Ai}\left(\Theta_{-L}\right)\right]\left[gk_x^2\left(\widehat{\rho}_{0e}-\widehat{\rho}_{0i}\right)-\mathrm{i}\widehat{\rho}_{0e}\omega^2\kappa\right]}, \tag{4.49}$$

$$C_1=\frac{\left[\widehat{\rho}_{0i}\omega^2\Theta'\mathrm{Bi}'\left(\Theta_0\right)-\left(\widehat{\rho}_{0e}\omega^2\kappa\mathrm{i}+gk_x^2\left(\widehat{\rho}_{0i}-\widehat{\rho}_{0e}\right)\right)\mathrm{Bi}\left(\Theta_0\right)\right]D_1}{\omega^2\Theta'\widehat{\rho}_{0e}W\left(\mathrm{Ai}\left(\Theta_0\right),\mathrm{Bi}\left(\Theta_0\right)\right)}, \tag{4.50}$$

$$C_2=-\frac{\left[\widehat{\rho}_{0i}\omega^2\Theta'\mathrm{Ai}'\left(\Theta_0\right)+\left(gk_x^2\left(\widehat{\rho}_{0e}-\widehat{\rho}_{0i}\right)-\widehat{\rho}_{0e}\omega^2\kappa\mathrm{i}\right)\mathrm{Ai}\left(\Theta_0\right)\right]D_1}{\omega^2\Theta'\widehat{\rho}_{0e}W\left(\mathrm{Ai}\left(\Theta_0\right),\mathrm{Bi}\left(\Theta_0\right)\right)}. \tag{4.51}$$

The Wronskian of the Airy functions is given by

$$W\left(\mathrm{Ai}\left(\Theta_0\right),\mathrm{Bi}\left(\Theta_0\right)\right)=\frac{1}{\pi}. \tag{4.52}$$

upon considering the form of D_1, there may be singular frequencies. We also notice that C_1 and C_2 are proportional to D_1, just like in the previous case of vertically propagating sound waves, so any resonance is global in nature. Let us now investigate these resonant frequencies. Making use of the fact that

$$\Theta_{-L}=-\frac{z_0}{N_0^2}\left(\frac{k_x^2N_0^2}{\omega^2z_0}\right)^{\frac{1}{3}}\left(N_0^2-\omega^2\right)+\frac{z_0}{N_0^2}\left(\frac{k_x^2N_0^2}{\omega^2z_0}\right)^{\frac{1}{3}}\frac{L}{z_0}=\Theta_0\left(1-\frac{N_0^2}{N_0^2-\omega^2}\frac{L}{z_0}\right), \tag{4.53}$$

and that the lower layer is thin $L/z_0\ll 1$ we may Taylor expand the Airy functions,

$$\mathrm{Ai}\left(\Theta_0\left(1-\frac{N_0^2}{N_0^2-\omega^2}\frac{L}{z_0}\right)\right)\approx\mathrm{Ai}\left(\Theta_0\right)-\mathrm{Ai}'\left(\Theta_0\right)\frac{\Theta_0N_0^2}{N_0^2-\omega^2}\frac{L}{z_0}, \tag{4.54}$$

$$\mathrm{Bi}\left(\Theta_0\left(1-\frac{N_0^2}{N_0^2-\omega^2}\frac{L}{z_0}\right)\right)\approx\mathrm{Bi}\left(\Theta_0\right)-\mathrm{Bi}'\left(\Theta_0\right)\frac{\Theta_0N_0^2}{N_0^2-\omega^2}\frac{L}{z_0}. \tag{4.55}$$

Note that Θ_0 is order $O\left(\left(k_xz_0\right)^{\frac{2}{3}}\right)$. k_xz_0 is a large parameter due to the Boussinesq approximation, there are therefore terms in the Taylor expansion which may not be considered small as we do not specify the magnitude of the product k_xL outright. We may, however, use the first two terms in the series if we make the assumption that the driving frequency is comparable to the Brunt-Väisälä frequency $\omega\approx N_0$ (or under the assumption that $k_xL\ll 1$

but this will have consequences on the resonant frequency as we shall see). Under this assumption $1-\omega^2/N_0^2$ is small. Θ_0 is now the product of the large parameter to the 2/3 power and a small term to the first power. The term $N_0/\left(N_0^2-\omega^2\right)$ is large. The Taylor expansion now forms a decreasing series and may be approximated by the expression above. This is restricted to the case $(k_x z_0)^{\frac{2}{3}} L/z_0 < 1$ (this guarantees convergence but a more detailed analysis shows that the condition is closer to $(k_x z_0)^{\frac{2}{3}} L/z_0 < 3$). Using the Wronskian property above,

$$\mathrm{Ai}'(\Theta_0)\,\mathrm{Bi}(\Theta_{-L}) - \mathrm{Bi}'(\Theta_0)\,\mathrm{Ai}(\Theta_{-L}) \approx -\frac{1}{\pi}, \tag{4.56}$$

$$\mathrm{Ai}(\Theta_0)\,\mathrm{Bi}(\Theta_{-L}) - \mathrm{Bi}(\Theta_0)\,\mathrm{Ai}(\Theta_{-L}) \approx \frac{L}{\pi}\left(\frac{k_x^2 N_0^2}{\omega^2 z_0}\right)^{\frac{1}{3}}. \tag{4.57}$$

Driving above the cut-off frequency in the upper layer $\omega > N$, we may simplify D_1 to

$$D_1 \approx \frac{\omega^2 \widehat{\rho}_{0i}\widehat{\rho}_{0e} I(\omega)\left(1+\frac{mL}{z_0}\right)}{\widehat{\rho}_{0i}\omega^2 + \left(g k_x^2(\widehat{\rho}_{0e}-\widehat{\rho}_{0i}) + \widehat{\rho}_{0e}\omega^2 k_x\left(1-\frac{N^2}{\omega^2}\right)^{\frac{1}{2}}\right)L}, \tag{4.58}$$

hence the waves are amplified when driven at

$$\omega^2 = \frac{L k_x^2\left(N^2 L + 2g\alpha(1-\alpha)\right)}{2\left(k_x^2 L^2 - \alpha^2\right)} \pm \frac{L k_x^2}{2\left(\alpha^2 - k_x^2 L^2\right)}\left[\left(N^2 L + 2g\alpha(1-\alpha)\right)^2 - 4g^2\left(1-\alpha^2\right)\left(\alpha^2 - k_x^2 L^2\right)\right]^{\frac{1}{2}}, \tag{4.59}$$

where α is the ratio of densities at $z = 0$,

$$\alpha = \frac{\widehat{\rho}_{0i}}{\widehat{\rho}_{0e}}, \tag{4.60}$$

and $k_x^2 L^2 \neq \alpha^2$. For simplicity let us consider the case where the density is continuous, $\alpha = 1$. When this is the case the resonant frequency reduces to

$$\omega = N\left(\frac{1}{1-\frac{1}{k_x^2 L^2}}\right)^{\frac{1}{2}}, \tag{4.61}$$

where $k_x L > 1$ for a real frequency. The Boussinesq approximation is equivalent to assuming large wavenumbers so this inequality is likely to be valid. In the simplifications made previously, we assumed $(k_x z_0)^{\frac{2}{3}} L/z_0 < 1$ which may be rewritten $(k_x L)^{\frac{2}{3}} (L/z_0)^{\frac{1}{3}} < 1$. Hence, the inequalities $k_x L > 1$ and $(k_x L)^{\frac{2}{3}} (L/z_0)^{\frac{1}{3}} < 1$ may be satisfied if L/z_0 is sufficiently small.

This analysis shows that the resonance shown to exist for vertically propagating sound waves also exists for internal gravity waves in the Boussinesq approximation. Due to g-modes having an upper cut-off frequency, that is propagating solutions exist below the

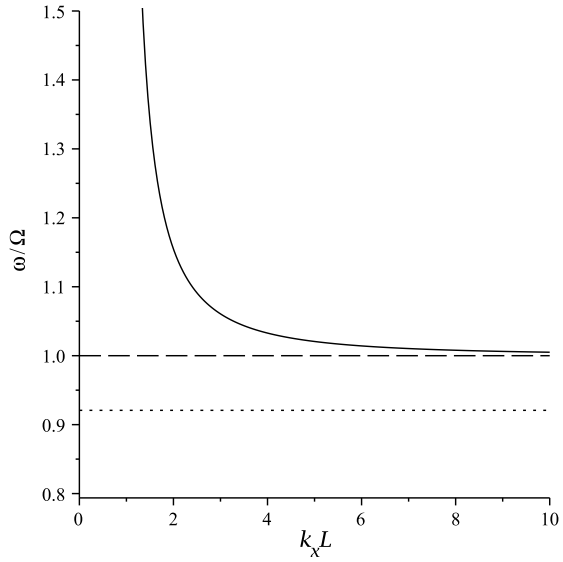

Fig. 4.1 A plot of the resonant frequencies (4.61), normalised to the Brunt-Väisälä frequency in the upper layer, for increasing k_xL (solid line). The dashed line represents the Brunt-Väisälä frequency in the upper layer, taken to be $N = 0.03$ rad s^{-1}. The dotted line is the Brunt-Väisälä in the lower layer N_0, the parameters are taken to be $z_0 = 1.5$ Mm and $g = 0.274$ km s^{-2}.

Brunt-Väisälä frequency, the resonance is located above the Brunt-Väisälä in the upper layer. For the case of continuous sound speed, it can be shown $N_0^2 = N^2 - g/z_0$, *i.e.* $N_0 < N$ and so the resonant frequencies are also located above the cut-off frequency of the lower layer. The solution in the lower layer also represents evanescent modes.

The resonant frequency given by Equation (4.61) is plotted in Figure 4.1 for increasing k_xL. As k_xL increases the resonant frequency tends to the Brunt-Väisälä frequency in the upper layer. The resonant frequency becomes infinite as $k_xL \to 1$, and becomes complex for $k_xL < 1$. The physical significance for this limit is, perhaps, linked to the Boussinesq approximation. It was discussed previously that the Boussinesq approximation is valid for large wavenumbers. The fact that the resonance stops for this value may not be linked to the physical process of the resonance, rather it may be due to the fact that the region $kL < 1$ is outside of the scope of the underlying approximations. In the next section we discuss the resonance for hydrodynamic waves without any limitation placed on the wavelength.

Although drastic simplifications must be made to find an analytical expression for the resonant frequency, the analysis unveils that a global resonance does indeed exist. The analytical expression allows, however, a simple investigation of the resonant frequencies and shall provide a useful comparison to the MHD case in what follows.

4.3 Non-Vertical Wave Propagation

It is also possible to find solutions and investigate the driven problem for the case of combined buoyancy and compression. The general governing equation for linear waves in

a gravitationally stratified fluid, describing both p-modes and g-modes, when $k_y \neq 0$ is

$$\frac{\mathrm{d}^2\Delta}{\mathrm{d}z^2} + \frac{1}{c_s^2}\left(\frac{\mathrm{d}c_s^2}{\mathrm{d}z} - g\gamma\right)\frac{\mathrm{d}\Delta}{\mathrm{d}z} + \left[\frac{1}{c_s^2}\left(\omega^2 - c_s^2k_\perp^2\right) + \frac{k_\perp^2N^2}{\omega^2}\right]\Delta = 0, \tag{4.62}$$

where $\Delta = \nabla\cdot\mathbf{v}$, as derived by *e.g.* Lamb (1932). This equation was used to study uncoupled p- and g-modes via a local (WKB) dispersion relation in Chapter 2.

Solutions, in terms of confluent hypergeometric functions, may be found for a polytropic background as in Campbell & Roberts (1989),

$$\Delta = e^{-k_\perp z}\left(C_1M(a,b,\alpha) + C_2U(a,b,\alpha)\right), \tag{4.63}$$

where

$$\alpha = -2k_\perp(z_0 - z), \quad a = \frac{1}{2} + \frac{\gamma g z_0}{2\widehat{c_s^2}} + \frac{\omega^2 z_0}{2\widehat{c_s^2}k_\perp} + \frac{k_\perp N_0^2 z_0}{2\omega^2}, \quad b = 1 + \frac{\gamma g z_0}{\widehat{c_s^2}}. \tag{4.64}$$

The outgoing solution in the upper layer, for the case of an isothermal, non-magnetic fluid (where $k_\perp \neq 0$) is

$$\xi_z = D_1\exp\left(\frac{z}{2H_e} + \mathrm{i}\kappa z\right), \quad \kappa = \frac{1}{2H_e}\left(4H_e^2A - 1\right)^{\frac{1}{2}}, \tag{4.65}$$

where

$$A = \frac{N^2k^2}{\omega^2} + \frac{\omega^2 - c_{se}^2k^2}{c_{se}^2}. \tag{4.66}$$

For propagating waves, κ is real and positive. This translates to the condition

$$\omega^4 - \left(c_{se}^2k^2 + \Omega^2\right)\omega^2 + N^2c_{se}^2k^2 > 0, \tag{4.67}$$

where $\Omega^2 = c_{se}^2/4H_e^2, N^2 = g^2(\gamma-1)/c_{se}^2$. Wave propagation is therefore possible when the waves are driven above (or below) the cut-off frequencies

$$\omega^2 > \frac{c_{se}^2k^2 + \Omega^2}{2} + \frac{1}{2}\sqrt{\left(c_{se}^2k^2 + \Omega^2\right)^2 - 4N^2c_{se}^2k^2} > \Omega^2$$

or

$$\omega^2 < \frac{c_{se}^2k^2 + \Omega^2}{2} - \frac{1}{2}\sqrt{\left(c_{se}^2k^2 + \Omega^2\right)^2 - 4N^2c_{se}^2k^2} < N^2. \tag{4.68}$$

Note we assume the terms under the square root to be positive for real cut-off frequencies; this is ensured by $\Omega^2 > 2N^2$ or $\gamma^2/4 > \gamma - 1$. The first of these is the acoustic cut-off for sound wave modified by gravity. The inequality $\omega^2 > \Omega^2$ holds as the first inequality increases from the minimum value Ω^2, monotonically and without bound, with k. The second of these cut-offs is the internal gravity wave modified by compression. The inequality $\omega^2 < N^2$ may be deduced by the fact that the right hand side of the inequality

increases monotonically with k^2 (when $\Omega^2 > N^2$) and asymptotically tends to N^2 when $k^2 \to \infty$.

Connecting the layers together we apply boundary conditions of continuity of the vertical component of the Lagrangian displacement vector and the Lagrangian perturbation to the total pressure at the interface. We drive the waves at the lower boundary as in the cases of vertical wave propagation. The first boundary condition is given by

$$\xi_{zi} = I(\omega) \quad \text{at} \quad z = -L. \tag{4.69}$$

where it can be shown that

$$\xi_{zi} = \frac{\mathrm{i}}{\omega} u_{zi} = \frac{\mathrm{i}\omega}{g^2 k_\perp^2 - \omega^4} \left(c_{si}^2 \frac{\mathrm{d}\Delta}{\mathrm{d}z} - g\left(\gamma - \frac{k_\perp^2 c_{si}^2}{\omega^2} \right) \Delta \right). \tag{4.70}$$

The continuity of displacement at $z = 0$ is given by

$$\xi_{zi} = \xi_{ze} \quad \text{at} \quad z = 0. \tag{4.71}$$

The final boundary condition is

$$\delta p_i = \delta p_e \quad \text{at} \quad z = 0, \tag{4.72}$$

where δf is the Lagrangian change of f given by $\delta f = f_1 + \xi \cdot \nabla f_0$; and it may be shown that

$$\delta p_i = p_{1i} - g\rho_{0i}\xi_{zi} = -\frac{\mathrm{i}\rho_{0i} c_{si}^2}{\omega} \Delta, \quad \delta p_e = \frac{\rho_{0e} c_{se}^2}{\omega^2 - c_{se}^2 k_\perp^2} \left(g k_\perp^2 \xi_{ze} - \omega^2 \frac{\mathrm{d}\xi_{ze}}{\mathrm{d}z} \right). \tag{4.73}$$

Applying the above boundary conditions, we may solve for the system of coefficients

$$D_1 = \frac{\left(c_{se}^2 k^2 - \omega^2\right)\left(g^2 k^2 - \omega^4\right) I(\omega) e^{-kL} \left[M(a,b,\alpha_0) Q_0 + U(a,b,\alpha_0) P_0 \right]}{\left(\omega^2 - c_{se}^2 k^2\right)\left(\omega^4 - g^2 k^2\right)\left[M(a,b,\alpha_0) Q_{-L} + U(a,b,\alpha_0) P_{-L} \right] + \omega^2 \frac{c_{se}^2 \widehat{\rho_e}}{\widehat{c_{si}^2}\widehat{\rho_i}} \left(\frac{\omega^2}{2H_e} + \mathrm{i}\omega^2\kappa - g k^2 \right) \left[P_0 Q_{-L} - P_{-L} Q_0 \right]}, \tag{4.74}$$

$$C_1 = \frac{\begin{array}{c} \mathrm{i}[\widehat{\rho_e}\omega^2 c_{se}^2 \left(\omega^2 + 2\mathrm{i}H_e\omega^2\kappa - 2H_e g k^2\right) Q_0 \\ - 2H_e \widehat{c_{si}^2}\widehat{\rho_i} \left(\omega^4 - g^2 k^2\right)\left(\omega^2 - c_{se}^2 k^2\right) U(a,b,\alpha_0)] D_1 \end{array}}{2H_e \widehat{c_{si}^2}\widehat{\rho_i}\omega \left(c_{se}^2 k^2 - \omega^2\right)\left[M(a,b,\alpha_0) Q_0 + U(a,b,\alpha_0) P_0 \right]}, \tag{4.75}$$

$$C_2 = \frac{\begin{array}{c} \mathrm{i}[\widehat{\rho_e}\omega^2 c_{se}^2 \left(\omega^2 + 2\mathrm{i}H_e\omega^2\kappa - 2H_e g k^2\right) P_0 \\ + 2H_e \widehat{c_{si}^2}\widehat{\rho_i} \left(\omega^4 - g^2 k^2\right)\left(\omega^2 - c_{se}^2 k^2\right) U(a,b,\alpha_0)] D_1 \end{array}}{2H_e \widehat{c_{si}^2}\widehat{\rho_i}\omega \left(c_{se}^2 k^2 - \omega^2\right)\left[M(a,b,\alpha_0) Q_0 + U(a,b,\alpha_0) P_0 \right]}, \tag{4.76}$$

where

$$P_0 = 2k\widehat{c}_{si}^2 M'(a,b,\alpha_0) - \left[\widehat{c}_{si}^2 k + g\gamma - \frac{gk^2\widehat{c}_{si}^2}{\omega^2}\right] M(a,b,\alpha_0), \tag{4.77}$$

$$P_{-L} = 2k\widehat{c}_{si}^2\left(1+\frac{L}{z_0}\right) M'(a,b,\alpha_{-L}) - \left[\widehat{c}_{si}^2\left(1+\frac{L}{z_0}\right)k + g\gamma - \frac{gk^2\widehat{c}_{si}^2\left(1+\frac{L}{z_0}\right)}{\omega^2}\right] M(a,b,\alpha_{-L}), \tag{4.78}$$

$$Q_0 = \left[\widehat{c}_{si}^2 k + g\gamma - \frac{gk^2\widehat{c}_{si}^2}{\omega^2}\right] U(a,b,\alpha_0) - 2k\widehat{c}_{si}^2 U'(a,b,\alpha_0), \tag{4.79}$$

$$Q_{-L} = \left[\widehat{c}_{si}^2\left(1+\frac{L}{z_0}\right)k + g\gamma - \frac{gk^2\widehat{c}_{si}^2\left(1+\frac{L}{z_0}\right)}{\omega^2}\right] U(a,b,\alpha_{-L}) - 2k\widehat{c}_{si}^2\left(1+\frac{L}{z_0}\right) U'(a,b,\alpha_{-L}). \tag{4.80}$$

Using the above expressions, we may write D_1 as

$$\mathrm{Num}\, D_1 = -2k\left(c_{se}^2k^2 - \omega^2\right)\left(g^2k^2 - \omega^4\right) I(\omega) e^{-kL} W(M(\alpha_0), U(\alpha_0)), \tag{4.81}$$

$$\begin{aligned}
\mathrm{Denom}\, D_1 = {} & \left\{\left(\omega^2 - c_{se}^2k^2\right)\left(\omega^4 - g^2k^2\right) - \frac{c_{se}^2\widehat{\rho}_e}{\widehat{\rho}_i}\left(k\omega^2 + \frac{\omega^2}{H_i} - gk^2\right)\left(\frac{\omega^2}{2H_e} + \mathrm{i}\omega^2\kappa - gk^2\right)\right\} \times \\
& \left\{2k\left(1+\frac{L}{z_0}\right)\left[M'(\alpha_{-L})U(\alpha_0) - M(\alpha_0)U'(\alpha_{-L})\right] + \right. \\
& \left.\left(\left(1+\frac{L}{z_0}\right)k + \frac{1}{H_i} - \frac{gk^2}{\omega^2}\left(1+\frac{L}{z_0}\right)\right)\left[M(\alpha_0)U(\alpha_{-L}) - M(\alpha_{-L})U(\alpha_0)\right]\right\} \\
& + 2k\omega^2c_{se}^2\frac{\widehat{\rho}_e}{\widehat{\rho}_i}\left(\frac{\omega^2}{2H_e} + \mathrm{i}\omega^2\kappa - gk^2\right)\left\{2k\left(1+\frac{L}{z_0}\right)\left[M'(\alpha_{-L})U'(\alpha_0) - M'(\alpha_0)U'(\alpha_{-L})\right] + \right. \\
& \left.\left(\left(1+\frac{L}{z_0}\right)k + \frac{1}{H_i} - \frac{gk^2}{\omega^2}\left(1+\frac{L}{z_0}\right)\right)\left[M'(\alpha_0)U(\alpha_{-L}) - M(\alpha_{-L})U'(\alpha_0)\right]\right\},
\end{aligned} \tag{4.82}$$

where we use the notation $D_1 = \mathrm{Num}\, D_1/\mathrm{Denom}\, D_1$ and $M(\alpha_0) = M(a,b,\alpha_0)$ etc. for simplicity.

The resonant frequencies are located between the upper cut-off frequency of g-modes, ω_{cg}, and the lower cut-off of p-modes, ω_{cp}. The exact expressions for these quantities were given previously. It is instructive to consider the asymptotic limits of these frequencies. In the limit of small wavenumber the cut-off of g-modes tends to zero, $\omega_{cg} \sim 0$, while the cut-off of p-modes tends to the acoustic cut-off frequency, $\omega_{cp} \sim \Omega$; hence a resonance may exist when

$$0 < \omega < \Omega, \quad k \to 0. \tag{4.83}$$

In the opposite limit of large wavenumber the cut-off of g-modes tends to the Brunt-Väisälä frequency, $\omega_{cg} \sim N$, whereas the cutoff of p-modes tends to the Lamb frequency, $\omega_{cp} \sim c_s k$;

meaning a resonance may exist when

$$N < \omega < c_s k, \quad k \to \infty. \tag{4.84}$$

In order to deduce the modification to the resonant frequency of p-modes due to non-vertical wave propagation we shall apply the long wavelength approximation. This has the consequence of removing IGWs, hence p-modes are the only wave solutions. In the long wavelength approximation

$$kL \ll 1, \quad kH_e \ll 1, \quad kH_i \ll 1, \tag{4.85}$$

although we do not specify the magnitude of the ratio of these term. $\alpha_{-L} = -2kL + \alpha_0$, where $\alpha_0 = -2kz_0$. We may Taylor expand the Kummer functions, making use of the properties

$$\frac{\mathrm{d}}{\mathrm{d}x} M(a,b,x) = \frac{a}{b} M(a+1,b+1,x), \quad \frac{\mathrm{d}}{\mathrm{d}x} U(a,b,x) = -aU(a+1,b+1,x), \tag{4.86}$$

$$M(a,b,\alpha_{-L}) \approx M(a,b,\alpha_0) - 2kL\frac{a}{b} M(a+1,b+1,\alpha_0) = M(a,b,\alpha_0) - 2kLM'(a,b,\alpha_0), \tag{4.87}$$

$$U(a,b,\alpha_{-L}) \approx U(a,b,\alpha_0) + 2kLaU(a+1,b+1,\alpha_0) = U(a,b,\alpha_0) - 2kLU'(a,b,\alpha_0), \tag{4.88}$$

$$\begin{aligned} \frac{\mathrm{d}}{\mathrm{d}z} M(a,b,\alpha)\bigg|_{-L} &= \alpha' \frac{a}{b} M(a+1,b+1,\alpha_{-L}) \\ &\approx \alpha' M'(a,b,\alpha_0) - \alpha' 2kL \frac{a(a+1)}{b(b+1)} M(a+2,b+2,\alpha_0), \end{aligned} \tag{4.89}$$

$$\begin{aligned} \frac{\mathrm{d}}{\mathrm{d}z} U(a,b,\alpha)\bigg|_{-L} &= -\alpha' aU(a+1,b+1,\alpha_{-L}) \\ &\approx \alpha' U'(a,b,\alpha_0) - \alpha' 2kLa(a+1) U(a+2,b+2,\alpha_0). \end{aligned} \tag{4.90}$$

Using the recurrence relations (Abramowitz & Stegun, 1972)

$$b(1-b+x) M(a,b,x) + b(b-1) M(a-1,b-1,x) - axM(a+1,b+1,x) = 0, \tag{4.91}$$

$$U(a-1,b-1,x) - (1-b+x) U(a,b,x) - axU(a+1,b+1,x) = 0, \tag{4.92}$$

we may determine that

$$M(a+2,b+2,\alpha_0) = \frac{b+1}{\alpha_0(a+1)}\left[(\alpha_0-b)M(a+1,b+1,\alpha_0)+bM(a,b,\alpha_0)\right], \tag{4.93}$$

and

$$U(a+2,b+2,\alpha_0) = \frac{1}{\alpha_0(a+1)}\left[(b-\alpha_0)U(a+1,b+1,\alpha_0)+U(a,b,\alpha_0)\right]. \tag{4.94}$$

The Taylor expansions and the recurrence relations allow us to make the following approximations

$$\begin{aligned}\frac{\mathrm{d}}{\mathrm{d}z}M(a,b,\alpha)\Big|_{-L}U(a,b,\alpha_0) - M(a,b,\alpha_0)\frac{\mathrm{d}}{\mathrm{d}z}U(a,b,\alpha)\Big|_{-L}\\ \approx 2kW(M(a,b,\alpha_0),U(a,b,\alpha_0))\left(\frac{L}{z_0}(b+2kz_0)-1\right)\\ = 2kW(M(a,b,\alpha_0),U(a,b,\alpha_0))\left(\frac{L}{z_0}+\frac{L}{H_i}+2kL-1\right),\end{aligned} \tag{4.95}$$

$$M(a,b,\alpha_0)U(a,b,\alpha_{-L}) - M(a,b,\alpha_{-L})U(a,b,\alpha_0) \approx -2kLW(M(a,b,\alpha_0),U(a,b,\alpha_0)), \tag{4.96}$$

$$M(a,b,\alpha_{-L})\frac{\mathrm{d}}{\mathrm{d}z}U(a,b,\alpha)\Big|_0 - \frac{\mathrm{d}}{\mathrm{d}z}M(a,b,\alpha)\Big|_0 U(a,b,\alpha_{-L}) \approx 2kW(M(a,b,\alpha_0),U(a,b,\alpha_0)), \tag{4.97}$$

$$\begin{aligned}\frac{\mathrm{d}}{\mathrm{d}z}M(a,b,\alpha)\Big|_0\frac{\mathrm{d}}{\mathrm{d}z}U(a,b,\alpha)\Big|_{-L} - \frac{\mathrm{d}}{\mathrm{d}z}M(a,b,\alpha)\Big|_{-L}\frac{\mathrm{d}}{\mathrm{d}z}U(a,b,\alpha)\Big|_0\\ \approx -\frac{4ak^2L}{z_0}W(M(a,b,\alpha_0),U(a,b,\alpha_0))\\ = -2k^2W(M(a,b,\alpha_0),U(a,b,\alpha_0))\left(\frac{L}{z_0}+\frac{L}{H_i}+\frac{\omega^2L}{\widehat{c}_{si}^2k}+\frac{kN_0^2L}{\omega^2}\right).\end{aligned} \tag{4.98}$$

As in the case of only vertical wave propagation, for the series expansions used above to be strictly valid we assume that L/H_i is small. Let us apply these simplifications to D_1, neglecting terms higher than first order in kL and kH leads us to

$$\begin{aligned}D_1 \approx \frac{-\omega^2H_i^2H_eI(\omega)(1-kL)}{\omega^2H_iH_e\left[kLH_i\left(1+\frac{L}{z_0}\right)+\frac{L^2}{z_0}\left(1+\frac{H_i}{z_0}\right)-H_i\right]}\\ +c_{se}^2\frac{\widehat{\rho}_e}{\widehat{\rho}_i}\left(\frac{1}{2}+\mathrm{i}\kappa H_e\right)\left[\frac{\omega^2LH_i^2}{\widehat{c}_{si}^2}\left(1+\frac{L}{z_0}\right)-\frac{L^2}{z_0}\left(1+\frac{H_i}{z_0}\right)-\frac{L^2kH_i}{z_0}\right]\end{aligned}, \tag{4.99}$$

where

$$H_e^2 A \approx \frac{\omega^2 H_e^2}{c_{se}^2}, \quad \text{and so} \quad H_e\kappa \approx \frac{\mathrm{i}}{2}\left(1-\frac{4\omega^2 H_e^2}{c_{se}^2}\right)^{\frac{1}{2}}, \tag{4.100}$$

when the waves are driven below the acoustic cut-off frequency. The expression for the simplified κ shows the removal of terms due to buoyancy in the long wavelength limit. We must retain terms to first order in kH and kL in order to see the effect of non-vertical wave propagation; to zero-th order in these parameters, D_1 is identical to the case of $k = 0$ studied previously, as expected.

To determine the resonant frequency, we must determine the roots of

$$\omega^2 H_i H_e\left[kLH_i\left(1+\frac{L}{z_0}\right)+\frac{L^2}{z_0}\left(1+\frac{H_i}{z_0}\right)-H_i\right]+ \\ \frac{c_{se}^2\widehat{\rho}_e}{2\widehat{\rho}_i}\left[1-\left(1-\frac{4\omega^2 H_e^2}{c_{se}^2}\right)^{\frac{1}{2}}\right]\left[\frac{\omega^2 LH_i^2}{\widehat{c}_{si}^2}\left(1+\frac{L}{z_0}\right)-\frac{L^2}{z_0}\left(1+\frac{H_i}{z_0}\right)-\frac{L^2 kH_i}{z_0}\right]=0. \tag{4.101}$$

Equation (4.101) results in a fairly complex sixth order polynomial in ω (a cubic in ω^2). Expressions for the solution are given by Cardano's formula. The resonant frequency, given by Cardano's formula, is very complicated so it is convenient to further simplify Equation (4.101). Let us make the assumption $L/z_0 \ll 1$. This will allow a simpler solution, for which we may deduce the effect of $k \neq 0$. Perhaps more importantly, it also allows us a comparison to the $k = 0$ case, in which the assumption of a thin lower layer (*i.e.* $L/z_0 \ll 1$) was applied.

Under this assumption, Equation (4.101) reduces to

$$H_e(kL-1)+\frac{c_{se}^2\widehat{\rho}_e}{2\widehat{c}_{si}^2\widehat{\rho}_i}L\left[1-\left(1-\frac{4\omega^2 H_e^2}{c_{se}^2}\right)^{\frac{1}{2}}\right]=0, \tag{4.102}$$

hence

$$\omega=\frac{\widehat{c}_{si}\widehat{\rho}_i}{L\widehat{\rho}_e}\left(\frac{L\widehat{\rho}_e}{H_e\widehat{\rho}_i}(1-kL)+\frac{\widehat{c}_{si}^2}{c_{se}^2}(2kL-1)\right)^{\frac{1}{2}}. \tag{4.103}$$

Note that to strictly justify the above we make the assumption that $L/z_0 \ll kL \ll 1$. The above may be rewritten, using the relationship between $\widehat{\rho}_i$ and $\widehat{\rho}_e$, as

$$\omega=\frac{c_{se}}{L}\left(\frac{L}{H_e}(1-kL)+2kL-1\right)^{\frac{1}{2}}. \tag{4.104}$$

For the case of $kL = 0$, the condition for a global resonance to exist is $L/H_e > 1$. This is modified to the condition

$$\frac{L}{H_e} > \frac{1-2kL}{1-kL} \approx 1-kL, \tag{4.105}$$

hence there may exist a global resonance for the case of $kL \neq 0$, where it may not exist when $kL = 0$. The angle of propagation means that there may be enough space to trap the waves, where there would not be in the case of purely vertical propagation. The resonant frequency may be written

$$\omega = \frac{c_{se}}{L}\left(\frac{L}{H_e} - 1 + kL\left(2 - \frac{L}{H_e}\right)\right)^{\frac{1}{2}}. \tag{4.106}$$

When $L/H_e = 2$, the resonant frequency is equal to the case of $k = 0$, and $\omega = \Omega$. When $L/H_e < 2$ the resonant frequency is greater than the previous case while it is lower when $L/H_e > 2$. This behaviour is shown in Figure 4.2, where L/H_e is varied for a fixed kL. The effect of changing KL for for a fixed L/H_e is plotted in Figure 4.3. Figure 4.3 shows the effect of changing kL is dependent on the value of L/H_e. When $L/H_e < 2$, ω increases with kL. When $L/H_e > 2$, increasing kL causes ω to decrease.

Note that a requirement for the global resonance to occur, based on the assumption of small wavenumbers, is that $\omega < \Omega$. We see from Figure 4.2 that there are some regions for which $L/H \leq 2$ where the resonance ceases to exist. For some values of kL the resonance may occur again for smaller values of L/H; whereas it appears that for larger values of kL the resonance is limited to $L/H > 2$. The analytical results, however, are unreliable for such wavenumbers. It should be noted that the restriction of $\omega < \Omega$, is valid only for small wavenumbers and is an approximation (not exact); so it may be possible that a resonance occurs. A numerical study is needed to determine the true effect of larger wavenumbers.

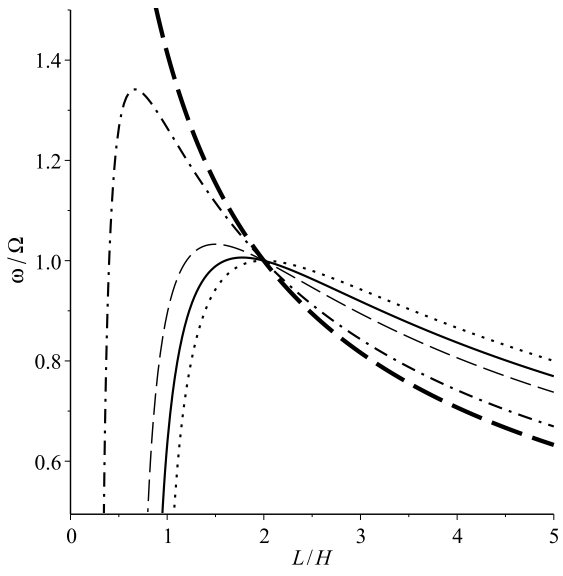

Fig. 4.2 A plot of the resonant frequencies (4.104), normalised to the acoustic cut-off frequency, for varying values of L/H_e. The dotted line represents $kL = 0$, the solid line is $kL = 0.1$, the dashed line is $kL = 0.2$, the dot-dash line is $kL = 0.4$ and the bold dashed line is $kL = 0.5$.

Let us make a note of when $kL = 0.5$; at this point there will exist a resonance for any value of L/H_e, as seen in Equation (4.105). Although this may stretch the assumption

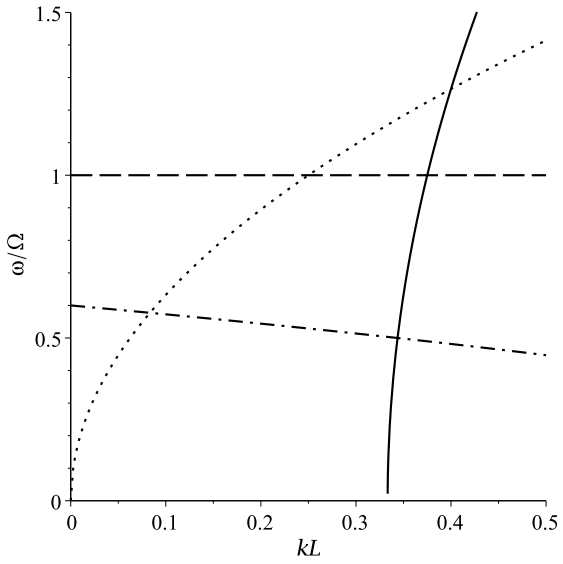

Fig. 4.3 A plot of the resonant frequencies (4.104), normalised to the acoustic cut-off frequency, for varying values of kL. The solid line represents $L/H_e = 0.5$, the dotted line is $L/H_e = 1$, the dashed line is $L/H_e = 2$, the dot-dash line is $L/H_e = 10$.

of $kL \ll 1$, it is interesting to note the change in behaviour. When $kL > 0.5$, and so the approximate expression for the frequency becomes inaccurate, we may investigate the frequencies numerically.

Analytical progress is, to our knowledge, not possible for the case of a short wavelength. When the wavelength is small, we may make the assumptions $kL \gg 1$ and $kz_0 \gg 1$. Asymptotic expressions are not known for the Kummer hypergeometric functions in the limit of the parameter $a \to \infty$, and the argument $\alpha \to -\infty$, based on our relations between α, a, and b.

We now consider, numerically the effect of a large wavenumber. In order to circumvent some difficulties in evaluating the Kummer functions we first 'flip' the coordinate system, that is the region $z \in [0, L]$ is the lower polytropic layer and $z \in (-\infty, 0]$ is the isothermal upper layer. These difficulties owe their nature to the fact that the Kummer U function is a many valued function (c.f. the logarithm function); this flip of coordinate system ensures we use the principle branch of the function. Gravity points towards the solar centre, *i.e* in the positive z-direction. The driven boundary is located at $z = L$. This may be achieved by applying the mappings $g \to -g$, (and so $H \to -H$) $z_0 \to -z_0$, $L \to -L$. The Brunt-Väisälä frequency and the quantity A are invariant under these mappings. In the isothermal layer the kinetic energy density tends to 0 when $z \to -\infty$, if $4H^2A < 1$. When the coordinate system is flipped in this manner, the governing equations and solutions are as in previous studies *e.g.* Campbell and Roberts (1989).

We let kH_e vary from 1 to 10, *i.e.* outside the region in which the analytical results are valid. We also assume $\widehat{c_{si}} = c_{se}$, $L = z_0$, $\widehat{\rho_i} = \widehat{\rho_e}$, in order to show that the global resonance is not dependent on the inequalities used in the analytical study, rather they were made for simplicity. We use typical lower solar values for the parameters, $\gamma = 5/3$, $g = 0.274$

km s^{-2}, $c_{se} = 8$ km s^{-1}. We also set $L = z_0 = 5H_e$. This choice for z_0 returns typical values for the Brunt-Väisälä frequency ($N_0 \approx 0.03$) and allows for a significant temperature change throughout the layer. We use Halley's method, a modified Newton's method that converges to the root cubically if the first and second derivatives are given, to find the roots of Equation (4.82). The roots are plotted in Figure 4.4.

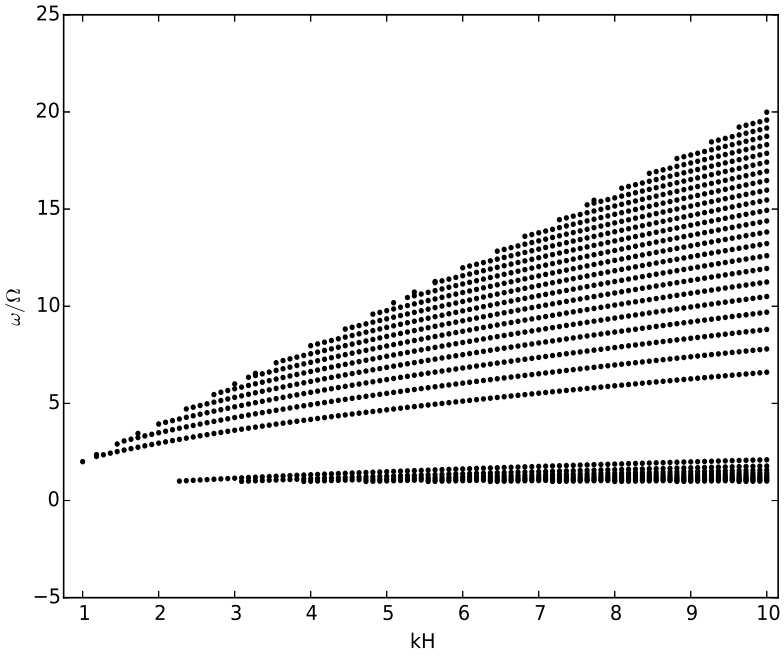

Fig. 4.4 A plot of the numerical resonant frequencies, normalised to the acoustic cut-off frequency, for varying values of kH.

We immediately see that there are two branches of solutions. The higher frequency modes, which form distinct parabolas are the resonant p-modes. The lower frequency branch are the g-modes. Increasing kH causes the arrival of more solutions both from above, in the case of p-modes; and below for g-modes. For a given root, the frequency of a p-mode increases with increasing wavenumber. This is in contrast to the behaviour when kH is small. The value of the resonant frequency, for a given root, increases at a lower rate when kH increases, resulting in the parabolic curves. The behaviour of the resonant frequency for larger kH is in contrast to the behaviour for small wavenumber. This is due to the omission of the higher-order terms which become dominant when $kH > 1$. These terms change the character of the solution, hence we have two regimes for the resonance. The physical cause is the interaction of the different scales present in the problem. To see this we would ideally extend the problem for the case $kH < 1$, although numerical investigation is difficult in this region. The behaviour of the low frequency g-modes, however, is difficult to determine exactly due to the clustering effect caused by the arrival of more roots.

It can be shown that when $kH = 1$ there is 1 root (based on the parameters specified previously) located at $\omega/\Omega \approx 2$. When $kH = 10$ there are 33 roots with $\min(\omega/\Omega) \approx 1.0$ and

$\max(\omega/\Omega) \approx 20.0$. The Brunt-Väisälä frequency in the upper layer is such that $N/\Omega \approx 0.96$. The resonant g-modes are located above the Brunt-Väisälä frequency, as shown analytically with the application of the Boussinesq approximation. For the parameters used, it is also the case that they are above the acoustic cut-off.

Also of note from Figure 4.4 is that the p-mode solutions are above Ω. This is due to the dependence of the interval in which resonant modes may exist being dependent on k. When kH is small we have that resonant modes may exist only below Ω, but we see that this is not that case for kH is not small. When k is not small, the more significant cut-off for the waves is the Lamb frequency. Figure 4.4 also demonstrates the upper bound to the roots, which is approximately the Lamb frequency.

This numerical study is notable as it shows the global resonance is not dependent on the specific values used in the analytical study. Rather, the resonance is a robust phenomenon that occurs for all wave modes through the spectrum of frequencies. That is, it is not simply vertically propagating sound waves of low frequency (below the acoustic cut-off) that are subject to a resonance. Higher frequency, non-radial modes may also become trapped in the solar atmosphere. This a potentially very important mechanism for supplying energy to the chromosphere and beyond.

This study does not take into account several important aspects at play in the Sun. The effects of curvature, rotation and magnetism are neglected. In the next sections we build a more realistic model, starting with the effect of a large scale flow.

4.3.1 Influence of a Steady State Flow

We seek to consider the effect of large scale motion on the resonant p-modes. Such a large scale flow is representative of, for example, meridional flow or differential rotation. In helioseismology, rotational effects can be measured by the splitting of p-modes. Such an analysis has allowed the internal rotation rate of the Sun to be inferred. The modification to the frequency of p-modes by a large scale flow has been analysed analytically by *e.g.* Erdélyi & Taroyan (1999), Erdélyi *et al.* (1999), Varga & Erdélyi (2001), Taroyan (2004); see Pintér & Erdélyi (2011) for a review. The analytical results are in agreement with observations made by *e.g.* Braun & Fan (1998). The changes in travel times of the waves, due to a steady flow and magnetic field, and its implications for time-distance helioseismology was studied by Taroyan & Doyle (2004).

We consider only a horizontal, steady state flow of the form $\mathbf{u_0} = (V,0,0)$, where V is constant. A horizontal, uniform flow is inertia-less ($\mathbf{u_0} \cdot \nabla \mathbf{u_0} = \mathbf{0}$) hence there is no modification to the pressure via Bernoulli's principle. The equation of hydrostatic equilibrium is, therefore, as in the previous sections and the equilibrium quantities depend on z only. The governing equations for linearised perturbations around such a background are

$$\rho_0 \frac{\partial \mathbf{u_1}}{\partial t} + \rho_0 V \frac{\partial \mathbf{u_1}}{\partial x} = -\nabla p_1 + \rho_1 \mathbf{g}, \tag{4.107}$$

$$\frac{\partial \rho_1}{\partial t} + V\frac{\partial \rho_1}{\partial x} = -\rho_0 \nabla \cdot \mathbf{u_1} - \nabla \rho_0 \cdot \mathbf{u_1}, \tag{4.108}$$

$$\frac{\partial p_1}{\partial t} + V\frac{\partial p_1}{\partial x} = -\mathbf{u_1} \cdot \nabla p_0 - \gamma p_0 \nabla \cdot \mathbf{u_1}. \tag{4.109}$$

Assuming normal nodes and letting $\Delta = \nabla \cdot \mathbf{u_1}$, we may eliminate several quantities from our governing equations leaving us with

$$\frac{\mathrm{d}u_z}{\mathrm{d}z} = \frac{gk_\perp^2}{\omega_D^2}u_z + \left(1 - \frac{k_\perp^2 c_s^2}{\omega_D^2}\right)\Delta, \tag{4.110}$$

$$c_s^2\omega_D^2\frac{\mathrm{d}\Delta}{\mathrm{d}z} - g\left(\gamma\omega_D^2 - k_\perp^2 c_s^2\right)\Delta = \left(g^2k_\perp^2 - \omega_D^4\right)u_z, \tag{4.111}$$

where

$$\omega_D \equiv \omega - Vk_x \tag{4.112}$$

is the Doppler shifted frequency. A single governing equation may be formed

$$\frac{\mathrm{d}^2\Delta}{\mathrm{d}z^2} + \left(\frac{1}{c_s^2}\frac{\mathrm{d}c_s^2}{\mathrm{d}z} - \frac{g\gamma}{c_s^2}\right)\frac{\mathrm{d}\Delta}{\mathrm{d}z} + \left(\frac{\omega_D^2 - k_\perp^2 c_s^2}{c_s^2} + \frac{gk_\perp^2}{c_s^2\omega_D^2}\left[\frac{\mathrm{d}c_s^2}{\mathrm{d}z} + g(\gamma - 1)\right]\right)\Delta = 0. \tag{4.113}$$

We see that the influence of a horizontal, unidirectional flow is to modify the local frequency of the waves via the Doppler shift. There is only an effect when there is some component of wave propagation in the x-direction. Let us now apply the boundary conditions for the two-layer model to see the *global* influence of the flow on the frequency of resonant sound waves.

The solution for a polytropic background, *i.e.* the lower layer, is given by

$$\Delta = e^{-k_\perp z}\left(C_1 M(a,b,\alpha) + C_2 U(a,b,\alpha)\right), \tag{4.114}$$

where

$$\alpha = -2k_\perp(z_0 - z), \quad a = \frac{1}{2} + \frac{\gamma g z_0}{2c_s^2} + \frac{\omega_D^2 z_0}{2c_s^2 k_\perp} + \frac{k_\perp N_0^2 z_0}{2\omega_D^2}, \quad b = 1 + \frac{\gamma g z_0}{c_s^2}. \tag{4.115}$$

The upper layer, and so the solution to the governing equation, is as in the previous subsection. The appropriate boundary conditions at the interface $z = 0$ are the continuity of the *Lagrangian* vertical displacement and pressure,

$$[[\xi_z]] = 0, \quad [[P - \rho_0 g \xi_z]] = 0. \tag{4.116}$$

Due to the flow, the quantities in the lower layer can be shown to be

$$\xi_{zi} = \frac{\mathrm{i}}{\omega_D} u_{zi} = \frac{\mathrm{i}\omega_D}{g^2 k_\perp^2 - \omega_D^4}\left(c_s^2 \frac{\mathrm{d}\Delta}{\mathrm{d}z} - g\left(\gamma - \frac{k_\perp^2 c_s^2}{\omega_D^2}\right)\Delta\right), \quad \delta p_i = -\frac{\mathrm{i}c_s^2 \rho_0}{\omega_D}\Delta. \tag{4.117}$$

The coefficient D_1 is given by

$$\text{Num } D_1 = 2kh_e \widehat{\rho_i} I(\omega) e^{-kL}\left(c_{se}^2 k^2 - \omega^2\right)\left(\omega_D^4 - g^2 k^2\right) W(M(\alpha_0), U(\alpha_0)), \tag{4.118}$$

$$\begin{aligned}
\text{Denom } D_1 = &\left\{H_e \widehat{\rho_i}\left(\omega^2 - c_{se}^2 k^2\right)\left(\omega_D^4 - g^2 k^2\right) - c_{se}^2 \widehat{\rho_e} \omega_D^2 \left(\frac{\omega^2}{2} + H_e \omega^2 \mathrm{i}\kappa - H_e g k^2\right)\left(k + \frac{1}{H_i} - \frac{gk^2}{\omega_D^2}\right)\right\} \times \\
&\left\{2k\left(1 + \frac{L}{z_0}\right)\left[M'(\alpha_{-L}) U(\alpha_0) - M(\alpha_0) U'(\alpha_{-L})\right] + \right. \\
&\left.\left(\left(1 + \frac{L}{z_0}\right)k + \frac{1}{H_i} - \frac{gk^2}{\omega_D^2}\left(1 + \frac{L}{z_0}\right)\right)\left[M(\alpha_0) U(\alpha_{-L}) - M(\alpha_{-L}) U(\alpha_0)\right]\right\} \\
&+ k\omega_D^2 c_{se}^2 \widehat{\rho_e}\left(\omega^2 + 2H_e \mathrm{i}\omega^2 \kappa - 2H_e g k^2\right)\left\{2k\left(1 + \frac{L}{z_0}\right)\left[M'(\alpha_{-L}) U'(\alpha_0) - M'(\alpha_0) U'(\alpha_{-L})\right] + \right. \\
&\left.\left(\left(1 + \frac{L}{z_0}\right)k + \frac{1}{H_i} - \frac{gk^2}{\omega_D^2}\left(1 + \frac{L}{z_0}\right)\right)\left[M'(\alpha_0) U(\alpha_{-L}) - M(\alpha_{-L}) U'(\alpha_0)\right]\right\}.
\end{aligned} \tag{4.119}$$

An analysis as in the previous section leads us to

$$H_e H_i \widehat{\rho_i} \omega_D^2 \left(kLH_i - H_i + \frac{L^2}{z_0}\right) + \widehat{\rho_e} c_{se}^2 \left(\frac{1}{2} + H_e \mathrm{i}\kappa\right)\left[\frac{\omega_D^2 L H_i^2}{\widehat{c}_{si}^2}\left(1 + \frac{L}{z_0}\right) - \frac{L^2}{z_0}\right] = 0. \tag{4.120}$$

Neglecting the terms in L/z_0 returns the resonant frequencies (4.104), hence the flow does not modify the resonance either to leading order or in the kL term.

We may study the influence of the flow numerically when the propagation angle is such that the waves feel the flow. We may see the effect of a flow in Figure 4.5. In this plot the parameters used are $L = 5H/2$, $L = z_0$, $kH = 5$, $\widehat{c}_{si} = c_{se} = 8\text{km s}^{-1}$, $\rho_i = \rho_e$, $N_0 = 0\ \text{s}^{-1}$. We see that for no flow, there are 6 resonant solutions. The effect of a flow is to increase the frequency linearly, until they no longer remain in the interval for which resonant frequencies may occur. Turning on the flow we have the appearance of a new singular frequency, further investigation is needed to determine the nature of this resonant mode (it should be noted that the background is unstable, this mode may be related to the well known Kelvin-Helmholtz instability). Note that the curve representing the new solution appears to be broken, this may be attributed to numerical error.

In this numerical analysis we have considered an adiabatic polytrope for simplicity. To analyse the effect of a flow of g-modes in this model a more sophisticated numerical study is needed. This is due to the dispersion relation being difficult to analyse when g-modes

are included. Alternatively, we may use the Boussinesq approximation with a background flow.

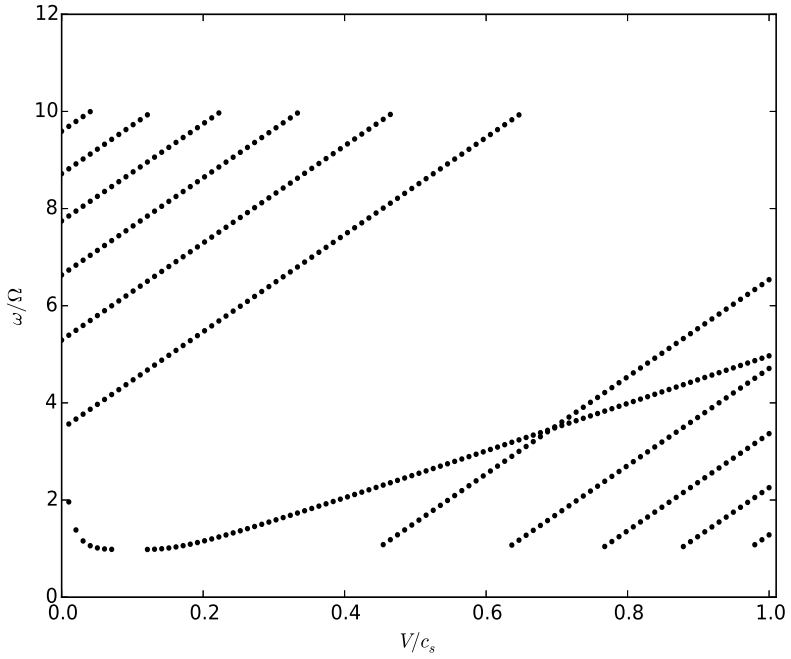

Fig. 4.5 A plot of the numerical resonant frequencies, normalised to the acoustic cut-off frequency, for varying values of V.

Figure 4.5 shows the appearance of new resonant frequencies for Mach numbers greater than 0.4. To determine what these solutions are we note in a stationary medium waves may propagate in the positive and negative direction without any bias. This is expressed in the governing equations by the fact the the frequency appears as a squared quantity. When the flow is absent, left and right propagating waves may be resonant modes. When a flow is present, the waves are Doppler shifted. There is also a preferred direction to the problem due to the flow. For a sufficiently strong flow, a wave propagating against the flow may have its direction reversed. This accounts for the appearance of new solutions; waves propagating against the flow (in the negative x-direction) have their direction reversed. The frequency of these waves may be taken into the interval in which resonance occurs.

4.4 Conclusions

The partial trapping of waves due to a variable temperature profile may be an efficient mechanism to supply energy to the upper solar atmosphere. The solar convection zone is constantly generating waves through turbulent motion. The conditions of the upper interior and lower solar atmosphere are such that the temperature decreases. This may cause partial reflection of waves driven within specific frequency ranges. The trapping leads to an amplification of the wave amplitude throughout the entire unbounded atmosphere. An

increase in the amplitude leads to non-linear effects, such as the steepening into a shock wave. Shocks are efficient ways to heat the solar medium.

In this chapter we focus only on hydrodynamic waves. In the solar atmosphere this is applicable to regions where magnetism has a very small effect and may be neglected. Regions where we may apply the hydrodynamic theory are in the so-called quiet Sun. Recent high resolution observations suggest that the quiet Sun is not free of magnetic activity, rather contains many small-scale, dynamic magnetic events. The plasma in this region can often be said to be in the high-β regime. When, to leading order, these magnetic elements do not have a significant influence on the dynamics of the plasma, we may apply the hydrodynamic theory. We address the case of magnetism in the next chapter.

Previous studies of the hydrodynamic global resonance focus only on vertically propagating waves. In this chapter we generalise this to include the effects of non-vertical wave propagation. There are several effects that become important when we introduce non-vertical propagation angle, which have an important influence on the global resonance.

Perhaps the most significant result is that the frequency range for which the resonance exists is much greater when considering non-vertical wave propagation. This is due to the effect of the wavenumber on the acoustic cut-off frequency. Resonance exists only for waves driven below the cut-off frequency; for near vertical propagation the cut-off is the quantity $g\gamma/2c_s$. For large wavenumber the cut-off tends to the Lamb frequency, which may be much greater than the previously stated quantity. Analytical expressions for the frequency are possible for near vertical wave propagation. The large range of resonant frequencies means that we may expect this resonance to be a common phenomenon.

When propagation is vertical only, the effects of buoyancy are not included. This means that not only are the effects of buoyancy neglected from the acoustic wave, the internal gravity wave is not present. In this chapter we show that internal gravity waves may also be trapped. While internal gravity waves have been observed in the solar atmosphere, less attention has been paid to them. It is not yet known how efficiently IGWs are generated in the solar atmosphere.

The real solar atmosphere is much more highly structured than the models used in this chapter. In this chapter we have presented the essential physics at work using relatively simple models. Future work would include studying the resonant trapping of waves numerically using detailed simulations with a real solar atmosphere. Such an experiment is needed to determine the importance of the mechanisms in the real solar atmosphere. Waves driven with a given frequency may be propagating or evanescent in different regions of the solar atmosphere, with more subtlety than the models used here. This will change or perhaps even inhibit the resonance.

Chapter 5

Global Resonance in a Magnetohydrodynamic Model

5.1 Introduction

Magnetic activity is ubiquitous throughout the solar atmosphere. We observe magnetic fields to have an influence on all scales; with large prominences and sunspots and small-scale magnetic bright points and chromospheric flux tubes. A proper treatment of physical phenomena in the solar atmosphere is not complete without the addition of magnetism. In the previous chapter we discussed the global resonance of hydrodynamic waves caused by stratification. In this chapter we generalise the previous work to magnetohydrodynamic waves.

We begin by considering a horizontal magnetic field, representative of canopy fields in the chromosphere. In the interest of simplicity we begin by considering vertically propagating waves as in Taroyan & Erdélyi (2008). This gives a straightforward generalisation of this previous study to include magnetism. By studying vertically propagating waves we study only the fast MHD waves, analogous to a hydrodynamic *p*-mode; the slow wave does not propagate in this limit. We consider two models: a constant and exponentially varying Alfvén speed. We see that the inclusion of a magnetic field has a significant effect on the global resonance. We, then, move onto the case of non-vertical wave propagation. Due to the increased complexity, we study the case of constant Alfvén speed.

We end this chapter by considering briefly the global resonance in a model with a vertical magnetic field. As seen previously, the mathematical treatment of MHD waves in a vertical field is difficult for even simple background states. Due to this difficulty we study some limiting forms of the governing equations. We find that the resonance does indeed exist for some models. We are led to the conclusion that the global resonance is a robust phenomenon which may be very important in the supplying of energy into the upper solar atmosphere.

It should be noted that the resonance discussed here is cavity resonance due to the trapping of driven waves and not resonant absorption. We stress this here as resonant absorption is often referred to as simply resonance. Resonant absorption is a popular, and mathematically elegant, method for the damping of MHD modes which may excite other waves. For a review of resonant absorption see *e.g.* Goossens, Erdélyi & Ruderman (2011).

5.2 Vertical Wave Propagation in a Horizontal Field

In this section, we consider a non-magnetic lower layer coupled to a layer in which the magnetic field is horizontal. Oscillations in such a model have been studied by *e.g.* Campbell & Roberts (1989), Evans & Roberts (1990), Pintér *et al.* (1998), Pintér & Goossens (1999), and Pintér & Erdélyi (2011), just to name a few.

Let us first assume that the horizontal wavenumber is zero, that is wave propagation is strictly in the vertical direction. To begin with, we add a magnetic field to the hydrodynamic case in the simplest possible way. In the lower layer the solution is as in Taroyan & Erdélyi

(2008),

$$\xi_z = (z - z_0)^{-m/2} \left(C_1 J_m(\theta) + C_2 Y_m(\theta)\right), \tag{5.1}$$

where

$$\theta = \frac{2\omega\sqrt{z_0}}{\widehat{c_s}} \sqrt{z_0 - z}. \tag{5.2}$$

The linearised ideal MHD equations (in Fourier space), for a gravitationally stratified plasma embedded in a horizontal, z-dependent magnetic field, may be written after some algebra as two coupled ordinary differential equations

$$D\frac{\mathrm{d}\xi_z}{\mathrm{d}z} = A_1\xi_z - A_2 P_T, \tag{5.3}$$

$$D\frac{\mathrm{d}P_T}{\mathrm{d}z} = A_3\xi_z - A_1 P_T, \tag{5.4}$$

where the functions D, A_1, A_2 and A_3 are

$$D = \rho_0\left(c_s^2 + v_A^2\right)\left(\omega^2 - c_T^2 k_x^2\right)\left(\omega^2 - v_A^2 k_x^2\right), \quad A_1 = g\rho_0\omega^2\left(\omega^2 - v_A^2 k_x^2\right), \tag{5.5}$$

$$A_2 = \omega^4 - \left(c_s^2 + v_A^2\right)\left(\omega^2 - c_T^2 k_x^2\right)k^2, \quad A_3 = \rho_0^2 g^2\left(\omega^2 - v_A^2 k_x^2\right)^2 + \rho_0\left(\omega^2 - v_A^2 k_x^2 + \frac{g}{\rho_0}\frac{\mathrm{d}\rho_0}{\mathrm{d}z}\right)D. \tag{5.6}$$

Here, $k^2 = k_x^2 + k_y^2$. A single governing equation may be formed as in *e.g.* Goedbloed & Poedts (2004). In the limit of $k_x = k_y = 0$ these functions reduce to

$$D = \rho_0\left(c_s^2 + v_A^2\right)\omega^4, \quad A_1 = g\rho_0\omega^4, \quad A_2 = \omega^4, \quad A_3 = \rho_0^2 g^2\omega^2 + \left(\rho_0\omega^2 + g\frac{\mathrm{d}\rho_0}{\mathrm{d}z}\right)D, \tag{5.7}$$

and so the governing equations may be combined to yield

$$\rho_0\left(c_s^2 + v_A^2\right)\frac{\mathrm{d}^2\xi_z}{\mathrm{d}z^2} + \left(\frac{\mathrm{d}}{\mathrm{d}z}\rho_0\left(c_s^2 + v_A^2\right)\right)\frac{\mathrm{d}\xi_z}{\mathrm{d}z} + \rho_0\omega^2\xi_z = 0. \tag{5.8}$$

We shall use Equation (5.8) to investigate the upper atmospheric layer. We consider separately the cases of constant and varying Alfvén speeds.

5.2.1 Model with a Constant Alfvén Speed

We assume an isothermal background, so the sound speed, c_s, is constant. We also assume, for simplicity, that the magnetic field varies like the square root of the density. In such a system the Alfvén speed is constant. In this case, the governing equation reduces to

$$\frac{\mathrm{d}^2\xi_z}{\mathrm{d}z^2} - \frac{1}{H_B}\frac{\mathrm{d}\xi_z}{\mathrm{d}z} + \frac{\omega^2}{c_s^2 + v_A^2}\xi_z = 0, \tag{5.9}$$

where H_B is the magnetically modified pressure scale-height given by

$$H_B = \frac{c_s^2 + \frac{1}{2}\gamma v_A^2}{g\gamma}. \tag{5.10}$$

The modified pressure scale-height is greater than the hydrodynamic scale-height, $H_B > H$. Solutions are easily found to be

$$\xi_z = D_1 \exp\left(\frac{z}{2H_B} + \kappa z\right) + D_2 \exp\left(\frac{z}{2H_B} - \kappa z\right), \tag{5.11}$$

where

$$\kappa = \frac{\mathrm{i}}{2}\left(\frac{4\omega^2}{c_s^2 + v_A^2} - \frac{1}{H_B^2}\right)^{\frac{1}{2}}. \tag{5.12}$$

The square of the modified cut-off frequency is

$$\Omega^2 = \frac{c_s^2 + v_A^2}{4H_B^2}. \tag{5.13}$$

Note that exact solutions are available for the isothermal case when $k_\perp \neq 0$, and v_A is constant (Campbell & Roberts, 1989) or when $k_\perp = 0$ and the horizontal magnetic field is uniform in terms of Legendre polynomials (see Section 5.2.2). Exact solutions also exist when the magnetic field is uniform and the wave propagation is oblique (*e.g.* Nye & Thomas, 1976; Pintér & Erdélyi, 2011). As a straightforward possible generalisation to the hydrodynamic case we first use the solution above.

We select the outgoing wave solution,

$$\xi_z = D_1 \exp\left(\frac{z}{2H_B} + \kappa z\right). \tag{5.14}$$

The Lagrangian perturbation to the total pressure, in the upper layer, may be shown to be

$$\delta P_T = -\rho_0 \left(c_s^2 + v_A^2\right) \frac{\mathrm{d}\xi_z}{\mathrm{d}z}, \tag{5.15}$$

hence the pressure boundary condition is expressed as

$$\rho_{0i} c_{si}^2 \frac{\mathrm{d}\xi_{zi}}{\mathrm{d}z} = \rho_{0e} \left(c_{se}^2 + v_{Ae}^2\right) \frac{\mathrm{d}\xi_{ze}}{\mathrm{d}z}, \quad \text{at} \quad z = 0. \tag{5.16}$$

Applying the driven boundary conditions we have the relations

$$(-L - z_0)^{-\frac{m}{2}} \left(C_1 J_m(\theta_{-L}) + C_2 Y_m(\theta_{-L})\right) = I(\omega), \tag{5.17}$$

$$(-z_0)^{-\frac{m}{2}} \left(C_1 J_m(\theta_0) + C_2 Y_m(\theta_0)\right) = D_1, \tag{5.18}$$

$$-\widehat{\rho}_{0i}\widehat{c}_{si}^2\theta_0'\left[(-z_0)^{-\frac{m}{2}}J_{m+1}(\theta_0)C_1+(-z_0)^{-\frac{m}{2}}Y_{m+1}(\theta_0)C_2\right]=\widehat{\rho}_{0e}\left(\widehat{c}_{se}^2+\widehat{v}_A^2\right)\left(\frac{1}{2H_B}+\kappa\right)D_1. \tag{5.19}$$

Here, we have used the property (Abramowitz & Stegun, 1972)

$$\mathscr{C}_m'(x)=-\mathscr{C}_{m+1}(x)+\frac{m}{x}\mathscr{C}_m(x), \tag{5.20}$$

where, again, $\mathscr{C}$ denotes either of the Bessel functions J and Y (and also the Hankel functions and linear combinations of the Bessel functions). The coefficients may be determined to be

$$D_1=\frac{(-z_0)^{-\frac{m}{2}}\widehat{\rho}_{0i}\widehat{c}_{si}^2\theta_0'I(\omega)W(J_m(\theta_0),Y_m(\theta_0))(-L-z_0)^{\frac{m}{2}}}{\begin{aligned}&\widehat{\rho}_{0i}\widehat{c}_{si}^2\theta_0'\left[J_{m+1}(\theta_0)Y_m(\theta_{-L})-J_m(\theta_{-L})Y_{m+1}(\theta_0)\right]\\&+\widehat{\rho}_{0e}\left(\tfrac{1}{2H_B}+\kappa\right)\left(c_{se}^2+v_A^2\right)\left[J_m(\theta_0)Y_m(\theta_{-L})-J_m(\theta_{-L})Y_m(\theta_0)\right]\end{aligned}}, \tag{5.21}$$

$$C_1=\frac{-(-z_0)^{\frac{m}{2}}\left[\widehat{\rho}_{0e}\left(\frac{1}{2H_B}+\kappa\right)\left(c_{se}^2+v_A^2\right)Y_m(\theta_0)+\widehat{\rho}_{0i}\widehat{c}_{si}^2\theta_0'Y_{m+1}(\theta_0)\right]D_1}{\widehat{\rho}_{0i}\widehat{c}_{si}^2\theta_0'W(J_m(\theta_0),Y_m(\theta_0))}, \tag{5.22}$$

$$C_2=\frac{(-z_0)^{\frac{m}{2}}\left[\widehat{\rho}_{0e}\left(\frac{1}{2H_B}+\kappa\right)\left(c_{se}^2+v_A^2\right)J_m(\theta_0)+\widehat{\rho}_{0i}\widehat{c}_{si}^2\theta_0'J_{m+1}(\theta_0)\right]D_1}{\widehat{\rho}_{0i}\widehat{c}_{si}^2\theta_0'W(J_m(\theta_0),Y_m(\theta_0))}, \tag{5.23}$$

where "i" and "e" denote the interior and exterior layers. The functions θ evaluated at $z=-L,0$ are

$$\theta_0=\frac{2\omega z_0}{\widehat{c}_{si}},\quad \theta_{-L}=\frac{2\omega z_0}{\widehat{c}_{si}}\sqrt{1+\frac{L}{z_0}},\quad \theta_0'=-\frac{\omega}{\widehat{c}_{si}}, \tag{5.24}$$

and the Wronskian of the Bessel functions is

$$W(J_m(\theta_0),Y_m(\theta_0))=\frac{2}{\pi\theta_0}=\frac{\widehat{c}_{si}}{\pi\omega z_0}. \tag{5.25}$$

Any singularities are located below the modified acoustic cut-off frequency, Ω, in the upper layer. We may determine the resonant frequencies if we assume the temperature varies slowly,

$$\frac{L}{z_0}\ll 1. \tag{5.26}$$

Making this assumption we have

$$\theta_{-L}\approx\frac{2\omega z_0}{\widehat{c}_{si}}\left(1+\frac{L}{2z_0}\right)=\theta_0\left(1+\frac{L}{2z_0}\right). \tag{5.27}$$

By Taylor's theorem we may approximate the Bessel functions to first order,

$$J_m(\theta_{-L})\approx J_m\left(\theta_0\left(1+\frac{L}{2z_0}\right)\right)\approx J_m(\theta_0)\left(1+\frac{mL}{2z_0}\right)-J_{m+1}(\theta_0)\frac{\omega L}{\widehat{c}_{si}}, \tag{5.28}$$

$$Y_m(\theta_{-L}) \approx Y_m(\theta_0)\left(1+\frac{mL}{2z_0}\right) - Y_{m+1}(\theta_0)\frac{\omega L}{\widehat{c}_{si}}, \tag{5.29}$$

and so

$$J_{m+1}(\theta_0)\,Y_m(\theta_{-L}) - J_m(\theta_{-L})\,Y_{m+1}(\theta_0) \approx \frac{\widehat{c}_{si}}{\pi\omega z_0}, \tag{5.30}$$

$$J_m(\theta_0)\,Y_m(\theta_{-L}) - J_m(\theta_{-L})\,Y_m(\theta_0) \approx \frac{L}{\pi z_0}. \tag{5.31}$$

The coefficient D_1 may be simplified to

$$D_1 \approx \frac{\widehat{\rho}_{0i}\widehat{c}_{si}^2 I(\omega)\left(1+\frac{mL}{2z_0}\right)}{\widehat{\rho}_{0i}\widehat{c}_{si}^2 - \widehat{\rho}_{0e}L\left(\frac{1}{2H_B} - \frac{1}{2}\left(\frac{1}{H_B^2} - \frac{4\omega^2}{c_{se}^2+v_A^2}\right)^{\frac{1}{2}}\right)\left(c_{se}^2+v_A^2\right)}. \tag{5.32}$$

The global resonance then occurs when the driving frequency is

$$\omega = \frac{\widehat{\rho}_{0i}\widehat{c}_{si}}{\widehat{\rho}_{0e}L}\left(\frac{L\widehat{\rho}_{0e}}{H_B\widehat{\rho}_{0i}} - \frac{\widehat{c}_{si}^2}{c_{se}^2+v_A^2}\right)^{\frac{1}{2}}. \tag{5.33}$$

This frequency is the generalisation of the hydrodynamic case with zero horizontal wavenumber, when the upper layer contains a horizontal magnetic field. In the limit $v_A = 0$, such that $H_B = H_e$ then the resonant frequency reduces to that found by Taroyan & Erdélyi (2008) as expected. Note that the frequency (5.33) represents only the fundamental harmonic of the resonant cavity due to the simplifications made in its derivation.

To maintain equilibrium, there must be no discontinuity in the total pressure at the boundary $z = 0$,

$$p_{0i} = p_{0e} + \frac{B_0^2}{2\mu}, \quad \text{at} \quad z = 0. \tag{5.34}$$

This may be expressed as

$$\frac{\widehat{\rho}_{0i}}{\widehat{\rho}_{0e}} = \frac{c_{se}^2}{\widehat{c}_{si}^2} + \frac{\gamma v_A^2}{2\widehat{c}_{si}^2}. \tag{5.35}$$

The resonant frequency may be written

$$\omega = \left(1+\frac{\gamma v_A^2}{2c_{se}^2}\right)\frac{c_{se}^2}{L}\left(\frac{L}{H_e+\frac{v_A^2}{2g}}\cdot\frac{1}{c_{se}^2+\frac{\gamma v_A^2}{2}} - \frac{1}{c_{se}^2+v_A^2}\right)^{\frac{1}{2}}. \tag{5.36}$$

The resonant frequencies are lower than the hydrodynamic frequencies as shown in Figure 5.1. As the Alfvén speed increases, for a given L and c_{se}, the resonant frequency decreases monotonically. As in the hydrodynamic case, the resonant frequencies are complex when $L/H_e < 1$, although, the modified condition is $L/H_B < \left(c_{se}^2+\gamma v_A^2/2\right)/\left(c_{se}^2+v_A^2\right) < 1$ (based on $\gamma = 5/3$). At some point the resonant frequencies may become complex as H_B increases to the point where $L < H_B$.

We may see these properties analytically, as well as numerically. Let us rewrite the resonant frequency as

$$\omega = \frac{c_{se}}{L}\left(\frac{L}{H_e} - \frac{\left(1+\frac{\gamma}{2}\epsilon\right)^2}{1+\epsilon}\right)^{\frac{1}{2}}, \tag{5.37}$$

where H_e is the hydrodynamic scale height and we let $\epsilon = v_A^2/c_{se}^2$. If the magnetic field is weak, $\epsilon \ll 1$,

$$\frac{\left(1+\frac{\gamma}{2}\epsilon\right)^2}{1+\epsilon} \approx 1 + (\gamma-1)\epsilon + \left(\frac{\gamma}{2}-1\right)^2\epsilon^2 + \ldots. \tag{5.38}$$

Keeping terms to first order in ϵ (in ω^2) we have

$$\omega \approx \frac{c_{se}}{L}\left(\frac{L}{H_e} - 1 - (\gamma-1)\epsilon\right)^{\frac{1}{2}}. \tag{5.39}$$

This is the approximation for the resonant frequency when the magnetic field is weak. We see that this is lower than the hydrodynamic case when we take $\gamma = 5/3$. Let us now examine the other extreme of a strong magnetic field, $\epsilon \gg 1$. When this is the case

$$\frac{\left(1+\frac{\gamma}{2}\epsilon\right)^2}{1+\epsilon} \sim \frac{\gamma^2}{4}\epsilon + \gamma - \frac{\gamma^2}{4} + \left(\frac{\gamma}{2}-1\right)^2\frac{1}{\epsilon} + O\left(\frac{1}{\epsilon^2}\right) \quad \text{as} \quad \epsilon \to \infty, \tag{5.40}$$

and so

$$\omega \sim \frac{c_{se}}{L}\left(\frac{L}{H_e} - \frac{\gamma^2}{4}\epsilon - \gamma + \frac{\gamma^2}{4}\right)^{\frac{1}{2}} \quad \text{as} \quad \epsilon \to \infty. \tag{5.41}$$

If $L/H_e > 1$, so the hydrodynamic and weak field resonance exists, but is $O(1)$ (which is valid for the lower solar atmosphere) the dominant term inside the square root is $-\gamma^2\epsilon/4$, hence the resonance does not exist for the case of a strong magnetic field. Note that the possibility of L/H_e being large enough to be the dominant term is unlikely, as it may violate the assumption of $L/z_0 \ll 1$.

The effect of changing the length of the lower layer is shown in Figures 5.2 and 5.3 for the case of a weak magnetic field ($v_A/c_s = 0.1$). Figure 5.2 shows the analytical frequency for increasing L. The dotted line indicates the point where $L/H_e = 1$, below which the resonant frequencies are complex, as L increases the resonant frequency increases rapidly to it maximum value just beyond the point where $L/H_e = 1$. The frequencies then decrease with increasing L. The analytical expression becomes less reliable as the parameter L/z_0 increases (although the Taylor expansions are passable for $L/z_0 < 1$).

Let us investigate the dependence on L when the assumption of small L/z_0 is no longer valid. The numerical values are found using a simple root finding technique on the denominator of Equation (5.21). These numerical frequencies are plotted in Figure 5.3. We immediately see that the trend of decreasing frequency as L increases, as shown by the analytical solution, is indeed true when the assumptions underlying its derivation are no longer valid. The temperature profile in the numerical solution is continuous at

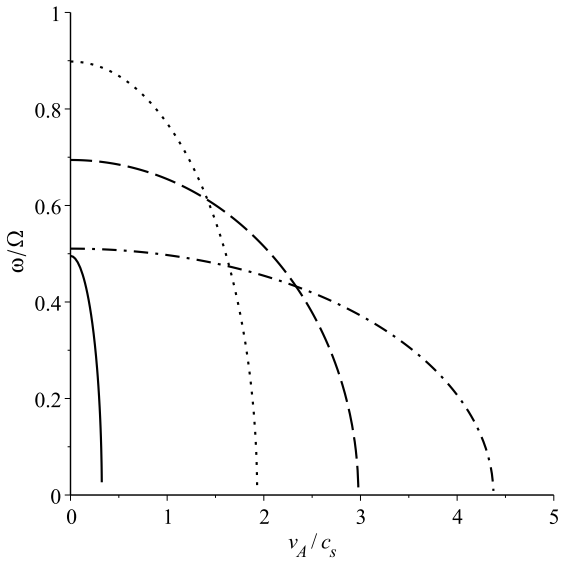

Fig. 5.1 A plot of the resonant frequencies (5.36), normalised to the *hydrodynamic* acoustic cut-off in the upper layer (denoted by Ω) , for increasing Alfvén speed. Typical photospheric values are used $c_{se} = 8$ km s^{-1}, $\gamma = 5/3, g = 0.274$ km s^{-2}. The solid line represents $L = 150$ km, the dotted line $L = 500$ km, the dashed line $L = 1$ Mm, and the dot-dashed line $L = 2$ Mm.

$z = 0$, hence $\widehat{c}_{si} = c_{se}$. The value of ω/Ω given by the numerical solution for $L/z_0 = 1$ is slightly below 0.8, suggesting that the decrease shown by the analytical solution is somewhat drastic. This discrepancy is attributed to the increase in the parameter L/z_0 and that $L/H_i = L/H_e$. Although there is a difference, the analytical and numerical frequencies are the same order of magnitude; despite the conditions, used in the analytical derivation, not being satisfied. This analysis shows that the analytical result is a good indicator of the resonant frequencies.

Another feature shown by the numerical solutions is the appearance of higher harmonics as the length of the lower layer increases. In addition to the fundamental mode, the first and second harmonics are plotted. The frequency of these modes also decreases with increasing L. Note that the three modes are not the only modes that exist for these values of L/z_0, in fact it can be shown that six harmonics in addition to the fundamental mode may be present for $L/z_0 \in [1, 10]$ (based on the values of the parameters used in Figure 5.3). As L/z_0 increases more harmonics are present, subject to the limitation that $\omega < \Omega$.

In the limit $L \to \infty$ the frequency, given by Equation (5.36), tends to 0. This is because the cavity in which the waves are trapped ceases to exist in this limit, *i.e.* waves driven at real positive frequencies are not trapped and no resonance occurs. This may also be seen in Figure 5.3 for the numerically plotted frequencies (including higher harmonics).

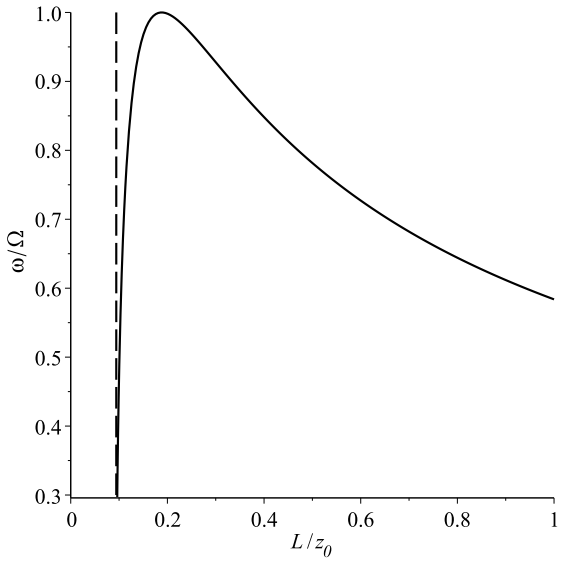

Fig. 5.2 A plot of the resonant frequencies (5.36), normalised to the *modified* acoustic cut-off in the upper layer, for L. Typical photospheric values are used $c_{se} = 8$ km s^{-1}, $\gamma = 5/3, g = 0.274$ km s^{-2}. The temperature scale height in the lower layer is fixed at $z_0 = 1500$ km and the Alfvén speed is such that $v_{A0}/c_{se} = 0.1$.

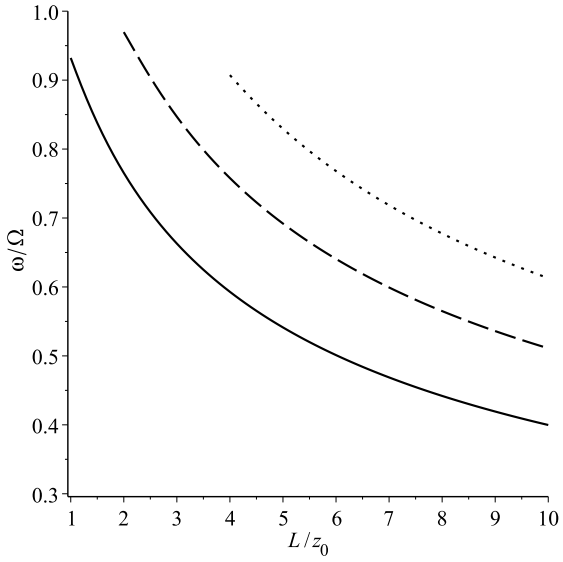

Fig. 5.3 A plot of the numerical resonant frequencies, normalised to the *modified* acoustic cut-off in the upper layer, for L. Typical photospheric values are used $c_{se} = 8$ km s^{-1}, $\gamma = 5/3, g = 0.274$ km s^{-2}. The temperature scale height in the lower layer is fixed at $z_0 = 1500$ km and the Alfvén speed is such that $v_{A0}/c_{se} = 0.1$.

5.2.2 Model with a Uniform Magnetic Field

Let the magnetic field be uniform $\mathbf{B}_0 = (B_0, 0, 0)$, B_0 is constant. The equation of magneto-hydrostatic equilibrium reduces to

$$\frac{\mathrm{d}p_0}{\mathrm{d}z} = -g\rho_0. \tag{5.42}$$

In the upper layer we again take the temperature to be uniform, hence the density and pressure decrease exponentially. When this is the case the square of the Alfvén speed increases exponentially

$$v_A^2 = \widehat{v}_A^2 e^{z/H}. \tag{5.43}$$

The governing equation of motion,

$$\rho_0\left(c_s^2 + v_A^2\right)\frac{\mathrm{d}^2\xi_z}{\mathrm{d}z^2} + \left(\frac{\mathrm{d}}{\mathrm{d}z}\rho_0\left(c_s^2 + v_A^2\right)\right)\frac{\mathrm{d}\xi_z}{\mathrm{d}z} + \rho_0\omega^2\xi_z = 0, \tag{5.44}$$

becomes

$$\left(c_s^2 e^{-z/H} + \widehat{v}_A^2\right)\frac{\mathrm{d}^2\xi_z}{\mathrm{d}z^2} - \frac{c_s^2}{H}e^{-z/H}\frac{\mathrm{d}\xi_z}{\mathrm{d}z} + \omega^2 e^{-z/H}\xi_z = 0. \tag{5.45}$$

We may find exact solutions to this equation by making the variable change

$$\varphi = 1 + \frac{2c_s^2}{\widehat{v}_A^2}e^{-z/H}. \tag{5.46}$$

Under this transformation Equation (5.45) becomes

$$\left(1-\varphi^2\right)\frac{\mathrm{d}^2\xi_z}{\mathrm{d}\varphi^2} - 2\varphi\frac{\mathrm{d}\xi_z}{\mathrm{d}\varphi} - \frac{H^2\omega^2}{c_s^2}\xi_z = 0. \tag{5.47}$$

Equation (5.47) is Legendre's equation (Abramowitz & Stegun, 1972),

$$\left(1-x^2\right)\frac{\mathrm{d}^2 f}{\mathrm{d}x^2} - 2x\frac{\mathrm{d}f}{\mathrm{d}x} + \left[\nu(\nu+1) - \frac{\mu^2}{1-x^2}\right]f = 0, \tag{5.48}$$

which has regular singular points at $x = -1, 1, \infty$. Equation (5.47) has solutions in terms of Legendre functions (the special case of the associated Legendre functions when $\mu = 0$)

$$\xi_z = D_1 P_\nu(\varphi) + D_2 Q_\nu(\varphi), \tag{5.49}$$

where

$$\nu = -\frac{1}{2} + \frac{H\mathrm{i}}{c_s}\sqrt{\omega^2 - \frac{c_s^2}{4H^2}}, \tag{5.50}$$

and P_ν and Q_ν denote the Legendre functions of degree ν of the first and second kind respectively.

The solution valid around the singular point $\varphi = 1$ has radius of convergence $|(1-\varphi)/2| < 1$, which translates to the condition

$$\frac{c_s^2}{\widehat{v}_A^2}e^{-z/H} < 1. \tag{5.51}$$

As $z/H \geq 0$ this is satisfied when $c_s^2/\widehat{v}_A^2 < 1$, *i.e.*, the case of low plasma-β. The solution valid around the singular point $z = \infty$ may not be used for the case of a weak magnetic

field as $\varphi \to 1$ as $z \to \infty$. We continue this analysis with the condition that the plasma-β is low. We return to the high-β case later. These solutions to the governing equations have been derived previously by Thomas (1983) although the finite radius of convergence was not commented upon.

Both P_ν and Q_ν are regular at $z = 0$. We seek non-leaky modes, hence we require the perturbation of the kinetic energy density, $\rho_0 v_z^2$, to tend to zero as $z \to \infty$. Let us examine the behaviour of the solutions as $z \to \infty$. As $z \to \infty$, $\varphi \to 1$, around the singular point $\varphi = 1$ the Legendre functions have the expansions (leading order behaviour is given by *e.g.* Erdélyi, 1953; higher order terms can be deduced by using the well-known recurrence relations which may be shown using the relationship between Legendre functions and Hypergeometric functions, Abramowitz & Stegun, 1972),

$$P_\nu(\varphi) = 1 - \frac{-\nu(1+\nu)}{2}(\varphi - 1) + O\Big((\varphi-1)^2\Big), \quad \left|\frac{1-\varphi}{2}\right| < 1, \tag{5.52}$$

$$\begin{aligned} Q_\nu(\varphi) = \left(\frac{1}{2}(\log(1+\varphi) - \log(1-\varphi)) - \psi(\nu+1)\right)\left(1 + \frac{\nu(\nu+1)}{2}(\varphi-1) - O\Big((\varphi-1)^2\Big)\right) \\ -\widetilde{\gamma} + \frac{\nu(\nu+1)}{2}(1-\widetilde{\gamma})(\varphi-1) - O\Big((\varphi-1)^2\Big), \quad \left|\frac{1-\varphi}{2}\right| < 1, \nu \notin \mathbb{Z}, \end{aligned} \tag{5.53}$$

where $\widetilde{\gamma}$ is the Euler-Mascheroni constant (not the ratio of specific heats of the plasma) and ψ is the digamma function $\psi(x) = \frac{\mathrm{d}}{\mathrm{d}x}\log(\Gamma(x))$. We see from the leading order behaviour that P_ν remains finite while Q_ν has a logarithmic singularity as $z \to \infty$. To satisfy the boundary condition of vanishing kinetic energy density (and also magnetic energy density $\mathbf{B}_0 \cdot \mathbf{B}_1/\mu$) we must set $D_2 = 0$, hence our solution is

$$\xi_z = D_1 P_\nu(\varphi). \tag{5.54}$$

The boundary conditions are the same as the case of constant Alfvén speed. Applying these gives the relations

$$(-L - z_0)^{-\frac{m}{2}}\left[C_1 J_m(\theta_{-L}) + C_2 Y_m(\theta_{-L})\right] = I(\omega), \tag{5.55}$$

$$(-z_0)^{-\frac{m}{2}}\left[C_1 J_m(\theta_0) + C_2 Y_m(\theta_0)\right] - D_1 P_\nu(\varphi_0) = 0, \tag{5.56}$$

$$\begin{aligned} \widehat{\rho}_{0i}\widehat{c}_{si}^2\omega(-z_0)^{-\frac{m}{2}}\left[C_1 J_{m+1}(\theta_0) + C_2 Y_{m+1}(\theta_0)\right] + \\ \frac{\widehat{\rho}_{0e}\nu\widehat{v}_A^2}{2H_e}\left[\left(1 + \frac{2c_{se}^2}{\widehat{v}_A^2}\right)P_\nu(\varphi_0) - P_{\nu-1}(\varphi_0)\right]D_1 = 0, \end{aligned} \tag{5.57}$$

where we have used the property

$$\frac{\mathrm{d}P_\nu(x)}{\mathrm{d}x} = \frac{\nu}{x^2-1}\left(xP_\nu(x) - P_{\nu-1}(x)\right). \tag{5.58}$$

Inverting the system of equations leads us to

$$D_1 = \frac{-2\widehat{c_{si}}\omega\widehat{\rho_{0i}}H_e\left(1+L/z_0\right)^{\frac{m}{2}} I(\omega)W\left(J_m(\theta_0), Y_m(\theta_0)\right)}{\begin{array}{l}2\widehat{c_{si}}\widehat{\rho_{0i}}\omega H_e P_\nu(\varphi_0)\left(J_{m+1}(\theta_0)Y_m(\theta_{-L}) - J_m(\theta_{-L})Y_{m+1}(\theta_0)\right) \\ \quad + \widehat{\rho_{0e}}\nu\left(\left(\widehat{v_A^2} + 2c_{se}^2\right)P_\nu(\varphi_0) - \widehat{v_A^2}P_{\nu-1}(\varphi_0)\right)\left[J_m(\theta_0)Y_m(\theta_{-L}) - J_m(\theta_{-L})Y_m(\theta_0)\right]\end{array}}, \tag{5.59}$$

$$C_1 = \frac{\begin{array}{l}[\nu\widehat{\rho_{0e}}\widehat{v_A^2}Y_m(\theta_0)P_{\nu-1}(\varphi_0) \\ \quad -(2\widehat{\rho_{0i}}\widehat{c_{si}}\omega H_e Y_{m+1}(\theta_0) + \nu\widehat{\rho_{0e}}\left(\widehat{v_A^2} + 2c_{se}^2\right)Y_m(\theta_0))P_\nu(\varphi_0)]I(\omega)(-L-z_0)^{\frac{m}{2}}\end{array}}{\begin{array}{l}2\widehat{c_{si}}\widehat{\rho_{0i}}\omega H_e P_\nu(\varphi_0)\left(J_{m+1}(\theta_0)Y_m(\theta_{-L}) - J_m(\theta_{-L})Y_{m+1}(\theta_0)\right) \\ \quad + \widehat{\rho_{0e}}\nu\left(\left(\widehat{v_A^2} + 2c_{se}^2\right)P_\nu(\varphi_0) - \widehat{v_A^2}P_{\nu-1}(\varphi_0)\right)\left[J_m(\theta_0)Y_m(\theta_{-L}) - J_m(\theta_{-L})Y_m(\theta_0)\right]\end{array}}, \tag{5.60}$$

$$C_2 = \frac{\begin{array}{l}[\left(2\widehat{\rho_{0i}}\widehat{c_{si}}\omega H_e J_{m+1}(\theta_0) + \nu\widehat{\rho_{0e}}\left(\widehat{v_A^2} + 2c_{se}^2\right)J_m(\theta_0)\right)P_\nu(\varphi_0) \\ \quad -\nu\widehat{\rho_{0e}}\widehat{v_A^2}J_m(\theta_0)P_{\nu-1}(\varphi_0)]I(\omega)(-L-z_0)^{\frac{m}{2}}\end{array}}{\begin{array}{l}2\widehat{c_{si}}\widehat{\rho_{0i}}\omega H_e P_\nu(\varphi_0)\left(J_{m+1}(\theta_0)Y_m(\theta_{-L}) - J_m(\theta_{-L})Y_{m+1}(\theta_0)\right) \\ \quad + \widehat{\rho_{0e}}\nu\left(\left(\widehat{v_A^2} + 2c_{se}^2\right)P_\nu(\varphi_0) - \widehat{v_A^2}P_{\nu-1}(\varphi_0)\right)\left[J_m(\theta_0)Y_m(\theta_{-L}) - J_m(\theta_{-L})Y_m(\theta_0)\right]\end{array}}. \tag{5.61}$$

The fundamental mode of the resonant frequency may be investigated analytically by making the assumption that the lower layer is thin, $L/z_0 \ll 1$. The Bessel functions may be approximated as in Section 4.1. The eigenfunction in the upper layer is restricted to the low-β case of $c_{se}^2 < \widehat{v_A^2}$; let us make the stronger assumption that $c_{se}^2/\widehat{v_A^2} \ll 1$. We may then approximate the Legendre functions by

$$P_\nu(\varphi_0) \approx 1 + \frac{\nu(1+\nu)}{2}(\varphi_0 - 1) = 1 + \nu(1+\nu)\frac{c_{se}^2}{\widehat{v_A^2}}. \tag{5.62}$$

The coefficient D_1 may be simplified to

$$D_1 \approx \frac{-2H_e\left(1 + \frac{mL}{2z_0}\right)I(\omega)}{\begin{array}{l}2H_e\left[1 + \nu(1+\nu)\frac{c_{se}^2}{\widehat{v_A^2}}\right] \\ \quad + \left(c_{se}^2 + \frac{\gamma\widehat{v_A^2}}{2}\right)^{-1}\widehat{v_A^2}L\nu\left(\left(1 + \frac{2c_{se}^2}{\widehat{v_A^2}}\right)\left[1 + \nu(1+\nu)\frac{c_{se}^2}{\widehat{v_A^2}}\right] - 1 + \nu(1-\nu)\frac{c_{se}^2}{\widehat{v_A^2}}\right)\end{array}}. \tag{5.63}$$

Using the approximation

$$(1+\beta)^{-1} \approx 1 - \beta \quad \text{when} \quad \beta \ll 1, \tag{5.64}$$

and neglecting terms of order $O\left(\beta^2\right)$ and higher, D_1 becomes (after substitution in ν as given by Equation (5.50)),

$$D_1 \approx \frac{-2H_e\left(1+\frac{mL}{2z_0}\right)I(\omega)}{2H_e\left[1-\frac{\omega^2 c_{se}^2\beta}{2\gamma g^2}\right]-2L\frac{\omega^2 c_{se}^2}{g^2\gamma^2}\beta}, \tag{5.65}$$

where $\beta = 2c_{se}^2/\gamma\widehat{v}_A^2$. The fundamental mode of the resonant frequency is then given by

$$\omega^2 = \frac{H_e}{L}\frac{\gamma^2 g^2\widehat{v}_A^2}{2c_{se}^4}\left(\frac{H_e}{2L}+\frac{1}{\gamma}\right)^{-1}, \tag{5.66}$$

which may be written as

$$\omega = 2\Omega\widehat{v}_A\left(2Lg+c_{se}^2\right)^{-\frac{1}{2}}, \tag{5.67}$$

where Ω is the cut-off frequency in the upper layer, $\Omega = g\gamma/2c_{se}$.

The first key point to make about this resonant frequency is that it does not tend to the hydrodynamic case when $v_A = 0$. This is due to the solution being valid only around the singular point $\varphi = 1$. In the limit $v_A \to 0$, $\varphi \to \infty$ hence the solution around $\varphi = 1$ does no longer apply and so a direct comparison cannot be made.

The resonant frequency is real for all L. Unlike the hydrodynamic and constant Alfvén speed model there is no requirement that the resonant frequencies are located below the acoustic cut-off frequency. The denominator of the simplified D_1 is real, to order $O(\beta)$, whether ν is real or complex. This may be verified by assuming $\omega > g\gamma/2c_{se}$ in ν and keeping terms of order $O(\beta)$. The resulting resonant frequency is given by Equation (5.67). As $L \to \infty$, $\omega \to 0$ as in the hydrodynamic case.

The resonant frequency for the case of constant Alfvén speed tends to zero, and becomes complex, as v_A increases. The resonant frequency for the variable Alfvén speed increases with increasing $\widehat{v}_A$ and is only valid for the case of low-β plasma. The cause of this discrepancy is that the pressure scale-height and so the acoustic cut-off frequency for the case constant Alfvén speed is modified by the gradient of magnetic pressure. As the magnetic field increases the modified scale-height increases and so the resonance may no longer occur. There is no such restriction for the case of constant magnetic field, *i.e.*, the effect of a gradient in the background magnetic field is to decrease and stop the resonant frequency for increasing magnetic field strength.

Due to the solution being valid only for the case of low-β plasma, a comparison to hydrodynamic and constant Alfvén cases is difficult. We now seek to extend to the solution to high-β plasma cases for a more direct comparison.

We assume that the upper layer is such that we may consider the plasma to be in the high-β regime near the interface. At the interface $z = 0$, we then assume that the Alfvén

speed is small in comparison to the sound speed,

$$\frac{\widehat{v_A^2}}{c_s^2} = \epsilon \ll 1. \tag{5.68}$$

The magnetic field is constant so the Alfvén speed increases as the density decreases. The plasma-β, therefore, transitions from high to low through the atmosphere.

The governing equation may then be written

$$\left(e^{-z/H} + \epsilon\right)\frac{\mathrm{d}^2\xi_z}{\mathrm{d}z^2} - \frac{1}{H}e^{-z/H}\frac{\mathrm{d}\xi_z}{\mathrm{d}z} + \frac{\omega^2}{c_s^2}e^{-z/H}\xi_z = 0. \tag{5.69}$$

We may naively try to solve this equation using a regular perturbation series, although this approach will give an incomplete solution. This is because of the exponential term which becomes small as z increases. When $z \sim -H\log\epsilon$, the exponential term and the ϵ term are the same order. This results in a loss of regularity in the perturbation series, that is, the first and second terms in the perturbation series are the same order.

Solving this problem requires the use of the method of matched asymptotic expansions, as in the study of slow modes in an isothermal medium considered previously in Section 3.2.3. We begin by making the change of variable

$$\alpha = e^{-z/H}. \tag{5.70}$$

The domain $z \in [0, \infty)$ corresponds to $\alpha \in (0, 1]$. This transforms our governing equation to

$$\alpha(\alpha + \epsilon)\frac{\mathrm{d}^2\xi_z}{\mathrm{d}\alpha^2} + (2\alpha + \epsilon)\frac{\mathrm{d}\xi_z}{\mathrm{d}\alpha} + \frac{\omega^2 H^2}{c_s^2}\xi_z = 0. \tag{5.71}$$

This transformation has been made to write our governing equation in a form more suitable to the method of matched asymptotic expansions. We must perform a variable scaling to determine the "inner solution". The choice of scaling is simpler to identify when dealing with polynomial coefficients in the governing equation rather than exponential coefficients.

We find the outer solution by finding a regular asymptotic expansion for ξ_z. Note that the terms outer and inner solutions refer to the variable α rather than the physical variable z. We let

$$\xi_z \sim \Psi_0 + \epsilon\Psi_1 + \epsilon^2\Psi_2 + \ldots. \tag{5.72}$$

Substituting this perturbation series into the governing equation we have

$$\alpha^2\frac{\mathrm{d}^2\Psi_0}{\mathrm{d}\alpha^2} + 2\alpha\frac{\mathrm{d}\Psi_0}{\mathrm{d}\alpha} + \frac{\omega^2 H^2}{c_s^2}\Psi_0 + \epsilon\left[\alpha^2\frac{\mathrm{d}^2\Psi_1}{\mathrm{d}\alpha^2} + \alpha\frac{\mathrm{d}^2\Psi_0}{\mathrm{d}\alpha^2} + 2\alpha\frac{\mathrm{d}\Psi_1}{\mathrm{d}\alpha} + \frac{\mathrm{d}\Psi_0}{\mathrm{d}\alpha} + \frac{\omega^2 H^2}{c_s^2}\Psi_1\right] + O\left(\epsilon^2\right) = 0. \tag{5.73}$$

To $O(\epsilon)$ we have the equation

$$\alpha^2 \frac{\mathrm{d}^2\Psi_0}{\mathrm{d}\alpha^2} + 2\alpha \frac{\mathrm{d}\Psi_0}{\mathrm{d}\alpha} + \frac{\omega^2 H^2}{c_s^2}\Psi_0 = 0. \tag{5.74}$$

This ODE is an Euler (or Euler-Cauchy) type (Zwillinger, 1989) which has solutions of the form $\Psi_0 = \alpha^n$ where

$$n^2 + n + \frac{\omega^2 H^2}{c_s^2} = 0, \tag{5.75}$$

or

$$n = -\frac{1}{2} \pm \frac{1}{2c_s}\sqrt{c_s^2 - 4\omega^2 H^2} \equiv -\frac{1}{2} \pm \kappa. \tag{5.76}$$

Our solution for the first term in the perturbation series is then

$$\Psi_0 = C_1 \alpha^{-\frac{1}{2}+\kappa} + C_2 \alpha^{-\frac{1}{2}-\kappa}. \tag{5.77}$$

The order ϵ terms give us

$$\frac{\mathrm{d}^2\Psi_1}{\mathrm{d}\alpha^2} + \frac{2}{\alpha}\frac{\mathrm{d}\Psi_1}{\mathrm{d}\alpha} + \frac{\omega^2 H^2}{c_s^2 \alpha^2}\Psi_1 = -\frac{1}{\alpha}\frac{\mathrm{d}^2\Psi_0}{\mathrm{d}\alpha^2} - \frac{1}{\alpha^2}\frac{\mathrm{d}\Psi_0}{\mathrm{d}\alpha}. \tag{5.78}$$

The homogeneous solution is of the same form as the solution for Ψ_0,

$$\Psi_1 = D_1 \alpha^{-\frac{1}{2}+\kappa} + D_2 \alpha^{-\frac{1}{2}-\kappa}. \tag{5.79}$$

The inhomogeneous solution may be found by applying the method of variation of parameters (Zwillinger, 1989). For an inhomogeneous linear second order ODE

$$y'' + P(x)y' + Q(x)y = R(x), \tag{5.80}$$

the inhomogeneous solution is given by

$$y = -y_1 \int \frac{y_2 R}{W(y_1, y_2)} dx + y_2 \int \frac{y_1 R}{W(y_1, y_2)} dx, \tag{5.81}$$

where y_1 and y_2 are the homogeneous solutions and $W(y_1, y_2) = y_1 y_2' - y_2 y_1'$ is the Wronskian. The method of variation of parameters is equivalent to other methods for solving inhomogeneous equations such as Green's functions. Letting

$$y_1 = \alpha^{-\frac{1}{2}+\kappa}, \quad y_2 = \alpha^{-\frac{1}{2}-\kappa}, \quad R = -\frac{1}{\alpha}\frac{\mathrm{d}^2\Psi_0}{\mathrm{d}\alpha^2} - \frac{1}{\alpha^2}\frac{\mathrm{d}\Psi_0}{\mathrm{d}\alpha}, \tag{5.82}$$

we may calculate that

$$W(y_1, y_2) = -2\kappa\alpha^2. \tag{5.83}$$

The inhomogeneous solution is then

$$C_1\alpha^{-\frac{3}{2}+\kappa}\left(-\frac{1}{4}+\frac{\kappa}{2}\right)+C_2\alpha^{-\frac{3}{2}-\kappa}\left(-\frac{1}{4}-\frac{\kappa}{2}\right), \tag{5.84}$$

and so the second term in the asymptotic series is

$$\Psi_1 = D_1\alpha^{-\frac{1}{2}+\kappa}+D_2\alpha^{-\frac{1}{2}-\kappa}+C_1\alpha^{-\frac{3}{2}+\kappa}\left(-\frac{1}{4}+\frac{\kappa}{2}\right)+C_2\alpha^{-\frac{3}{2}-\kappa}\left(-\frac{1}{4}-\frac{\kappa}{2}\right). \tag{5.85}$$

Combining the expressions for Ψ_0 and Ψ_1 gives the asymptotic outer solution

$$\begin{aligned}\xi_z \sim\ & C_1\alpha^{-\frac{1}{2}+\kappa}+C_2\alpha^{-\frac{1}{2}-\kappa}\\ &+\epsilon\left[D_1\alpha^{-\frac{1}{2}+\kappa}+D_2\alpha^{-\frac{1}{2}-\kappa}+C_1\alpha^{-\frac{3}{2}+\kappa}\left(-\frac{1}{4}+\frac{\kappa}{2}\right)+C_2\alpha^{-\frac{3}{2}-\kappa}\left(-\frac{1}{4}-\frac{\kappa}{2}\right)\right]+\ldots.\end{aligned} \tag{5.86}$$

We see that when $\alpha \sim \epsilon$, the third and fourth terms in the square brackets are the same order as the first and second terms in the series, hence the loss of regularity in the perturbation series.

In order to determine the inner solution we make the variable scaling

$$\widetilde{\alpha} = \frac{\alpha}{\epsilon}, \tag{5.87}$$

such that $\widetilde{\alpha}$ is order 1 when α is order ϵ. The boundary condition to be applied at $z \to \infty$ corresponds to $\widetilde{\alpha} \to 0$. When $\alpha = \epsilon$, where the outer solution fails, $\widetilde{\alpha} = 1$. The region we are interested in then corresponds to $\widetilde{\alpha} \in (0,1)$.

Under this variable scaling the governing equation is

$$\widetilde{\alpha}(\widetilde{\alpha}+1)\frac{\mathrm{d}^2\xi_z}{\mathrm{d}\widetilde{\alpha}^2}+(2\widetilde{\alpha}+1)\frac{\mathrm{d}\xi_z}{\mathrm{d}\widetilde{\alpha}}+\frac{\omega^2H^2}{c_s^2}\xi_z = 0. \tag{5.88}$$

Making another variable change,

$$\widehat{\alpha} = -\widetilde{\alpha}, \tag{5.89}$$

the governing equation may be written

$$\widehat{\alpha}(1-\widehat{\alpha})\frac{\mathrm{d}^2\xi_z}{\mathrm{d}\widehat{\alpha}^2}+(1-2\widehat{\alpha}+1)\frac{\mathrm{d}\xi_z}{\mathrm{d}\widehat{\alpha}}-\frac{\omega^2H^2}{c_s^2}\xi_z = 0. \tag{5.90}$$

This is the standard form of the Gauss hypergeometric equation (Abramowitz & Stegun, 1974)

$$x(1-x)\frac{\mathrm{d}^2w}{\mathrm{d}x^2}+[c-(a+b+1)x]\frac{\mathrm{d}w}{\mathrm{d}x}-abw = 0, \tag{5.91}$$

where

$$a+b = 1, \quad ab = \frac{\omega^2H^2}{c_s^2}, \quad c = 1, \tag{5.92}$$

that is

$$a = \frac{1}{2} - \kappa, \quad b = \frac{1}{2} + \kappa. \tag{5.93}$$

We apply the boundary condition at $z \to \infty$, hence we seek the solution valid around the singular point $\widetilde{\alpha} = 0$. Selecting the appropriate solution from Kummer's 24 solutions (Abramowitz & Stegun, 1974) for the case of $c = 1$ we have

$$\xi_z \sim A_1 {}_2F_1(a,b;1;-\widetilde{\alpha}) + A_2 \Big\{ {}_2F_1(a,b;1;-\widetilde{\alpha}) \log(-\widetilde{\alpha}) + \sum_{n=1}^{\infty} \frac{(a)_n (b)_n}{(n!)^2} (-\widetilde{\alpha})^n \left[\psi(a+n) - \psi(a) + \psi(b+n) - \psi(b) - 2\psi(n+1) + 2\psi(1) \right] \Big\}, \quad |\widetilde{\alpha}| < 1 \tag{5.94}$$

where $\psi(x)$ is the digamma function. We note that $c - a - b = 0$, hence the series representation of the hypergeometric function converges within/on the unit circle, except the point $\widetilde{\alpha} = -1$.

Let us apply the boundary condition of finite energy density as $z \to \infty$. As $\widetilde{\alpha} \to 0$, ${}_2F_1(a,b;1;-\widetilde{\alpha}) \to 1$, and $\Re(\log -\widetilde{\alpha}) \to -\infty$. To satisfy the boundary condition, $A_2 = 0$, and the inner solution is

$$\xi_z \sim A_1 {}_2F_1(a,b;1;-\widetilde{\alpha}). \tag{5.95}$$

We must now match the inner solution to the outer solution. We do this via Van Dyke's matching rule as discussed previously in Section 3.2.3. First, we consider the outer solution (5.86) in terms of the inner variable, that is we make the substitution $\alpha = \epsilon\widetilde{\alpha}$,

$$\xi_z \sim C_1 \widetilde{\alpha}^{-\frac{1}{2}+\kappa} \epsilon^{-\frac{1}{2}+\kappa} + C_2 \widetilde{\alpha}^{-\frac{1}{2}-\kappa} \epsilon^{-\frac{1}{2}-\kappa} + D_1 \widetilde{\alpha}^{-\frac{1}{2}+\kappa} \epsilon^{\frac{1}{2}+\kappa} + D_2 \widetilde{\alpha}^{-\frac{1}{2}-\kappa} \epsilon^{\frac{1}{2}-\kappa} + C_1 \widetilde{\alpha}^{-\frac{3}{2}+\kappa} \left(-\frac{1}{4} + \frac{\kappa}{2} \right) \epsilon^{-\frac{1}{2}+\kappa} + C_2 \widetilde{\alpha}^{-\frac{3}{2}-\kappa} \left(-\frac{1}{4} - \frac{\kappa}{2} \right) \epsilon^{-\frac{1}{2}-\kappa}. \tag{5.96}$$

In order to determine the leading order behaviour when $\epsilon \to 0$, let us make the assumption that the driving frequency is below the acoustic cut-off frequency, Ω, as in the hydrodynamic problem. The parameter κ may be written

$$\kappa = \frac{1}{2} \sqrt{1 - \frac{\omega^2}{\Omega^2}}. \tag{5.97}$$

Under the assumption $\omega < \Omega$, we see that κ is real and positive and is bounded $0 < \kappa < 1/2$. The dominant terms when $\epsilon \to 0$, are

$$\xi_z \sim C_2 \widetilde{\alpha}^{-\frac{1}{2}-\kappa} \epsilon^{-\frac{1}{2}-\kappa} + C_2 \widetilde{\alpha}^{-\frac{3}{2}-\kappa} \left(-\frac{1}{4} - \frac{\kappa}{2} \right) \epsilon^{-\frac{1}{2}-\kappa} = C_2 \alpha^{-\frac{1}{2}-\kappa} + C_2 \epsilon \alpha^{-\frac{3}{2}-\kappa} \left(-\frac{1}{4} - \frac{\kappa}{2} \right). \tag{5.98}$$

Substituting the outer variable into the inner solution, *i.e.* $\widetilde{\alpha} = \alpha/\epsilon$, we have

$$\xi_z \sim A_1 {}_2F_1\left(a,b;1;-\frac{\alpha}{\epsilon}\right). \tag{5.99}$$

We let $\epsilon \to 0$, and use the asymptotic property of the hypergeometric function (Abramowitz & Stegun, 1974),

$$ {}_2F_1\left(a,b;1;-\frac{\alpha}{\epsilon}\right) \sim \frac{\Gamma(1)\Gamma(b-a)}{\Gamma(b)\Gamma(1-a)}\left(\frac{\alpha}{\epsilon}\right)^{-a} {}_2F_1\left(a,a;1-b+a;-\frac{\epsilon}{\alpha}\right) + \frac{\Gamma(1)\Gamma(a-b)}{\Gamma(a)\Gamma(1-b)}\left(\frac{\alpha}{\epsilon}\right)^{-b} {}_2F_1\left(b,b;1-a+b;-\frac{\epsilon}{\alpha}\right). \quad (5.100) $$

We have a and b expressed in terms of κ, hence the first term is the dominant term. We may also Taylor expand the hypergeometric functions appearing in the asymptotic formula. In order to match the solutions we keep the first two terms in the series expansion. The inner solution is then

$$ \xi_z \sim A_1 \frac{\Gamma(b-a)}{\Gamma(b)\Gamma(1-a)} \alpha^{-\frac{1}{2}+\kappa} \epsilon^{\frac{1}{2}-\kappa}\left(1-\frac{a^2}{1-b+a}\frac{\epsilon}{\alpha}\right). \quad (5.101) $$

We see at this stage that the inner solution must be scaled in order to match the orders of ϵ. Before we do this, we note that the solutions do not match. The inner solution has a term α to the power $-1/2+\kappa$, whereas the outer solution is to the power $-1/2-\kappa$. In order to match the solutions we must therefore set $C_2 = 0$ and go to the next dominant term in the outer solution. Physically, this is intuitive as the leading term in the outer solution represented an incoming wave. When $\omega < \Omega$, this term would not satisfy the boundary condition of finite energy density. The method of matched asymptotic expansions has therefore allowed us to transmit the correct information from the boundary conditions, via the inner solution, to the outer solution. Setting $C_2 = 0$, the outer solution is

$$ \xi_z \sim C_1 \widetilde{\alpha}^{-\frac{1}{2}+\kappa} \epsilon^{-\frac{1}{2}+\kappa} + C_1 \widetilde{\alpha}^{-\frac{3}{2}+\kappa}\left(-\frac{1}{4}+\frac{\kappa}{2}\right)\epsilon^{-\frac{1}{2}+\kappa} = C_1 \alpha^{-\frac{1}{2}+\kappa} + C_1 \alpha^{-\frac{3}{2}+\kappa}\left(-\frac{1}{4}+\frac{\kappa}{2}\right)\epsilon. \quad (5.102) $$

Rescaling the inner solution by

$$ \epsilon^{-\frac{1}{2}+\kappa}, \quad (5.103) $$

$$ \xi_z \sim A_1 \frac{\Gamma(b-a)}{\Gamma(b)\Gamma(1-a)} \alpha^{-\frac{1}{2}+\kappa}\left(1-\frac{a^2}{1-b+a}\frac{\epsilon}{\alpha}\right) = A_1 \frac{\Gamma(b-a)}{\Gamma(b)\Gamma(1-a)} \alpha^{-\frac{1}{2}+\kappa} - A_1 \frac{\Gamma(b-a)}{\Gamma(b)\Gamma(1-a)} \frac{a}{2} \epsilon \alpha^{-\frac{3}{2}+\kappa}, \quad (5.104) $$

as $1-b+a = 2a$. We see that the inner and outer solutions match when

$$ C_1 = \frac{\Gamma(b-a)}{\Gamma(b)\Gamma(1-a)} A_1. \quad (5.105) $$

The complete asymptotic solution is then

$$\xi_z \sim \frac{\Gamma(b)\Gamma(1-a)}{\Gamma(b-a)} A_1 e^{\left(\frac{1}{2H}-\frac{\kappa}{H}\right)z} + \epsilon\left[D_1 e^{\left(\frac{1}{2H}-\frac{\kappa}{H}\right)z} + D_2 e^{\left(\frac{1}{2H}+\frac{\kappa}{H}\right)z} + \frac{\Gamma(b)\Gamma(1-a)}{\Gamma(b-a)} A_1 \left(-\frac{1}{4}+\frac{\kappa}{2}\right) e^{\left(\frac{3}{2H}-\frac{\kappa}{H}\right)z}\right], \quad (5.106)$$

when z/H is smaller than $-\log\epsilon$; and

$$\xi_z \sim A_1 \, {}_2F_1\left(\frac{1}{2}-\kappa, \frac{1}{2}+\kappa; 1; -\frac{e^{-\frac{z}{H}}}{\epsilon}\right)\epsilon^{-\frac{1}{2}+\kappa}, \quad (5.107)$$

when z/H is larger than $-\log\epsilon$. Using these asymptotic solutions, a composite solution may be constructed to approximate the solution in the whole of the domain. We shall not do this as we will now apply boundary conditions to the solution to study the global resonance of the system. The method of matched asymptotic expansion has allowed us to consider the case of an initially weak field and apply a boundary condition from a region where the solution is no longer valid. Note that it may seem that we have too many constants of integration to find with our two remaining boundary conditions at $z = 0$. This is not the case, however, as we have the boundary conditions applied to order 1 and order ϵ. The order ϵ boundary conditions allow D_1 and D_2 to be determined in terms of A_1.

We may wish to construct a uniformly valid composite (although non-unique) solution, that will allow us to investigate the region $z \sim -H\log\epsilon$ more accurately. The procedure to derive this solution is (take the limit $\epsilon \to 0, \alpha$ fixed in the outer solution) + (take the limit $\epsilon \to 0, \widetilde{\alpha}$ fixed in the inner solution) − ($\epsilon \to 0$ with the outer variable in the inner solution). See Hinch (1991) for details and examples.

It should be noted that, for the case of $k_\perp \neq 0$, the validity of the hypergeometric solution for only a strong magnetic field was commented upon by Nye & Thomas (1976) (see also Musielak *et al.* 1993). In their analysis, analytic continuation was used to extend the solution outside of its radius of convergence. Instead of using this method to solve the problem, we have opted to use the matched asymptotic solution. The strength of the matched asymptotic solution is that it, firstly, gives a relatively simple solution which expresses the relevant information. That is, the important features of the solution may be expressed in a simple way. More importantly, perhaps, the character of the waves is explicit in this solution. The behaviour in the high-β regime is clear and includes the effect of the boundary conditions applied in the low-β regime. The dependence of the behaviour of the wave on the plasma-β is not as clear in the solution with analytic continuation. For these reasons (not to mention the elegance in deriving the solution), we feel that the method of matched asymptotic expansions, which to our knowledge has not been previously applied to MAG waves in the solar atmosphere, has its place in analysing wave behaviour in a stratified atmosphere. The method of matched asymptotic expansions has been applied to problems in MHD by *e.g.* Furth *et al.* (1963) in the context of the tearing mode instability (see also Goedbloed *et al.* , 2010); Ruderman *et al.* (1997), Ballai *et al.* (1998), Ballai &

Erdélyi (1998), Ballai & Erdelyi (2002), Clack *et al.* (2009) in the study of non-linear resonant absorption; and Heyvaerts & Norman (2003) in relativistic jets and winds.

Let us apply the boundary conditions at $z = -L$ and $z = 0$, for the two-layer model. The boundary condition at $z = -L$ is as in the previous cases

$$(-L - z_0)^{-\frac{m}{2}} \left[C_1 J_m(\theta_{-L}) + C_2 Y_m(\theta_{-L})\right] = I(\omega). \tag{5.108}$$

The continuity of vertical displacement, $\xi_{zi} = \xi_{ze}$, is

$$(-z_0)^{-\frac{m}{2}} \left[C_1 J_m(\theta_0) + C_2 Y_m(\theta_0)\right] = \frac{\Gamma(b)\Gamma(1-a)}{\Gamma(b-a)} A_1 + \epsilon \left[D_1 + D_2 + \frac{\Gamma(b)\Gamma(1-a)}{\Gamma(b-a)} A_1 \left(-\frac{1}{4} + \frac{\kappa}{2}\right)\right]. \tag{5.109}$$

To order ϵ^0 the boundary condition gives the relation

$$(-z_0)^{-\frac{m}{2}} \left[C_1 J_m(\theta_0) + C_2 Y_m(\theta_0)\right] - \frac{\Gamma(b)\Gamma(1-a)}{\Gamma(b-a)} A_1 = 0, \tag{5.110}$$

while the boundary condition to order ϵ term gives

$$D_1 + D_2 + \frac{\Gamma(b)\Gamma(1-a)}{\Gamma(b-a)} A_1 \left(-\frac{1}{4} + \frac{\kappa}{2}\right) = 0. \tag{5.111}$$

The boundary condition of Lagrangian perturbation of the total pressure may be written

$$\left(1 + \frac{\gamma}{2}\epsilon\right) \left.\frac{\mathrm{d}\xi_{zi}}{\mathrm{d}z}\right|_{z=0} = (1+\epsilon) \left.\frac{\mathrm{d}\xi_{ze}}{\mathrm{d}z}\right|_{z=0}. \tag{5.112}$$

Substituting the solutions into this boundary condition,

$$\begin{aligned} &\frac{\omega}{\widehat{c_{si}}} (-z_0)^{-\frac{m}{2}} \left[C_1 J_{m+1}(\theta_0) + C_2 Y_{m+1}(\theta_0)\right] + \frac{\gamma\omega}{2\widehat{c_{si}}} \epsilon (-z_0)^{-\frac{m}{2}} \left[C_1 J_{m+1}(\theta_0) + C_2 Y_{m+1}(\theta_0)\right] = \\ &\qquad \frac{\Gamma(b)\Gamma(1-a)}{\Gamma(b-a)} \left(\frac{1}{2H} - \frac{\kappa}{H}\right) A_1 + \epsilon \frac{\Gamma(b)\Gamma(1-a)}{\Gamma(b-a)} \left(\frac{1}{2H} - \frac{\kappa}{H}\right) A_1 + \\ &\epsilon \left[D_1 \left(\frac{1}{2H} - \frac{\kappa}{H}\right) + D_2 \left(\frac{1}{2H} + \frac{\kappa}{H}\right) + \frac{\Gamma(b)\Gamma(1-a)}{\Gamma(b-a)} A_1 \left(-\frac{1}{4} + \frac{\kappa}{2}\right)\left(\frac{3}{2H} - \frac{\kappa}{H}\right)\right] + O\left(\epsilon^2\right). \end{aligned} \tag{5.113}$$

The order ϵ^0 and order ϵ boundary conditions are therefore

$$\frac{\omega}{\widehat{c_{si}}} (-z_0)^{-\frac{m}{2}} \left[C_1 J_{m+1}(\theta_0) + C_2 Y_{m+1}(\theta_0)\right] - \frac{\Gamma(b)\Gamma(1-a)}{\Gamma(b-a)} \left(\frac{1}{2H} - \frac{\kappa}{H}\right) A_1 = 0, \tag{5.114}$$

and

$$\frac{\gamma\omega}{2\widehat{c_{si}}}(-z_0)^{-\frac{m}{2}}\left[C_1 J_{m+1}(\theta_0)+C_2 Y_{m+1}(\theta_0)\right]- \frac{\Gamma(b)\Gamma(1-a)}{\Gamma(b-a)}A_1\left[\left(\frac{1}{2H}-\frac{\kappa}{H}\right)+\left(-\frac{1}{4}+\frac{\kappa}{2}\right)\left(\frac{3}{2H}-\frac{\kappa}{H}\right)\right]-D_1\left(\frac{1}{2H}-\frac{\kappa}{H}\right)-D_2\left(\frac{1}{2H}+\frac{\kappa}{H}\right)=0. \tag{5.115}$$

Inverting the system of equations gives

$$A_1=\frac{\Gamma(b-a)}{\Gamma(b)\Gamma(1-a)}\cdot\frac{-2\omega HI(\omega)(1+L/z_0)^m 2W(J_m(\theta_0),Y_m(\theta_0))}{2H\omega\left[Y_{m+1}(\theta_0)J_m(\theta_{-L})-Y_m(\theta_{-L})J_{m+1}(\theta_0)\right]+\widehat{c}_{si}(2\kappa-1)\left[Y_m(\theta_0)J_m(\theta_{-L})-Y_m(\theta_{-L})J_m(\theta_0)\right]}, \tag{5.116}$$

$$C_1=\frac{\Gamma(b-a)}{\Gamma(b)\Gamma(1-a)}\cdot\frac{-\left[2HY_{m+1}(\theta_0)+\widehat{c}_{si}(2\kappa-1)Y_m(\theta_0)\right](-z_0)^m 2A_1}{2\omega HW(J_m(\theta_0),Y_m(\theta_0))}, \tag{5.117}$$

$$C_2=\frac{\Gamma(b-a)}{\Gamma(b)\Gamma(1-a)}\cdot\frac{\left[2HJ_{m+1}(\theta_0)+\widehat{c}_{si}(2\kappa-1)J_m(\theta_0)\right](-z_0)^m 2A_1}{2\omega HW(J_m(\theta_0),Y_m(\theta_0))}, \tag{5.118}$$

$$D_1=\frac{\Gamma(b-a)}{\Gamma(b)\Gamma(1-a)}\frac{1}{8\kappa}\left(2\gamma\kappa-4\kappa^2-\gamma+1\right)A_1, \tag{5.119}$$

$$D_2=-\frac{\Gamma(b-a)}{\Gamma(b)\Gamma(1-a)}\frac{1}{8\kappa}(2\gamma\kappa-2\kappa-\gamma+1)A_1. \tag{5.120}$$

Making the assumption of slowly varying temperature, we may approximate

$$A_1\approx\frac{\Gamma(b-a)}{\Gamma(b)\Gamma(1-a)}\frac{I(\omega)\left(1+\frac{mL}{2z_0}\right)}{1+L\left(\frac{\kappa}{H}-\frac{1}{2H}\right)}. \tag{5.121}$$

The resonant frequency is then found to be

$$\omega=\frac{c_{se}}{L}\left(\frac{L}{H}-1\right)^{\frac{1}{2}}, \tag{5.122}$$

the same as in the hydrodynamic case, the properties of which were discussed earlier. We conclude that the effect of a weak magnetic field above the interface is to modify the solutions and the amplitude of the oscillations in relation to the hydrodynamic case but does not change the frequency of the trapped waves.

In comparison to the weak field case of a constant Alfvén speed, Equation (5.39), we also see that a constant Alfvén speed has a more significant effect on the resonant frequency as it has a term of order ϵ. This is due to the magnetic field modifying the scale-height and vertical wavenumber. This is in-line with the conclusion of Evans & Roberts (1990) who found that in a two-layer model, a constant Alfén speed profile has a much greater effect on the eigenfrequencies of the system in comparison to a uniform magnetic field profile.

5.3 Non-Vertical Wave Propagation in a Horizontal Field

We have so far considered vertically propagating waves, *i.e.* $k_\perp = 0$. In this section we shall relax this assumption in order to study waves in a magnetic atmosphere with arbitrary propagation angle.

In the upper magnetic layer we, again, assume constant Alfvén speed. The governing equation is

$$\frac{\mathrm{d}^2\xi_z}{\mathrm{d}z^2} - \frac{1}{H_B}\frac{\mathrm{d}\xi_z}{\mathrm{d}z} + A\xi_z = 0, \tag{5.123}$$

where

$$A = \frac{\begin{array}{r}(\Gamma-1)k^2g^2\left(\omega^2 - v_A^2k_x^2\right) + v_A^4k^2k_x^2\left(\omega^2 - c_s^2k_x^2\right) + \omega^4\left(\omega^2 - c_s^2k^2\right) + \frac{1}{H_B}k_y^2gv_A^2\omega^2 \\ + v_A^2\omega^2\left(2k_x^2k^2c_s^2 - k_x^2\omega^2 - k^2\omega^2\right)\end{array}}{\left(\omega^2 - v_A^2k_x^2\right)\left(c_s^2 + v_A^2\right)\left(\omega^2 - c_T^2k_x^2\right)}. \tag{5.124}$$

Γ is the magnetically modified adiabatic index,

$$\Gamma = \frac{2c_s^2\gamma}{2c_s^2 + \gamma v_A^2}, \quad H_B = \frac{c_s^2}{\Gamma g}. \tag{5.125}$$

This is the generalisation of Equation (5.9) to the case of non-zero horizontal wavenumber. It reduces to the equation used by Campbell & Roberts (1989) when $k_y = 0$. The plane wave solution, *i.e.* in terms of complex exponential functions, has been given previously by *e.g.* Yu (1965), Campbell & Roberts (1989) and Pintér & Erdélyi (2011),

$$\xi_z \propto \exp\left(\frac{z}{2H_B}\left[1 \pm \mathrm{i}\left(4H_B^2A - 1\right)^{\frac{1}{2}}\right]\right). \tag{5.126}$$

Selecting the out-going wave, the solution in the upper layer is

$$\xi_z = D_1\exp\left(\left[\frac{1}{2H_B} + \mathrm{i}\kappa\right]z\right), \quad \kappa = \frac{1}{2H_B}\left(4H_B^2A - 1\right)^{\frac{1}{2}}. \tag{5.127}$$

In the lower layer we may show, via some algebra on the governing equations, that

$$\xi_{zi} = \frac{\omega\mathrm{i}}{\left(g^2k^2 - \omega^4\right)}\left[c_s^2\frac{\mathrm{d}\Delta}{\mathrm{d}z} - g\left(\gamma - \frac{c_s^2k^2}{\omega^2}\right)\Delta\right], \tag{5.128}$$

$$\delta p_i = -\frac{\mathrm{i}\rho_0c_s^2}{\omega}\Delta. \tag{5.129}$$

In the upper layer

$$\delta P_{Te} = \left(\frac{A_1}{A_2} - g\rho_0\right)\xi_z - \frac{D}{A_2}\frac{\mathrm{d}\xi_z}{\mathrm{d}z}. \tag{5.130}$$

for the case of $k_y = 0$ these quantities reduce to the boundary conditions used by Campbell & Roberts (1989) and Pintér & Erdélyi (2011). The coefficients for the driven problem,

which may be determined by applying the appropriate boundary conditions, are

$$D_1 = \frac{2\widehat{\rho_i}\widehat{c_{si}^2}H_B A_{20}\left(g^2k^2-\omega^4\right)I(\omega)\left[Q_0 M(a,b,\alpha_0)+P_0 U(a,b,\alpha_0)\right]e^{-kL}}{\begin{array}{r}2\widehat{\rho_i}\widehat{c_{si}^2}H_B A_{20}\left(g^2k^2-\omega^4\right)\left[Q_{-L}M(a,b,\alpha_0)+P_{-L}U(a,b,\alpha_0)\right]+\\ \omega^2\left(D_0-2A_{10}H_B+2g\widehat{\rho_e}H_B A_{20}+2\mathrm{i}H_B D_0\kappa\right)\left(P_{-L}Q_0-P_0Q_{-L}\right)\end{array}}, \tag{5.131}$$

$$C_1 = \frac{\begin{array}{r}\mathrm{i}[\omega^2\left(2A_{10}H_B-D_0-2A_{20}H_B g\widehat{\rho_e}-2\mathrm{i}D_0H_B\kappa\right)Q_0+\\ 2A_{20}\widehat{c_{si}^2}\widehat{\rho_i}H_B\left(\omega^4-g^2k^2\right)U(a,b,\alpha_0)]D_1\end{array}}{2\omega A_{20}H_B\widehat{c_{si}^2}\widehat{\rho_i}\left[Q_0M(a,b,\alpha_0)+P_0U(a,b,\alpha_0)\right]}, \tag{5.132}$$

$$C_2 = \frac{\begin{array}{r}\mathrm{i}[\omega^2\left(2A_{10}H_B-D_0-2A_{20}H_B g\widehat{\rho_e}-2\mathrm{i}D_0H_B\kappa\right)P_0+\\ 2A_{20}\widehat{c_{si}^2}\widehat{\rho_i}H_B\left(g^2k^2-\omega^4\right)M(a,b,\alpha_0)]D_1\end{array}}{2\omega A_{20}H_B\widehat{c_{si}^2}\widehat{\rho_i}\left[Q_0M(a,b,\alpha_0)+P_0U(a,b,\alpha_0)\right]}, \tag{5.133}$$

where P_0, P_{-L}, Q_0, Q_{-L} are as in the previous section; and

$$D_0 = \widehat{\rho_e}\left(c_{se}^2+\widehat{v_{Ae}^2}\right)\left(\omega^2-\widehat{c_{Te}^2}k_x^2\right)\left(\omega^2-\widehat{v_{Ae}^2}k_x^2\right), \tag{5.134}$$

$$A_{10} = g\widehat{\rho_e}\omega^2\left(\omega^2-\widehat{v_{Ae}^2}k_x^2\right), \tag{5.135}$$

$$A_{20} = \omega^4-\left(c_{se}^2+\widehat{v_{Ae}^2}\right)\left(\omega^2-\widehat{c_{Te}^2}k_x^2\right)k^2. \tag{5.136}$$

Let us simplify the expression for D_1. Using the expression for Q_0 and P_0, the numerator is

$$\mathrm{Num}\,D_1 = -2kA_{20}\widehat{\rho_i}I(\omega)e^{-kL}\left(g^2k^2-\omega^4\right)W\left(M(a,b,\alpha_0),U(a,b,\alpha_0)\right), \tag{5.137}$$

and the denominator is

$$\begin{aligned}\mathrm{Denom}\,D_1 = &\left\{A_{20}\widehat{\rho_i}\left(g^2k^2-\omega^4\right)+\left(k\omega^2+\frac{\omega^2}{H_i}-gk^2\right)\left(A_{20}g\widehat{\rho_e}+\mathrm{i}D_0\kappa-A_{10}+\frac{D_0}{2H_B}\right)\right\}\times\\ &\left\{2k\left(1+\frac{L}{z_0}\right)\left[M'(\alpha_{-L})U(\alpha_0)-M(\alpha_0)U'(\alpha_{-L})\right]+\right.\\ &\left.\left(\left(1+\frac{L}{z_0}\right)k+\frac{1}{H_i}-\frac{gk^2}{\omega^2}\left(1+\frac{L}{z_0}\right)\right)\left[M(\alpha_0)U(\alpha_{-L})-M(\alpha_{-L})U(\alpha_0)\right]\right\}\\ &-2k\omega^2\left(A_{20}g\widehat{\rho_e}+\mathrm{i}D_0\kappa-A_{10}+\frac{D_0}{2H_B}\right)\left\{2k\left(1+\frac{L}{z_0}\right)\left[M'(\alpha_{-L})U'(\alpha_0)-M'(\alpha_0)U'(\alpha_{-L})\right]\right.\\ &\left.+\left(\left(1+\frac{L}{z_0}\right)k+\frac{1}{H_i}-\frac{gk^2}{\omega^2}\left(1+\frac{L}{z_0}\right)\right)\left[M'(\alpha_0)U(\alpha_{-L})-M(\alpha_{-L})U'(\alpha_0)\right]\right\}.\end{aligned} \tag{5.138}$$

Investigating the resonant frequencies is difficult due to the complexity of Equation (5.138), although analytical progress may be made with some simplification. Let us make the long wavelength approximation, $kL \ll 1$, as in the hydrodynamic case. The Taylor

expansions and so the simplified expressions for terms including the Kummer functions *e.g.* $M'(a,b,\alpha_0)U(a,b,\alpha_{-L}) - M(a,b,\alpha_{-L})U'(a,b,\alpha_0)$ were given previously in Section 4.3. To simplify the expression, enough such that analytical progress may be made, we assume that the wavelength is much smaller than other length scales in the problem. That is, in addition to the assumption of $kL \ll 1$ we also assume

$$kH_i \ll 1, \quad \text{and} \quad kH_B \ll 1. \tag{5.139}$$

The assumption that $kH_B \ll 1$ implies that in addition to kH_e being small, the term $kv_A^2/2g \ll 1$. While simplifying D_1, we shall also make the assumption $L/z_0 \ll 1$. As previously stated, the assumption of a thin lower layer is made not just to simplify the result but for the purposes of comparison to previous problems. Applying these assumptions, some algebra leads to

$$D_1 \approx \frac{\left(c_{se}^2 + v_A^2 - 1\right)\widehat{\rho_i} I(\omega) H_B (1 - kL)}{\widehat{\rho_i} H_B (kL - 1) + \frac{L\widehat{\rho_e}}{\widehat{c_{si}^2}}\left(c_{se}^2 + v_A^2\right)\left(\frac{1}{2} + \mathrm{i}\kappa H_B\right)}, \tag{5.140}$$

where, when we drive below the cut-off frequency

$$H_B\kappa = \frac{\mathrm{i}}{2}\left(1 - 4H_B^2 A\right)^{\frac{1}{2}}, \tag{5.141}$$

and

$$H_B^2 A \approx \frac{\omega^6 H_B^2 + H_B k_y^2 g v_A^2 \omega^2}{\left(\omega^2 - v_A^2 k_x^2\right)\left(c_s^2 + v_A^2\right)\left(\omega^2 - c_T^2 k_x^2\right)}. \tag{5.142}$$

The waves are resonantly amplified when Denom $D_1 = 0$. Substituting the expression for κ into the simplified denominator of D_1 gives us, after some manipulation and keeping only small terms to first order, the polynomial

$$\widehat{\rho_e}^2\left(c_{se}^2 + v_A^2\right) H_B L^2 \omega^6 + \widehat{\rho_i}\widehat{c_{si}^2}\left[\widehat{\rho_i}\widehat{c_{si}^2} H_B (1 - 2kL) + \widehat{\rho_e} L\left(c_{se}^2 + v_A^2\right)(kL - 1)\right]\omega^4 +$$
$$\widehat{\rho_i}\widehat{c_{si}^2} k_x^2\left(c_T^2 + v_A^2\right)\left[\widehat{\rho_e}\left(c_{se}^2 + v_A^2\right)L - \widehat{\rho_i}\widehat{c_{si}^2} H_B\right]\omega^2 + \widehat{\rho_i}\widehat{c_{si}^2} v_A^2 c_T^2 k_x^4\left[\widehat{\rho_i}\widehat{c_{si}^2} H_B - \widehat{\rho_e}\left(c_{se}^2 + v_A^2\right)L\right] = 0. \tag{5.143}$$

Solving Equation (5.143) gives the the resonant frequency for the case of $k \neq 0$, and a constant Alfvén speed in the upper layer. Let us note some limits of Equation (5.143). In the limit $v_A \to 0$, Equation (5.143) gives the non-magnetic solution, Equation (4.103), as expected. Taking the limit $k_x \to 0$, gives Equation (5.33). The solution which we now investigate is the generalisation of these previous cases.

Equation (5.143) is cubic in ω^2, hence an explicit solution is given by Cardano's formula. This solution is complicated, so for simplicity let us try a perturbation series

approach based on the small parameter kL. Let us assume a solution of the form

$$\omega^2 = \omega_0^2 + kL\omega_1^2 + O\left(k^2L^2\right). \tag{5.144}$$

As Equation (5.143) neglected terms of higher order than kL, we may only go as far as $O(kL)$ in the perturbation series. Substituting the expression for ω^2 into Equation (5.143),

$$\begin{aligned}\widehat{\rho_e^2}\left(c_{se}^2+v_A^2\right)H_BL^2\omega_0^4\left(\omega_0^2+3kL\omega_1^2\right)+\widehat{\rho_i c_{si}^2}\Big[\widehat{\rho_i c_{si}^2}H_B(1-2kL)+\\ \widehat{\rho}_eL\left(c_{se}^2+v_A^2\right)(kL-1)\Big]\omega_0^2\left(\omega_0^2+2kL\omega_1^2\right)+\widehat{\rho_i c_{si}^2}k_x^2\left(c_T^2+v_A^2\right)\Big[\widehat{\rho}_e\left(c_{se}^2+v_A^2\right)L-\\ \widehat{\rho_i c_{si}^2}H_B\Big]\left(\omega_0^2+\omega_1^2\right)+\widehat{\rho_i c_{si}^2}v_A^2c_T^2k_x^4\left[\widehat{\rho_i c_{si}^2}H_B-\widehat{\rho}_e\left(c_{se}^2+v_A^2\right)L\right]+O\left(k^2L^2\right)=0,\end{aligned} \tag{5.145}$$

where we have made use of the fact that

$$\omega^6 = \left(\omega_0 + kL\omega_1^2 + O\left(k^2L^2\right)\right)^3 = \omega_0^6 + 3kL\omega_0^4\omega_1^2 + O\left(k^2L^2\right), \tag{5.146}$$

$$\omega^4 = \left(\omega_0 + kL\omega_1^2 + O\left(k^2L^2\right)\right)^2 = \omega_0^4 + 2kL\omega_0^2\omega_1^2 + O\left(k^2L^2\right). \tag{5.147}$$

Keeping only terms $O\left(k^0L^0\right)$, gives

$$\widehat{\rho_e^2}\left(c_{se}^2+v_A^2\right)H_BL^2\omega_0^6+\widehat{\rho_i c_{si}^2}\left[\widehat{\rho_i c_{si}^2}H_B-\widehat{\rho}_eL\left(c_{se}^2+v_A^2\right)\right]\omega_0^4=0. \tag{5.148}$$

The zero-th order solution is then

$$\omega_0^2 = \frac{\widehat{\rho_i^2 c_{si}^2}}{\widehat{\rho_e^2}L^2}\left[\frac{L\widehat{\rho}_e}{H_B\widehat{\rho}_i} - \frac{\widehat{c_{si}^2}}{c_{se}^2+v_A^2}\right]. \tag{5.149}$$

This is, as we should expect, the solution given by Equation (5.33) for the case of $k = 0$. To determine the correction due to a non-zero horizontal wavenumber, let us simplify Equation (5.145) by keeping terms of order $O(kL)$,

$$\begin{aligned}\widehat{\rho_e^2}\left(c_{se}^2+v_A^2\right)H_BL^2\omega_0^4\left(\omega_0^2+3kL\omega_1^2\right)+\widehat{\rho_i^2 c_{si}^4}H_B\omega_0^2\left(\omega_0^2-2kL\omega_0^2+2kL\omega_1^2\right)\\ +\widehat{\rho_i\rho_e c_{si}^2}L\left(c_{se}^2+v_A^2\right)L\omega^2\left(kL\omega_0^2-\omega_0^2-2kL\omega_1^2\right)=0.\end{aligned} \tag{5.150}$$

Let us substitute the solution for ω_0^2 into Equation (5.145). After some algebra, it is simple to show that

$$\omega_1^2 = \frac{\widehat{\rho_i^2 c_{si}^2}}{\widehat{\rho_e^2}L^2}\left[\frac{2\widehat{c_{si}^2}}{c_{se}^2+v_A^2} - \frac{L\widehat{\rho}_e}{H_B\widehat{\rho}_i}\right]. \tag{5.151}$$

The asymptotic solution for ω^2 is

$$\omega^2 \approx \omega_0^2 + kL\omega_1^2 = \frac{\widehat{\rho_i^2}\widehat{c_{si}^2}}{\widehat{\rho_e^2}L^2}\left[\frac{L\widehat{\rho_e}}{H_B\widehat{\rho_i}}(1-kL) + \frac{\widehat{c_{si}^2}}{c_{se}^2+v_A^2}(2kL-1)\right] \tag{5.152}$$

$$= \left(1+\frac{\gamma v_A^2}{2c_{se}^2}\right)^2 \frac{c_{se}^4}{L^2}\left[\frac{L}{H_B}\left(c_{se}^2+\frac{\gamma v_A^2}{2}\right)^{-1}(1-kL) + \frac{2kL-1}{c_{se}^2+v_A^2}\right]. \tag{5.153}$$

This is the acoustic global resonance with the combined effects of a non-zero horizontal wavenumber and a magnetic field in the upper layer. In the limit of $v_A \to 0$,

$$\omega^2 = \frac{c_s^2}{L^2}\left[\frac{L}{H_e}(1-kL) + 2kL - 1\right]. \tag{5.154}$$

The effect of oblique wave propagation on the frequency in the MHD case is the same as on the hydrodynamic case.

The condition for the global resonance to exist is that the term in the square brackets is positive (so $\omega^2 > 0$), this condition is expressed as

$$\frac{L\widehat{\rho_e}}{H_B\widehat{\rho_i}} > \frac{\widehat{c_{si}^2}}{c_{se}^2+v_A^2}\frac{1-2kL}{1-kL} \approx \frac{\widehat{c_{si}^2}}{c_{se}^2+v_A^2}(1-kL). \tag{5.155}$$

The condition may be rewritten as

$$\frac{L}{H_e} > \frac{\left(1+\dfrac{\gamma v_A^2}{2c_{se}^2}\right)^2(1-2kL)}{\left(1+\dfrac{v_A^2}{c_{se}^2}\right)(1-kL)} \approx \frac{\left(1+\dfrac{\gamma v_A^2}{2c_{se}^2}\right)^2}{\left(1+\dfrac{v_A^2}{c_{se}^2}\right)}[1-kL]. \tag{5.156}$$

The disadvantage to using a perturbation series is a possible loss of regularity in the solution. There is a breakdown when $|\omega_0^2/kL\omega_1^2|$ is $O(1)$, or

$$\left|\frac{\dfrac{L\widehat{\rho_e}}{H_B\widehat{\rho_i}} - \dfrac{\widehat{c_{si}^2}}{c_{se}^2+v_A^2}}{\dfrac{2\widehat{c_{si}^2}}{c_{se}^2+v_A^2} - \dfrac{L\widehat{\rho_e}}{H_B\widehat{\rho_i}}}\right| = \left|\frac{L\left(1+\dfrac{v_A^2}{c_{se}^2}\right) - H_e\left(1+\dfrac{\gamma v_A^2}{2c_{se}^2}\right)^2}{2H_e\left(1+\dfrac{\gamma v_A^2}{2c_{se}^2}\right)^2 - L\left(1+\dfrac{v_A^2}{c_{se}^2}\right)}\right| = O(kL). \tag{5.157}$$

The condition for the solution to be valid can be expressed as

$$\left|\frac{L\left(1+\dfrac{v_A^2}{c_{se}^2}\right) - H_e\left(1+\dfrac{\gamma v_A^2}{2c_{se}^2}\right)^2}{2H_e\left(1+\dfrac{\gamma v_A^2}{2c_{se}^2}\right)^2 - L\left(1+\dfrac{v_A^2}{c_{se}^2}\right)}\right| \gg kL, \tag{5.158}$$

so $|\omega_0| \gg kL|\omega_1|$, solving this inequality shows that the solution is valid when

$$\frac{L}{H_e} \gg \frac{\left(1+\frac{\gamma v_A^2}{2c_{se}^2}\right)^2}{\left(1+\frac{v_A^2}{c_{se}^2}\right)} \frac{1+kL-2k^2L^2}{1-k^2L^2} \approx \frac{\left(1+\frac{\gamma v_A^2}{2c_{se}^2}\right)^2}{\left(1+\frac{v_A^2}{c_{se}^2}\right)} [1+kL], \tag{5.159}$$

or

$$\frac{L}{H_e} \ll \frac{\left(1+\frac{\gamma v_A^2}{2c_{se}^2}\right)^2}{\left(1+\frac{v_A^2}{c_{se}^2}\right)} \frac{1-kL-2k^2L^2}{1-k^2L^2} \approx \frac{\left(1+\frac{\gamma v_A^2}{2c_{se}^2}\right)^2}{\left(1+\frac{v_A^2}{c_{se}^2}\right)} [1-kL]. \tag{5.160}$$

The second of these inequalities contradicts the condition of $\omega^2 > 0$, Equation (5.156). There is a problem if the inequality (5.156) is satisfied but inequality (5.159) is not satisfied. That is, L/H_e is greater than the right hand side of inequality (5.156), but is the same order as the right hand side of inequality (5.159). When this is the case, the more complicated solution given by Cardano's formula should be used.

Letting $v_A^2/c_{se}^2 = \epsilon$, the resonant frequency may be written

$$\omega = \frac{c_{se}}{L}\left[\frac{L}{H_e}(1-kL) + (2kL-1)\frac{\left(1+\frac{\gamma}{2}\epsilon\right)^2}{1+\epsilon}\right]^{\frac{1}{2}}. \tag{5.161}$$

For the case of high-β plasma, $\epsilon \ll 1$ and so the resonant frequency may be approximated by

$$\omega = \frac{c_{se}}{L}\left[\frac{L}{H_e}(1-kL) + 2kL - 1 - (\gamma-1)\epsilon\right]^{\frac{1}{2}}, \tag{5.162}$$

where we have kept first order terms in the expression for ω^2 (note that terms in $kL\epsilon$ have also been neglected). For a fixed kL we see that a weak magnetic field will decrease the resonant frequency as in the case of $kL = 0$. We do not make the strong field assumption as $H_B = H_e(1+\gamma\epsilon/2)$. Hence making the assumptions $kH_e \ll 1$ and $\epsilon \gg 1$ means that there may be terms in $kH_e\epsilon$, that should not be neglected, missing from the simplified expression. The condition for the perturbation series solution to be valid can be approximated, when $\epsilon \ll 1$, by

$$\frac{L}{H_e} \gg 1 + kL + (\gamma-1)\epsilon. \tag{5.163}$$

The resonant frequency is plotted in Figure 5.4 for varying values of v_A^2/c_s^2. It is clear, as in the $k_\perp \neq 0$, that as the magnetic field strength increases the resonant frequency fall and eventually ceases to occur. The effect of non-vertical wave propagation is to decrease the rate at which the resonant frequency falls, with increasing magnetic field.

We also see in Figure 5.4 that there is some critical value of v_A^2/c_s^2 where the resonant frequency does not depend on kL. Below this critical value the values of the resonant

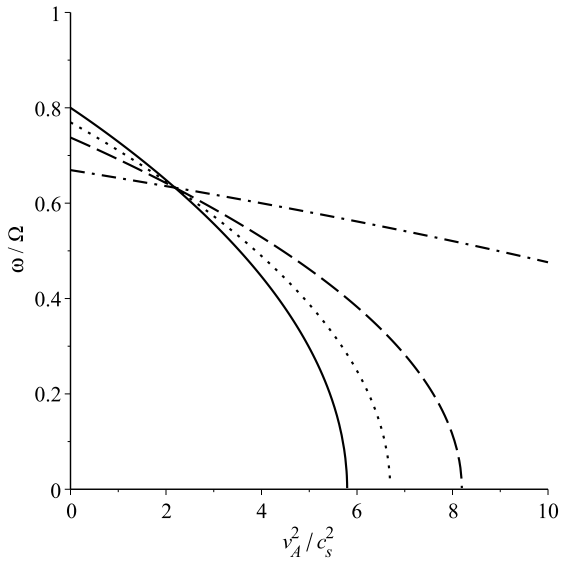

Fig. 5.4 A plot of the resonant frequencies (5.161), normalised to the *hydrodynamic* acoustic cut-off frequency $c_{se}/2H_e$, for varying values of v_A^2/c_{se}^2. The solid line represents $kL = 0$, the dotted line is $kL = 0.1$, the dashed line is $kL = 0.2$, the dot-dash line is $kL = 0.4$. The other parameters take the values $L/H_e = 5$, $\gamma = 5/3$.

frequency are below the case of $kL = 0$, whereas above this value they are greater. We may find this value analytically as follows. We solve

$$\frac{\partial}{\partial(kL)}\frac{\omega}{\Omega} = 0 \implies -\frac{L}{H_e} + \frac{2\left(1+\frac{\gamma v_A^2}{2}\right)^2}{1+\frac{v_A^2}{c_s^2}} = 0, \tag{5.164}$$

or

$$\frac{v_A^2}{c_s^2} = \frac{L}{\gamma^2 H_e} - \frac{2}{\gamma} + \frac{1}{\gamma^2}\left[\frac{L^2}{H_e^2} + \frac{2\gamma L}{H_e}(\gamma-2)\right]^{\frac{1}{2}}. \tag{5.165}$$

For the values $L/H_e = 5, \gamma = 5/3$, used in Figure 5.4, this value is $3(1+\sqrt{7})/5 \approx 2.19$.

It was previously noted that the assumption of a strong magnetic field may be inconsistent with the small wavenumber approximation. This is due to terms which were neglected in the small wavenumber approximation may no longer be considered small and so should be retained. We shall now investigate the effect of a strong magnetic field. Let us start from the assumption of a strong magnetic field hence the plasma in the upper layer is in the low-β regime, $\beta \ll 1$. Making this assumption, before any assumptions about the wavelength, will allow us to see the effect of a strong magnetic field without losing terms which may be important. Using the fact that

$$\widehat{\rho_i} = \frac{c_{se}^2}{\widehat{c_{si}^2}}\left(1+\frac{1}{\beta}\right)\widehat{\rho_e}, \quad H_B = H_e\left(1+\frac{1}{\beta}\right), \tag{5.166}$$

D_1 may be written

$$\mathrm{Num}\, D_1 = -2kA_{20}\frac{c_{se}^2}{\widetilde{c}_{si}^2} I(\omega) e^{-kL}\left(g^2k^2-\omega^4\right)H_i^2 H_e^2 W(M_0,U_0)), \tag{5.167}$$

$$\begin{aligned}\mathrm{Denom}\, D_1 = &\left\{A_{20}\frac{c_{se}^2}{\widetilde{c}_{si}^2}\left(g^2k^2-\omega^4\right)H_iH_e+\left(kH_i\omega^2+\omega^2-gk^2H_i\right)\left(1+\frac{1}{\beta}\right)^{-1}\left(A_{20}gH_e\right.\right.\\ &\left.\left.-\frac{A_{10}}{\widetilde{\rho}_e}H_e+\frac{D_0}{\widetilde{\rho}_e}\left(1+\frac{1}{\beta}\right)^{-1}\left(\frac{1}{2}+\mathrm{i}\kappa H_B\right)\right)\right\}\left\{2kH_i\left(1+\frac{L}{z_0}\right)\left[M'_{-L}U_0-M_0U'_{-L}\right]\right.\\ &\left.+\left(\left(1+\frac{L}{z_0}\right)kH_i+1-\frac{gk^2H_i}{\omega^2}\left(1+\frac{L}{z_0}\right)\right)\left[M_0U_{-L}-M_{-L}U_0\right]\right\}\\ &-2kH_i\omega^2\left(1+\frac{1}{\beta}\right)^{-1}\left(A_{20}gH_e-\frac{A_{10}}{\widetilde{\rho}_e}H_e+\frac{D_0}{\widetilde{\rho}_e}\left(1+\frac{1}{\beta}\right)^{-1}\left(\frac{1}{2}+\mathrm{i}\kappa H_B\right)\right)\left\{2kH_i\left(1+\frac{L}{z_0}\right)\times\right.\\ &\left.\left[M'_{-L}U'_0-M'_0U'_{-L}\right]+\left(\left(1+\frac{L}{z_0}\right)kH_i+1-\frac{gk^2H_i}{\omega^2}\left(1+\frac{L}{z_0}\right)\right)\left[M'_0U_{-L}-M_{-L}U'_0\right]\right\},\end{aligned} \tag{5.168}$$

where we use the shorthand notation $M_0 = M(a,b,\alpha_0), M_{-L} = M(a,b,\alpha_{-L})$ etc. Under the assumption $\beta \ll 1$, we apply the expansions

$$\left(1+\frac{1}{\beta}\right)^{-1} \approx \beta-\beta^2+\ldots, \quad \left(1+\frac{1}{\beta}\right)^{-2} \approx \beta^2-2\beta^3+\ldots. \tag{5.169}$$

We keep only terms to first order in β, and making note of the fact that

$$\begin{aligned}\beta^2 H_{B\kappa} = \frac{\mathrm{i}}{2}\beta^2\left(1-4H_e^2\left(1+\frac{1}{\beta}\right)A\right)^{\frac{1}{2}} &= \frac{\mathrm{i}}{2}\left(\beta^4-4H_e\left(\beta^4+2\beta^3+\beta^2\right)A\right)^{\frac{1}{2}}\\ &\approx \frac{\mathrm{i}}{2}\left(-4H_e^2\beta^2A\right)^{\frac{1}{2}} = \mathrm{i}\beta\left(-H_e^2A\right)^{\frac{1}{2}},\end{aligned} \tag{5.170}$$

the denominator of D_1 may be simplified somewhat (not stated for simplicity). It may be shown that for any possible resonance $H_e^2A \le 0$. Next, we simplify further by applying the long wavelength approximation as above ($kL, kH_i, kH_e \ll 1$), where terms in, *e.g.*, βkL are considered second order small and neglected. D_1 may be approximated

$$\mathrm{Num}\, D_1 \approx \frac{c_{se}^2}{\widetilde{c}_{si}^2} I(\omega)(1-kL)H_i^2H_e\omega^2, \tag{5.171}$$

$$\begin{aligned}\mathrm{Denom}\, D_1 \approx &-\frac{c_{se}^2}{\widetilde{c}_{si}^2}\omega^2H_iH_e\left[kH_iL\left(1+\frac{L}{z_0}\right)-H_i+\frac{L^2}{z_0}\left(1+\frac{H_i}{z_0}\right)\right]\\ &+\beta\left(c_{se}^2+v_A^2\right)\left(-H_e^2A\right)^{\frac{1}{2}}\left[\frac{\omega^2LH_i}{\widetilde{c}_{si}^2}\left(1+\frac{L}{z_0}\right)-\frac{L^2}{z_0}\left(1+\frac{H_i}{z_0}\right)\right],\end{aligned} \tag{5.172}$$

where

$$H_e^2 A \approx \frac{H_e^2 \omega^6}{\left(\omega^2 - v_A^2 k_x^2\right)\left(c_{se}^2 + v_A^2\right)\left(\omega^2 - c_T^2 k_x^2\right)}. \tag{5.173}$$

For a resonance to occur $H_e^2 A < 0$, and so $c_T^2 k_x^2 < \omega^2 < v_A^2 k_x^2$ which may be approximated by $c_{se}^2 k_x^2 < \omega^2 < v_A^2 k_x^2$. That is, the waves are driven below the local frequency of fast MHD waves. If we also assume the layer is thin, $L/z_0 \ll 1$, again as above, and attempt to locate the fundamental resonant frequency *i.e.* Denom $D_1 = 0$,

$$-c_{se}^2 H_i (kL - 1)\left(v_A^2 k_x^2 - \omega^2\right)^{\frac{1}{2}}\left(\omega^2 - c_T^2 k_x^2\right)^{\frac{1}{2}} + \beta\left(c_{se}^2 + v_A^2\right)^{\frac{1}{2}} \omega^3 L = 0. \tag{5.174}$$

This may be simplified to

$$c_{se}^4 H_i^2 \omega^4 (1 - 2kL) = 0, \tag{5.175}$$

hence there is no global resonance when the magnetic field is sufficiently strong. This behaviour was seen for the case of $k_\perp = 0$ where the resonant frequency ceased to occur when β became small.

Let us now consider the case of large horizontal wavelength; we study this problem numerically. We begin by studying the effect of a weak magnetic field. The roots of Equation (5.138) are plotted in Figure 5.5 for the parameter $\widehat{v}_A/c_s$ varying from 0 to 0.5. The other parameters are as in the hydrodynamic case, Figure 4.4. The value of kH is fixed at 2 (note that $k_y = 0$ for simplicity). When the Alfvén speed is equal to zero the three solutions are those in the hydrodynamic case. We increase the Alfvén speed from 0, due to the computational complexity of solving Equation (5.138) numerically we choose to use 26 points for $\widehat{v}_A/c_s$ (including 1 point for the field free case), more points will make the curves appear solid, although some information in available using only this, relatively low, number of points.

It is clear that there are three types of resonant solutions. The hydrodynamic solutions are the p-modes, the g-modes do not exist for the value of kH used. As the magnetic field increases, these modes are the p-type fast modes. The frequency increases very slowly, with increasing magnetic field strength. This is, as in the hydrodynamic case, in contrast to the near-vertical propagation properties. When non-vertical propagation is included the resonance may exist above the modified cut-off. Increasing the magnetic field does not cause the resonance to stop. This is, again, due to the difference in the lower cut-off of fast modes for vertical and non-vertical wave propagation. For a discussion on the cut-off frequency of fast MHD modes in an isothermal atmosphere see *e.g.* Stark & Musielak (1993).

The lowest frequency modes are the g-type slow modes. The effect of increasing the magnetic field strength is that these modes may exist, where they would not exist in the hydrodynamic limit. Increasing the Alfvén speed increases the cut-off frequency, and so more modes may exist. It seems to be the case that the cut-off tends to Ω_B as $\widehat{v}_A$ increases.

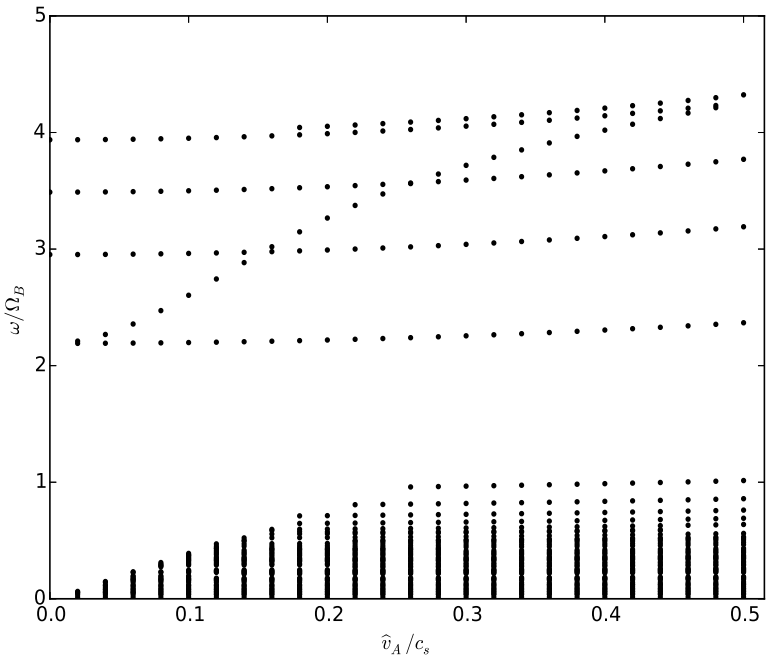

Fig. 5.5 A plot of the numerical resonant frequencies, normalised to the modified cut-off frequency, for varying values of $\widehat{v}_A/c_s$.

The behaviour of these modes is unclear due to the fact there are many modes below $\Omega_B = 1$.

The third solution is the mode which increase with $\widehat{v}_A/c_s$ through the same frequency range as the p-modes. It is unclear what this solution is exactly. It is not present in the hydrodynamic model which leads us to conjecture that it is either magnetic in nature or a surface mode caused by the density discontinuity. As the magnetic field increases the frequency of this mode meets the fast modes, possibly in avoided crossings. The mode is not present for $\widehat{v}_A = 0$, although it exists for the first non-zero value of the Alfvén speed. The absence of this solution (and the lowest fast mode solution) in the hydrodynamic limit, suggests it is present due to the magnetic field. When the magnetic field is non-zero there must be a discontinuity in the background density to maintain a pressure balance. The presence of a discontinuity may lead to the existence of surface modes.

It may also be the case that this mode is purely magnetic in nature, rather than a surface mode. If so, this mode may be described as a magnetic slow mode (as opposed to a g-type slow mode). The points where this mode meets the fast modes may be sites of mode conversion.

We may investigate the effect of a more significant magnetic field by plotting the full spectrum of modes, varying kH. These are plotted in Figures 5.6 and 5.7 for the case of $v_A/\widehat{c_s} = 0.1$ and 1, respectively. As in the hydrodynamic case, resonant frequencies may exist well above the acoustic cut-off frequency. It can be shown that for stronger magnetic fields, a huge number of modes may exist. Note that the modes shown are for

an adiabatically stratified polytrope. When this is the case, there are no effects due to buoyancy in the lower polytropic layer. The polytrope is adiabatically stratified when the temperature variation is such that $\gamma = 1 + 1/m$, so $m = 3/2$ when $\gamma = 5/3$. To account for this the temperature scale height z_0 must be equal to $5H/2$, where H is evaluated at $z = 0$. The motivation for removing the effects of buoyancy is for numerical simplicity. As seen in Figure 5.5, there are a large number of resonant g-modes the frequencies of which are located close together. This presents a significant problem for a numerical analysis in terms of finding these roots, without skipping over roots, and the speed of the algorithm.

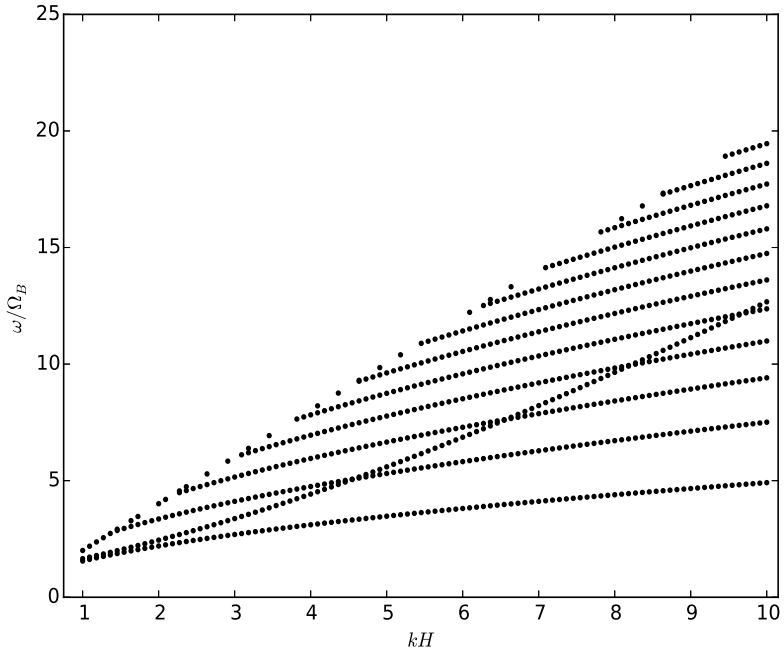

Fig. 5.6 A plot of the numerical resonant frequencies when $v_A/c_s = 0.1$ and $N_0 = 0$, normalised to the modified cut-off frequency, for varying values of kH.

5.3.1 Boussinesq Approximation

Let us apply the Boussinesq approximation in order to study internal gravity waves. In the non-magnetic lower layer, the governing equation was derived previously. The solution, for a slowly varying background, is given by

$$q = C_1 \mathrm{Ai}(\Theta) + C_2 \mathrm{Bi}(\Theta), \tag{5.176}$$

where

$$\Theta = -\frac{1}{N_0^2}\left(\frac{k_\perp^2 N_0^2}{\omega^2 z_0}\right)^{\frac{1}{3}}\left(N_0^2(z+z_0) - \omega^2 z_0\right). \tag{5.177}$$

Note that $k_y \neq 0$, and $k_\perp^2 = k_x^2 + k_y^2$.

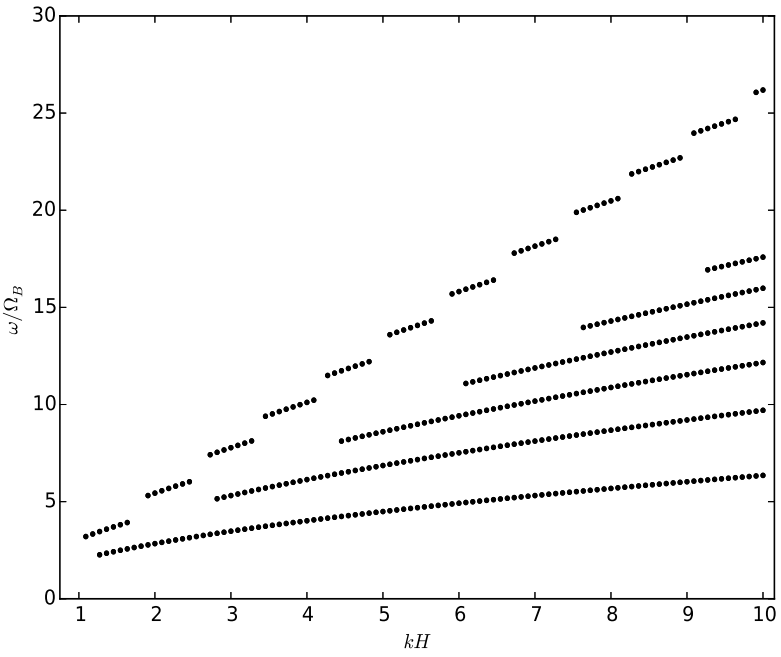

Fig. 5.7 A plot of the numerical resonant frequencies when $v_A/c_s = 1$ and $N_0 = 0$, normalised to the modified cut-off frequency, for varying values of kH.

In the upper layer the solution is

$$\xi_z = D_1 e^{m_+ z} + D_2 e^{m_- z}, \tag{5.178}$$

where

$$m_\pm = \frac{1}{2H_B}\left(\frac{\omega^2}{\omega^2 - v_A^2 k_x^2} + 1\right) \pm \mathrm{i}\left[\frac{k_\perp^2\left(v_A^2 k_x^2 + N^2 - \omega^2\right)}{\omega^2 - v_A^2 k_x^2} - \frac{v_A^4 k_x^4}{4H_B^2\left(\omega^2 - v_A^2 k_x^2\right)^2}\right]^{\frac{1}{2}}. \tag{5.179}$$

Note that N is the magnetically modified Brunt-Väisälä frequency. The modified scale-height is determined by

$$H_B = \frac{c_s^2 + \frac{1}{2}\gamma v_A^2}{g\gamma} \tag{5.180}$$

and so the term

$$\frac{v_A^4 k_x^4}{4H_B^2} \tag{5.181}$$

is $O\left(1/\beta^2\right)$. In applying the Boussinesq approximation we are implicitly assuming a high-β approximation and so the second term in the square root above may be neglected, reducing Equation (5.179) to

$$m_\pm = \frac{1}{2H_B}\left(\frac{\omega^2}{\omega^2 - v_A^2 k_x^2} + 1\right) \pm \mathrm{i}\left[\frac{k_\perp^2 N^2}{\omega^2 - v_A^2 k_x^2} - k_\perp^2\right]^{\frac{1}{2}}. \tag{5.182}$$

When the medium is stable to convection, $N^2 > 0$, the solution is oscillatory when

$$v_A^2 k_x^2 < \omega^2 < k_x^2 v_A^2 + N^2, \tag{5.183}$$

if $\omega^2 < v_A^2 k_x^2$ or $\omega^2 > v_A^2 k_x^2 + N^2$ the solution is evanescent (or develops into an instability). The magnetic field may inhibit convection and so wave propagation may be possible even when $N^2 < 0$. When this is the case the solution oscillates when

$$k_x^2 v_A^2 + N^2 < \omega^2 < v_A^2 k_x^2, \tag{5.184}$$

and decays/becomes unstable when $\omega^2 > v_A^2 k_x^2$ or $\omega^2 < v_A^2 k_x^2 + N^2$.

For outgoing waves or finite energy when the solution is not oscillatory the solution is given by

$$\xi_z = D_1 e^{m_+ z}. \tag{5.185}$$

The boundary conditions to be applied are as in the previous cases with the note that the continuity of Lagrangian pressure takes the form

$$\frac{\mathrm{i}\omega}{k_\perp^2}\frac{\mathrm{d}q_i}{\mathrm{d}z} - \frac{\mathrm{i}g}{\omega}q_i = \frac{\rho_{0e}}{k_\perp^2}\left(\omega^2 - v_A^2 k_x^2\right)\frac{\mathrm{d}\xi_{ze}}{\mathrm{d}z} + \left(\frac{\omega^2}{k_\perp^2}\frac{\mathrm{d}\rho_{0e}}{\mathrm{d}z} - g\rho_{0e}\right)\xi_{ze} \quad \text{at} \quad z = 0. \tag{5.186}$$

The coefficients can be shown to be

$$D_1 = \frac{-\omega^2\Theta_0'\widehat{\rho}_i H_B\left(1+\frac{L}{z_0}\right)^m I(\omega)\, W\left(\mathrm{Ai}(\Theta_0), \mathrm{Bi}(\Theta_0)\right)}{\begin{array}{l}\widehat{\rho}i H_B\omega^2\Theta_0'\left[\mathrm{Ai}'(\Theta_0)\mathrm{Bi}(\Theta_{-L}) - \mathrm{Ai}(\Theta_{-L})\mathrm{Bi}'(\Theta_0)\right] + \left[gH_B k_\perp^2\left(\widehat{\rho}_i - \widehat{\rho}_e\right)\right. \\ \left. + \widehat{\rho}_e m_+ H_B\left(\omega^2 - v_A^2 k_x^2\right) - \widehat{\rho}_e\omega^2\right]\left(\mathrm{Ai}(\Theta_{-L})\mathrm{Bi}(\Theta_0) - \mathrm{Ai}(\Theta_0)\mathrm{Bi}(\Theta_{-L})\right)\end{array}}, \tag{5.187}$$

$$C_1 = \frac{\mathrm{i}\left[\mathrm{Bi}(\Theta_0)\left(gH_B k_\perp^2\left(\widehat{\rho}_i - \widehat{\rho}_e\right) - \widehat{\rho}_e\omega^2 + \widehat{\rho}_e m_+ H_B\left(\omega^2 - v_A^2 k_x^2\right)\right) - \omega^2\Theta_0'\widehat{\rho}_i H_B\mathrm{Bi}(\Theta_0)\right]D_1}{\Theta_0' H_B W\left(\mathrm{Ai}(\Theta_0), \mathrm{Bi}(\Theta_0)\right)}, \tag{5.188}$$

$$C_2 = \frac{\mathrm{i}\left[\mathrm{Ai}(\Theta_0)\left(gH_B k_\perp^2\left(\widehat{\rho}_e - \widehat{\rho}_i\right) + \widehat{\rho}_e\omega^2 - \widehat{\rho}_e m_+ H_B\left(\omega^2 - v_A^2 k_x^2\right)\right) + \omega^2\Theta_0'\widehat{\rho}_i H_B\mathrm{Ai}(\Theta_0)\right]D_1}{\Theta_0' H_B W\left(\mathrm{Ai}(\Theta_0), \mathrm{Bi}(\Theta_0)\right)}. \tag{5.189}$$

Under the same simplifications as the non-magnetic case we may approximate D_1 as

$$D_1 \approx \frac{\omega^2 H_B I(\omega)\left(1+\frac{mL}{z_0}\right)}{\begin{array}{l}H_B\omega^2 - L\left[gH_B k_\perp^2(1-\alpha)\right. \\ \left. + \frac{\alpha}{2}\left(2\omega^2 - v_A^2 k_x^2\right) - \alpha H_B k_\perp\left(1 - \frac{N^2}{\omega^2 - v_A^2 k_x^2}\right)^{\frac{1}{2}}\left(\omega^2 - v_A^2 k_x^2\right) - \alpha\omega^2\right]\end{array}}. \tag{5.190}$$

Assuming continuous sound speed and high-β plasma (in accordance with the Boussinesq approximation), we may assume

$$\alpha = \frac{\widehat{\rho}_{0e}}{\widehat{\rho}_{0i}} = \frac{1}{1 + \frac{\gamma}{2}\frac{v_A^2}{\widehat{c}_s^2}} \approx 1. \tag{5.191}$$

The resonant frequency is then given by

$$\omega^2 = \frac{L\left[LH_B k_\perp^2\left(2v_A^2k_x^2 + N^2\right) - v_A^2k_x^2\right]}{2H_B\left(k_\perp^2L^2 - 1\right)} + \frac{L}{2H_B\left(k_\perp^2L^2-1\right)}\Bigg(\left[v_A^2k_x^2 - LH_Bk_\perp^2\left(2v_A^2k_x^2 + N^2\right)\right]^2 + 4\left(k_\perp^2L^2-1\right)k_x^2v_A^2\left[\frac{v_A^2k_x^2}{4} + H_B^2k_\perp^2\left(N^2 - v_A^2k_x^2\right)\right]\Bigg)^{\frac{1}{2}}. \tag{5.192}$$

The first point to note is that there are two resonant solutions, corresponding to the two roots in the above expression. We have seen that (for $N^2 > 0$) a resonance may occur if $\omega^2 < k_x^2v_A^2$ or $\omega^2 > k_x^2v_A^2 + N^2$, hence there are two regions for which driven waves may become resonant. Physically, this is a consequence of the magnetic field introducing a lower cut-off for magnetic IGWs. In the hydrodynamic limit, the lower root in the above solution reduces to the hydrodynamic IGW solution

$$\omega^2 = \frac{N^2L^2k_x^2}{k_x^2L_x^2 - 1}. \tag{5.193}$$

The upper root returns $\omega^2 = 0$. This corresponds to the lower cut-off reducing to 0, hence this branch of resonant frequencies no longer exist. We may also investigate the frequencies in the limit of large wavenumber. Taking the asymptotic limit $k_xL \to \infty$, it may be shown that Equation (5.192) reduces to

$$\omega^2 \sim k_x^2v_A^2 \tag{5.194}$$

that is, to leading order the resonant frequencies are asymptotic to the Alfvén frequency. We may contrast this to the hydrodynamic case where the resonant frequencies tend to the Brunt-Väisälä frequency. The Brunt-Väisälä frequency is a constant quantity in the upper isothermal layer, whereas the Alfvén frequency varies with wavenumber. Note that we do not lose any solutions in this asymptotic limit; retaining the next term in the series would highlight this fact. To leading order, the solutions corresponding to the upper and lower root each tend to the Alfvén frequency, from above and below, respectively.

5.4 Wave Propagation in a Vertical Magnetic Field

In this section, we investigate the driven boundary in a magnetohydrodynamic setting when the plasma is embedded in a vertical magnetic field. Our aim is to show that the resonance discovered by Taroyan & Erdélyi (2008) still exists for MHD waves in a plasma

embedded in a vertical field and to investigate it analytically. A resonance was investigated numerically by Scheuer & Thomas (1981). It was shown that fast MHD modes may be trapped by varying sound and Alfvén speeds. Fast MHD modes may be thought of as analogous to sound waves and so the resonance here is somewhat different in nature as it occurs at frequencies above the acoustic cut-off in the upper isothermal layer.

A resonance was also discovered by Hollweg (1979). This resonance was an interaction between horizontally propagating fast MHD waves which drive vertical motion along rigid magnetic field lines. The amplitude of the vertically propagating acoustic waves (slow MHD waves in low-β plasma) may become infinite due to the driving fast modes.

The coupled linearised equations for magnetoacoustic-gravity waves, in plasma embedded in a vertical magnetic field, are given by Equations (3.1) and (3.2). Our aim to analyse the global resonance in a two-layer system requires us to have solutions for a polytropic density profile. We limit our analysis to the cases where analytical solutions are available in terms of special functions. The complexity of the linearised MHD equations when a magnetic field is parallel to gravity means that general exact solutions are not available. This requires us to make some simplifications to the governing equations.

We shall take the approach of Roberts (2006) and restrict our attention to slow MAG waves. This firstly, allows us to find analytical solutions and secondly focuses on a different resonance than that of Scheuer & Thomas (1981).

Under the assumption of small horizontal wavelength the governing equation is

$$c_T^2 \frac{\partial^2 \xi_z}{\partial z^2} - g\gamma \frac{c_T^4}{c_s^4} \frac{\partial \xi_z}{\partial z} + \left(\omega^2 - \frac{c_T^2}{v_A^2} \left(N^2 + \frac{g}{H} \frac{c_T^2}{c_s^2} \right) \right) \xi_z = 0. \tag{5.195}$$

Assuming plane waves in the x-direction we can write the partial derivatives instead as ordinary derivatives. Let us first consider the case of low-β plasma, the governing equation under this simplification is

$$c_s^2 \frac{\mathrm{d}^2 \xi_z}{\mathrm{d}z^2} - g\gamma \frac{\mathrm{d}\xi_z}{\mathrm{d}z} + \omega^2 \xi_z = 0. \tag{5.196}$$

This is a description of sound waves propagating vertically along rigid magnetic field lines. This equation can be solved in the same way as the non-magnetic case of Taroyan & Erdélyi (2008). We can therefore state that the resonance exits in an MHD model with a vertical field. The resonant frequencies for slow MHD waves in low-β plasma are the same as those of sound waves in a hydrodynamic model. The magnetic field does not change the resonant frequency, rather the magnetic field acts only as a waveguide.

Let us consider a second case of a vertical magnetic field that also reduces to the same analysis as the non-magnetic case. We make the assumption of long horizontal wavelength, in contrast to the analysis of Roberts (2006). Letting $k_x H \to 0$, Equations (3.1) and (3.2) become

$$v_A^2 \frac{\partial^2 \xi_x}{\partial z^2} + \omega^2 \xi_x = 0, \tag{5.197}$$

$$c_s^2 \frac{\partial^2 \xi_z}{\partial z^2} - g\gamma \frac{\partial \xi_z}{\partial z} + \omega^2 \xi_z = 0. \tag{5.198}$$

The equations have been studied by *e.g.* Ferraro & Plumpton (1958) and Hasan & Christensen-Dalsgaard (1992). The horizontal and vertical displacements are decoupled in this limit. The waves determined by the horizontal and vertical perturbations were labeled A-waves and S-waves, respectively, by Ferraro & Plumpton (1958). In the limit of a weak magnetic field, Hasan & Christensen-Dalsgaard (1992) noted that Equation (5.197) represents magnetic contributions to the slow MAG mode and (5.198) is a sound wave. Equations (5.197) and (5.198) are valid for arbitrary magnetic field strength.

As we have another equation that takes the form of vertically propagating sound waves we, again, have resonance, with no modification due to the magnetic field.

5.4.1 Magnetic IGWs: Slowly Varying Interior

Let us turn our attention to slow magnetoacoustic-gravity waves. We first begin by considering magnetic IGWs, before allowing a more general treatment of slow MAG waves. In order to consider buoyancy-driven motion we make the assumption that the medium consists only of high-β plasma. This approach, as discussed previously, is analogous the applying the Boussinesq approximation. This approximation is, however, not without limitation. In applying the Boussinesq approximation we assume the plasma-β to be large; as the medium is stratified this approximation is not valid for the whole of the atmosphere. We may proceed, despite limitations, with this approach as an approximation to a very weakly stratified layer. That is, the case where the density scale-height is very large. We are interested in primarily magnetic IGWs so we will not include "non-Boussinesq" effects here; this will be relaxed in a following section. The governing equation is

$$v_A^2 \frac{\mathrm{d}^2 \xi_z}{\mathrm{d}z^2} + \left(\omega^2 - N^2\right)\xi_z = 0. \tag{5.199}$$

In the lower layer, the Alfvén speed and the Brunt-Väisälä frequency takes the form

$$v_A^2 = \widehat{v}_A^2 \left(1 - \frac{z}{z_0}\right)^{-m}, \quad N^2 = N_0^2 \left(1 - \frac{z}{z_0}\right)^{-1}, \quad N_0^2 = g\left(\frac{m}{z_0} - \frac{g}{c_{s0}^2}\right). \tag{5.200}$$

It can be shown that the governing equations, when the temperature is considered to vary slowly or rapidly, can be solved in terms of special functions. We first treat the case of slow variation, the solutions of which are given by

$$\xi_z = C_1 \mathrm{Ai}(Q) + C_2 \mathrm{Bi}(Q), \tag{5.201}$$

where

$$Q = \left(\frac{1}{\widehat{v_A^2} z_0}\right)^{1/3} \left(N_0^2 (m-1) - m\omega^2\right)^{-2/3} \left[\omega^2 (mz - z_0) + N_0^2 (z_0 + z(1-m))\right]. \tag{5.202}$$

In the upper, isothermal layer the vertical displacement is given by

$$\xi_z = D_1 J_0(j) + D_2 Y_0(j), \tag{5.203}$$

where

$$j = \frac{2H}{\widehat{v_A}} \left(\omega^2 - N^2\right)^{\frac{1}{2}} e^{-\frac{z}{2H}}. \tag{5.204}$$

In our model the upper layer is semi-infinite. As $z \to \infty$, $j \to 0$. In this limit $J_0 \to 1$ and $Y_0 \to -\infty$. For the solution to remain finite, that is, for the kinetic energy density to remain finite $D_2 = 0$. The solution in the upper layer is then

$$\xi_z = D_1 J_0(j). \tag{5.205}$$

When $\omega < N$, we may write

$$j = \mathrm{i} \frac{2H}{\widehat{v_A}} \left(N^2 - \omega^2\right)^{\frac{1}{2}} e^{-\frac{z}{2H}} \equiv \mathrm{i}\widehat{j}. \tag{5.206}$$

The governing equation may then be written

$$\frac{\mathrm{d}^2 \xi_z}{\mathrm{d}\widehat{j}^2} + \frac{1}{\widehat{j}} \frac{\mathrm{d}\xi_z}{\mathrm{d}\widehat{j}} - \xi_z = 0, \tag{5.207}$$

which has the solution, in terms of modified Bessel functions,

$$\xi_z = D_1 I_0\left(\widehat{j}\right) + D_2 K_0\left(\widehat{j}\right). \tag{5.208}$$

In the limit $\widehat{j} \to 0$ ($z \to \infty$) I_0 remains finite, whereas K_0 becomes infinite. The solution is therefore

$$\xi_z = D_1 I_0\left(\widehat{j}\right). \tag{5.209}$$

This is consistent with Equation (5.205) as $I_0(x) = J_0(ix)$.

Two of the required boundary conditions are as those of Taroyan & Erdélyi (2008),

$$\xi_z = I(\omega) \quad \text{at} \quad z = -L, \tag{5.210}$$

and

$$[[\xi_z]] = 0 \quad \text{at} \quad z = 0, \tag{5.211}$$

where $[[f]]$ denotes the jump in the quantity f. The final boundary condition at the interface is the continuity of the vertical component of the perturbed magnetic field. This is due to

the continuity of Lagrangian pressure being a restatement of the continuity of displacement when the density is continuous (as a consequence of the coordinate stretching used to simplify the governing equations). When the density is discontinuous the continuity of pressure implies a reflecting boundary condition; the singular frequencies are then the eigenvalues of the bottom layer but the resonance does not extend to the upper layer.

The continuity of magnetic field gives the relation

$$\left[\left[\frac{B_0}{c_s^2+v_A^2}\left(c_s^2\frac{\mathrm{d}\xi_z}{\mathrm{d}z}-g\xi_z\right)\right]\right]=0 \quad \text{at} \quad z=0. \tag{5.212}$$

We require the continuity of background pressure to maintain equilibrium, and the continuity of density in order to avoid total reflection at the boundary. This reduces the boundary condition to

$$\left[\left[\frac{\mathrm{d}\xi_z}{\mathrm{d}z}\right]\right]=0 \quad \text{at} \quad z=0. \tag{5.213}$$

Applying these boundary conditions, we may determine the coefficients to be

$$D_1=\frac{-W(\mathrm{Ai}(Q_0),\mathrm{Bi}(Q_0))\,Q'I(\omega)}{\begin{array}{r}Q'J_0(j_0)(\mathrm{Ai}'(Q_0)\mathrm{Bi}(Q_{-L})-\mathrm{Ai}(Q_{-L})\mathrm{Bi}'(Q_0))\\ +j_0'J_1(j_0)(\mathrm{Ai}(Q_0)\mathrm{Bi}(Q_{-L})-\mathrm{Ai}(Q_{-L})\mathrm{Bi}(Q_0))\end{array}}, \tag{5.214}$$

$$C_1=\frac{\left[j_0'\mathrm{Bi}(Q_0)J_1(j_0)+Q'J_0(j_0)\mathrm{Bi}'(Q_0)\right]D_1}{W(\mathrm{Ai}(Q_0),\mathrm{Bi}(Q_0))\,Q'}, \tag{5.215}$$

$$C_2=\frac{-\left[j_0'\mathrm{Ai}(Q_0)J_1(j_0)+Q'J_0(j_0)\mathrm{Ai}'(Q_0)\right]D_1}{W(\mathrm{Ai}(Q_0),\mathrm{Bi}(Q_0))\,Q'}. \tag{5.216}$$

Any singular points of D_1 represent a global resonance as C_1 and C_2 are proportional to D_1. We note that the local (WKB) dispersion relation for slow magnetoacoustic-gravity waves, determined by applying the Boussinesq approximation, is

$$\omega^2=v_A^2k_z^2+\frac{k_x^2}{k_x^2+k_z^2}N^2. \tag{5.217}$$

In the limit of large horizontal wavenumber, the approximation under which the solutions have been derived, this reduces to

$$\omega^2=v_A^2k_z^2+N^2. \tag{5.218}$$

The waves propagate at frequencies above the Brunt-Väisälä frequency. The first thing we can learn from the expression for D_1 is that the global resonance is not limited to the case of evanescent solutions. For the hydrodynamic cases of vertically propagating sound waves and internal gravity waves, or slow waves in a low-β plasma in a vertical magnetic field the resonance exists below the cut-off frequency in the upper layer (or above for g-modes). For slow MHD waves in high-β plasma in a vertical magnetic field the solutions may oscillate

in the upper layer. This is due to the Bessel function solutions automatically satisfying the boundary condition of finite kinetic energy density as $z \to \infty$ for both oscillating and evanescent perturbations.

The plasma is in the high-β regime and the temperature varies slowly, hence we may consider Q_0, Q_{-L} and j_0 to be large. An asymptotic expansion of D_1 is possible. Let us assume $\omega > N$, then $Q < 0, j > 0$. This is not a fundamental assumption in the analysis, rather it is made to avoid technicalities in the asymptotic expansion of the Airy functions (the presence of Stokes' phenomena, for details see *e.g.* Bender & Orszag, 1978). We return to the case of $Q > 0$ later. The first term in the asymptotic expansion of the Bessel function of the first kind is (Abramowitz & Stegun, 1972)

$$J_\nu(x) \sim \sqrt{\frac{2}{\pi x}}\cos\left(x - \frac{\nu\pi}{2} - \frac{\pi}{4}\right), \quad \nu \text{ fixed}, \quad |x| \to \infty, \quad |\arg x| < \pi. \tag{5.219}$$

The first terms in the asymptotic expansions of the Airy functions are given in Equation (2.65); Their derivatives, are

$$\mathrm{Ai}'(-x) \sim -\pi^{-1/2}x^{1/4}\cos\left(\zeta + \frac{\pi}{4}\right), \quad \mathrm{Bi}'(-x) \sim \pi^{-1/2}x^{1/4}\sin\left(\zeta + \frac{\pi}{4}\right), \quad x \to \infty, \tag{5.220}$$

where

$$\zeta = \frac{2}{3}x^{3/2}, \quad \text{and} \quad |\arg x| < \frac{2}{3}\pi. \tag{5.221}$$

Applying these expansions we may simplify D_1,

$$D_1 \sim \frac{Q'I(\omega)}{\sqrt{\frac{2}{\pi j_0}}\widetilde{Q}_{-L}^{-\frac{1}{4}}\left[\widetilde{Q}_0^{\frac{1}{4}}Q'\cos\left(j_0 - \frac{\pi}{4}\right)\cos(\zeta_0 - \zeta_{-L}) - j_0'\widetilde{Q}_0^{-\frac{1}{4}}\cos\left(j_0 - \frac{3\pi}{4}\right)\sin(\zeta_0 - \zeta_{-L})\right]}, \tag{5.222}$$

where

$$\widetilde{Q}_{0,-L} = -Q_{0,-L}, \quad \zeta_{0,-L} = \frac{2}{3}\widetilde{Q}_{0,-L}^{\frac{3}{2}}. \tag{5.223}$$

The waves are resonantly amplified when

$$\widetilde{Q}_0^{\frac{1}{4}}Q'\cos\left(j_0 - \frac{\pi}{4}\right)\cos(\zeta_0 - \zeta_{-L}) - j_0'\widetilde{Q}_0^{-\frac{1}{4}}\cos\left(j_0 - \frac{3\pi}{4}\right)\sin(\zeta_0 - \zeta_{-L}) = 0, \tag{5.224}$$

or, substituting the expressions for Q and j,

$$\left(\omega^2 - N_0^2\right)^{\frac{1}{2}}\sin\left(j_0 + \frac{\pi}{4}\right)\cos(\zeta_0 - \zeta_{-L}) + \left(\omega^2 - N^2\right)^{\frac{1}{2}}\cos\left(j_0 + \frac{\pi}{4}\right)\sin(\zeta_0 - \zeta_{-L}) = 0, \tag{5.225}$$

when $\omega^2 \neq N_0^2(m-1)/m$ and we have used the fact that $\cos(j_0 - \pi/4) = \sin(j_0 + \pi/4)$, $\cos(j_0 - 3\pi/4) = -\cos(j_0 + \pi/4)$. Further simplification is possible if we make the assumption $N \approx N_0$, or

$$1 - \frac{N_0^2}{N^2} \ll 1. \tag{5.226}$$

This is equivalent to assuming $g/\left(z_0 N^2\right) \ll 1$. Using conditions representative of the lower solar atmosphere, the parameters take the values $g = 0.274\text{km s}^{-2}$, $N = 0.03$ rad s^{-1} and choosing $z_0 = 1.5$ Mm, $g/\left(z_0 N^2\right) \approx 0.2$ and may be considered small. This term is even smaller when z_0 is larger. When this approximation is made

$$\left(\omega^2 - N^2\right)^{\frac{1}{2}} \sin\left(j_0 + \frac{\pi}{4} + \zeta_0 - \zeta_{-L}\right) = 0. \tag{5.227}$$

The resonant frequencies may found to be solutions of

$$j_0 + \frac{\pi}{4} + \zeta_0 - \zeta_{-L} = n\pi, \quad n = 1, 2, 3, \ldots, \tag{5.228}$$

or

$$\frac{2H}{\widehat{v}_A}\left(\omega^2 - N^2\right)^{\frac{1}{2}} + \frac{\pi}{4} + \frac{2}{3}\widetilde{Q}_0^{\frac{3}{2}} - \frac{2}{3}\left[\widetilde{Q}_0\left(1 + \frac{(m-1)N^2 - m\omega^2}{N^2 - \omega^2}\frac{L}{z_0}\right)\right]^{\frac{3}{2}} = n\pi, \tag{5.229}$$

note that we have written $N_0 \approx N$. Taylor expanding this expression around the small parameter L/z_0 we may approximate the resonant frequencies as

$$\omega^2 = N^2 + \frac{\widehat{v}_A^2 \pi^2 \left(n - \frac{1}{4}\right)^2}{(L + 2H)^2}, \quad n = 1, 2, 3, \ldots. \tag{5.230}$$

This expression represents the resonant frequencies of a two-layer solar atmosphere consisting of high-β plasma in the presence of a vertical magnetic field. The waves are slow MAG waves in the limit of small horizontal wavenumber, *i.e.* magnetically modified g-modes. As in the non-magnetic cases the resonant frequencies are located above the Brunt-Väisälä frequency. In contrast to the non-magnetic case this represents oscillating solutions due to the influence of the magnetic field and the small horizontal wavelength. We see that, as in the case of a uniform horizontal magnetic field, a magnetic field allows the trapping of waves *above* the cut-off frequency in the isothermal layer.

The expression for D_1 is such that the resonant frequencies may be found without the same level of simplification as in the other cases. This results in the fact that we may find analytical expressions for higher harmonics of the resonant cavity. The first three harmonics (the fundamental mode and the first and second harmonics) are plotted in Figure 5.8 for increasing L. The values of the parameters parameters used are typical of the lower solar atmosphere, *i.e.* $N = 0.03$ rad s^{-1}, $\widehat{c_s} = 8$ km s^{-1}, $g = 0.274$ km s^{-2}, $\gamma = 5/3$ (so $H \approx 140$ km). The dotted line indicates the Brunt-Väisälä frequency in the upper layer. As L increases, the resonant frequencies tend to the Brunt-Väisälä frequency in the upper layer as in the non-magnetic Bousinesq case, Figure 4.1. In contrast to the non-magnetic case, there are no values of L such that $k_x L$ is close to unity due to assumption of large horizontal wavelength, hence the resonant frequencies stay real and finite for all L.

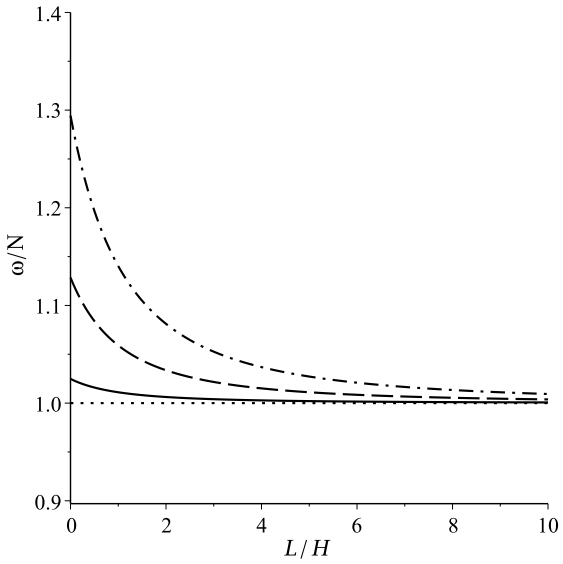

Fig. 5.8 A plot of the resonant frequencies (5.230), normalised to the Brunt-Väisälä frequency in the upper layer, for increasing L. The solid line represents the fundamental mode ($n = 1$), the dashed line is the first harmonic ($n = 2$), and the dot-dash line is the second harmonic ($n = 3$). The dotted line represents the Brunt-Väisälä in the upper layer, taken to be $N = 0.03$ rad s^{-1}. The parameters are taken to be $\widehat{v_A}/\widehat{c_s} = 0.1$, $\gamma = 5/3$ and $g = 0.274$ km s^{-2}.

In the previous analysis, we made the assumption $\omega > N_0$ so the asymptotic expansion of the Airy functions is well defined. The resonant frequencies (5.230) are located above the Brunt-Väisälä frequency N, but we may question whether this is a product of the assumption $\omega > N_0$. Lets us seek to answer this question by making the assumption $\omega < N_0$. As $N > N_0$, we have $N > N_0 > \omega$, and now $Q > 0$. $j_0 = \mathrm{i}\widehat{j_0}$, $J_0(j_0) = I_0\left(\widehat{j_0}\right), J_1(j_0) = \mathrm{i}I_1\left(\widehat{j_0}\right)$, where I_ν is the modified Bessel function of the first kind. We may write

$$D_1 = \frac{-\pi^{-1}Q'I(\omega)}{\begin{array}{r}Q'I_0\left(\widehat{j_0}\right)[\mathrm{Ai}'(Q_0)\mathrm{Bi}(Q_{-L}) - \mathrm{Ai}(Q_{-L})\mathrm{Bi}'(Q_0)] \\ + \mathrm{i}j_0'I_1\left(\widehat{j_0}\right)[\mathrm{Ai}(Q_0)\mathrm{Bi}(Q_{-L}) - \mathrm{Ai}(Q_{-L})\mathrm{Bi}(Q_0)]\end{array}}. \tag{5.231}$$

The asymptotic expansions of the modified Bessel function and Airy functions (for a large positive argument) are

$$I_\nu(x) \sim \frac{e^x}{\sqrt{2\pi x}}\left(1 - \frac{4\nu^2 - 1}{8x} + \ldots\right), \quad \nu \text{ fixed}, \quad |x| \to \infty, \quad |\arg x| < \frac{\pi}{2}, \tag{5.232}$$

$$\mathrm{Ai}(x) \sim \frac{1}{2}\pi^{-\frac{1}{2}}x^{-\frac{1}{4}}e^{-\zeta} + \ldots, \quad \mathrm{Ai}'(x) \sim -\frac{1}{2}\pi^{-\frac{1}{2}}x^{\frac{1}{4}}e^{-\zeta} + \ldots, \quad x \to \infty, \tag{5.233}$$

$$\mathrm{Bi}(x) \sim \pi^{-\frac{1}{2}}x^{-\frac{1}{4}}e^{\zeta} + \ldots, \quad \mathrm{Bi}'(x) \sim \pi^{-\frac{1}{2}}x^{\frac{1}{4}}e^{\zeta} + \ldots, \quad x \to \infty, \tag{5.234}$$

where $\zeta = \frac{2}{3}x^{3/2}$ and $|\arg x| < \pi$. Approximating the above functions by the first term in their expansion we may approximate D_1 as

$$D_1 \sim \frac{-Q_{-L}^{\frac{1}{4}} Q_0^{\frac{1}{4}} \sqrt{2\pi\widehat{j_0}} Q' I(\omega)\widehat{v}_A}{e^{\widehat{j_0}}\left[\left(N_0^2-\omega^2\right)^{\frac{1}{2}}\cosh(\zeta_{-L}-\zeta_0)+(N^2-\omega^2)^{\frac{1}{2}}\sinh(\zeta_{-L}-\zeta_0)\right]}. \tag{5.235}$$

Under the assumption $N \approx N_0$, made earlier for the case $\omega > N_0$, we have

$$D_1 \sim \frac{-Q_{-L}^{\frac{1}{4}} Q_0^{\frac{1}{4}} \sqrt{2\pi\widehat{j_0}} Q' I(\omega)\widehat{v}_A}{e^{\widehat{j_0}}\left(N^2-\omega^2\right)^{\frac{1}{2}} e^{(\zeta_{-L}-\zeta_0)}}. \tag{5.236}$$

This shows that D_1 is not singular when $\omega < N_0$ and $N_0 \approx N$. Let us consider the case where we do not make the approximation $N_0 \approx N$,

$$D_1 \sim \frac{-Q_{-L}^{\frac{1}{4}} Q_0^{\frac{1}{4}} \sqrt{2\pi\widehat{j_0}} Q' I(\omega)\widehat{v}_A}{e^{\widehat{j_0}}\left(N_0^2-\omega^2\right)^{\frac{1}{2}}\cosh(\zeta_{-L}-\zeta_0)\left[1+\frac{N^2-\omega^2}{N_0^2-\omega^2}\tanh(\zeta_{-L}-\zeta_0)\right]}. \tag{5.237}$$

By Taylor's theorem we may approximate

$$\zeta_{-L}-\zeta_0 \approx Q_0^{\frac{3}{2}}\frac{(m-1)N_0^2-m\omega^2}{N_0^2-\omega^2}\frac{L}{z_0} = \frac{L}{\widehat{v}_A}\left(N_0^2-\omega^2\right)^{\frac{1}{2}}. \tag{5.238}$$

As $\omega < N_0$, $\zeta_{-L}-\zeta_0$ is real and positive. This implies $\tanh(\zeta_{-L}-\zeta_0) > 0$. Finally, $N > N_0$ so $\left(N^2-\omega^2\right)/\left(N_0^2-\omega^2\right) > 0$. D_1 is non-singular, hence there are no resonant frequencies located below the Brunt-Väisälä frequency in the lower layer, N_0.

Note that it is also possible that $N > \omega > N_0$, if we do not assume $N \approx N_0$. When this is the case we may use the asymptotic expansion of the modified Bessel I function leading to the relation

$$\left(\omega^2-N_0^2\right)^{\frac{1}{2}}\cos(\zeta_0-\zeta_{-L})+\left(N^2-\omega^2\right)^{\frac{1}{2}}\sin(\zeta_0-\zeta_{-L}) = 0. \tag{5.239}$$

This is consistent with Equation (5.225). Under the assumption that L/z_0 is small, the dispersion relation may be written

$$\mathrm{i}\tanh\left(\frac{L}{\widehat{v}_A}\left(N_0^2-\omega^2\right)^{1/2}\right) = -\frac{\left(\omega^2-N_0^2\right)^{1/2}}{\left(N^2-\omega^2\right)^{1/2}}, \tag{5.240}$$

or

$$\frac{\omega^2-N_0^2}{N^2-\omega^2}+\tanh^2\left(\frac{L}{\widehat{v}_A}\left(N_0^2-\omega^2\right)^{1/2}\right) = 0. \tag{5.241}$$

We see that there are no real frequencies that satisfy the dispersion relation in the interval $N_0 < \omega < N$. A global resonance then may only occur at frequencies above the Brunt-Väisälä

frequency in the upper layer. This model is equivalent to considering the Boussinesq approximation as discussed in the previous chapters. A comparison to the hydrodynamic Boussinesq case shows that the magnetic field does not change the threshold for a resonance to occur, but the frequencies themselves do not coincide.

5.4.2 Magnetic IGWs: Varying Plasma-β in the Upper Layer

The analysis in the previous section is equivalent to applying the Boussinesq approximation; that is, it is applicable to magnetically modified IGWs. We previously showed, in Chapter 3, that the Boussinesq approximation is equivalent to assuming large wavelength and a high-β medium. The previous models were built on the assumption that we could treat the waves in the Boussinesq approximation. In a more realistic atmosphere we do not expect that the Boussinesq approximation should be valid in all parts of the medium. The present model is equivalent to relaxing the Boussinesq approximation somewhat.

It is possible to investigate the governing equation asymptotically to find a solution that allows the background plasma-β to decrease from an initial large value, close to the lower polytropic layer, to a small value higher in the atmosphere. In reality, the density decreases significantly so the plasma-β does indeed vary in such a manner. This model, therefore, can be considered to be the most applicable for magnetic IGWs in a vertical background magnetic field.

The solution in the upper isothermal layer is found via an asymptotic method, assuming that the plasma-β is initially large. The asymptotic high-β solution is connected to the low-β via the method of matched asymptotic expansions. We apply the upper boundary condition of no incoming waves to the low-β solution, this information is transmitted to the high-β solution in the matching process. To determine the constants of integration, and so to investigate a possible global resonance, we apply boundary conditions to the leading order solutions at $z = 0$.

The solution to leading order in the upper layer, valid in the region $z < -H \log \epsilon$ where $\epsilon = \widehat{v}_A^2/c_s^2$, is

$$\xi_{ze} \sim D_1 e^{z/4H} e^{-S_e/\epsilon^{1/2}}, \tag{5.242}$$

where

$$S_e = -\frac{2H}{c_s}\left(N^2 - \omega^2\right)^{1/2} \alpha_e^{-1/2}. \tag{5.243}$$

The leading order solution in the lower layer is given by

$$\xi_{zi} \sim C_1 \left[\frac{\alpha_i^{1-m}}{\alpha_i \omega^2 - N_0^2}\right]^{1/4} e^{S_i/\epsilon^{1/2}} + C_2 \left[\frac{\alpha_i^{1-m}}{\alpha_i \omega^2 - N_0^2}\right]^{1/4} e^{-S_i/\epsilon^{1/2}}, \tag{5.244}$$

where

$$S_i = \mathrm{i}\frac{2\omega z_0}{\widehat{c_s}(m+2)} \alpha_i^{\frac{m+2}{2}} {}_2F_1\left(-\frac{1}{2}, -1 - \frac{m}{2}; -\frac{m}{2}; \frac{N_0^2}{\alpha_i \omega^2}\right), \tag{5.245}$$

$$\alpha_i = 1 - \frac{z}{z_0}. \tag{5.246}$$

We now apply appropriate boundary conditions. As we are implementing conditions to an asymptotic series we apply the boundary conditions at order *e.g.* $\epsilon^0, \epsilon^{1/2}$, etc. To determine the coefficients of the leading order solution, we need only apply boundary conditions to lowest orders. Higher order boundary conditions fix the coefficients of higher terms in the asymptotic series in terms of the already found coefficients. The first boundary condition is that we drive the waves at $z = -L$, this is expressed as

$$C_1\left(1+\frac{L}{z_0}\right)^{\frac{1-m}{4}}\left(\left(1+\frac{L}{z_0}\right)\omega^2 - N_0^2\right)^{-1/4} e^{S_i(-L)/\epsilon^{1/2}} + C_2\left(1+\frac{L}{z_0}\right)^{\frac{1-m}{4}}\left(\left(1+\frac{L}{z_0}\right)\omega^2 - N_0^2\right)^{-1/4} e^{-S_i(-L)/\epsilon^{1/2}} = I(\omega). \tag{5.247}$$

Note that $S_i(-L)$ represents S_i evaluated at $z = -L$ (not $\alpha = -L$). The following two boundary conditions are applied at $z = 0$. The first is the continuity of displacement $\xi_{zi} = \xi_{ze}$; to leading order this is

$$C_1\left(\omega^2 - N_0^2\right)^{-1/4} e^{S_i(0)/\epsilon^{1/2}} + C_2\left(\omega^2 - N_0^2\right)^{-1/4} e^{-S_i(0)/\epsilon^{1/2}} - D_1 e^{-S_e(0)/\epsilon^{1/2}} = 0. \tag{5.248}$$

The next condition is the continuity of the vertical component of the perturbed magnetic field, when the density and temperature are continuous this takes the form $\mathrm{d}\xi_{zi}/\mathrm{d}z = \mathrm{d}\xi_{ze}/\mathrm{d}z$. To order $\epsilon^{-1/2}$ this condition leaves us with the equation

$$C_1\frac{1}{z_0}\frac{\mathrm{d}S_i}{\mathrm{d}\alpha_i}\bigg|_{z=0}\left(\omega^2 - N_0\right)^{-1/4} e^{S_i(0)/\epsilon^{1/2}} - C_2\frac{1}{z_0}\frac{\mathrm{d}S_i}{\mathrm{d}\alpha_i}\bigg|_{z=0}\left(\omega^2 - N_0\right)^{-1/4} e^{-S_i(0)/\epsilon^{1/2}} - D_1\frac{1}{H}\frac{\mathrm{d}S_e}{\mathrm{d}\alpha_e}\bigg|_{z=0} e^{-S_e(0)/\epsilon^{-1/2}} = 0. \tag{5.249}$$

The system of three equations may be solved to give

$$D_1 = \frac{(1/z_0)\left(\omega^2 - N_0^2\right)^{-1/4}\left(\omega^2\left(1+\frac{L}{z_0}\right) - N_0^2\right)^{1/4}\left(1+\frac{L}{z_0}\right)^{\frac{m-1}{4}} S_i'(0) e^{S_e(0)/\epsilon^{1/2}} I(\omega)}{\frac{1}{H}S_e'(0)\sinh\left(\epsilon^{-1/2}\left[S_i(-L) - S_i(0)\right]\right) + \frac{1}{z_0}S_i'(0)\cosh\left(\epsilon^{-1/2}\left[S_i(-L) - S_i(0)\right]\right)}, \tag{5.250}$$

$$C_1 = \frac{\left(\frac{1}{H}S_e'(0) + \frac{1}{z_0}S_i'(0)\right) z_0\left(\omega^2 - N_0^2\right)^{1/4} e^{-S_i(0)/\epsilon^{1/2}} e^{-S_e(0)/\epsilon^{1/2}}}{2S_i'(0)} D_1, \tag{5.251}$$

$$C_2 = \frac{\left(\frac{1}{z_0}S_i'(0) - \frac{1}{H}S_e'(0)\right) z_0\left(\omega^2 - N_0^2\right)^{1/4} e^{S_i(0)/\epsilon^{1/2}} e^{-S_e(0)/\epsilon^{1/2}}}{2S_i'(0)} D_1. \tag{5.252}$$

We see that the condition for a resonant instability may be written

$$\tan(Q) = -\omega\left(N^2-\omega^2\right)^{-1/2}\left[{}_2F_1\left(-\frac{1}{2},-1-\frac{m}{2};-\frac{m}{2};\frac{N_0^2}{\omega^2}\right)+\frac{N_0^2}{m\omega^2}\,{}_2F_1\left(\frac{1}{2},-\frac{m}{2};1-\frac{m}{2};\frac{N_0^2}{\omega^2}\right)\right], \tag{5.253}$$

where

$$Q = \frac{2\omega z_0}{\widehat{v}_A(m+2)}\left[\left(1+\frac{L}{z_0}\right)^{\frac{m+2}{2}}{}_2F_1\left(-\frac{1}{2},-1-\frac{m}{2};-\frac{m}{2};\frac{N_0^2}{\omega^2}\left(1+\frac{L}{z_0}\right)^{-1}\right) - {}_2F_1\left(-\frac{1}{2},-1-\frac{m}{2};-\frac{m}{2};\frac{N_0^2}{\omega^2}\right)\right]. \tag{5.254}$$

Before we consider solution to the above equation let us note an apparent consequence. As in the case of the eigenmodes of the non-driven two-layer model, real frequency solutions are only available when $\omega < N$. That is, a resonance may only occur for waves driven below the Brunt-Väisälä frequency in the upper layer. The physical reason for this is that waves driven above the Brunt-Väisälä frequency are propagating rather than decaying, so the waves may carry energy away from the trapping cavity, hence the global resonance may not form. It should be noted that in previous models, the global resonance occurred for oscillatory solutions so this may not fully explain why the resonance occurs only below the Brunt-Väisälä frequency.

The fact that a resonance may only exist below the Brunt-Väisälä frequency is in contrast to the results obtained by considering the upper layer to be high-β only. To understand why we have different results let us consider the expansion of the Bessel function

$$\begin{aligned}&\xi_{ze} = D_1 J_0(j) + D_2 Y_0(j) \sim \\ &\alpha_e^{1/4} e^{S_e/\epsilon^{1/2}}\left\{D_1 - D_2 - \mathrm{i}(D_1+D_2)\right\}\frac{\lambda}{2} + \alpha_e^{1/4} e^{-S_e/\epsilon^{1/2}}\left\{D_1 - D_2 + \mathrm{i}(D_1+D_2)\right\}\frac{\lambda}{2}, \quad \epsilon \to 0,\end{aligned} \tag{5.255}$$

where λ represents the constant factors in the asymptotic expansion. This is equivalent to the leading order asymptotic WKB solution. The boundary conditions applied to the low-β regime of the asymptotic solution led to the condition that the coefficient of the term $\exp(S_e/\epsilon^{1/2})$ is zero. This condition made the high-β solution feel the effects of the low-β solution. If we were to apply this to the Bessel function solution, the equivalent condition would be $D_1 - D_2 - \mathrm{i}(D_1+D_2) = 0$. In the high-$\beta$ only case, the boundary condition of finite kinetic energy density led to the condition that $D_2 = 0$. We see that the two approaches are not equivalent and so the two models are different. The more realistic model is the present one, where the solutions are allowed to feel the effects of the upper atmosphere. That is not to say that the previous results are incorrect, it is that they relate to a simpler, more limited model. When the background varies very slowly, so that for practical purposes

the oscillations do not feel any low-β effects, a global oscillation may occur above the Brunt-Väisälä frequency. In a model where the stratification has a more significant effect, a resonance may form only below the Brunt-Väisälä frequency.

The key difference to the previous model is due to the inclusion of "non-Boussinesq" effects. When the waves do not feel these low-β effects the resonant frequencies were as in the previous section. When we include low-β effects the character of the resonance is significantly changed. The drastic changes seem to imply that the the non-Boussinesq effects become dominant when they are included.

Also of note is the similarity of resonant frequencies to the eigenfrequencies of the non-driven two layer model. In fact, it can be shown that the resonant frequencies are the same as the eigenfrequencies; that is, Equation 5.253 is simply a restatement of the dispersion relation found in Chapter 3. This implies that the resonant cavity that the waves may be trapped in is representative of the whole lower layer. Analytical results obtained by studying Equation 5.253 are given in Appendix B.

5.5 Conclusions

In this chapter we have generalised the previous results of the global resonance of hydrodynamic waves to magnetohydrodyanmic waves. To study the effects of magnetism we made use of several magnetic field profiles and inclinations. The inclusion of magnetism is crucial when attempting to model the solar atmosphere. In this chapter we were able to determine several key effects on the global resonance due to a magnetic atmosphere.

We began by considering a horizontal magnetic field. Such a field is applicable to the canopy fields that are observed in the solar chromosphere. A horizontal magnetic field is the most simple field to consider mathematically as there is limited inhomogeneity in the direction of the magnetic field in a first approximation. Due to the complexity of the problem, we first studied the case of vertically propagating waves, that is the wave vector and the magnetic field are perpendicular. This approach represents a straightforward generalisation of the hydrodynamic problem to magnetohydrodynamics. We use two magnetic field profiles to study the magnetic effects. Firstly, we use a field that decays as the square root of the density, so the Alfvén speed remains constant. The key effect here is that the resonant frequencies are lower than the hydrodynamic frequencies. A sufficiently strong field may even inhibit the resonance. This is due to the fact that a variable magnetic field, and so a magnetic pressure gradient, reduces the acoustic cut-off frequency. This means that the range of frequencies that may be trapped is reduced.

Next, we studied a uniform magnetic field. This has the consequence that we may study the effect of a variable Alfvén speed. In reality, the Alfvén speed does increase with height, though not as rapidly as we model here. The mathematical analysis is such that we categorise the effects by whether the magnetic pressure is initially strong or weak when compared to the kinetic pressure. When strong, the resonance may always exist, hence

one of the significant effects of a magnetic field is that resonance may occur for oscillatory solutions rather than evanescent solutions. This is due to effect of the magnetic field on the eigenfunctions. The inhibiting effect seen previously is not present as there is no gradient in the magnetic pressure. We study the weak field case using the method of matched asymptotic expansions. We show that when the field is initially weak the magnetic field modifies the wave amplitude, although the resonant frequencies are unchanged.

The effects of non-vertical wave propagation are studied next. Analytical expressions are given for the case of near vertical wave propagation. For simplicity, we limit our analysis to the case of a constant Alfvén speed. This will be relaxed in future work. As in the hydrodynamic case the range of resonant frequencies is greater due to the values of the cut-off frequency. In the magnetic case, there may be multiple cut-offs hence there may be distinct branches of resonant frequencies. The large number of resonant frequencies again suggests that the resonance is a robust phenomenon which may be an important mechanism at work in the solar atmosphere.

A horizontal magnetic field may be studied with relative simplicity. In contrast, the effects of a vertical magnetic field are more difficult to analyse as solutions in terms of special functions are not widely available. We were able to show that the resonance does indeed exist for some limiting cases but a more general treatment requires further study. In particular, a sophisticated numerical study, in the manner of *e.g.* Shelyag *et al.* (2009), Fedun, Shelyag & Erdélyi (2011) and Mumford, Fedun & Erdélyi (2015) is required to further determine the effects of a vertical field.

Future work includes extending the work here to a more realistic solar atmosphere. This includes using a realistic background profile as in *e.g.* Vernazza *et al.* (1981) and localised, structured magnetic fields. Due to the complexity of the governing equations a numerical study is needed to include these effects.

Chapter 6

Discussion, Conclusions and Future Work

In this thesis we have worked on problems related to magnetohydrodynamic waves in a gravitationally stratified medium. The theory of MHD waves has a long history, undergoing significant development since the discovery by Alfvén (1942). The topic was expanded to explain phenomena associated with plasmas, in particular the Sun. It has been known since Hale's groundbreaking discovery of magnetic fields in sunspots (Hale, 1908) that magnetism is very important in explaining the physical processes associated with solar phenomena. Plasmas embedded within a magnetic field are able to support MHD waves; hence, the study of MHD waves in the solar atmosphere has been a popular area of study. Particular attention has been paid to the possibility that MHD waves are responsible for the heating of the solar atmosphere. While MHD waves are a prime candidate to explain this heating (along with small-scale magnetic reconnection events), the problem has yet to be resolved. The study of MHD waves received attention yet again when new space missions observed oscillating coronal loops (Ashwanden *et al.* , 1999). The use of MHD waves as a diagnostic tool to deduce information about the coronal plasma has since become a very active area of research.

The properties of linear MHD waves in a homogeneous medium are well understood. We briefly reviewed some of this theory in Chapter 2, although see *e.g.* Goedbloed & Poedts (2004) for a comprehensive treatment. Studying MHD waves in such a medium has the advantage that the mathematical treatment is very simple and so some of the key properties of MHD waves may be understood. In reality, the real solar atmosphere is far from homogeneous. The properties of MHD waves are highly dependent on inhomogeneity. Magnetic structures in the solar atmosphere are most often present in the form of flux tubes. MHD waves in flux tubes is a rich area of study used chiefly in the analysis of coronal loop oscillations. Another important cause of inhomogeneity is the stratification of the fluid due to the presence of a gravitational field.

The plasma in the solar atmosphere is subject to a gravitational force from the entire Sun. The compressible plasma is therefore stratified by gravity. The theory of hydrodynamic waves in a gravitationally stratified fluid is well established, as summarised in *e.g.* Lamb (1932). Gravitational stratification modifies the acoustic wave in several key ways. The amplitude of the wave varies and the wave is subject to a cut-off. Gravity also introduces a buoyancy force which modifies the acoustic wave and introduces a new wave, the internal gravity wave. While pressure is the key restoring force in acoustic waves, buoyancy is responsible for IGWs. The motivation for developing the theory was the application to Earth's atmosphere. Hydrodynamic waves are important in many atmospheric processes. The theory has found applications beyond terrestrial situations; an important example is helioseismology. Hydrodynamic waves were discussed in Chapter 2.

MHD waves in a gravitationally stratified plasma are less understood. The properties of MHD waves are more subtle and complex when gravitational stratification is introduced. A significant amount of work has been undertaken, with many successes, although the

field is far from complete. Much of the previous work has been focused on the behaviour of p-modes in an MHD context. This is motivated by observations of p-mode interaction with a magnetic field, in particular the damping of the waves, when propagating through local magnetically active regions. It has also been established that the frequencies of helioseismic p-modes vary throughout the solar cycle due to the Sun's large scale magnetic fields. MHD waves in a stratified medium have also been studied due to their application to sunspot oscillations. It has long been known that there are oscillations with periods of 3 to 5 minutes in sunspots, these are interpreted to be slow MHD modes in the low-β atmosphere generated by mode conversion of incoming p-modes (fast MHD modes in the high-β surroundings).

The role of buoyancy in the theory of MHD waves has received less attention. The theory of MHD waves where buoyancy plays a key role in the dynamics of the fluid has not been well developed. We address this in Chapter 3. We began by using the Boussinesq approximation in order to treat the problem. The problem of propagating waves was studied in both a vertical and horizontal field. Previous studies, in particular in the case of a vertical magnetic field, have misinterpreted the situation due to a convoluted mathematical treatment of the governing equations. For the case of a vertical magnetic field, buoyancy-driven MHD waves have been identified as Alfvén waves. By employing a more careful analysis we were able to derived a generalised governing equation for the waves and show that this was not the case. Buoyancy-driven MHD waves are actually slow MHD waves. This fact has been touched upon in previous studies, but here we provide a more rigorous justification. While it may seem that this is only a matter of semantics, this is not the case. Alfvén waves and slow waves are both present in the analysis and represent distinct solutions (they are orthogonal eigenmodes of the differential operator) and have distinct properties. These distinctions include phase speed, group speed, polarisation and the way in which energy is carried and dissipated. The difference between slow and Alfvén waves may also be very important in identifying these waves observationally.

The equations under the Boussinesq approximation are difficult to solve analytically, hence we apply another approximation equivalent to small horizontal wavelength (which captures some of the key physics of the Boussinesq approximation) to study slow MHD waves. With this approximation we are able to determine the eigenfunctions for a rather complex polytropic background state; generalising previous work.

With the frequency expressions derived in this section we can determine the properties of magnetic IGWs. An important feature is that the frequency may depart significantly from the Brunt-Väisälä frequency for very weak fields if the vertical wavelength is small. This means that IGWs may easily become dominated by magnetic effects. An understanding of the properties of magnetic IGWs is important in observing these waves in the solar atmosphere. IGWs have been observed by Komm *et al.* (1991), Stodilka (2008) and Straus *et al.* (2008), although the observations were such that a detailed study of the magnetic effects was not determined. An exception was that Straus *et al.* (2008) observed IGWs

to be suppressed in a region of strong magnetic field; this may be due to the frequency of the range increasing so that frequencies were too high to observe as suggested by the frequency expressions derived in Chapter 3. A possible alternative explanation is that a magnetic field may cause reflection of IGWs as discussed by Newington & Cally (2010).

When the waves are in the gravitationally dominated regime they may be observable in the same manner as Straus *et al.* (2008). Intensity variations are unlikely to be useful in observing the waves as they are not compressible in nature. Doppler velocities, however, may be used to identifying these waves. IGWs in the lower solar atmosphere were observed by Straus *et al.* (2008) using line of sight Doppler velocities using the Interferometric Bidimensional Spectrograph (IBIS) and Echelle spectrograph instruments at the Dunn Solar Telescope (DST) and the Michelson Doppler Imager (MDI) onboard the Solar and Heliospheric Observatory (SOHO) spacecraft. In the hydrodynamic regime we expect the waves may be observed using similar methods. In the magnetic regime, periods may be too low for current instruments to observe so other methods may be needed. In this limit it may be difficult to distinguish between Alfvén modes, although in principle, it is possible. The frequency is greater than the Alfvén frequency, although the difference may be difficult to observe. A more significant difference may be observed in the phase and group velocities, expressions for which are easily determined. When the waves have a magnetic character, the velocity perturbations relative to the magnetic field may be used to distinguish these waves from Alfvén waves.

The Boussinesq approximation may be applied to regions of the solar atmosphere in which the plasma dynamics are dominated by hydrodynamic effects (high-β plasma). In the lower solar atmosphere the plasma-β may be considered high, even in region of strong magnetic field. The density decreases with height hence the plasma-β decreases, typically reaching unity in the chromosphere. The corona is magnetically dominated with very low plasma-β. The Boussinesq approximation may then be applied to the lower atmosphere, such as the photosphere or low chromosphere. To accurately model the solar atmosphere we should apply a model with this feature. We do this with the small horizontal wavelength approximation. We are able to find asymptotic solutions for an isothermal atmosphere with varying plasma-β. Studying the eigenmodes we find the curious feature that an upper cut-off frequency is introduced by the upper atmosphere. This means that when the waves are such that they feel the effect of the entire chromosphere/corona, they may only propagate in a narrow frequency range. This possibly explains why g-modes are observed infrequently in the solar atmosphere. It is known that p-modes may leak into the solar corona, as seen in observation by *e.g.* Didkovsky *et al.* (2011), Didkovsky *et al.* (2013), Ireland, McAteer & Inglis (2015). Our analytical work suggests that the atmosphere itself does not allow g-modes to propagate into the higher atmosphere. The g-modes that exist in the solar interior are evanescent in the solar convection zone. They may propagate again in the solar photosphere along magnetic structures but are suppressed by the atmosphere itself.

After the case of a vertical field we briefly considered a horizontal field. We study g-modes with a horizontal canopy field in the atmosphere. While the equations of motion may be solved with relative ease, compared to a vertical field, the dispersion relations are difficult to solve. Limiting solutions to the dispersion relation may be found. An important fact is that an upper cut-off frequency, depending on the Alfvén speed, is introduced. This means that a magnetic field allows propagating solutions to exist where they could not in the hydrodynamic limit. Contrast this to the case of a vertical field where wave propagation is inhibited. Another key point is that there are two types of solutions: modes with a magnetic character and modes with a g-mode character. A numerical study suggests that there is a lower cut-off frequency. Further analytical investigation is needed to study this cut-off. To determine the effect of a horizontal field on g-modes in a more realistic solar atmosphere, a more sophisticated numerical study should be performed. This would be an excellent avenue for future study.

In Chapter 3 we have provided a more in-depth treatment of magnetic IGWs, generalising previous studies to situations applicable to the solar atmosphere. An understanding of the theory is important because it allows us to gain greater insight into the physical processes at play in the solar atmosphere. Such an understanding is vital when attempting to determine how energy is transferred and supplied to the solar plasma. The temperature of the solar corona is orders of magnitude greater than the lower solar atmosphere. How is this heat supplied and maintained? Attempting to answer this question has guided solar physics for many years. MHD waves are often identified as a likely candidate for supplying this energy. The various MHD waves have different properties, including capability to carry and dissipate energy. It is, therefore, important to understand the theory of MHD waves in detail.

A secondary motivation for the study of MHD waves is the potential for seismology of the solar plasma. Magneto-seismology of the corona may be performed by observing coronal loop oscillations. Fast kink modes are particularly useful for magneto-seismology in the corona. A knowledge of the theory of MHD waves allows the measurements to be inverted to infer the properties of the plasma. Such properties are the density scale-height and the much sought after magnetic field. Other techniques used to measure the magnetic field, such as Zeeman splitting, are less applicable to the corona so magneto-seismology is an invaluable diagnostic tool. The techniques of magneto-seismology are analogous to helioseismology, the study of p-modes propagating through the solar interior. The application of helioseismology allows us the deduce the conditions of the solar interior. The conditions of the lower solar atmosphere, in particular the chromosphere, are less well known. Magneto-seismology has not yet been widely applied to the chromosphere, although we expect this to grow in the coming years. A deep knowledge of MHD waves is needed to perform magneto-seismology, hence the work in this thesis may be useful in the application of seismology to atmospheric g-modes. As observing technologies and techniques progress, seismology may be applied to g-modes in the lower solar atmosphere.

We have developed further the theory of buoyancy-driven MHD waves, although the topic is not complete. Here, we focus on the theory of linear waves; with this now rather well established a clear next step would be to consider the theory of non-linear waves. In a stratified medium the amplitude of the waves may increase as the wave propagates. We may expect non-linear effects to become important in some region in the solar atmosphere. Non-linear effects may be important in the dissipation of energy. The steepening of the waves into shocks and non-linear interaction between the separate wave modes, such as non-linear coupling of magnetic IGWs and Alfvén waves, is potentially important in the dynamics of the solar atmosphere and so deserves further study. Future work also includes, as mentioned previously, a sophisticated numerical study of the waves as in *e.g.* Shelyag *et al.* (2009), Fedun *et al.* (2011) and Mumford *et al.* (2015). We have discussed waves in a relatively complex atmosphere although this does not capture the nuances of the real solar plasma. Numerical simulations will allow us to determine how the waves we discuss here propagate in a more complex, realistic atmosphere.

In Chapter 3 we made the first steps towards including the effects of partial ionisation. We used a two-fluid MHD model to study the effects of partial ionisation on buoyancy-driven MHD waves. MHD waves in a homogeneous two-fluid model were studied by *e.g.* Zaqarashvili *et al.* (2011b). The effects of partial ionisation in a single-fluid model, in particular the damping of Alfvén waves, have been studied by numerous authors. Here, we include the effects of buoyancy in a stratified plasma. To our knowledge, this is the first study of its kind. We studied waves using a local WKB dispersion relation. Corrections to the case of a fully ionised plasma, and damping rates due to ion-neutral collisions were found in several limits. Some key results include the fact that magnetic effects can have a significant effect in weakly ionised plasmas. When the collision frequency is low the two fluids interact weakly and so each may support oscillatory wave motion which is damped due to collisions. When the collision frequency is high the gasses act as a single-fluid; two of the oscillatory waves become purely damped solutions denoted vortex modes. The buoyancy-driven MHD wave is weakly damped in this limit. We used a simplified two-fluid description, neglecting effects such as the Hall effect, magnetic diffusion and collisions with electrons. In the future these effects may be included resulting in a more general two-fluid model. Our analysis was based on a local WKB method. Studying the effect of partial ionisation on the eigenfunctions, and so finding corrections to other work in this thesis, would be an interesting avenue for future study. Extending the theory of MHD waves in a stratified, partially ionisation medium would be an interesting, and potentially important, topic of future study. The effect of partial ionisation on, for example, mode conversion would be particularly interesting.

The second section of this thesis focused on the global resonance of driven waves in a gravitationally stratified medium. A variable temperature, and so variable acoustic cut-off frequency may lead to the trapping of waves. This trapping essentially forms standing waves in an effective cavity. Driving waves at the natural frequencies of this cavity leads

to a resonance which extends to the entire unbounded atmosphere. This problem was discussed by Taroyan & Erdélyi (2008) for the case of vertically propagating acoustic waves. In Chapters 4 and 5 we generalise these results. Chapter 4 deals with hydrodynamic waves in a field free atmosphere. The key results in this chapter are that this resonance also exists for IGWs; and that the range of resonant frequencies for non-vertically propagating acoustic modes may be large. This is due to the dependence of the cut-off on the horizontal wave number. These resonant frequencies may be investigated analytically when the propagation is close to vertical. The work in this chapter shows that the global resonance discovered by Taroyan & Erdéyi (2008) may occur for a wide range of waves.

There have been many observations of p-modes with varying spherical degree. The waves generated in the convection zone are therefore non-radial modes. There is increasing evidence that these modes are not only trapped in the solar interior but may leak into the solar atmosphere. The complex temperature profile in the lower solar atmosphere may lead to trapping of these modes as described previously. As these waves may have a significant horizontal component, we should not limit the discussion to radial propagation. This was the basis of Chapter 4. There are several next steps which may extend this work. A numerical study with a more realistic atmospheric temperature profile is clearly an important next step. As we see in Chapter 4, analytical progress is limited due to the complexity of the system. The dispersion relations derived in Chapter 4 are difficult to solve for relatively simplistic background set ups; for a realistic solar atmosphere an analytical investigation is not possible. The effect of the spherical nature of the Sun was neglected in this study. While this assumption can often be employed, in a general study we should not neglect the curvature of the Sun. This may or may not have a significant effect on the physics we study here. A numerical investigation may be required to establish the effect of the spherical Sun.

A hydrodynamic model may be applicable to regions of the Sun where there is little magnetic activity. We observe the solar atmosphere to be magnetically dominated. More recent observations suggest that the so called quiet sun is not devoid from magnetism; rather small-scale magnetic elements are ubiquitous. These magnetic elements are the foot-points of chromospheric loops. Magnetism is, therefore, very important and should be taken into account when dealing with solar processes.

Including the effect of a magnetic field on the global resonance was the subject of Chapter 5. For simplicity, we began by focusing on the case of vertically propagating waves with a horizontal magnetic field. Two magnetic field profiles were considered: an exponentially varying field and a uniform field. We saw that the magnetic field had significant effects on the global resonance. A strong decaying field inhibited the resonance due to the varying magnetic pressure and so the scale-height. Waves that would be trapped and amplified in a field-free atmosphere would not be trapped when a magnetic field is present. On the other hand, a uniform field is able to trap waves when the plasma-β is low. The resonance occurs even for oscillatory solutions due to the eigenfunctions in this model.

The effect of a weak field was studied using the method of matched asymptotic expansions; we saw that, to leading order, the amplitude of the wave was modified but the resonant frequencies were unchanged. The effect of non-vertical wave propagation was included when the magnetic field varied exponentially. The effects of horizontal propagation were analogous to the hydrodynamic case in that the range of possible resonant frequencies is very large.

The case of a vertical field was briefly considered. The number of models is limited due to that fact that exact solutions are difficult to find for MAG waves in a polytropic atmosphere. We were able to establish that resonance may occur in certain situations including vertically propagating MAG waves (in the limit $k_x H \to 0$) and slow MAG waves in low-β plasma in the small horizontal wavelength limit. We also found expressions for the resonance for buoyancy-driven MHD waves. Numerical simulations are needed to establish the effect of a vertical field on the global resonance in a wider range of models.

We conclude that the mechanism discussed by Taroyan & Erdéyi (2008) is a robust phenomenon that persists in many different situations. We have shown that the range of resonant frequencies is large where both high and low frequency waves may be trapped. We therefore expect that the trapping of waves by a varying background to be common in the solar atmosphere. This may be an important mechanism for transferring energy to the upper atmosphere. The solar corona is significantly hotter than the lower photosphere; the question of how this heat is supplied and maintained is not yet answered. We suggest that the mechanism discussed here may be important in addressing this. The key to establishing the importance of the global resonance in the solar atmosphere is with observational data. With the increasing spatial and temporal resolution of solar telescopes we expect that waves generated in the solar convection zone will be observed propagating throughout the solar chromosphere. Observing the reflection of such waves will allow us to determine the efficient of the global resonance discussed here. We urge observers to undertake such a study.

The field of magneto-seismology of the solar atmosphere has been very successful in recent years. The results in this thesis will be very useful in interpreting results as the field continues to develop. While we are motivated primarily by solar applications the results in this work may be applicable to other situations. The field of astroseismology is relatively new although it has undergone significant developments recently. We anticipate that magneto-seismology of other stars will be possible in the future. Results developed with solar applications in mind may be found to be very useful in this new context.

References

[1] Abramowitz, M. and Stegun, I. A. (1972). *Handbook of Mathematical Functions*. Dover, New York.

[2] Aizenman, M., Smeyers, P., and Weigert, A. (1977). Avoided Crossing of Modes of Non-radial Stellar Oscillations. *Astron. Astrophys.*, 58:41.

[3] Alboussière, T., Cardin, P., Debray, F., La Rizza, P., Masson, J., Plunian, F., Ribeiro, A., and Schmitt, D. (2011). Experimental evidence of alfvén wave propagation in a gallium alloy. *Physics of Fluids*, 23(9).

[4] Alfvén, H. (1942). Existence of Electromagnetic-Hydrodynamic Waves. *Nat*, 150:405–406.

[5] Andries, J., Arregui, I., and Goossens, M. (2005). Determination of the Coronal Density Stratification from the Observation of Harmonic Coronal Loop Oscillations. *Astrophys. J. Lett.*, 624:L57–L60.

[6] Appourchaux, T., Belkacem, K., Broomhall, A.-M., Chaplin, W. J., Gough, D. O., Houdek, G., Provost, J., Baudin, F., Boumier, P., Elsworth, Y., García, R. A., Andersen, B. N., Finsterle, W., Fröhlich, C., Gabriel, A., Grec, G., Jiménez, A., Kosovichev, A., Sekii, T., Toutain, T., and Turck-Chièze, S. (2010). The quest for the solar g modes. *Astron. Astrophys. Rev.*, 18:197–277.

[7] Aschwanden, M. J. (2005). *Physics of the Solar Corona. An Introduction with Problems and Solutions (2nd edition)*. Springer.

[8] Aschwanden, M. J., Fletcher, L., Schrijver, C. J., and Alexander, D. (1999). Coronal Loop Oscillations Observed with the Transition Region and Coronal Explorer. *Astrophys. J.*, 520:880–894.

[9] Ballai, I. and Erdelyi, R. (1998). Resonant Absorption of Nonlinear Slow MHD Waves in Isotropic Steady Plasmas - I. Theory. *Solar Phys.*, 180:65–79.

[10] Ballai, I. and Erdelyi, R. (2002). Nonlinear theory of resonant slow mhd waves in twisted magnetic flux tubes. *J. Plasma Phys.*, 67:79.

[11] Ballai, I., Oliver, R., and Alexandrou, M. (2015). Dissipative instability in partially ionised prominence plasmas. *Astron. Astrophys.*, 577:A82.

[12] Ballai, I., Ruderman, M. S., and Erdélyi, R. (1998). Nonlinear theory of slow dissipative layers in anisotropic plasmas. *Phys. Plasmas*, 5:252–260.

[13] Banerjee, D., Hasan, S. S., and Christensen-Dalsgaard, J. (1995). The Influence of a Vertical Magnetic Field on Oscillations in an Isothermal Stratified Atmosphere. II. *Astrophys. J.*, 451:825.

[14] Barnes, G., MacGregor, K. B., and Charbonneau, P. (1998). Gravity Waves in a Magnetized Shear Layer. *Astrophys. J. Lett.*, 498:L169.

[15] Batchelor, G. K. (1967). *An Introduction to Fluid Dynamics*. Cambridge University Press.

[16] Bel, N. and Leroy, B. (1981). Propagation of waves in an atmosphere in the presence of a magnetic field. IV - Alfven waves in sunspot umbrae. *Astron. Astrophys.*, 104:203–206.

[17] Bender, C. M. and Orszag, S. A. (1978). *Advanced Mathematical Methods for Scientists and Engineers*. McGraw-Hill.

[18] Berthold, W. K., Harris, A. K., and Hope, H. J. (1960). World-wide effects of hydromagnetic waves due to argus. *Journal of Geophysical Research*, 65(8):2233–2239.

[19] Bogdan, T. J., Hindman, B. W., Cally, P. S., and Charbonneau, P. (1996). Absorption of p-Modes by Slender Magnetic Flux Tubes and p-Mode Lifetimes. *Astrophys. J.*, 465:406.

[20] Bogdan, T. J. and Judge, P. G. (2006). Observational aspects of sunspot oscillations. *Philosophical Transactions of the Royal Society of London Series A*, 364:313–331.

[21] Bostick, W. H. and Levine, M. A. (1952). Experimental demonstration in the laboratory of the existence of magneto-hydrodynamic waves in ionized helium. *Phys. Rev.*, 87:671–671.

[22] Braginskii, S. I. (1965). Transport Processes in a Plasma. *Reviews of Plasma Physics*, 1:205.

[23] Braun, D. C., Duvall, Jr., T. L., and Labonte, B. J. (1987). Acoustic absorption by sunspots. *Astrophys. J. Lett.*, 319:L27–L31.

[24] Braun, D. C. and Fan, Y. (1998). Helioseismic Measurements of the Subsurface Meridional Flow. *Astrophys. J. Lett.*, 508:L105–L108.

[25] Cally, P. S. (2001). Note on an Exact Solution for Magnetoatmospheric Waves. *Astrophys. J.*, 548:473–481.

[26] Cally, P. S. (2005). Local magnetohelioseismology of active regions. *Mon. Not. Roy. Astron. Soc.*, 358:353–362.

[27] Cally, P. S. (2006). Dispersion relations, rays and ray splitting in magnetohelioseismology. *Royal Society of London Philosophical Transactions Series A*, 364:333–349.

[28] Cally, P. S. and Bogdan, T. J. (1993). Solar p-modes in a vertical magnetic field - Trapped and damped pi-modes. *Astrophys. J.*, 402:721–732.

[29] Campbell, W. R. and Roberts, B. (1989). The influence of a chromospheric magnetic field on the solar p- and f-modes. *Astrophys. J.*, 338:538–556.

[30] Campos, L. M. B. C. (1986). On umbral oscillations as a sunspot diagnostic. In Gough, D. O., editor, *NATO Advanced Science Institutes (ASI) Series C*, volume 169 of *NATO Advanced Science Institutes (ASI) Series C*, pages 293–301.

[31] Carbonell, M., Forteza, P., Oliver, R., and Ballester, J. L. (2010). The spatial damping of magnetohydrodynamic waves in a flowing partially ionised prominence plasma. *Astron. Astrophys.*, 515:A80.

[32] Carlsson, M. and Stein, R. F. (2002). Dynamic Hydrogen Ionization. *Astrophys. J.*, 572:626–635.

[33] Cavallini, F. (2006). IBIS: A New Post-Focus Instrument for Solar Imaging Spectroscopy. *Solar Phys.*, 236:415–439.

[34] Chandrasekhar, S. (1961). *Hydrodynamic and hydromagnetic stability*. International Series of Monographs on Physics, Oxford: Clarendon, 1961.

[35] Chaplin, W. J. (2006). *Music of the Sun*. Oneworld Publications.

[36] Chaplin, W. J., Elsworth, Y., Miller, B. A., Verner, G. A., and New, R. (2007). Solar p-Mode Frequencies over Three Solar Cycles. *Astrophys. J.*, 659:1749–1760.

[37] Chaplin, W. J. and Miglio, A. (2013). Asteroseismology of Solar-Type and Red-Giant Stars. *Ann. Rev. Astron. Astrophys.*, 51:353–392.

[38] Chen, C. J. and Lykoudis, P. S. (1972). Velocity Oscillations in Solar Plage Regions. *Solar Phys.*, 25:380–401.

[39] Choudhuri, A. R. (1998). *The Physics of Fluids and Plasmas*. Cambridge University Press.

[40] Christensen-Dalsgaard, J. (1980). On adiabatic non-radial oscillations with moderate or large L. *Mon. Not. Roy. Astron. Soc.*, 190:765–791.

[41] Christensen-Dalsgaard, J. (2002). Helioseismology. *Reviews of Modern Physics*, 74:1073–1129.

[42] Christensen-Dalsgaard, J., Dappen, W., Ajukov, S. V., Anderson, E. R., Antia, H. M., Basu, S., Baturin, V. A., Berthomieu, G., Chaboyer, B., Chitre, S. M., Cox, A. N., Demarque, P., Donatowicz, J., Dziembowski, W. A., Gabriel, M., Gough, D. O., Guenther, D. B., Guzik, J. A., Harvey, J. W., Hill, F., Houdek, G., Iglesias, C. A., Kosovichev, A. G., Leibacher, J. W., Morel, P., Proffitt, C. R., Provost, J., Reiter, J., Rhodes, Jr., E. J., Rogers, F. J., Roxburgh, I. W., Thompson, M. J., and Ulrich, R. K. (1996). The Current State of Solar Modeling. *Science*, 272:1286–1292.

[43] Christensen-Dalsgaard, J. and Gough, D. O. (1976). Towards a heliological inverse problem. *Nature*, 259:89–92.

[44] Clack, C. T. M., Ballai, I., and Ruderman, M. S. (2009). On the validity of nonlinear Alfvén resonance in space plasmas. *Astron. Astrophys.*, 494:317–327.

[45] Cowling, T. G. (1941). The non-radial oscillations of polytropic stars. *Mon. Not. Roy. Astron. Soc.*, 101:367.

[46] Cox, J. P. (1980). *Theory of Stellar Pulsation*. Princeton University Press, Princeton.

[47] de Moortel, I. (2009). Longitudinal Waves in Coronal Loops. *Space Sci. Rev.*, 149:65–81.

[48] de Pontieu, B. and Haerendel, G. (1998). Weakly damped Alfven waves as drivers for spicules. *Astron. Astrophys.*, 338:729–736.

[49] Decarreau, A., Maroni, P., and Robert, A. (1978). Heun's Differential Equations. *Ann. Soc. Buxelles*, 92.

[50] Deubner, F. L. (1975). Observations of low wavenumber nonradial eigenmodes of the sun. *Astron. Astrophys.*, 44:371–375.

[51] Deubner, F. L. and Gough, D. (1984). Helioseismology: Oscillations as a Daignostic of the Solar Interior. *Ann. Rev. Astron. Astrophys.*, 22:593–619.

[52] Díaz, A. J., Soler, R., and Ballester, J. L. (2012). Rayleigh-Taylor Instability in Partially Ionized Compressible Plasmas. *Astrophys. J.*, 754:41.

[53] Didkovsky, L., Judge, D., Kosovichev, A. G., Wieman, S., and Woods, T. (2011). Observations of Five-minute Solar Oscillations in the Corona Using the Extreme Ultraviolet Spectrophotometer (ESP) On Board the Solar Dynamics Observatory Extreme Ultraviolet Variability Experiment (SDO/EVE). *Astrophys. J. Lett.*, 738:L7.

[54] Didkovsky, L., Kosovichev, A., Judge, D., Wieman, S., and Woods, T. (2013). Variability of Solar Five-Minute Oscillations in the Corona as Observed by the Extreme Ultraviolet Spectrophotometer (ESP) on the Solar Dynamics Observatory/Extreme Ultraviolet Variability Experiment (SDO/EVE). *Solar Phys.*, 287:171–184.

[55] Duvall, Jr., T. L., Dziembowski, W. A., Goode, P. R., Gough, D. O., Harvey, J. W., and Leibacher, J. W. (1984). Internal rotation of the sun. *Nature*, 310:22–25.

[56] Duvall, Jr., T. L. and Harvey, J. W. (1984). Rotational frequency splitting of solar oscillations. *Nature*, 310:19–22.

[57] Edwin, P. M. and Roberts, B. (1983). Wave propagation in a magnetic cylinder. *Solar Phys.*, 88:179–191.

[58] El-Jaick, L. J. and Figueiredo, B. D. B. (2009). A limit of the confluent Heun equation and the Schroedinger equation for an inverted potential and for an electric dipole. *Journal of Mathematical Physics*.

[59] Erdélyi, A., editor (1953). *Higher Transcendental Functions Volume 1*. McGraw-Hill, US.

[60] Erdélyi, R. (2006a). Magnetic coupling of waves and oscillations in the lower solar atmosphere: can the tail wag the dog? *R. Soc. Lond. Philos. Trans. A*.

[61] Erdélyi, R. (2006b). Magnetic seismology of the lower solar atmosphere. In *Proceedings of SOHO 18/GONG 2006/HELAS I, Beyond the spherical Sun*.

[62] Erdélyi, R., Hague, A., and Nelson, C. J. (2014). Effects of Stratification and Flows on P_1/P_2 Ratios and Anti-node Shifts Within Closed Loop Structures. *Solar Phys.*, 289:167–182.

[63] Erdélyi, R. and James, S. P. (2004). Can ion-neutral damping help to form spicules?. II. Random driver. *Astron. Astrophys.*, 427:1055–1064.

[64] Erdélyi, R. and Taroyan, Y. (2008). Hinode EUV spectroscopic observations of coronal oscillations. *Astron. Astrophys.*, 489:L49–L52.

[65] Erdélyi, R. and Taroyan, Y. A. (1999). The Influence of a Steady State on p- and f-Modes. In Wilson, A. and et al., editors, *Magnetic Fields and Solar Processes*, volume 448 of *ESA Special Publication*, page 81.

[66] Erdélyi, R., Varga, E., and Zétényi, M. (1999). Magnetoacoustic-Gravity Surface Waves in Steady Plasmas. In Wilson, A. and et al., editors, *Magnetic Fields and Solar Processes*, volume 448 of *ESA Special Publication*, page 269.

[67] Evans, D. J. and Roberts, B. (1990). The influence of a chromospheric magnetic field on the solar p- and f-modes. II - Uniform chromospheric field. *Astrophys. J.*, 356:704–719.

[68] Evans, J. W. and Michard, R. (1962). Observational Study of Macroscopic Inhomogeneities in the Solar Atmosphere. III. Vertical Oscillatory Motions in the Solar Photosphere. *Astrophys. J.*, 136:493.

[69] Fedun, V., Shelyag, S., and Erdélyi, R. (2011). Numerical Modeling of Footpoint-driven Magneto-acoustic Wave Propagation in a Localized Solar Flux Tube. *Astrophys. J.*, 727:17.

[70] Ferraro, C. A. and Plumpton, C. (1958). Hydromagnetic waves in a horizontally stratified atmosphere. v. *Astrophys. J.*, 127:459.

[71] Figueiredo, B. D. B. (2005). Ince's limits for confluent and double-confluent Heun equations. *Journal of Mathematical Physics*, 46(11):113503.

[72] Fontenla, J. M., Avrett, E. H., and Loeser, R. (1990). Energy balance in the solar transition region. I - Hydrostatic thermal models with ambipolar diffusion. *Astrophys. J.*, 355:700–718.

[73] Forteza, P., Oliver, R., and Ballester, J. L. (2008). Time damping of non-adiabatic MHD waves in an unbounded partially ionised prominence plasma. *Astron. Astrophys.*, 492:223–231.

[74] Forteza, P., Oliver, R., Ballester, J. L., and Khodachenko, M. L. (2007). Damping of oscillations by ion-neutral collisions in a prominence plasma. *Astron. Astrophys.*, 461:731–739.

[75] Fraenkel, L. E. (1969a). On the method of matched asymptotic expansions I. *Mathematical Proceedings of the Cambridge Philosophical Society*, 65:209–231.

[76] Fraenkel, L. E. (1969b). On the method of matched asymptotic expansions II. *Mathematical Proceedings of the Cambridge Philosophical Society*, 65:209–231.

[77] Fraenkel, L. E. (1969c). On the method of matched asymptotic expansions III. *Mathematical Proceedings of the Cambridge Philosophical Society*, 65:209–231.

[78] Gent, F. A., Fedun, V., Mumford, S. J., and Erdélyi, R. (2013). Magnetohydrostatic equilibrium - I. Three-dimensional open magnetic flux tube in the stratified solar atmosphere. *Mon. Not. Roy. Astron. Soc.*, 435:689–697.

[79] Giovanelli, R. G. (1980). An exploratory two-dimensional study of the coarse structure of network magnetic fields. *Solar Phys.*, 68:49–69.

[80] Goedbloed, J. P. (1971). Stabilization of magnetohydrodynamic instabilities by force-free magnetic fields. I. Plane plasma layer. *Physica*, 53:412–444.

[81] Goedbloed, J. P., Keppens, R., and Poedts, S. (2010). *Advanced Magnetohydrodynamics*. Cambridge University Press.

[82] Goedbloed, J. P. H. and Poedts, S. (2004). *Principles of Magnetohydrodynamics*. Cambridge University Press, Cambridge.

[83] Goossens, M., Erdélyi, R., and Ruderman, M. S. (2011). Resonant MHD Waves in the Solar Atmosphere. *Space Sci. Rev.*, 158:289–338.

[84] Gough, D. O. (1969). The Anelastic Approximation for Thermal Convection. *Journal of Atmospheric Sciences*, 26:448–456.

[85] Haerendel, G. (1992). Weakly damped Alfven waves as drivers of solar chromospheric spicules. *Nature*, 360:241–243.

[86] Hague, A. and Erdélyi, R. (2016). Buoyancy-driven Magnetohydrodynamic Waves. *Astrophys. J.*, 828:88.

[87] Hale, G. E. (1908). On the Probable Existence of a Magnetic Field in Sun-Spots. *Astrophys. J.*, 28:315.

[88] Hasan, S. S. and Christensen-Dalsgaard, J. (1992). The influence of a vertical magnetic field on oscillations in an isothermal stratified atmosphere. *Astrophys. J.*, 396:311–332.

[89] Heyvaerts, J. and Norman, C. (2003). Global Asymptotic Solutions for Nonrelativistic Magnetohydrodynamic Jets and Winds. *Astrophys. J.*, 596:1270–1294.

[90] Heyvaerts, J. and Priest, E. R. (1983). Coronal heating by phase-mixed shear Alfven waves. *Astron. Astrophys.*, 117:220–234.

[91] Hinch, E. J. (1991). *Perturbation Methods*. Cambridge University Press, Cambridge, Uk.

[92] Hindman, B. W. and Jain, R. (2008). The Generation of Coronal Loop Waves below the Photosphere by p-Mode Forcing. *Astrophys. J.*, 677:769–780.

[93] Hindman, B. W., Zweibel, E. G., and Cally, P. S. (1996). Driven Acoustic Oscillations within a Vertical Magnetic Field. *Astrophys. J.*, 459:760.

[94] Hollweg, J. V. (1979). A new resonance in the solar atmosphere. I - Theory. *Solar Phys.*, 62:227–240.

[95] Hollweg, J. V. (1986). Viscosity and the Chew-Goldberger-Low equations in the solar corona. *Astrophys. J.*, 306:730–739.

[96] Hood, A. W., Brooks, S. J., and Wright, A. N. (2002). Coronal heating by the phase mixing of individual pulses propagating in coronal holes. *Proceedings of the Royal Society of London Series A*, 458:2307.

[97] Ireland, J., McAteer, R. T. J., and Inglis, A. R. (2015). Coronal Fourier Power Spectra: Implications for Coronal Seismology and Coronal Heating. *Astrophys. J.*, 798:1.

[98] Jain, R., Hindman, B. W., Braun, D. C., and Birch, A. C. (2009). Absorption of p Modes by Thin Magnetic Flux Tubes. *Astrophys. J.*, 695:325–335.

[99] Jain, R. and Roberts, B. (1994a). Effects of non-parallel propagation on p- and f-modes. *Astron. Astrophys.*.

[100] Jain, R. and Roberts, B. (1994b). Surface effects of a magnetic field on p-modes: two layer atmosphere. *Astron. Astrophys.*, 286:254–262.

[101] James, S. P. and Erdélyi, R. (2002). Spicule formation by ion-neutral damping. *Astron. Astrophys.*, 393:L11–L14.

[102] James, S. P., Erdélyi, R., and De Pontieu, B. (2003). Can ion-neutral damping help to form spicules? *Astron. Astrophys.*, 406:715–724.

[103] Jess, D. B., Mathioudakis, M., Erdélyi, R., Crockett, P. J., Keenan, F. P., and Christian, D. J. (2009). Alfvén Waves in the Lower Solar Atmosphere. *Science*, 323:1582.

[104] Jovanović, G. (2014). Reflection Properties of Gravito-MHD Waves in an Inhomogeneous Horizontal Magnetic Field. *Solar Phys.*, 289:4085–4104.

[105] Khodachenko, M. L., Arber, T. D., Rucker, H. O., and Hanslmeier, A. (2004). Collisional and viscous damping of MHD waves in partially ionized plasmas of the solar atmosphere. *Astron. Astrophys.*, 422:1073–1084.

[106] Komm, R., Mattig, W., and Nesis, A. (1991). The decay of granular motions and the generation of gravity waves in the solar photosphere. *Astron. Astrophys.*, 252:827–834.

[107] Lamb, H. (1932). *Hydrodynamics*. Dover, New York.

[108] Landau, L. D. and Lifshitz, E. M. (1987). *Fluid Mechanics 2nd edition*. Butterworth-Heinemann.

[109] Leake, J. E., Arber, T. D., and Khodachenko, M. L. (2005). Collisional dissipation of Alfvén waves in a partially ionised solar chromosphere. *Astron. Astrophys.*, 442:1091–1098.

[110] Lehnert, B. (1954). Magneto-Hydrodynamic Waves in Liquid Sodium. *Physical Review*, 94:815–824.

[111] Leibacher, J. W. and Stein, R. F. (1971). A New Description of the Solar Five-Minute Oscillation. *Astrophys. Lett.*, 7:191–192.

[112] Leighton, R. B., Noyes, R. W., and Simon, G. W. (1962). Velocity Fields in the Solar Atmosphere. I. Preliminary Report. *Astrophys. J.*, 135:474.

[113] Leroy, B. (1980). Propagation of waves in an atmosphere in the presence of a magnetic field. II - The reflection of Alfven waves. *Astron. Astrophys.*, 91:136–146.

[114] Leroy, B. (1981). Propagation of waves in an atmosphere in the presence of a magnetic field. III - Alfven waves in the solar atmosphere. *Astron. Astrophys.*, 97:245–250.

[115] Leroy, B. and Schwartz, S. J. (1982). Propagation of waves in an atmosphere in the presence of a magnetic field. V - The theory of magneto-acoustic-gravity oscillations. *Astron. Astrophys.*, 112:84.

[116] Lighthill, J. (1978). *Waves in Fluids*. Cambridge University Press, Cambridge.

[117] Lundquist, S. (1949). Experimental Investigations of Magneto-Hydrodynamic Waves. *Physical Review*, 76:1805–1809.

[118] MacDonald, G. J. F. (1961). Spectrum of Hydromagnetic Waves in the Exosphere. *J. Geophys. Res.*, 66:3639–3670.

[119] Mather, J. F. and Erdélyi, R. (2016). Magneto-Acoustic Waves in a Gravitationally Stratified Magnetized Plasma: Eigen-Solutions and their Applications to the Solar Atmosphere. *Astrophys. J.*, 822:116.

[120] Mathioudakis, M., Jess, D. B., and Erdélyi, R. (2013). Alfvén Waves in the Solar Atmosphere. From Theory to Observations. *Space Sci. Rev.*, 175:1–27.

[121] McDougall, A. M. D. and Hood, A. W. (2007). A New Look at Mode Conversion in a Stratified Isothermal Atmosphere. *Solar Phys.*, 246:259–271.

[122] McKenzie, J. F. and Axford, W. I. (2000). Hydromagnetic Gravity Waves in the Solar Atmosphere. *Astrophys. J.*, 537:516–523.

[123] Miles, A. J., Allen, H. R., and Roberts, B. (1992). Magnetoacoustic-gravity surface waves. II - Uniform magnetic field. *Solar Phys.*, 141:235–251.

[124] Miles, A. J. and Roberts, B. (1992). Magnetoacoustic-gravity surface waves. I - Constant Alfven speed. *Solar Phys.*, 141:205–234.

[125] Moreno-Insertis, F. and Spruit, H. C. (1989). Stability of sunspots to convective motions. I - Adiabatic instability. *Astrophys. J.*, 342:1158–1171.

[126] Mumford, S. J., Fedun, V., and Erdélyi, R. (2015). Generation of Magnetohydrodynamic Waves in Low Solar Atmospheric Flux Tubes by Photospheric Motions. *Astrophys. J.*, 799:6.

[127] Musielak, Z. E., Moore, R. L., Suess, S. T., and An, C.-H. (1989). Propagating and nonpropagating compression waves in an isothermal atmosphere with uniform horizontal magnetic field. *Astrophys. J.*, 344:478–493.

[128] Nakariakov, V. M. and Ofman, L. (2001). Determination of the coronal magnetic field by coronal loop oscillations. *Astron. Astrophys.*, 372:L53–L56.

[129] Newington, M. E. and Cally, P. S. (2010). Reflection and conversion of magnetogravity waves in the solar chromosphere: windows to the upper atmosphere. *Mon. Not. Roy. Astron. Soc.*, 402:386–394.

[130] Nye, A. H. and Thomas, J. H. (1976). Solar magneto-atmospheric waves. I - an exact solution for a horizontal magnetic field. *Astrophys. J.*, 204:573–588.

[131] Ogura, Y. and Phillips, N. A. (1962). Scale Analysis of Deep and Shallow Convection in the Atmosphere. *Journal of Atmospheric Sciences*, 19:173–179.

[132] Pintér, B. (1999). *PhD Thesis*. Katholieke Universiteit Leuven, Belgium.

[133] Pintér, B. (2008). Modelling the Coupling Role of Magnetic Fields in Helioseismology. *Solar Phys.*, 251:329–340.

[134] Pinter, B., Cadez, V. M., and Goossens, M. (1998). MHD eigenmodes in a semi-infinite structured solar atmosphere. *Astron. Astrophys.*, 332:775–785.

[135] Pintér, B. and Erdélyi, R. (2011). Effects of Magnetic Fields in the Solar Atmosphere on Global Oscillations. *Space Sci. Rev.*, 158:471–504.

[136] Pintér, B., Erdélyi, R., and Goossens, M. (2007). Global oscillations in a magnetic solar model. II. Oblique propagation. *Astron. Astrophys.*, 466:377–388.

[137] Pintér, B., Erdélyi, R., and New, R. (2001). Damping of helioseismic modes in steady state. *Astron. Astrophys.*, 372:L17–L20.

[138] Pintér, B. and Goossens, M. (1999). Oscillations in a magnetic solar model. I. Parallel propagation in a chromospheric and coronal magnetic field with constant Alfvén speed. *Astron. Astrophys.*, 347:321–334.

[139] Pintér, B., Čadež , V. M., and Roberts, B. (1999). Waves and instabilities in a stratified isothermal atmosphere with constant Alfvén speed - revisited. *Astron. Astrophys.*, 346:190–198.

[140] Priest, E. (2014). *Magnetohydrodynamics of the Sun*. Cambridge University Press, Cambridge, UK.

[141] Reardon, K. P., Wang, Y.-M., Muglach, K., and Warren, H. P. (2011). Evidence for Two Separate but Interlaced Components of the Chromospheric Magnetic Field. *Astrophys. J.*, 742:119.

[142] Roberts, B. (1981a). Wave Propagation in a Magnetically Structured Atmosphere - Part Two - Waves in a Magnetic Slab. *Solar Phys.*, 69:39–56.

[143] Roberts, B. (1981b). Wave propagation in a magnetically structured atmosphere. I - Surface waves at a magnetic interface. *Solar Phys.*, 69:27–38.

[144] Roberts, B. (2000). Waves and Oscillations in the Corona - (Invited Review). *Solar Phys.*, 193:139–152.

[145] Roberts, B. (2006). Slow magnetohydrodynamic waves in the solar atmosphere. *Royal Society of London Philosophical Transactions Series A*, 364:447.

[146] Roberts, B., Edwin, P. M., and Benz, A. O. (1984). On coronal oscillations. *Astrophys. J.*, 279:857–865.

[147] Ronveaux, A., editor (1995). *Heun's Differential Equations*. Oxford University Press, Oxford.

[148] Rosenberg, H. (1970). Evidence for MHD Pulsations in the Solar Corona. *Astron. Astrophys.*, 9:159.

[149] Ruderman, M. S. and Erdélyi, R. (2009). Transverse Oscillations of Coronal Loops. *Space Sci. Rev.*, 149:199–228.

[150] Scherrer, P. H., Bogart, R. S., Bush, R. I., Hoeksema, J. T., Kosovichev, A. G., Schou, J., Rosenberg, W., Springer, L., Tarbell, T. D., Title, A., Wolfson, C. J., Zayer, I., and MDI Engineering Team (1995). The Solar Oscillations Investigation - Michelson Doppler Imager. *Solar Phys.*, 162:129–188.

[151] Scheuer, M. A. and Thomas, J. H. (1981). Umbral oscillations as resonant modes of magneto-atmospheric waves. *Solar Phys.*, 71:21–38.

[152] Schunker, H. and Cally, P. S. (2006). Magnetic field inclination and atmospheric oscillations above solar active regions. *Mon. Not. Roy. Astron. Soc.*, 372:551–564.

[153] Schwartz, S. J. and Leroy, B. (1982). Propagation of Waves in an Atmosphere in the Presence of a Magnetic Field - Part Six - Application of Magneto-Acoustic Mode Theory to the Solar Atmosphere. *Astron. Astrophys.*, 112:93.

[154] Shelyag, S., Zharkov, S., Fedun, V., Erdélyi, R., and Thompson, M. J. (2009). Acoustic wave propagation in the solar sub-photosphere with localised magnetic field concentration: effect of magnetic tension. *Astron. Astrophys.*, 501:735–743.

[155] Soler, R., Carbonell, M., and Ballester, J. L. (2013a). Magnetoacoustic Waves in a Partially Ionized Two-fluid Plasma. *ApJS*, 209:16.

[156] Soler, R., Carbonell, M., Ballester, J. L., and Terradas, J. (2013b). Alfvén Waves in a Partially Ionized Two-fluid Plasma. *Astrophys. J.*, 767:171.

[157] Soler, R., Díaz, A. J., Ballester, J. L., and Goossens, M. (2012). Kelvin-Helmholtz Instability in Partially Ionized Compressible Plasmas. *Astrophys. J.*, 749:163.

[158] Soler, R., Díaz, A. J., Ballester, J. L., and Goossens, M. (2013c). Effect of partial ionization on wave propagation in solar magnetic flux tubes. *Astron. Astrophys.*, 551:A86.

[159] Soler, R., Oliver, R., and Ballester, J. L. (2009a). Magnetohydrodynamic Waves in a Partially Ionized Filament Thread. *Astrophys. J.*, 699:1553–1562.

[160] Soler, R., Oliver, R., and Ballester, J. L. (2009b). Resonantly Damped Kink Magnetohydrodynamic Waves in a Partially Ionized Filament Thread. *Astrophys. J.*, 707:662–670.

[161] Soler, R., Oliver, R., and Ballester, J. L. (2010). Time damping of non-adiabatic magnetohydrodynamic waves in a partially ionized prominence plasma: effect of helium. *Astron. Astrophys.*, 512:A28.

[162] Spiegel, E. A. and Unno, W. (1962). On Convective Growth-rates in a Polytropic Atmosphere. *Pub. Astron. Soc. Japan*, 14:28.

[163] Spiegel, E. A. and Veronis, G. (1960). On the Boussinesq Approximation for a Compressible Fluid. *Astrophys. J.*, 131:442.

[164] Spruit, H. C. and Bogdan, T. J. (1992). The conversion of p-modes to slow modes and the absorption of acoustic waves by sunspots. *Astrophys. J. Lett.*, 391:L109–L112.

[165] Staicova, D. (2012). *PhD Thesis*. Sofia University "Sv. Kliment Ohridski", Bulgaria.

[166] Stark, B. A. and Musielak, Z. E. (1993). The cutoff frequency for fast-mode magnetohydrodynamic waves in an isothermal atmosphere with a uniform horizontal magnetic field. *Astrophys. J.*, 409:450–454.

[167] Stodilka, M. I. (2008). On the detection of internal gravity waves in the solar photosphere. *Mon. Not. Roy. Astron. Soc.*, 390:L83–L87.

[168] Straus, T., Fleck, B., Jefferies, S. M., Cauzzi, G., McIntosh, S. W., Reardon, K., Severino, G., and Steffen, M. (2008). The Energy Flux of Internal Gravity Waves in the Lower Solar Atmosphere. *Astrophys. J. Lett.*, 681:L125–L128.

[169] Syrovatskii, S. I. and Zhugzhda, Y. D. (1968). Oscillatory Convection of a Conducting Gas in a Strong Magnetic Field. *Soviet Astron.*, 11:945.

[170] Taroyan, Y. (2004). *PhD Thesis*. The University of Sheffield, UK.

[171] Taroyan, Y. and Doyle, J. G. (2004). Solar Oscillations and the Magnetic Atmosphere. *Publications of the Astronomy Department of the Eotvos Lorand University*, 14:129–140.

[172] Taroyan, Y. and Erdélyi, R. (2008). Global Acoustic Resonance in a Stratified Solar Atmosphere. *Solar Phys.*, 251:523–531.

[173] Thomas, J. H. (1982). The local dispersion relation for magneto-atmospheric waves. *Astrophys. J.*, 262:760–767.

[174] Thomas, J. H. (1983). Magneto-atmospheric waves. *Annual Review of Fluid Mechanics*, 15:321–343.

[175] Thompson, M. J. (2006a). *An Introduction to Astrophysical Fluid Dynamics*. Imperial College Press.

[176] Thompson, M. J. (2006b). Magnetohelioseismology. *Royal Society of London Philosophical Transactions Series A*, 364:297–311.

[177] Thompson, M. J., Christensen-Dalsgaard, J., Miesch, M. S., and Toomre, J. (2003). The Internal Rotation of the Sun. *Ann. Rev. Astron. Astrophys.*, 41:599–643.

[178] Tirry, W. J., Goossens, M., Pinter, B., Cadez, V., and Vanlommel, P. (1998). Resonant Damping of Solar p-Modes by the Chromospheric Magnetic Field. *Astrophys. J.*, 503:422.

[179] Tracy, E. R., Kaufman, A. N., and Brizard, A. J. (2003). Ray-based methods in multidimensional linear wave conversion. *Physics of Plasmas*, 10:2147–2154.

[180] Uchida, Y. (1970). Diagnosis of Coronal Magnetic Structure by Flare-Associated Hydromagnetic Disturbances. *Pub. Astron. Soc. Japan*, 22:341.

[181] Ulrich, R. K. (1970). The Five-Minute Oscillations on the Solar Surface. *Astrophys. J.*, 162:993.

[182] Unno, W., Osaki, Y., Ando, H., Saio, H., and Shibahashi, H. (1989). *Nonradial Oscillations of Stars*. University of Tokyo Press, Tokyo.

[183] Van Dyke, M. (1975). *Perturbation Methods In Fluid Mechanics*. The Parabolic Press, Stanford, California.

[184] Vernazza, J. E., Avrett, E. H., and Loeser, R. (1981). Structure of the solar chromosphere. III - Models of the EUV brightness components of the quiet-sun. *ApJS*, 45:635–725.

[185] Verth, G., Erdélyi, R., and Jess, D. B. (2008). Refined Magnetoseismological Technique for the Solar Corona. *Astrophys. J. Lett.*, 687:L45.

[186] Vranjes, J., Poedts, S., Pandey, B. P., and de Pontieu, B. (2008). Energy flux of Alfvén waves in weakly ionized plasma. *Astron. Astrophys.*, 478:553–558.

[187] Waelkens, C. (1991). Slowly pulsating B stars. *Astron. Astrophys.*, 246:453–468.

[188] Wang, T. (2011). Standing Slow-Mode Waves in Hot Coronal Loops: Observations, Modeling, and Coronal Seismology. *Space Sci. Rev.*, 158:397–419.

[189] Whitham, G. B. (1974). *Linear and Nonlinear Waves*. Wiley, New York.

[190] Winget, D. E. and Kepler, S. O. (2008). Pulsating White Dwarf Stars and Precision Asteroseismology. *Ann. Rev. Astron. Astrophys.*, 46:157–199.

[191] Yu, C. P. (1965). Magneto-Atmospheric Waves in a Horizontally Stratified Conducting Medium. *Physics of Fluids*, 8:650–656.

[192] Zaqarashvili, T. V., Khodachenko, M. L., and Rucker, H. O. (2011a). Damping of Alfvén waves in solar partially ionized plasmas: effect of neutral helium in multi-fluid approach. *Astron. Astrophys.*, 534:A93.

[193] Zaqarashvili, T. V., Khodachenko, M. L., and Rucker, H. O. (2011b). Magnetohydrodynamic waves in solar partially ionized plasmas: two-fluid approach. *Astron. Astrophys.*, 529:A82.

[194] Zhugzhda, Y. D. (1979). Magnetogravity waves in an isothermal conductive atmosphere. *Soviet Astron.*, 23:42.

[195] Zhugzhda, Y. D. and Dzhalilov, N. S. (1981). Conversion of Magnetogravitational Waves in the Solar Atmosphere. *Soviet Astron.*, 25:477.

[196] Zhugzhda, Y. D. and Dzhalilov, N. S. (1982). Transformation of magnetogravitational waves in the solar atmosphere. *Astron. Astrophys.*, 112:16–23.

[197] Zhugzhda, Y. D. and Dzhalilov, N. S. (1984a). Magneto-acoustic-gravity waves on the Sun. I - Exact solution for an oblique magnetic field. *Astron. Astrophys.*, 132:45–51.

[198] Zhugzhda, Y. D. and Dzhalilov, N. S. (1984b). Magneto-acoustic-gravity waves on the Sun. II - Transformation and Propagation. *Astron. Astrophys.*, 132:52.

[199] Zhukov, V. I. (1985). On the linear transformation and resonant absorption of Alfven p-modes in sunspots. *Solar Phys.*, 98:39–50.

[200] Zhukov, V. I. (2002). Oscillations on the Sun in regions with a vertical magnetic field. I. Sunspot umbral oscillations. *Astron. Astrophys.*, 386:653–657.

[201] Zhukov, V. I. (2005). Oscillations on the Sun in regions with a vertical magnetic field. II. On the calculation of the sunspot umbral oscillations. *Astron. Astrophys.*, 433:1127–1132.

[202] Zhukov, V. I. and Efremov, V. I. (1988). Propagation of magnetohydrodynamic waves in the solar atmosphere - Alfven p-waves in sunspots. *Bulletin of the Astronomical Society of India*, 16:145–158.

[203] Zwillinger, D. (1989). *Handbook Of Differential Equations*. Academic Press, inc, London, Uk.

Appendix A

Approximate Analytical Frequencies Derived From Dispersion Relation (3.181)

In Section 3.2.3 the dispersion relation for waves in a two-layer model consisting of a finite, high-β lower layer and a semi-infinite atmosphere was found to be

$$\tan Q = \mathrm{i}\frac{\left(\omega^2 - N_0^2\right)^{1/2}}{\left(\omega^2 - N^2\right)^{1/2}}, \tag{A.1}$$

where

$$Q = \frac{2\omega z_0}{\widehat{v_A}\,(m+2)}\left[\left(1+\frac{L}{z_0}\right)^{\frac{m+2}{2}} {}_2F_1\left(-\frac{1}{2},-1-\frac{m}{2};-\frac{m}{2};\frac{N_0^2}{\omega^2}\left(1+\frac{L}{z_0}\right)^{-1}\right) - {}_2F_1\left(-\frac{1}{2},-1-\frac{m}{2};-\frac{m}{2};\frac{N_0^2}{\omega^2}\right)\right]. \tag{A.2}$$

The dispersion relation was derived using the integral expression for S_i, the phase function found in the WKB analysis. S_i may be written in terms of hypergeometric functions, which leads to the equivalent form of the dispersion relation

$$\tan(Q) = -\omega\left(N^2-\omega^2\right)^{-1/2}\left[{}_2F_1\left(-\frac{1}{2},-1-\frac{m}{2};-\frac{m}{2};\frac{N_0^2}{\omega^2}\right) + \frac{N_0^2}{m\omega^2}\,{}_2F_1\left(\frac{1}{2},-\frac{m}{2};1-\frac{m}{2};\frac{N_0^2}{\omega^2}\right)\right], \tag{A.3}$$

where

$$Q = \frac{2\omega z_0}{\widehat{v_A}\,(m+2)}\left[\left(1+\frac{L}{z_0}\right)^{\frac{m+2}{2}} {}_2F_1\left(-\frac{1}{2},-1-\frac{m}{2};-\frac{m}{2};\frac{N_0^2}{\omega^2}\left(1+\frac{L}{z_0}\right)^{-1}\right) - {}_2F_1\left(-\frac{1}{2},-1-\frac{m}{2};-\frac{m}{2};\frac{N_0^2}{\omega^2}\right)\right]. \tag{A.4}$$

By writing the dispersion relation in this form we may investigate it analytically in various, although limited, cases.

We begin by writing the equation as

$$Q = \arctan\left(-\omega\left(N^2-\omega^2\right)^{-1/2}\left[{}_2F_1\left(-\frac{1}{2},-1-\frac{m}{2};-\frac{m}{2};\frac{N_0^2}{\omega^2}\right)+\right.\right.$$
$$\left.\left.\frac{N_0^2}{m\omega^2}\,{}_2F_1\left(\frac{1}{2},-\frac{m}{2};1-\frac{m}{2};\frac{N_0^2}{\omega^2}\right)\right]\right)+n\pi, \quad n=0,1,2,3,\ldots, \tag{A.5}$$

where the term $n\pi$ is due to the periodicity of the tangent function.

Analytical progress is possible if we consider frequencies close to the Brunt-Väisälä frequency in the lower layer, that is $N_0^2/\omega^2 \approx 1$. Let us Taylor expand the hypergeometric function around the point $N_0^2/\omega^2 = 1$. We retain the first two terms in the series, *e.g.*

$${}_2F_1\left(N_0^2/\omega^2\right) = {}_2F_1(1) + {}_2F_1'(1)\left(\frac{N_0^2}{\omega^2}-1\right)+O\left(\left(\frac{N_0^2}{\omega^2}-1\right)^2\right). \tag{A.6}$$

Taylor expanding the hypergeometric functions in the argument of the inverse tangent term, it can be shown that the first non-zero term in the expansion is of order $(N_0^2/\omega^2-1)^2$. Making note of the series expansion of $\arctan(z)$ in the region $|z|<1$, we may therefore treat the arctan function as a second order small term. Keeping only small terms to first order, the dispersion relation may be approximated by

$$\frac{2\omega z_0}{\widehat{v_A}\,(m+2)}\left[A+B\left(\frac{N_0^2}{\omega^2}-1\right)\right]=n\pi, \tag{A.7}$$

or

$$(A-B)\,\omega^2-\frac{n\pi\widehat{v_A}\,(m+2)}{2z_0}\omega+BN_0^2=0, \tag{A.8}$$

where

$$A=\left(1+\frac{L}{z_0}\right)^{\frac{m+2}{2}}{}_2F_1\left(-\frac{1}{2},-1-\frac{m}{2};-\frac{m}{2};\left(1+\frac{L}{z_0}\right)^{-1}\right)-{}_2F_1\left(-\frac{1}{2},-1-\frac{m}{2};-\frac{m}{2};1\right), \tag{A.9}$$

$$B=\left(1+\frac{L}{z_0}\right)^{m/2}{}_2F_1'\left(-\frac{1}{2},-1-\frac{m}{2};-\frac{m}{2};\left(1+\frac{L}{z_0}\right)^{-1}\right)-{}_2F_1'\left(-\frac{1}{2},-1-\frac{m}{2};-\frac{m}{2};1\right). \tag{A.10}$$

The above equation can be simply solved to determine the resonant frequencies. Considering the fundamental mode $n=0$, the frequency takes the form

$$\omega^2=\frac{BN_0^2}{B-A}. \tag{A.11}$$

Note that in this limit magnetic effects are not felt by the fundamental mode of the resonance. To see magnetic effects we must look at higher harmonics. We may also consider the case that the lower layer is thin $L/z_0 \ll 1$, Taylor expanding A and B leads to

$$A \approx \frac{1}{2}B\left(\frac{1}{2},-\frac{m}{2}\right)\left[\frac{m(m+2)}{8}-\frac{(m+2)^2}{4}-\frac{1+(m/2)}{2-m}\right]\frac{L^2}{z_0^2}, \tag{A.12}$$

$$\begin{aligned} B \approx B\left(1-\frac{m}{2},-\frac{1}{2}\right)\left(\frac{5m}{8}-\frac{3}{4}\right)\frac{L}{z_0}+\frac{1}{2}\Bigg({}_2F_1'''\left(-\frac{1}{2},-1-\frac{m}{2};-\frac{m}{2};1\right) \\ -m\,{}_2F_1''\left(-\frac{1}{2},-1-\frac{m}{2};-\frac{m}{2};1\right)+m\left(\frac{m}{2}-1\right){}_2F_1'\left(-\frac{1}{2},-1-\frac{m}{2};-\frac{m}{2};1\right)\Bigg)\frac{L^2}{z_0^2}. \end{aligned} \tag{A.13}$$

To lowest order, A is second order small, whereas B is first order small. To leading order then, the fundamental mode takes the form

$$\omega^2 \approx N_0^2. \tag{A.14}$$

To calculate the correction, we keep the next term in L/z_0. Writing the series expansions of the parameters A and B as $A = A_2(L^2/z_0^2)$, $B = B_1(L/z_0) + B_2(L^2/z_0^2)$ we can write the fundamental frequency as

$$\omega^2 = N_0^2\frac{B_1+B_2(L/z_0)}{B_1+(B_2+A_2)(L/z_0)} \approx N_0^2\left(1+\frac{B_2}{B_1}\frac{L}{z_0}\right)\left(1-\frac{B_2+A_2}{B_1}\frac{L}{z_0}\right) \approx N_0^2\left(1-\frac{A_2}{B_1}\frac{L}{z_0}\right). \tag{A.15}$$

For typical solar parameters it can be shown that the quantity A_2/B_1 is negative, hence the frequencies are above the Brunt-Väisälä frequency in the lower layer.

Another route to simplification is to consider the case that the lower layer is close to adiabatic, that is the temperature variation is such that the effects of buoyancy are small. In terms of parameters, m is close to $3/2$. When this is the case $N_0 \approx 0$; to leading order the hypergeometric functions are evaluated at zero. Due to the complicated form of the dispersion relation, we consider only leading order behaviour, for simplicity. When this is the case, the dispersion relation may be written

$$\tan\left(\frac{2\omega z_0}{\widehat{v}_A\,(m+2)}\left(\left(1+\frac{L}{z_0}\right)^{\frac{m+2}{2}}-1\right)\right) = -\frac{\omega}{\left(N^2-\omega^2\right)^{1/2}}. \tag{A.16}$$

We shall also let the lower layer be thin, so $L/z_0 \ll 1$. Taylor expanding the interior of the tangent function and keeping terms to lowest order, the dispersion take the form

$$\tan\left(\frac{\omega L}{\widehat{v}_A}\right) = -\frac{\omega}{\left(N^2-\omega^2\right)^{1/2}}. \tag{A.17}$$

This equation is still transcendental in nature and so may no be analytically inverted. We noted previously that the resonant frequencies are located below the Brunt-Väisälä

frequency N. For most solar applications the medium is such that the Brunt-Väisälä frequency is low compared to the frequency of acoustic oscillations; that is the frequencies of g-modes are smaller than p-modes (this is one reason they are difficult to observe). If we suppose that ω is of comparable order to N, and noting that we supposed L was small compared to z_0. Applying typical photospheric parameters we may estimate that $\omega L/v_A \approx 0.5$. We may consider this to be small compared to $\pi/2$ and so Taylor expand the tangent function. To leading order the fundamental mode of the global resonance is given by

$$\omega^2 = N^2 - \frac{v_A^2}{L^2}. \tag{A.18}$$

The above expression is located below the Brunt-Väisälä frequency in the upper layer as the original equation suggested. Note that the same result would be achieved if we do not consider the layer to be close to adiabatic, but have a large separation in Brunt-Väisälä frequencies so that $N_0 \ll \omega < N$.

Finally, let us consider a final, simplification, that is $\omega \ll N$ and $N_0 \approx 0$. The dispersion relation may then be written

$$\frac{2\omega z_0}{\widehat{v_A}\,(m+2)}\left(\left(1+\frac{L}{z_0}\right)^{\frac{m+2}{2}} - 1\right) = n\pi + \arctan\left(-\frac{\omega}{N}\right) \approx -\frac{\omega}{N}. \tag{A.19}$$

The frequency is given by a simple rearrangement. Let us focus on the case of a thin layer. Taylor expanding and keeping the lowest order term gives us

$$\frac{\omega L}{\widehat{v_A}} = n\pi - \frac{\omega}{N} \implies \omega = \frac{n\pi \widehat{v_A} N}{LN + \widehat{v_A}}. \tag{A.20}$$

This expression grows without bound as n increases and so is clearly not valid for all n. The a priori assumption that $\omega \ll N$ translates to the conditions that

$$\frac{\widehat{v_A}}{L}(n\pi - 1) \ll N. \tag{A.21}$$

Using typical photospheric parameters $N \approx 0.03$ s^{-1}; let us take L to be 100km (so that we may apply $L/z_0 \ll 1$, with $z_0 = 400$km and so $m \approx 1.85$) and choose the value of $v_A = 0.25$ km s^{-1}. This choice of Alfvén speed is based on $\epsilon = 0.001$. When this is the case the above inequality becomes $n \ll\approx 4$. The values of $n = 0, 1$ may be considered satisfactory choices for n. Clearly, the validity of this expression for the frequencies depends on the choice of parameters. Provided that the underlying assumptions are satisfied, the expression for the frequencies may be applied to higher harmonics for different choices of the parameters.

Appendix B

Boussinesq Approximation in a Horizontal Field: Three-Layer Model

The temperature profile of the upper solar interior and lower solar atmosphere is much more structured than the two-layer model previously applied. Let us allow more variation in the temperature by adding a third non-magnetic polytropic layer of length L to the previous two-layer model. Such a model may be applied to model several solar phenomena such as a radiative interior/convection zone/magnetic chromosphere; convection zone/photosphere/chromosphere; or photosphere to temperature minimum/temperature increase in the low chromosphere/isothermal, magnetic chromosphere; depending on the relative magnitude or sign of the temperature scale height. The interior, central and exterior layers are denoted by the subscripts i, c and e. As in the two-layer model, the gravitational field is directed in the positive z-direction.

The boundary conditions at positive and negative infinity are as in the previous subsection. The solutions to the governing equations in each region are

$$z > L: \quad q = C_2 \left(2k\left(z + z_{0i}\right)\right) e^{-k\left(z+z_{0i}\right)} U\left(1 - \frac{k z_{0i} N_{0i}^2}{2\omega^2}, 2, 2k\left(z + z_{0i}\right)\right), \tag{B.1}$$

$$0 < z < L: \quad q = 2k\left(z + z_{0c}\right) e^{-k\left(z+z_{0c}\right)} \left[D_1 M\left(1 - \frac{k z_{0c} N_{0c}^2}{2\omega^2}, 2, 2k\left(z + z_{0c}\right)\right) + D_2 U\left(1 - \frac{k z_{0c} N_{0c}^2}{2\omega^2}, 2, 2k\left(z + z_{0c}\right)\right)\right], \tag{B.2}$$

$$z < 0: \quad \xi_z = E_2 e^{m-z}. \tag{B.3}$$

Connecting the layers together via continuity of displacement and Lagrangian pressure perturbations at $z = L$ and $z = 0$; a significant amount of algebra leads to the dispersion

relation

$$\Big[M_c(0)U_c(L)-M_c(L)U_c(0)\Big]\Big\{U_i(L)\Big(\frac{z_{0i}}{\widehat{\rho_i}}\Big[\omega^2-k_x(L+z_{0c})\Big(\omega^2-gk_x\Big)\Big]-\frac{z_{0c}}{\widehat{\rho_c}}[\omega^2-$$
$$k_x(L+z_{0i})\Big(\omega^2-gk_x\Big)]\Big)-\frac{2\omega^2 z_{0c}k_x(L+z_{0i})}{\widehat{\rho_c}}U_i'(L)\Big\}\Big\{\omega^2H_B-\omega^2z_{0c}k_xH_B+gk_x^2z_{0c}H_B-$$
$$z_{0c}\frac{\widehat{\rho_e}}{\widehat{\rho_c}}\Big[\Big(\omega^2-v_A^2k_x^2\Big)m_-H_B+\omega^2+gk_x^2H_B\Big]\Big\}+2\omega^2z_{0c}H_Bk_x\Big[M_c'(0)U_c(L)-M_c(L)U_c'(0)\Big]\Big\{U_i(L)\Big(\frac{z_{0i}}{\widehat{\rho_i}}[\omega^2$$
$$-k_x(L+z_{0c})\Big(\omega^2-gk_x\Big)]-\frac{z_{0c}}{\widehat{\rho_c}}[\omega^2-k_x(L+z_{0i})\Big(\omega^2-gk_x\Big)]\Big)-\frac{2\omega^2z_{0c}k_x(L+z_{0i})}{\widehat{\rho_c}}U_i'(L)\Big\}$$
$$+\frac{2z_{0i}k_x\omega^2(L+z_{0c})}{\widehat{\rho_i}}U_i(L)[M_c(0)U_c'(L)-M_c'(L)U_c(0)]\Big\{\omega^2H_B-\omega^2z_{0c}k_xH_B+gk_x^2z_{0c}H_B-$$
$$z_{0c}\frac{\widehat{\rho_e}}{\widehat{\rho_c}}\Big[\Big(\omega^2-v_A^2k_x^2\Big)m_-H_B+\omega^2+gk_x^2H_B\Big]\Big\}+\frac{4\omega^4z_{0c}z_{0i}k_x^2H_B(L+z_{0i})}{\widehat{\rho_i}}[M_c'(0)U_c'(L)-M_c'(L)U_c'(0)]=0, \tag{B.4}$$

where we, for simplicity, let $k_y = 0$ and use the notation

$$M_c(0)=M\left(1-\frac{kz_{0c}N_{0c}^2}{2\omega^2},2,2k_xz_{0c}\right),\ U_i'(L)=U'\left(1-\frac{kz_{0i}N_{0i}^2}{2\omega^2},2,2k(z+z_{0i})\right),\quad \text{ect.} \tag{B.5}$$

It may be shown that the three-layer dispersion relation reduces to the two-layer equation in the limit $L \to 0$, as we expect. We shall solve this dispersion relation numerically, although a limiting solution may be found via an asymptotic analysis as in the previous two-layer study. In the limit $k_xz_0 \to \infty$, the hypergeometric functions may be expanded (again with the a priori assumption that κ does not grow with k_x, which we will see to be justified). Keeping only the exponential term in the asymptotic expansion of the Kummer M functions, we have

$$M_c(0)U_c(L)-M_c(L)U_c(0)\sim\frac{1}{\Gamma(1-\kappa_c)}e^{2k_xz_{0c}}\Big[(2k_xz_{0c})^{-1-\kappa_c}(2k_x(z_{0c}+L))^{\kappa_c-1}-$$
$$e^{2k_xL}(2k_xz_{0c})^{\kappa_c-1}(2k_x(z_{0c}+L))^{-1-\kappa_c}\Big], \tag{B.6}$$

$$M_c'(0)U_c(L)-M_c(L)U_c'(0)\sim\frac{1}{\Gamma(1-\kappa_c)}e^{2k_xz_{0c}}\Big[(2k_xz_{0c})^{-1-\kappa_c}(2k_x(z_{0c}+L))^{\kappa_c-1}+$$
$$(1-\kappa_c)e^{2k_xL}(2k_xz_{0c})^{\kappa_c-2}(2k_x(z_{0c}+L))^{-1-\kappa_c}\Big], \tag{B.7}$$

$$M_c(0)U_c'(L)-M_c'(L)U_c(0)\sim-\frac{1}{\Gamma(1-\kappa_c)}e^{2k_xz_{0c}}\Big[(1-\kappa_c)(2k_xz_{0c})^{-1-\kappa_c}(2k_x(z_{0c}+L))^{\kappa_c-2}+$$
$$e^{2k_xL}(2k_xz_{0c})^{\kappa_c-1}(2k_x(z_{0c}+L))^{-1-\kappa_c}\Big], \tag{B.8}$$

$$M_c'(0)U_c'(L)-M_c'(L)U_c'(0)\sim(1-\kappa_c)\frac{1}{\Gamma(1-\kappa_c)}e^{2k_xz_{0c}}\Big[e^{2k_xL}(2k_xz_{0c})^{\kappa_c-2}(2k_x(z_{0c}+L))^{-1-\kappa_c}- (2k_xz_{0c})^{-1-\kappa_c}(2k_x(z_{0c}+L))^{\kappa_c-2}\Big]. \quad \text{(B.9)}$$

Keeping only the exponential terms, the dispersion relation may then be approximated by

$$\begin{aligned}
&\left\{\frac{z_{0c}}{\widehat{\rho_c}}\left[\omega^2-\omega^2k_x(L+z_{0i})+gk_x^2(L+z_{0i})\right]-\frac{z_{0i}}{\widehat{\rho_i}}[\omega^2-\omega^2k_x(L+z_{0c})+gk_x^2(L+z_{0c})]-\right.\\
&\left.\frac{z_{0c}}{\widehat{\rho_c}}\left(\omega^2-\frac{k_xz_{0i}N_{0i}^2}{2}\right)\right\}\left\{\omega^2H_B-\omega^2z_{0c}k_xH_B+gk_x^2z_{0c}H_B-z_{0c}\frac{\widehat{\rho_e}}{\widehat{\rho_c}}\left[\left(\omega^2-v_A^2k_x^2\right)m_-H_B+\omega^2+gk_x^2H_B\right]\right\}\\
&+H_B\left(\omega^2-\frac{k_xz_{0c}N_{0c}^2}{2}\right)\left\{\frac{z_{0i}}{\widehat{\rho_i}}[\omega^2-\omega^2k_x(L+z_{0c})+gk_x^2(L+z_{0c})]-\frac{z_{0c}}{\widehat{\rho_c}}[\omega^2-\omega^2k_x(L+z_{0i})+gk_x^2(L+z_{0i})]\right.\\
&\left.+\frac{z_{0c}}{\widehat{\rho_c}}\left(\omega^2-\frac{k_xz_{0i}N_{0i}^2}{2}\right)\right\}-\frac{2z_{0i}\omega^2(L+z_{0c})k_x}{\widehat{\rho_i}}\left\{\omega^2H_B-\omega^2z_{0c}k_xH_B+gk_x^2z_{0c}H_B-\right.\\
&\left.z_{0c}\frac{\widehat{\rho_e}}{\widehat{\rho_c}}\left[\left(\omega^2-v_A^2k_x^2\right)m_-H_B+\omega^2+gk_x^2H_B\right]\right\}+\frac{2\omega^2z_{0i}k_xH_B(L+z_{0c})}{\widehat{\rho_i}}\left(\omega^2-\frac{k_xz_{0c}N_{0c}^2}{2}\right)=0.
\end{aligned} \quad \text{(B.10)}$$

To simplify the problem further, we expand the m_- term asymptotically,

$$\begin{aligned}
\left(\omega^2-v_A^2k_x^2\right)m_-H_B&=-\frac{1}{2}\left(2\omega^2-v_A^2k_x^2\right)+k_x^2H_B\left[v_A^4+\left(\frac{v_A^4}{4H_B}+N^2-2\omega^2\right)\frac{z_{0c}^2}{\widetilde{k}^2}+\omega^2\left(\omega^2-N^2\right)\frac{z_{0c}^2}{\widetilde{k}^4}\right]^{1/2}\\
&\sim v_A^2H_Bk_x^3+\frac{v_A^2}{2}k_x^2+\frac{H_B}{2}\left(\frac{v_A^2}{4H_B}+N^2-2\omega^2\right)k_x-\omega^2+O\left(\widetilde{k}^{-1}\right), \quad \text{as} \quad \widetilde{k}\to\infty, \quad \text{(B.11)}
\end{aligned}$$

where $\widetilde{k}=k_xz_{0c}$. Using this in the simplified dispersion relation (B.10), we may find the dominant contribution to the frequency by keeping terms of orders k_x^5 and k_x^4,

$$\begin{aligned}
&\omega^2v_A^2\left[1+\frac{L}{z_{0c}}+\frac{\widehat{\rho_i}}{\widehat{\rho_c}}\left(1+\frac{L}{z_{0i}}\right)\right]=\\
&\left[gk_xv_A^2-g^2\frac{\widehat{\rho_c^2}}{\widehat{\rho_e^2}}\left(1-\frac{\widehat{\rho_e}}{\widehat{\rho_i}}\right)+\frac{gv_A^2}{2H_B}\right]\left[\frac{\widehat{\rho_i}}{\widehat{\rho_c}}\left(1+\frac{L}{z_{0i}}\right)-\frac{L}{z_{0c}}-1\right]+\frac{N_{0c}^2\widehat{\rho_i}z_{0c}v_A^2}{2\widehat{\rho_c}z_{0i}}.
\end{aligned} \quad \text{(B.12)}$$

The frequency is simply determined by rearranging the above. To leading order the frequency is given by

$$\omega^2\sim gk_x\left[\frac{\widehat{\rho_i}}{\widehat{\rho_c}}\left(1+\frac{L}{z_{0i}}\right)-\frac{L}{z_{0c}}-1\right]\left[\frac{\widehat{\rho_i}}{\widehat{\rho_c}}\left(1+\frac{L}{z_{0i}}\right)+\frac{L}{z_{0c}}+1\right]^{-1}. \quad \text{(B.13)}$$

We note again that the solution satisfies the a priori assumption on κ. We may use Equation (B.13) to study the effects of the the relative temperature variations *i.e.* using z_{0i} is either greater or smaller than z_{0c}. The various solar models which this model may be used to

discuss, noted previously, can be studied in this manner. To determine the nature of this solution, consider the limits $L/z_{0i,c} \ll 1$,

$$\omega \approx g k_x \frac{1-\rho}{1+\rho}, \tag{B.14}$$

where $\rho = \widehat{\rho_i}/\widehat{\rho_c}$. We see the solution is the g-mode solution, the corresponding two-layer solution of which is given by Equations (3.262) and (3.269), although the density ratio is now the ratio of the two hydrodynamic layers. When the central layer is thin and the magnetic field may be considered very weak or non-existent so that $\widehat{\rho_c} \approx$ or $= \widehat{\rho_e}$, the solution is comparable to the non-magnetic two-layer solution, as we expect. We see that if the fluid in the central region is denser than the lower layer, $\rho > 1$, we have the well-know Rayleigh-Taylor instability.

A key difference to the two-layer model is the leading order behaviour. In the two-layer model a magnetic term represented the dominant term, whereas here the dominant contribution is the term below the f-mode. In the small wavelength limit, the solution is dominated by the change in temperature in the hydrodynamic layers. Magnetic effects are therefore less significant.